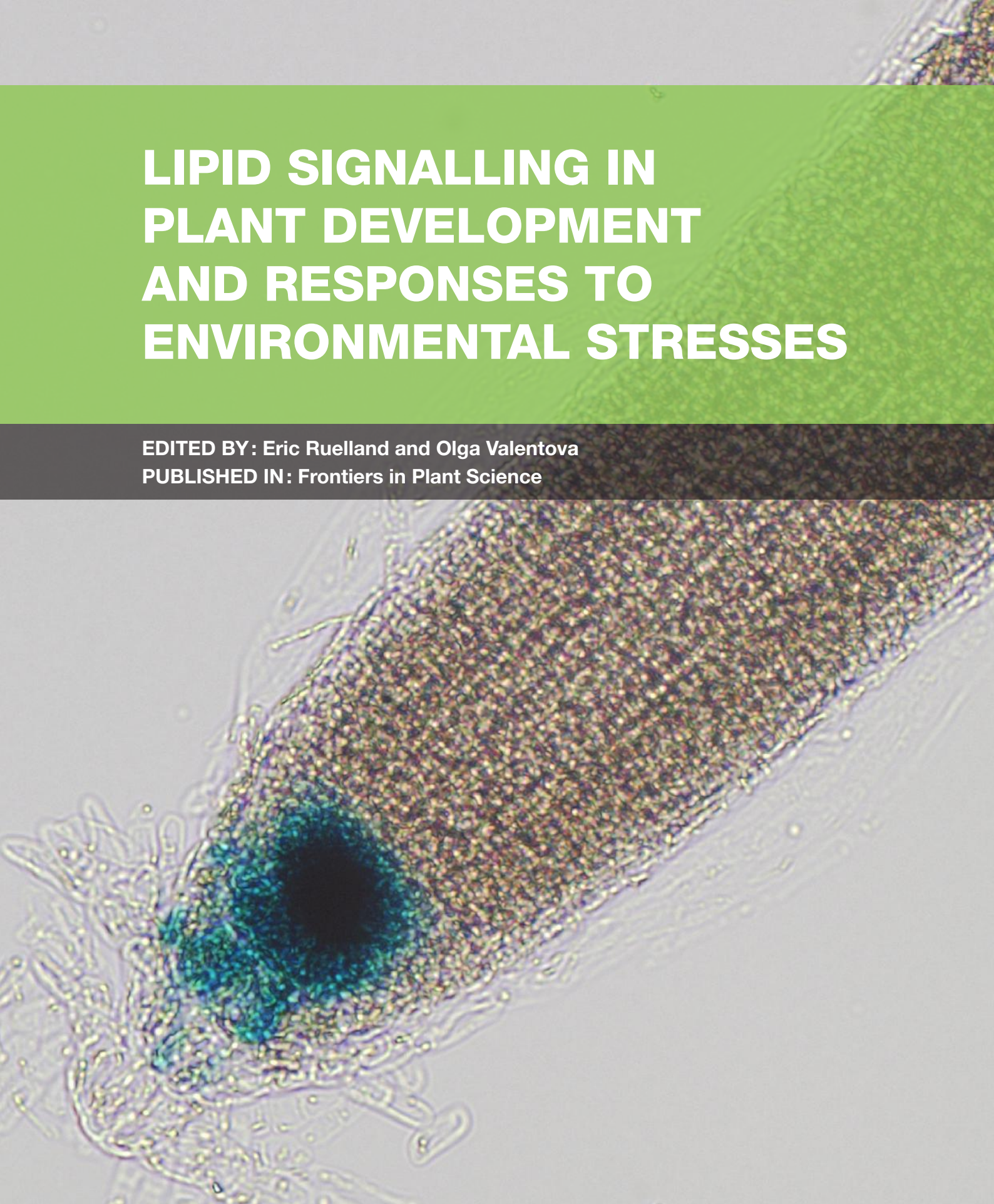
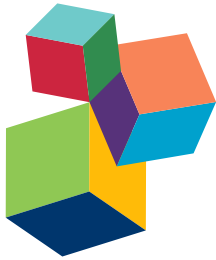


LIPID SIGNALLING IN PLANT DEVELOPMENT AND RESPONSES TO ENVIRONMENTAL STRESSES

EDITED BY: Eric Ruelland and Olga Valentova

PUBLISHED IN: Frontiers in Plant Science





frontiers

Frontiers Copyright Statement

© Copyright 2007-2016 Frontiers Media SA. All rights reserved.

All content included on this site, such as text, graphics, logos, button icons, images, video/audio clips, downloads, data compilations and software, is the property of or is licensed to Frontiers Media SA ("Frontiers") or its licensees and/or subcontractors. The copyright in the text of individual articles is the property of their respective authors, subject to a license granted to Frontiers.

The compilation of articles constituting this e-book, wherever published, as well as the compilation of all other content on this site, is the exclusive property of Frontiers. For the conditions for downloading and copying of e-books from Frontiers' website, please see the Terms for Website Use. If purchasing Frontiers e-books from other websites or sources, the conditions of the website concerned apply.

Images and graphics not forming part of user-contributed materials may not be downloaded or copied without permission.

Individual articles may be downloaded and reproduced in accordance with the principles of the CC-BY licence subject to any copyright or other notices. They may not be re-sold as an e-book.

As author or other contributor you grant a CC-BY licence to others to reproduce your articles, including any graphics and third-party materials supplied by you, in accordance with the Conditions for Website Use and subject to any copyright notices which you include in connection with your articles and materials.

All copyright, and all rights therein, are protected by national and international copyright laws.

The above represents a summary only. For the full conditions see the Conditions for Authors and the Conditions for Website Use.

ISSN 1664-8714

ISBN 978-2-88919-910-5

DOI 10.3389/978-2-88919-910-5

About Frontiers

Frontiers is more than just an open-access publisher of scholarly articles: it is a pioneering approach to the world of academia, radically improving the way scholarly research is managed. The grand vision of Frontiers is a world where all people have an equal opportunity to seek, share and generate knowledge. Frontiers provides immediate and permanent online open access to all its publications, but this alone is not enough to realize our grand goals.

Frontiers Journal Series

The Frontiers Journal Series is a multi-tier and interdisciplinary set of open-access, online journals, promising a paradigm shift from the current review, selection and dissemination processes in academic publishing. All Frontiers journals are driven by researchers for researchers; therefore, they constitute a service to the scholarly community. At the same time, the Frontiers Journal Series operates on a revolutionary invention, the tiered publishing system, initially addressing specific communities of scholars, and gradually climbing up to broader public understanding, thus serving the interests of the lay society, too.

Dedication to Quality

Each Frontiers article is a landmark of the highest quality, thanks to genuinely collaborative interactions between authors and review editors, who include some of the world's best academicians. Research must be certified by peers before entering a stream of knowledge that may eventually reach the public - and shape society; therefore, Frontiers only applies the most rigorous and unbiased reviews.

Frontiers revolutionizes research publishing by freely delivering the most outstanding research, evaluated with no bias from both the academic and social point of view.

By applying the most advanced information technologies, Frontiers is catapulting scholarly publishing into a new generation.

What are Frontiers Research Topics?

Frontiers Research Topics are very popular trademarks of the Frontiers Journals Series: they are collections of at least ten articles, all centered on a particular subject. With their unique mix of varied contributions from Original Research to Review Articles, Frontiers Research Topics unify the most influential researchers, the latest key findings and historical advances in a hot research area! Find out more on how to host your own Frontiers Research Topic or contribute to one as an author by contacting the Frontiers Editorial Office: researchtopics@frontiersin.org

LIPID SIGNALLING IN PLANT DEVELOPMENT AND RESPONSES TO ENVIRONMENTAL STRESSES

Topic Editors:

Eric Ruelland, Centre National de la Recherche Scientifique, France

Olga Valentova, University of Chemistry and Technology, Czech Republic



Histochemical analysis of *pNPC4:GUS* expression in main root of *Arabidopsis* seedlings. Ten-day-old *Arabidopsis* seedlings grown on agar were transferred to a 24-well plate containing 1 ml of 1/8 MS solution for 24 h. Plants were then immersed in X-Gluc buffer [2 mM X-Gluc, 50 mM NaPO₄ pH 7.0, 0.5% (v/v) Triton-X, 0.5 mM K-ferricyanide] for 16 h at 37°C. Final observations were done on a Nikon SMZ 1500 zoom stereoscopic microscope coupled to a Nikon DS-5M digital camera.

Image by Dr Přemysl Pejchar and Dr Jan Martinec (IEB, Prague).

bind them have been identified. Other important lipid mediators belong to the sphingolipid family such the phosphorylated phytosphingosine, or long-chain bases.

In response to environmental stresses, or during development, plant cells will produce lipids that will act as intracellular or intercellular mediators. Glycerophospholipid and/or sphingolipid second messengers resulting from the action of lipid metabolizing enzymes (e.g. lipid-kinases or lipases) are commonly found within cells. The importance of such mediating lipids in plants has become increasingly apparent. Responses to biotic and abiotic stresses, and to plant hormones, all appear to involve and require lipid signals. Likewise, developmental processes, in particular polarized growth, seem also to involve signalling lipids. Amongst these lipids, phosphatidic acid (PA) has received the most attention. It can be produced by phospholipases D, but also by diacylglycerol kinases coupled to phospholipases C. Proteins that bind phosphatidic acid, and for which the activity is altered upon binding, have been identified. Furthermore, other lipids are also important in signalling processes. PA can be phosphorylated into diacylglycerol-pyrophosphate, and plants are one of the first biological models where the production of this lipid has been reported, and its implication in signal transduction have been demonstrated. PA can also be deacylated into lyso- phosphatidic acid. The phosphorylated phosphatidylinositols, i.e. the phosphoinositides, can act as substrate of phospholipases C, but are also mediating lipids per se, since proteins that

Many questions remain unanswered concerning lipid signalling in plants. Understanding and discussing current knowledge on these mechanisms will provide insights into plant mechanisms in response to constraints, either developmental or environmental.

Citation: Ruelland, E., Valentova, O., eds. (2016). Lipid Signalling in Plant Development and Responses to Environmental Stresses. Lausanne: Frontiers Media. doi: 10.3389/978-2-88919-910-5

Table of Contents

- 06 Editorial: Lipid Signaling in Plant Development and Responses to Environmental Stresses**

Eric Ruelland and Olga Valentova

CHAPTER 1. THE USE OF MUTANT APPROACH TO FURTHER UNDERSTAND THE ROLES OF LIPID SIGNALING

- 09 Redundancy among phospholipase D isoforms in resistance triggered by recognition of the *Pseudomonas syringae* effector AvrRpm1 in *Arabidopsis thaliana***

Oskar N. Johansson, Per Fahlberg, Elham Karimi, Anders K. Nilsson, Mats Ellerström and Mats X. Andersson

- 18 Characterization of the inositol monophosphatase gene family in *Arabidopsis***

Aida Nourbakhsh, Eva Collakova and Glenda E. Gillaspy

- 32 Involvement of Phosphatidylinositol 3-kinase in the regulation of proline catabolism in *Arabidopsis thaliana***

Anne-Sophie Leprince, Nelly Magalhaes, Delphine De Vos, Marianne Bordenave, Emilie Crilat, Gilles Clément, Christian Meyer, Teun Munnik and Arnould Savouré

- 45 Ion and lipid signaling in apical growth—a dynamic machinery responding to extracellular cues**

Rui Malhó, Susana Serrazina, Laura Saavedra, Fernando V. Dias and Reiaz Ul-Rehman

CHAPTER 2. THE LIPID SIGNALING MACHINERY IS ACTIVE UNDER CONTROL CONDITIONS BUT CAN BE MODIFIED BY THE ACTION OF HORMONES OR ELICITORS VIA THEIR INHIBITION OF THIS BASAL PATHWAY

- 51 Non-specific phospholipase C4 mediates response to aluminum toxicity in *Arabidopsis thaliana***

Přemysl Pejchar, Martin Potocký, Zuzana Krčková, Jitka Brouzdová, Michal Daněk and Jan Martinec

- 59 Salicylic acid modulates levels of phosphoinositide dependent-phospholipase C substrates and products to remodel the *Arabidopsis* suspension cell transcriptome**

Eric Ruelland, Igor Pokotylo, Nabila Djafi, Catherine Cantrel, Anne Repellin and Alain Zachowski

- 78 Corrigendum: Salicylic acid modulates levels of phosphoinositide dependent-phospholipase C substrates and products to remodel the *Arabidopsis* suspension cell transcriptome**

Eric Ruelland, Igor Pokotylo, Nabila Djafi, Catherine Cantrel, Anne Repellin and Alain Zachowski

CHAPTER 3. IDENTIFICATION OF PUTATIVE NEW SIGNALING MOLECULES GENERATED BY THESE PATHWAYS

80 Biosynthesis and possible functions of inositol pyrophosphates in plants

Sarah P. Williams, Glenda E. Gillaspy and Imara Y. Perera

CHAPTER 4. CROSSTALK BETWEEN LIPID SIGNALING PATHWAYS

92 Overexpression of patatin-related phospholipase A_{IIIB} altered the content and composition of sphingolipids in Arabidopsis

Maoyin Li, Jonathan E. Markham and Xuemin Wang

CHAPTER 5. IDENTIFICATION OF THE MODE OF ACTIONS OF THE SIGNALING LIPIDS

100 Zn²⁺-dependent surface behavior of diacylglycerol pyrophosphate and its mixtures with phosphatidic acid at different pHs

Ana L. Villasuso, Natalia Wilke, Bruno Maggio and Estela Machado

CHAPTER 6. LIPIDS SIGNALLING IN ALGAE

109 Structural divergence and loss of phosphoinositide-specific phospholipase C signaling components during the evolution of the green plant lineage: implications from structural characteristics of algal components

Koji Mikami



Editorial: Lipid Signaling in Plant Development and Responses to Environmental Stresses

Eric Ruelland^{1,2*} and Olga Valentova³

¹ Université Paris-Est, Institut d'Ecologie et des Sciences de l'Environnement de Paris, Créteil, France, ² Centre National de la Recherche Scientifique, Unité Mixte de Recherche 7618, Institut d'Ecologie et des Sciences de l'Environnement de Paris, Créteil, France, ³ Department of Biochemistry and Microbiology, University of Chemistry and Technology, Prague, Prague, Czech Republic

Keywords: lipid signaling pathways, phospholipases, phosphatidic acid, diacylglycerol pyrophosphate, lipid-kinases, phosphoinositides, inositol phosphates

The Editorial on the Research Topic

Lipid Signaling in Plant Development and Responses to Environmental Stresses

In response to environmental stresses, or during development, plant cells will produce lipids that will act as intracellular mediators (Janda et al., 2013; Ruelland et al., 2015). Glycerophospholipid and/or sphingolipid second messengers resulting from the action of lipid metabolizing enzymes (e.g., lipid-kinases or lipases) are commonly found within cells. The articles published within this Research Topics clearly illustrate the trends of this research field that we can sum up as follows.

OPEN ACCESS

Edited and reviewed by:

Steven Carl Huber,
United States Department of
Agriculture - Agricultural Research
Service, USA

*Correspondence:

Eric Ruelland
eric.ruelland@upmc.fr

Specialty section:

This article was submitted to
Plant Physiology,
a section of the journal
Frontiers in Plant Science

Received: 02 December 2015

Accepted: 03 March 2016

Published: 17 March 2016

Citation:

Ruelland E and Valentova O (2016)
Editorial: Lipid Signaling in Plant
Development and Responses to
Environmental Stresses.
Front. Plant Sci. 7:324.
doi: 10.3389/fpls.2016.00324

THE USE OF MUTANT APPROACH TO FURTHER UNDERSTAND THE ROLES OF LIPID SIGNALING

A major contribution to understanding the role of phosphatidylinositol 3-kinase (PI3K), which catalyses the formation of phosphatidylinositol 3-phosphate (PI3P) from phosphatidylinositol, has been provided in this special issue. The PI3K inhibitor, LY294002, affects PI3P levels *in vivo* and triggers a decrease in proline accumulation in response to salt treatment of *Arabidopsis thaliana* seedlings. This is correlated with a higher transcript and protein levels of *Proline dehydrogenase 1* (*ProDH1*), a key-enzyme in proline catabolism. Interestingly the *ProDH1* expression is induced in a *pi3k*-hemizygous mutant, which clearly illustrates the role of PI3P in response to abiotic stresses (Leprince et al.). PI3P can be phosphorylated into phosphatidylinositol (3,5)-bisphosphate [PtdIns(3,5)P₂] by Fab1 phosphatidylinositol-3-phosphate 5-kinases. A reverse genetic approach by Malhó et al. has shown that these enzymes, localized to the endomembrane compartment, are involved in the regulation of plasma membrane recycling events and thus in the maintenance of polarity of pollen tube growth. However, a reverse genetic approach in plants can be tricky. In *Arabidopsis*, many enzymes of the lipid signaling machinery are encoded by multigenic families. For example, phospholipase D (PLD) has 12 gene members in *Arabidopsis*. In their study on plants response to pathogens, Johansson et al. elegantly combine a pharmacological approach with a reverse genetic one in order to cope with the PLD family redundancy. They clearly show that the decrease of PLD-dependent phosphatidic acid (PA) production by *n*-butanol strongly inhibits the hypersensitive response following *Pseudomonas syringae* effector recognition. Yet, the screening of different *pld* mutants (single or multiple mutants) in response to *P. syringae* AvrRpm1 recognition did not allow the identification of isoforms associated with the induction of HR following recognition. The authors reasoned that the PLD activity in response to AvrRpm1

recognition is therefore likely caused by the activation of several PLD isoforms and that the individual contributions might be so small that the single knock-outs show no phenotype. Yet, if the overall activity of PLD is lowered by addition of *n*-butanol, it might be possible to detect the effect of loss of single PLD isoforms. Doing so, i.e., screening again their mutants in response to AvrRpm1 recognition but in presence of *n*-butanol, they could identify several mutants for which the hypersensitive response was lower than that of WT plants (in presence of *n*-butanol). These mutants are impaired in isoforms that in WT plants participate in the bulk PLD activity downstream of AvrRpm1 recognition.

Another limitation of reverse genetic occurs in gene families with only a few members, for which a reverse genetic approach can result in the lack of production of viable mutants. This is illustrated by the *mpl1* mutant that is mutated in the *myo*-inositol monophosphatase (IMP) enzyme that hydrolyses D-*myo*-inositol 1-phosphate, a breakdown product of D-inositol (1,4,5) trisphosphate (Nourbakhsh et al.).

THE LIPID SIGNALING MACHINERY IS ACTIVE UNDER CONTROL CONDITIONS BUT CAN BE MODIFIED BY THE ACTION OF HORMONES OR ELICITORS VIA THEIR INHIBITION OF THIS BASAL PATHWAY

It is now well-accepted that such control states or steady states correspond to a state where some signaling events are active and participate in the maintenance of a metabolic equilibrium that we consider as the quiescent state. It is possible to inhibit such activities. Ruelland et al., show that in *Arabidopsis* suspension cells salicylic acid (SA) treatment leads to an increase in phosphoinositides and to a significant 20% decrease in PA, indicative of a decrease in the products of the phosphoinositide dependent phospholipase C (PI-PLC). Interestingly they could identify genes for which the response to SA was dependent on phosphoinositides. In addition, they were able to identify genes whose response to SA could be mimicked by inhibitors of the PI-PLC pathway. They propose a model in which SA inhibits PI-PLC activity and alters levels of PI-PLC products and substrates, thereby regulating gene expression divergently (Ruelland et al.). Since then the authors also showed that abscisic acid (ABA) also participates in a decrease of the PI-PLC pathway activity, and this could account for the important ABA- and SA-transcriptome response overlap observed in *Arabidopsis* suspension cells (Kalachova et al., 2016). Likewise, xenobiotics or metals could exert their negative effects on plants by acting on the basal lipid signaling machinery. Pejchar et al., illustrate this in their work with non-specific phospholipases C (NPCs) showing that phospholipase C acts on structural lipids such as phosphatidylcholine. Aluminum exposure leads to decreased expression of *NPC4* and decreased NPC activity in *Arabidopsis*. The *in vitro* activity and localization of *NPC4* were not affected by Al, thus excluding direct inhibition by Al ions or possible translocation of *NPC4* as mechanisms involved in the NPC-inhibiting effect (Pejchar et al.). Interestingly, overexpressing

NPC4 partly restored growth of Tobacco pollen tubes under Al stress. These observations suggest that NPCs play a role in the responses to Al stress because NPCs are likely inhibited by Al, and this inhibition is part of the deleterious effect of Al.

IDENTIFICATION OF PUTATIVE NEW SIGNALING MOLECULES GENERATED BY THESE PATHWAYS

Inositol phosphates (InsPs) are linked to lipid signaling, as at least one portion of the inositol phosphate signaling pool is derived from hydrolysis of phosphatidyl inositol (4,5) bisphosphate, a substrate of some phospholipases C. The inositol pyrophosphates are a novel group of InsP molecules containing diphosphate or triphosphate chains (i.e., PPx) attached to the inositol ring. They are emerging as critical players in the integration of cellular metabolism and stress signaling in non-plant eukaryotes. Williams et al., review data suggesting a signaling role for these molecules in plants.

CROSS TALK BETWEEN LIPID SIGNALING PATHWAYS

The first step of sphingolipid synthesis, which uses a fatty acid and a serine as substrates, is critical for sphingolipid homeostasis. Fatty acids are released by the action of phospholipases A. Interestingly, manipulating the level of phospholipases A can impact the level of sphingolipids. Indeed, 3-keto-sphinganine, the product of the first step of sphingolipid synthesis, had a 26% decrease in leaves of mutants plants defective in expression of *pPLAIIIB*, a patatin-related phospholipase A, while a 52% increase could be measured in plants overexpressing it (Li et al.).

IDENTIFICATION OF THE MODE OF ACTIONS OF THE SIGNALING LIPIDS

The lipids produced by the signaling pathways will trigger upstream signaling events. They can do so by binding to proteins, and thus modifying their localization and/or activity. But these lipids can also have effects on the physical properties of membranes. The work on diacylglycerol pyrophosphate (DGPP) and/or phosphatidic acid (PA) monolayers by Villasuso et al. illustrates this point. However, more work is necessary to fully describe the impact of signaling lipids on the physical states of membranes, such as in their fluidity, curvature, interaction with ions, and the consequent impacts on biological processes.

While most of the studies discussed so far concerned higher plants, we should not forget that lipid signaling pathways also exist in algae, including microalgae. Mikami provides a descriptive method to assess enzyme domain structures that provides suggestions as to the origin and evolution of signaling networks that regulate development and stress responses in terrestrial plants). Due to the importance of algae

and microalgae in ocean ecosystems, and as potential industrial source of renewable biodiesel, the article by Mikami is an invitation to develop our research field with these fascinating models.

REFERENCES

- Janda, M., Planchais, S., Djafi, N., Martinec, J., Burkettova, L., Valentova, O., et al. (2013). Phosphoglycerolipids are master players in plant hormone signal transduction. *Plant Cell Rep.* 32, 839–851. doi: 10.1007/s00299-013-1399-0
- Kalachova, T., Puga-Freitas, R., Kravets, V., Soubigou-Taconnat, L., Repellin, A., Balzergue, S., et al. (2016). The inhibition of basal phosphoinositide-dependent phospholipase C activity in *Arabidopsis* suspension cells by abscisic or salicylic acid acts as a signalling hub accounting for an important overlap in transcriptome remodelling induced by these hormones. *Environ. Exp. Bot.* 123, 37–49. doi: 10.1016/j.envexpbot.2015.11.003
- Ruelland, E., Kravets, V., Derevyanchuk, M., Martinec, J., Zachowski, A., and Pokotylo, I. (2015). Role of phospholipid signalling in plant

AUTHOR CONTRIBUTIONS

All authors listed, have made substantial, direct and intellectual contribution to the work, and approved it for publication.

environmental responses. *Environ. Exp. Bot.* 114, 129–143. doi: 10.1016/j.envexpbot.2014.08.009

Conflict of Interest Statement: The authors declare that the research was conducted in the absence of any commercial or financial relationships that could be construed as a potential conflict of interest.

Copyright © 2016 Ruellan and Valentova. This is an open-access article distributed under the terms of the Creative Commons Attribution License (CC BY). The use, distribution or reproduction in other forums is permitted, provided the original author(s) or licensor are credited and that the original publication in this journal is cited, in accordance with accepted academic practice. No use, distribution or reproduction is permitted which does not comply with these terms.



Redundancy among phospholipase D isoforms in resistance triggered by recognition of the *Pseudomonas syringae* effector AvrRpm1 in *Arabidopsis thaliana*

Oskar N. Johansson¹, Per Fahlberg¹, Elham Karimi², Anders K. Nilsson¹, Mats Ellerström¹ and Mats X. Andersson^{1*}

¹ Department of Biology and Environmental Sciences, University of Gothenburg, Gothenburg, Sweden

² Department of Plant Pathology, Faculty of Agriculture, Tarbiat Modares University, Tehran, Iran

Edited by:

Eric Ruelland, Centre National de la Recherche Scientifique, France

Reviewed by:

Xia Wu, University of Washington, USA

Eric Ruelland, Centre National de la Recherche Scientifique, France

Lenka Burketova, Academy of Sciences of the Czech Republic, Czech Republic

***Correspondence:**

Mats X. Andersson, Department of Biology and Environmental Sciences, University of Gothenburg, Box 461, SE-405 30 Gothenburg, Sweden
e-mail: mats.andersson@bioenv.gu.se

Plants possess a highly sophisticated system for defense against microorganisms. So called MAMP (microbe-associated molecular patterns) triggered immunity (MTI) prevents the majority of non-adapted pathogens from causing disease. Adapted plant pathogens use secreted effector proteins to interfere with such signaling. Recognition of microbial effectors or their activity by plant resistance (R)-proteins triggers a second line of defense resulting in effector triggered immunity (ETI). The latter usually comprises the hypersensitive response (HR) which includes programmed cell death at the site of infection. Phospholipase D (PLD) mediated production of phosphatidic acid (PA) has been linked to both MTI and ETI in plants. Inhibition of PLD activity has been shown to attenuate MTI as well as ETI. In this study, we systematically tested single and double knockouts in all 12 genes encoding PLDs in *Arabidopsis thaliana* for effects on ETI and MTI. No single PLD could be linked to ETI triggered by recognition of effectors secreted by the bacterium *Pseudomonas syringae*. However, repression of PLD dependent PA production by n-butanol strongly inhibited the HR following *Pseudomonas syringae* effector recognition. In addition some *pld* mutants were more sensitive to n-butanol than wild type. Thus, the effect of mutations of PLDs could become detectable, and the corresponding genes can be proposed to be involved in the HR. Only knockout of *PLD* caused a loss of MTI-induced cell wall based defense against the non-host powdery mildew *Erysiphe pisi*. This is thus in stark contrast to the involvement of a multitude of PLD isoforms in the HR triggered by AvrRpm1 recognition.

Keywords: phospholipase D, hypersensitive response, *Pseudomonas syringae*, *Arabidopsis thaliana*, phosphatidic acid, pathogen defense

INTRODUCTION

Plants employ a sophisticated multilayered immune system to defend themselves from pathogenic microbes (Jones and Dangl, 2006; Dodds and Rathjen, 2010). Early defenses are activated upon recognition of conserved molecular patterns of potential pathogens. Recognition of microbe-associated molecular patterns (MAMPs) activates MAMP triggered immunity (MTI) which entails strengthening of the cell wall, transcriptional activation of pathogenesis related (PR) proteins and secretion of low molecular weight antimicrobial substances (Boller and Felix, 2009). MTI is effective against pathogens from several kingdoms and is often sufficient to halt the intruder from colonizing the plant. Microbial co-evolution with plants has provided selective pressure for overcoming MTI and thus increases the possibility to proliferate on or in the plant tissue and cause disease. Adapted pathogens have developed means to suppress MTI. This often comprises the secretion of so called effector proteins, which can interfere with plant defense signaling (Dodds and Rathjen, 2010). In turn, plants have evolved resistance (R) proteins to detect the presence or activity of pathogenic effectors. Recognition of effectors results in a strong and robust defense known as effector triggered immunity

(ETI), which often includes the so called hypersensitive response (HR). ETI provides faster, stronger and more specific response to a pathogenic threat than MTI. Though more efficient at stopping adapted pathogens, ETI responses highly overlap those of MTI, the most prominent differential feature being HR leading to localized cell death at the site of infection (Tsuda and Katagiri, 2010). ETI also induces systemic transcriptional reprogramming and defense enhancement through the activation of systemic acquired resistance (SAR; Spoel and Dong, 2012) and long term immunity by epigenetic mechanisms (Molinier et al., 2006; Alvarez et al., 2010).

Phospholipase D (PLD) is a family of enzymes with prominent lipolytic activity in plant tissues that has been recognized for a long time (Hanahan and Chaikoff, 1947; Li et al., 2009). PLD cleaves phospholipids to produce phosphatidic acid (PA) and a free alcohol from the phospholipid head group. The former is known to be a potent second messenger in plants and other organisms (Wang, 2004; Li et al., 2009). PLD and PA dependent signals are implicated in responses to a wide range of abiotic and biotic stresses in higher plants (Laxalt and Munnik, 2002; Li et al., 2009). PA can also be produced by phosphorylation of diacylglycerol (DAG) by DAG

kinase (DAGK). DAG in its turn can be produced by phospholipase C (PLC) mediated degradation of phosphoinositides (Wang, 2004). Both pathways are implicated in PA production in response to abiotic as well as biotic stress. PLD dependent PA production can be “inhibited” by primary alcohols, whereas secondary alcohols are inefficient. The effect of primary alcohols is attributable to the preferential use of a primary alcohol for transphosphatidylation by PLD giving rise to an artificial phospholipid rather than PA.

The *Arabidopsis thaliana* (hereafter *Arabidopsis*) genome contains 12 genes encoding PLDs (Li et al., 2009). The PLDs are grouped according to their co-factor requirements and substrate preferences in α , β , γ , δ , ϵ , and ζ families. The *Arabidopsis* PLDs have roles in responses to various biotic and abiotic stresses. Several of the *Arabidopsis* PLDs have been implicated in responses to abiotic stress (Bargmann and Munnik, 2006): PLD α in drought-, salt- and PLD α , and PLD δ in cold stress (Sang et al., 2001b; Li et al., 2004, 2008; Hong et al., 2008). PLD α has also been implicated in senescence (Fan et al., 1997).

It is well known that PA accumulates in plant cells in response to both MTI and ETI (Bargmann and Munnik, 2006). The relative contribution of PLD and PLC-DAGK to the PA formation during MTI and ETI seems to differ between plant pathogen systems. PLD was previously directly linked to the induction of the HR after recognition of *Pseudomonas syringae* pv. tomato (*Pst*) and *Xanthomonas campestris* effectors (Andersson et al., 2006; Kirik and Mudgett, 2009). PA production is also associated with MTI (van der Luit et al., 2000) and inhibition of PLD was shown to increase the success of a non-adapted powdery mildew in cell wall penetration in *Arabidopsis* (Pinosa et al., 2013).

The individual contribution of different PLD isoforms to plant defense responses is poorly understood. Transcripts of *PLD α* are strongly induced by both virulent and avirulent strains of *Pst* and isoforms of *PLD β* are transiently induced by the same strains, whereas *PLD γ* isoforms are induced only after recognition of the avirulent strain (Zabela et al., 2002). Treatment with the fungal elicitor xylanase as well as both avirulent and virulent strains of *Pst* induce transcriptional activation of *PLD β 1* (Laxalt et al., 2001; Zhao et al., 2013). Recently we described how *PLD δ* is involved in the penetration resistance of *Arabidopsis* against the non-adapted fungal pathogen *Blumeria graminis* Sp *Hordei* (*Bgh*), the causal agent of powdery mildew on barley (Pinosa et al., 2013). The reduced penetration resistance also extended to the more adapted pathogen *Erysiphe pisi* (*Ep*), responsible for the powdery mildew disease of the garden pea. In contrast to the previously described instances where PA generated by PLD seems to act as a positive regulator of plant defense induced by both MTI and ETI, a recent study suggested that *PLD β 1* acts like a negative regulator of resistance responses to biotrophic pathogens, HR and salicylic acid dependent defenses in *Arabidopsis* (Zhao et al., 2013).

We herein show that several different *Arabidopsis* PLD isoforms contribute to HR induced by recognition of the *Pst* effector AvrRpm1. On the other hand, cell wall based MTI triggered by the pea powdery mildew *Ep*, which is a non-host pathogen for *Arabidopsis*, is exclusively regulated by a single PLD isoform, *PLD δ* . To the best

of our knowledge, this is the first complete reverse genetics screen of knock outs of all *Arabidopsis* PLD genes for involvement in defense against virulent and avirulent phytopathogenic bacteria.

MATERIALS AND METHODS

PLANT MATERIAL

Arabidopsis was cultivated on soil in a climate chambers (CLF climatics, Germany) under short day conditions (8 h light/16 h dark, 22°C/18°C, at 120 μmol photons $\text{m}^{-2} \text{s}^{-1}$ light intensity and 60% relative humidity). The *Arabidopsis rpm1-3* mutant line (Grant et al., 1995) and the *pld* mutant lines (Pinosa et al., 2013) used were all previously described. Garden pea (*Pisum sativum* cv. Kelvedon wonder) was cultivated under green house lights at 22°C.

ELECTROLYTE LEAKAGE AND BACTERIAL PROLIFERATION ASSAYS

Pseudomonas syringae pv. tomato DC3000 strains were maintained on solid *Pseudomonas* agar F (King's B medium, Biolife, Italy) supplemented with 50 mg l^{-1} rifampicin and 50 mg l^{-1} kanamycin. For electrolyte leakage experiments, exponentially growing cells from overnight plate culturing were suspended in 10 mM MgCl₂ and diluted to OD₆₀₀ 0.1. The bacterial suspension was vacuum infiltrated into leaf discs (7 mm diameter) of 6–8 week old *Arabidopsis* plants using a SpeedVac vacuum concentrator (Savant, Thermo Electron Corporation, USA). Leaf discs were washed in deionized water and transferred to six well cultivation plates containing 10 mL water (four discs per well). The release of electrolytes from the leaf discs was determined using a conductivity meter (Orion, Thermo scientific) as described (Johansson et al., 2014). In experiments with n- or tert-butanol, the bacteria were suspended in MgCl₂ solution containing the indicated concentration of n- or tert-butanol, infiltrated and put into culturing plates with 10 mL of deionized water and the same alcohol at the same concentrations.

Bacterial proliferation was measured after syringe infiltration of bacterial suspensions (OD₆₀₀ 0.00002) into the abaxial side of leaves attached to the plant with a needleless syringe. The bacteria were extracted directly or 3 days after infiltration and the number of colony-forming units (CFU) determined after serial dilution and plating as described (Johansson et al., 2014).

To determine the effect of tert- and n-butanol on the growth of *Pst*, exponentially growing cells from overnight culture were re-suspended in 10 mM MgCl₂ and transferred into liquid cultures of KB media containing n- or tert-butanol at the indicated concentrations. The preparation had an initial optical density of 0.05, corresponding to $2.5 \times 10^7 \text{ CFU} \cdot \text{mL}^{-1}$ and were cultivated on a shaker in room temperature for 6 h. An aliquot was taken, serially diluted, plated on KB plates and the number of colonies was determined after 2 days.

LIPID ANALYSIS

Lipids were extracted from three *Arabidopsis* leaf discs prepared and incubated as above by chloroform methanol extraction as previously described (Andersson et al., 2006) after addition of 0.1 μg of diheptadecanoyl phosphatidylcholine as internal standard. Phosphatidylbutanol (PBut) species were analyzed by LC-MS/MS using the chromatographic conditions and instrumental settings

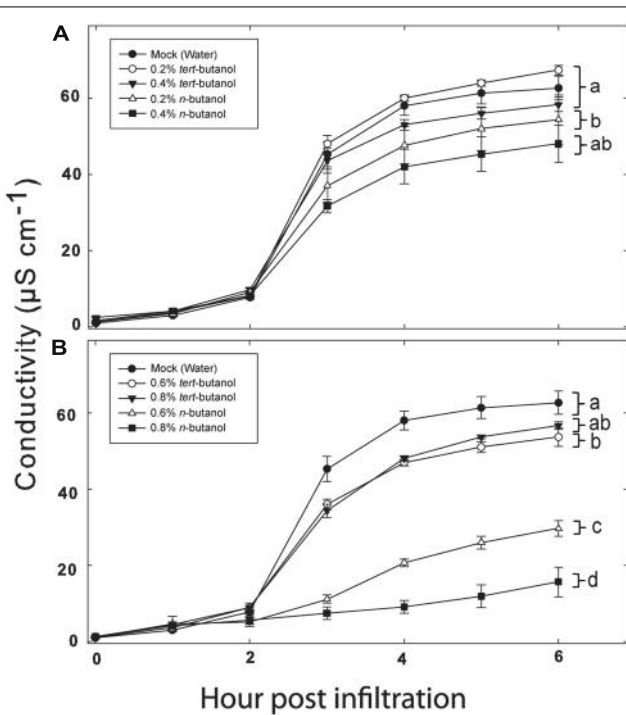


FIGURE 1 | Phospholipase D (PLD) dependence of hypersensitive response (HR) induction in *Arabidopsis* following recognition of AvrRpm1 expressed by *Pseudomonas syringae* pv. *tomato* (*Pst*). Leaf discs were prepared from wild type, Col-0, *Arabidopsis*, infiltrated with *Pst* DC3000:AvrRpm1 suspended in 0.2, 0.4 (A), 0.6 or 0.8 % (B) tert- or n-butanol solutions and incubated in deionized water with the same alcohol at the same concentration for 6 h. The conductivity of the bathing solution was measured at the indicated time points. Average of six replicates and SD is shown. Lower case letters represent statistically significant different groups (one way ANOVA, $p < 0.05$) for the 6 h time point. The experiment was performed twice with similar results.

previously described (Nilsson et al., 2014) using the MRM transitions described for PBut species (Rainteau et al., 2012). The following molecular species of PBut could be detected: 18:3/18:3, 18:2/18:3, 16:0/18:3, 18:2/18:2, 18:1/18:3, 16:0/18:2, 18:1/18:2, 18:0/18:2. The sum of the mass spectrometric signal for these species divided by that of the internal standard is presented in Figure 2.

Erysiphe pisi INOCULATION AND SCORING

The pea powdery mildew fungus *Ep* was maintained on its host plant garden pea. 4 weeks old *Arabidopsis* plants were brush inoculated with *Ep* spores and penetration rate scored at 2 dpi as described (Pinosa et al., 2013) after trypan blue staining (Koch and Slusarenko, 1990). In short, the infection state of at least 50 germinated spores on three separate leaves (3×50) was determined by visually inspecting the epidermal surface for stained cells or papillae using a light microscope (100–400 \times magnification).

STATISTICAL ANALYSIS

Statistical analysis was performed as described (Johansson et al., 2014) using GraphPad Prism 6 (GraphPad Software, La Jolla, CA,

USA). The final time point (6 h) of ion leakage assays, the penetration rate and the bacterial growth were subjected to one way ANOVA analysis with Tukey's *post hoc* analysis with $p < 0.05$ considered significant.

RESULTS

As PLDs are clearly involved in both PTI and ETI, we decided to test the involvement of individual *Arabidopsis* PLD genes on defense responses triggered by recognition of a bacterial effector. The tomato pathovar of *Pseudomonas syringae* DC3000 is normally highly virulent on wild type *Arabidopsis*. However, if the pathogen carries the AvrRpm1 effector gene, the AvrRpm1 protein is recognized by the *Arabidopsis* R-protein RPM1 (Grant et al., 1995). This recognition triggers induction of HR and programmed cell death in the plant. The latter can be measured as loss of electrolytes from leaf tissue into an aqueous solution (Hibberd, 1987; Mackey et al., 2002). To verify the involvement of PLD in HR triggered by AvrRpm1 recognition in *Arabidopsis*, leaf tissue infiltrated with *Pst* DC3000:AvrRpm1 was incubated in solution with different concentrations of n- or tert-butanol and the rate of cell death determined by measuring the electric conductance of the bathing solution (Figure 1). The primary alcohol n-butanol is known to inhibit PLD dependent formation of PA, as the alcohol is preferred over water to form an artificial phosphatidylalcohol by transphosphatidylation (Ella et al., 1997). Tert-butanol, on the other hand, is unable to do this. A concentration of 0.6% (v/v) n-butanol caused a decrease in the HR induced by AvrRpm1 recognition by about 40%, whereas 0.8% (v/v) of n-butanol caused an almost complete loss in cell death. Tert-butanol had only a slight effect on the HR as measured by electrolyte leakage, the effect of tert-butanol was apparent only at the two highest concentrations used.

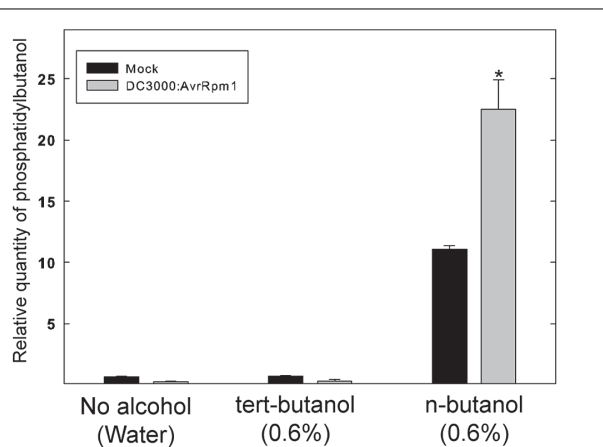
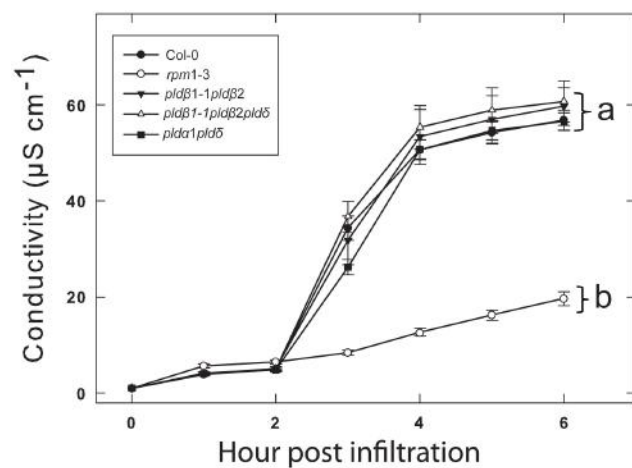
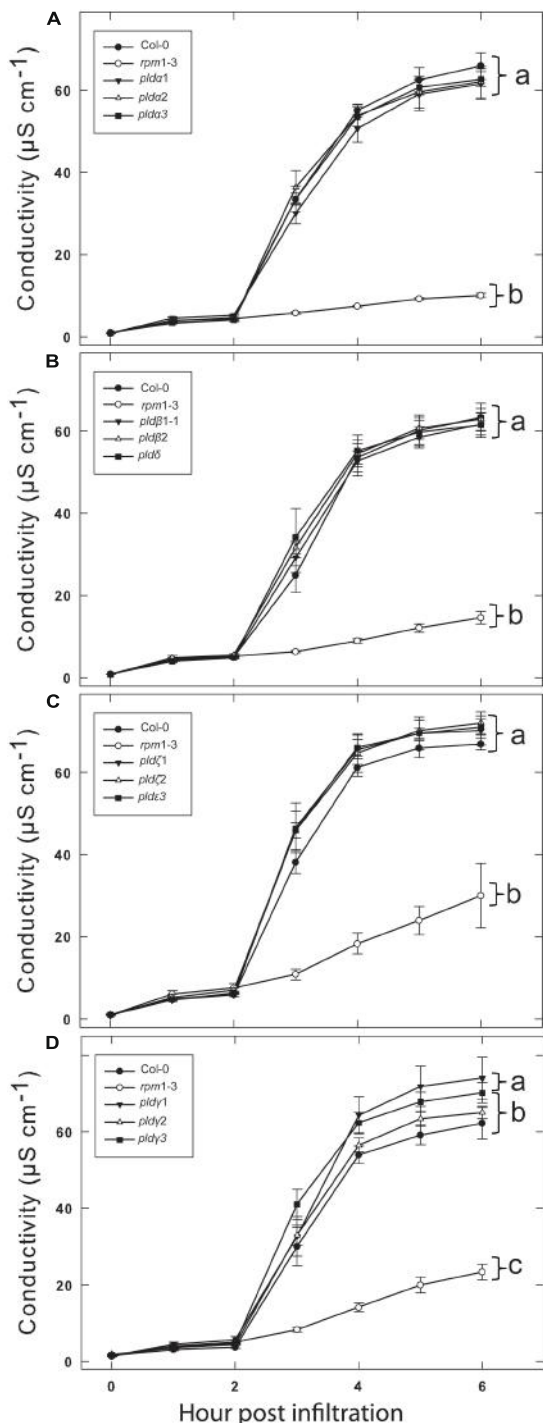


FIGURE 2 | Formation of Phosphatidylbutanol (PBut) in *Arabidopsis* leaf tissue during the HR in the presence of n-butanol. Leaf discs were prepared from wild type, Col-0, *Arabidopsis*, infiltrated with *Pst* DC3000:AvrRpm1 or $MgCl_2$ (mock treatment) in 0.6% tert- or n-butanol water solutions and incubated in deionized water with the same alcohol at the same concentration for 4 h. The lipids were extracted and the amount of PBut formed analyzed by LC-MS/MS. An asterisk indicates a statistically significant ($p < 0.05$, one way ANOVA) difference between mock treatment and infiltration with *Pst* DC3000:AvrRpm1.



To test whether the alcohol by itself had an effect on the bacteria, exponentially growing *Pst* DC3000:AvrRpm1 were incubated with n- or tert-butanol for 6 h and thereafter serially diluted, cultivated on solid medium and the number of colonies determined after 2 days (Figure S1). The alcohol treatment caused a significant growth inhibition over 6 h compared to mock treatment. However, there was no significant difference between treatments with tert- or n-butanol. Thus, the effect of n-butanol on the HR is unlikely to be caused by the growth inhibition of the bacteria as the latter did not differ from tert-butanol treatment which did not affect the HR related cell death. To further test that the n-butanol treatment really caused significant formation of PBut during the HR triggered by recognition of AvrRpm1, lipids were extracted from plant tissue treated with tert- or n-butanol 4 h following infiltration with *Pst* DC3000:AvrRpm1 and the amount of PBut formed analyzed by LC-MS/MS (Figure 2). There was a clear induction of PBut formation following recognition of AvrRpm1 in the presence of n-butanol at the same (0.6%) concentration that caused a significant decrease in HR related cell death. This thus confirms activation of PLD during the HR and formation of PBut in the presence of n-butanol. These results taken together support previously published data (Andersson et al., 2006; Kirik and Mudgett, 2009) that the HR induced by recognition of bacterial effectors in *Arabidopsis* is strongly dependent on formation of PA by PLD.

A HIGH DEGREE OF REDUNDANCY AMONG PLD ISOFORMS IN THE ETI SIGNALING

We previously tested a panel of PLD mutants for effects on cell wall based resistance to barley powdery mildew and found that PLD δ was involved in the MAMP triggered signaling involved

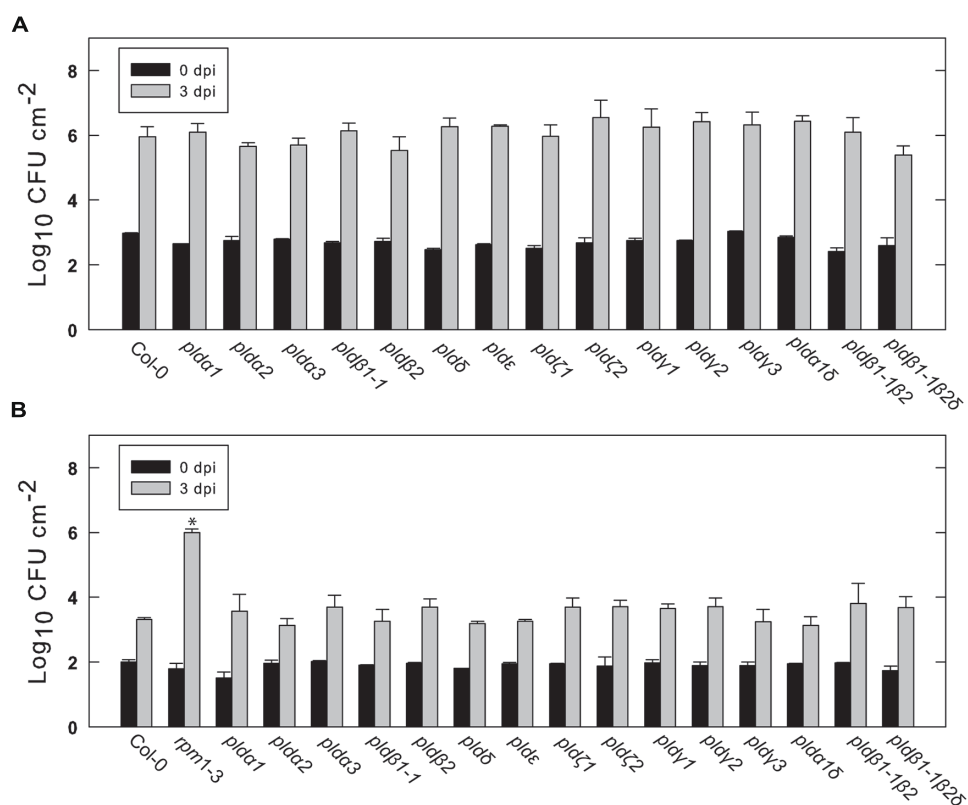


FIGURE 5 | Growth of virulent and avirulent *Pst* in various PLD knockout mutants. *Arabidopsis* leaves attached to the plant were infiltrated with a suspension of *Pst* DC3000 (A) or DC3000:AvrRpm1 (B). The bacteria in the leaves were extracted immediately or after 3 days and quantified by serial

dilution and cultivation on solid medium. Average and SD of three replicates is shown. An asterisk indicates statistically significant differences from wild type (Col-0) at 3 dpi. The experiments shown were repeated twice with similar results.

in the defense reaction (Pinosa et al., 2013). However, as effector triggered resistance differs significantly from MAMP triggered defense responses, we tested if the PLD-mediated effect on could be attributed to any particular of the 12 PLD genes in the *Arabidopsis* genome. Single (Figure 3), double and triple (Figure 4) *pld* T-DNA mutants (Pinosa et al., 2013) were assayed for HR induced after infiltration with *Pst* DC3000:AvrRpm1. This revealed no clear reduction in HR induced ion leakage for any of the tested mutants compared to wild type. The *pldy1* and *pldy3* mutants appeared to demonstrate a slightly elevated cell death response following AvrRpm1 recognition (Figure 3D). Taken together, this suggests that there is a high degree of genetic redundancy among the PLD isoforms activated during HR induced by AvrRpm1 recognition.

We next tested the different *Arabidopsis* lines for their ability to restrict growth of the virulent *Pst* DC3000 and the avirulent strain DC3000:AvrRpm1. As expected, over a period of 3 days DC3000 multiplied in wild type leaves by about a thousand times (Figure 5A). The growth of DC3000 was not significantly affected in any of the tested mutant lines. The avirulent strain DC3000:AvrRpm1 grew about 10-fold in 2 days in wild type Col-0 and this was not significantly affected in any of the tested mutants (Figure 5B). The *rpm1-3* mutant, which is unable to recognize AvrRpm1, demonstrated bacterial

multiplication by about 10000 times. To conclude, none of the tested PLD single, double or triple mutants demonstrated any apparent change in resistance toward virulent and avirulent *Pst* DC3000.

HR PHENOTYPES OF *pld* MUTANTS IN COMBINATION WITH INHIBITION OF PLD DEPENDENT PA FORMATION

While none of the tested *pld* mutants displayed a clear reduction in effector induced HR, the involvement of PLDs in this defense reaction was apparent as treatment with n-butanol clearly affected the plants ability to mount HR and formation of PBut in connection with this was observed. We thus reasoned that the PLD activity in response to AvrRpm1 recognition is likely caused by the activation of several PLD isoforms and that the individual contributions might be so small that the single knock outs show no phenotype. Thus, if the overall activity of PLD is lowered by addition of n-butanol, it might be possible to detect the effect of loss of single PLD isoforms. To test this, wild type (Col-0) and all the *pld* mutants were infiltrated with 0.6% n-butanol together with *Pst* DC3000:AvrRpm1 (Figure 6). As a control, the wild type was also treated with 0.6% tert-butanol. As expected, 0.6% n-butanol caused a significant reduction in ion leakage following AvrRpm1 recognition compared to treatment with 0.6% tert-butanol in wild type. The single mutants *pld α 1*,

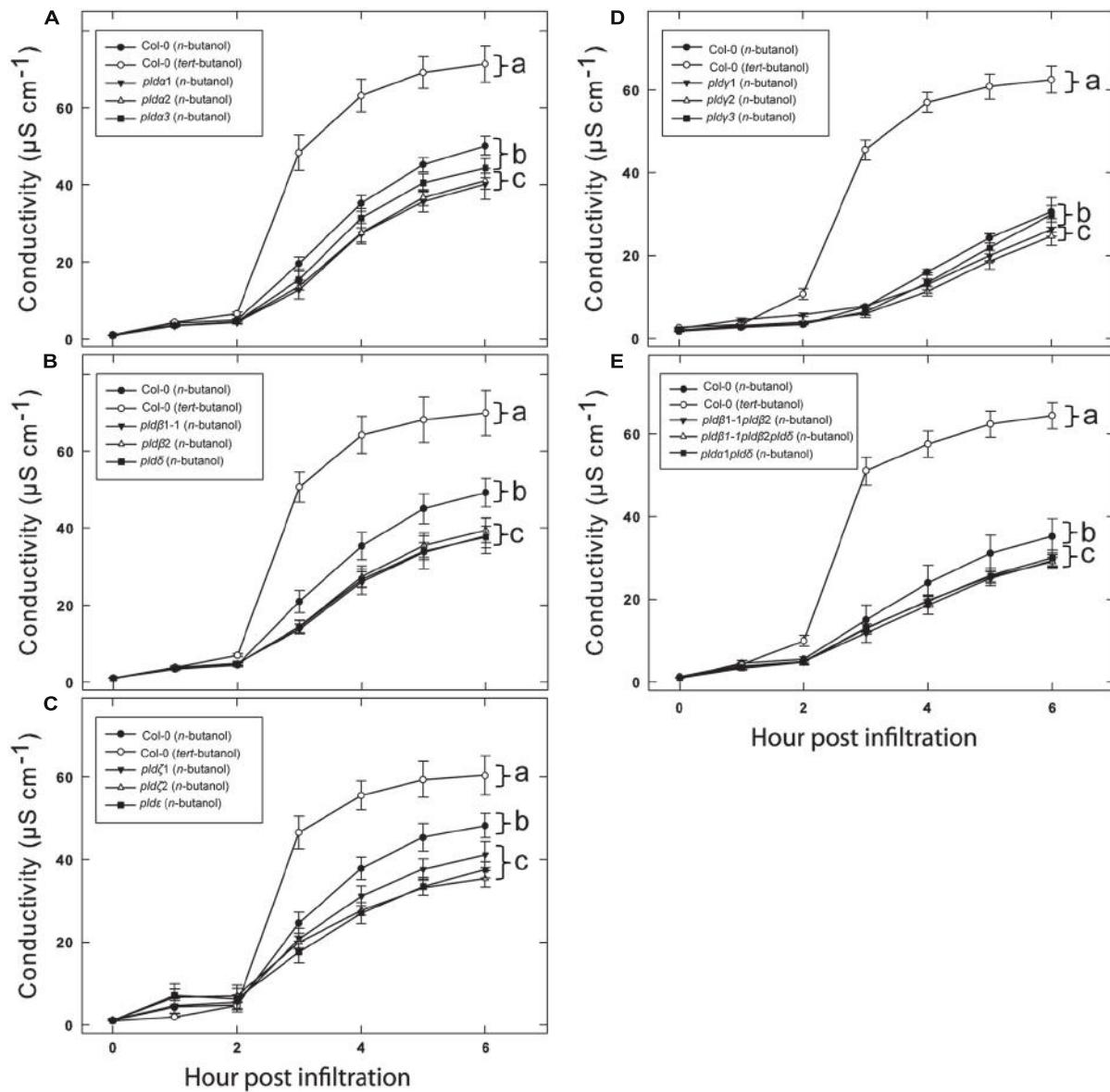


FIGURE 6 | Additive effects of n-butanol and loss of single PLD genes on HR cell death following recognition of AvrRpm1. Leaf discs were prepared from the indicated lines, infiltrated with *Pst* DC3000:AvrRpm1 in 0.6% tert- or n-butanol as indicated and incubated in deionized water with the same alcohol. Col-0 treated with tert- and n-butanol is included in all experiments (A–E) together with the indicated

subset of PLD knock out mutants. The loss of cellular electrolytes was measured as the conductance of the bathing solution at the indicated time points. Average of six replicates and SD is shown. Lower case letters represent statistically significant different groups (one way ANOVA, $p < 0.05$) for the 6 h time point. The experiment was performed twice with similar results.

pld α 2, *pld β 1*, *pld β 2*, *pld δ* , *pld ζ 1*, *pld ζ 2*, and *pld ϵ* all displayed 10–20% statistically significant reductions in HR compared to wild type when treated with 0.6% n-butanol (Figures 6A–C). The mutants *pld γ 1* and *pld γ 2* also displayed a statistically significant reduction in ion leakage induced after AvrRpm1 recognition, this effect was however smaller than for the other mutants (Figure 6D). Finally, the double mutants *pld β 1 pld β 2* and *pld α 1 pld δ* , as well as the triple mutant *pld β 1 pld β 2 pld δ* , displayed a similar conditional reduction of ion leakage as shown for the single mutants (Figure 6E).

PLD δ IS THE ONLY PLD ISOFORM INVOLVED IN TRIGGERING CELL WALL BASED DEFENSE AGAINST A NON-HOST POWDERY MILDEW

We previously reported that PLD δ was the only isoform involved in PLD-dependent cell wall based defense against the non-host powdery mildew *Bgh* and that the *pld δ* mutant also demonstrated a loss of penetration resistance toward pea powdery mildew *Ep* (Pinosa et al., 2013). We thus tested the response of the full panel of PLD mutants to *Ep* (Figure 7). To this end plants were inoculated with *Ep*, leaves stained with trypan blue 2 days post infection and scored for disease progress. The *pen1-1* mutant was included as

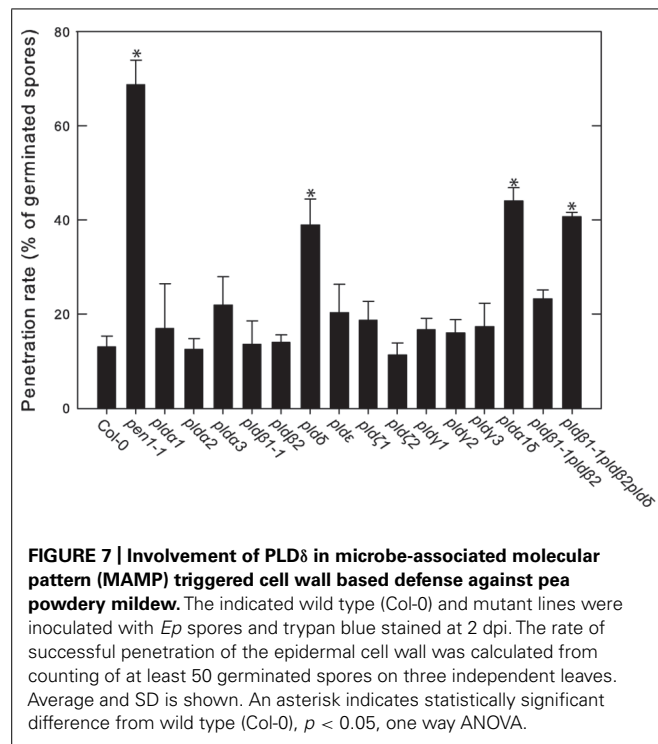


FIGURE 7 | Involvement of PLD δ in microbe-associated molecular pattern (MAMP) triggered cell wall based defense against pea powdery mildew. The indicated wild type (Col-0) and mutant lines were inoculated with *Ep* spores and trypan blue stained at 2 dpi. The rate of successful penetration of the epidermal cell wall was calculated from counting of at least 50 germinated spores on three independent leaves. Average and SD is shown. An asterisk indicates statistically significant difference from wild type (Col-0), $p < 0.05$, one way ANOVA.

a control as it has a severely deficient cell wall based resistance response against non-host powdery mildews (Collins et al., 2003). The number of germinated spores that successfully penetrated the epidermal cell wall was about 15% in wild type (Col-0), whereas *pen1-1* allowed about 70% of the germinated spores to penetrate the epidermal cell wall. Among the tested PLD single mutants, only *pld δ* displayed any increase in penetration rate compared to wild type. Higher order mutants containing the *pld δ* displayed the same phenotype as the single mutant. There was no change in frequency of single epidermal cell death following successful penetration in any of the tested mutants compared to wild type.

DISCUSSION

The HR was described a century ago, only recently has the molecular details of the process from the recognition of pathogenic effectors to the “auto destruction” of the host cell begun to be elucidated (Mur et al., 2008). PLDs have been shown to play an important role in the induction of HR following recognition of pathogenic effectors. This was previously demonstrated using a system where the *Pst* effector AvrRpm1 was expressed *in planta* after the selective inhibition of PLD dependent production of PA by primary alcohols (Andersson et al., 2006). We herein show that the same holds true for effector delivered by live *Pst* bacteria infiltrated into the tissue. Alcohol treatment caused a reduction in growth of *Pst* cultured *in vitro*. However, as the growth inhibition effect did not differ between tert- and n-butanol, and since n-butanol had a strong effect on the HR, we deem it most likely that this non-specific effect of the alcohol is not the primary cause of the inhibition of the HR related cell death. Furthermore, as formation of PBut could be observed in tissue after inoculation with *Pst* DC3000:AvrRpm1 in the presence of n-butanol, it is likely that

the effect of n-butanol was primarily exerted on PA production by PLD.

Phosphatidic acid has been shown to directly cause oxidative damage and cell death when infiltrated into plant tissue (Sang et al., 2001a; Park et al., 2004; Andersson et al., 2006). However, the contribution of PLD derived signals needed for the induction of HR and programmed cell death seems to vary between different effectors. HR induced by recognition of AvrRpm1 is highly PLD dependent, but is also inhibited by inhibition of PLC (Andersson et al., 2006). It was thus proposed that PLD activation is dependent of PLC activity in the case of AvrRpm1 triggered HR. On the other hand HR induced by AvrRpt2 is only inhibited if both PLD and PLC activity are affected at the same time and AvrBsT is of intermediate sensitivity to PLD inhibition (Kirik and Mudgett, 2009). This highlights that different effector recognition events trigger slightly different intracellular signaling pathways. Even though many components may be shared between the different effector response pathways, the extent to which specific signal transducers are involved in the responses appears to vary.

Of the 12 different PLDs encoded by the *Arabidopsis* genome no single gene knockout led to a decrease in HR induced after recognition of AvrRpm1. Since chemical inhibition of PLD dependent PA formation by primary alcohols strongly affects the HR, this point to a high degree of redundancy among the PLD genes in induction of HR following effector recognition. MTI, on the other hand, as tested here and previously (Pinosa et al., 2013) was found to be affected by the loss of a single gene, PLD δ . This difference is fully compatible with the notion that ETI is characterized by robust and redundant activation of intracellular signaling, whereas signaling leading to MTI is associated with a lower degree of redundancy (Sato et al., 2010). The lack of discernable HR phenotype of the tested PLD knockouts was also reflected in that none of the tested mutants displayed any difference in ability to restrict growth of *Pst* expressing AvrRpm1.

When combined with partial inhibition of the HR by n-butanol induced transphosphatidylation, several of the single knockout mutants revealed a decreased HR after recognition of AvrRpm1. Specifically, *pld α 1*, *pld α 2*, *pld β 1*, *pld β 2*, *pld δ* , *pld ζ 1*, *pld ζ 2*, and *pld ϵ* all displayed a conditional HR phenotype in the presence of n-butanol. We interpret this as that multiple PLDs are activated and contribute to PA production which stimulates the HR induced by AvrRpm1 recognition in *Arabidopsis*. However, alternative explanations exist such as that certain PLDs become more active in the absence of other isoforms. This regulation could be both at a transcriptional and/or at a post translational level. A small decrease in HR following AvrRpm1 recognition was previously reported for the double mutant *pld α 1 pld δ* . This finding was reported in a doctoral thesis, but never formally published in a journal (<http://dare.uva.nl/record/281626>). Although we found no phenotype of the double mutant, it can easily be envisioned that a small phenotype might sometimes be present as these two PLDs represent the most abundant PLD transcripts in *Arabidopsis*. Taken together, our data points to that the small contributions of many PLDs together provide enough PA to form an active signal. A likely activation mechanism for the multiple PLDs is the very strong and sustained increase in cytosolic calcium observed to follow recognition of bacterial effectors (Grant et al., 2000).

We found no evidence of that the *pldβ1* would contribute to increased HR in response to AvrRpm1 recognition as reported for recognition of AvrRpt2 (Zhao et al., 2013). This could be due to differences between the signaling pathways induced by different effector types. The *pen3* mutant for example demonstrates different phenotypes depending on whether it is treated with *Pst* expressing AvrRpm1 or AvrRpt2 (Kobae et al., 2006; Johansson et al., 2014). The previously reported strongly decreased proliferation in leaf tissue of virulent *Pst* DC3000 in the *pldβ1* mutant (Zhao et al., 2013) was not apparent in our hands. There are differences in the experimental setup such as light intensity and density of the bacterial inoculum which could influence the outcome. It should however be noted that the *pldβ1-1* line used herein is identical to the T-DNA line used in the study by Zhao et al. (2013). Further studies are needed to clarify this point and further investigate among other factors the effect of different bacterial titers on the defense reaction and the phenotype of the mutant.

To conclude, we herein report that at least eight different PLD isoforms in *Arabidopsis* contribute to signaling in HR triggered by AvrRpm1 recognition. In contrast, loss of just one of the major PLD isoforms is sufficient to significantly affect MTI dependent defense responses.

ACKNOWLEDGMENTS

The financial support of The Carl Tryggers foundation and The Olle Engkvist Byggmästare foundation is gratefully acknowledged.

SUPPLEMENTARY MATERIAL

The Supplementary Material for this article can be found online at: <http://www.frontiersin.org/journal/10.3389/fpls.2014.00639/abstract>

Figure S1 | Effect of tert- and n-butanol on the growth rate of

***Pseudomonas syringae* in vitro.** An overnight culture of *Pst* was diluted and transferred into liquid cultures with the respective concentration of butanol, grown for 6 h on shaker, serial diluted and plated on KB plates. The number of colonies was determined after 2 days incubation in room temperature. Shown are averages and SD of three replicates. An asterisk indicates statistically significant difference from water, $p < 0.05$, one way ANOVA. The experiment was performed twice with the same conclusion.

REFERENCES

- Alvarez, M. E., Nota, F., and Cambiagno, D. A. (2010). Epigenetic control of plant immunity. *Mol. Plant Pathol.* 11, 563–576. doi: 10.1111/j.1364-3703.2010.00621.X
- Andersson, M. X., Kourtchenko, O., Dangl, J. L., Mackey, D., and Ellerstrom, M. (2006). Phospholipase-dependent signalling during the AvrRpm1- and AvrRpt2-induced disease resistance responses in *Arabidopsis thaliana*. *Plant J.* 47, 947–959. doi: 10.1111/j.1365-313X.2006.02844.x
- Bargmann, B. O., and Munnik, T. (2006). The role of phospholipase D in plant stress responses. *Curr. Opin. Plant Biol.* 9, 515–522. doi: 10.1016/j.pbi.2006.07.011
- Boller, T., and Felix, G. (2009). A renaissance of elicitors: perception of microbe-associated molecular patterns and danger signals by pattern-recognition receptors. *Annu. Rev. Plant Biol.* 60, 379–406. doi: 10.1146/annurev.applant.57.032905.105346
- Collins, N. C., Thordal-Christensen, H., Lipka, V., Bau, S., Kombrink, E., Qiu, J. L., et al. (2003). SNARE-protein-mediated disease resistance at the plant cell wall. *Nature* 425, 973–977. doi: 10.1038/nature02076
- Dodds, P. N., and Rathjen, J. P. (2010). Plant immunity: towards an integrated view of plant-pathogen interactions. *Nat. Rev. Genet.* 11, 539–548. doi: 10.1038/Nrg2812
- Ella, K. M., Meier, K. E., Kumar, A., Zhang, Y., and Meier, G. P. (1997). Utilization of alcohols by plant and mammalian phospholipase D. *Biochem. Mol. Biol. Int.* 41, 715–724.
- Fan, L., Zheng, S. Q., and Wang, X. M. (1997). Antisense suppression of phospholipase D alpha retards abscisic acid- and ethylene-promoted senescence of postharvest *Arabidopsis* leaves. *Plant Cell* 9, 2183–2196. doi: 10.1105/tpc.9.12.2183
- Grant, M., Brown, I., Adams, S., Knight, M., Ainslie, A., and Mansfield, J. (2000). The RPM1 plant disease resistance gene facilitates a rapid and sustained increase in cytosolic calcium that is necessary for the oxidative burst and hypersensitive cell death. *Plant J.* 23, 441–450. doi: 10.1046/j.1365-313x.2000.00804.x
- Grant, M. R., Godiard, L., Straube, E., Ashfield, T., Lewald, J., Sattler, A., et al. (1995). Structure of the *Arabidopsis* Rpm1 gene enabling dual-specificity disease resistance. *Science* 269, 843–846. doi: 10.1126/science.7638602
- Hanahan, D. J., and Chaikoff, I. L. (1947). A new phospholipide-splitting enzyme specific for the ester linkage between the nitrogenous base and the phosphoric acid grouping. *J. Biol. Chem.* 169, 699–705.
- Hibberd, A. M. (1987). Different phenotypes associated with incompatible races and resistance genes in bacterial spot disease of pepper. *Plant Dis.* 71, 1075–1078. doi: 10.1094/pd-71-1075
- Hong, Y. Y., Pan, X. Q., Welti, R., and Wang, X. M. (2008). Phospholipase D alpha 3 is involved in the hyperosmotic response in *Arabidopsis*. *Plant Cell* 20, 803–816. doi: 10.1105/tpc.107.056390
- Johansson, O. N., Fantozzi, E., Fahlberg, P., Nilsson, A. K., Buhot, N., Tör, M., et al. (2014). Role of the penetration resistance genes PEN1, PEN2 and PEN3 in the hypersensitive response and race specific resistance in *Arabidopsis thaliana*. *Plant J.* 79, 466–476. doi: 10.1111/tpj.12571
- Jones, J. D., and Dangl, J. L. (2006). The plant immune system. *Nature* 444, 323–329. doi: 10.1038/nature05286
- Kirik, A., and Mudgett, M. B. (2009). SOBER1 phospholipase activity suppresses phosphatidic acid accumulation and plant immunity in response to bacterial effector AvrBsT. *Proc. Natl. Acad. Sci. U.S.A.* 106, 20532–20537. doi: 10.1073/pnas.0903859106
- Kobae, Y., Sekino, T., Yoshioka, H., Nakagawa, T., Martinoia, E., and Maeshima, M. (2006). Loss of AtPDR8, a plasma membrane ABC transporter of *Arabidopsis thaliana*, causes hypersensitive cell death upon pathogen infection. *Plant Cell Physiol.* 47, 309–318. doi: 10.1093/pcp/pcj001
- Koch, E., and Slusarenko, A. (1990). *Arabidopsis* is susceptible to infection by a downy mildew fungus. *Plant Cell* 2, 437–445. doi: 10.1105/tpc.2.5.437
- Laxalt, A. M., and Munnik, T. (2002). Phospholipid signalling in plant defence. *Curr. Opin. Plant Biol.* 5, 332–338. doi: 10.1016/S1369-5266(02)00268-6
- Laxalt, A. M., Ter Riet, B., Verdonk, J. C., Parigi, L., Tameling, W. I. L., Vossen, J., et al. (2001). Characterization of five tomato phospholipase D cDNAs: rapid and specific expression of LePLD beta 1 on elicitation with xylanase. *Plant J.* 26, 237–247. doi: 10.1046/j.1365-313X.2001.01023.x
- Li, M., Hong, Y., and Wang, X. (2009). Phospholipase D- and phosphatidic acid-mediated signalling in plants. *Biochim. Biophys. Acta* 1791, 927–935. doi: 10.1016/j.bbapplied.2009.02.017
- Li, W., Wang, R., Li, M., Li, L., Wang, C., Welti, R., et al. (2008). Differential degradation of extraplastidic and plastidic lipids during freezing and post-freezing recovery in *Arabidopsis thaliana*. *J. Biol. Chem.* 283, 461–468. doi: 10.1074/jbc.M706692200
- Li, W. Q., Li, M. Y., Zhang, W. H., Welti, R., and Wang, X. M. (2004). The plasma membrane-bound phospholipase D delta enhances freezing tolerance in *Arabidopsis thaliana*. *Nat. Biotechnol.* 22, 427–433. doi: 10.1038/nbt0404
- Mackey, D., Holt, B. E., Wiig, A., and Dangl, J. L. (2002). RIN4 interacts with *Pseudomonas syringae* type III effector molecules and is required for RPM1-mediated resistance in *Arabidopsis*. *Cell* 108, 743–754. doi: 10.1016/s0092-8674(02)00661-x
- Molinier, J., Ries, G., Zipfel, C., and Hohn, B. (2006). Transgeneration memory of stress in plants. *Nature* 442, 1046–1049. doi: 10.1038/Nature05022
- Mur, L. A. J., Kenton, P., Lloyd, A. J., Ougham, H., and Prats, E. (2008). The hypersensitive response; the centenary is upon us but how much do we know? *J. Exp. Bot.* 59, 501–520. doi: 10.1093/jxb/erm239
- Nilsson, A. K., Johansson, O. N., Fahlberg, P., Steinhart, F., Gustavsson, M. B., Ellerstrom, M., et al. (2014). Formation of oxidized phosphatidylinositol

- and 12-oxo-phytodienoic acid containing acylated phosphatidylglycerol during the hypersensitive response in *Arabidopsis*. *Phytochemistry* 101, 65–75. doi: 10.1016/j.phytochem.2014.01.020
- Park, J., Gu, Y., Lee, Y., and Yang, Z. B. (2004). Phosphatidic acid induces leaf cell death in *Arabidopsis* by activating the Rho-related small G protein GTPase-mediated pathway of reactive oxygen species generation. *Plant Physiol.* 134, 129–136. doi: 10.1104/pp.103.031393
- Pinosa, F., Buhot, N., Kwaaitaal, M., Fahlberg, P., Thordal-Christensen, H., Ellerstrom, M., et al. (2013). *Arabidopsis* phospholipase D delta 1s involved in basal defense and nonhost resistance to powdery mildew fungi. *Plant Physiol.* 163, 896–906. doi: 10.1104/pp.113.223503
- Rainteau, D., Humbert, L., Delage, E., Vergnolle, C., Cantrel, C., Maubert, M. A., et al. (2012). Acyl chains of phospholipase D transphosphatidylation products in *Arabidopsis* cells: a study using multiple reaction monitoring mass spectrometry. *PLoS ONE* 7:e41985. doi: 10.1371/journal.pone.0041985
- Sang, Y. M., Cui, D. C., and Wang, X. M. (2001a). Phospholipase D and phosphatidic acid-mediated generation of superoxide in arabidopsis. *Plant Physiol.* 126, 1449–1458. doi: 10.1104/pp.126.4.1449
- Sang, Y. M., Zheng, S. Q., Li, W. Q., Huang, B. R., and Wang, X. M. (2001b). Regulation of plant water loss by manipulating the expression of phospholipase D alpha. *Plant J.* 28, 135–144. doi: 10.1046/j.1365-313X.2001.01138.x
- Sato, M., Tsuda, K., Wang, L., Coller, J., Watanabe, Y., Glazebrook, J., et al. (2010). Network modeling reveals prevalent negative regulatory relationships between signaling sectors in *Arabidopsis* immune signaling. *PLoS Pathog.* 6:e1001011. doi: 10.1371/journal.ppat.1001011
- Spoel, S. H., and Dong, X. N. (2012). How do plants achieve immunity? Defence without specialized immune cells. *Nat. Rev. Immunol.* 12, 89–100. doi: 10.1038/Nri3141
- Tsuda, K., and Katagiri, F. (2010). Comparing signaling mechanisms engaged in pattern-triggered and effector-triggered immunity. *Curr. Opin. Plant Biol.* 13, 459–465. doi: 10.1016/j.pbi.2010.04.006
- van der Luit, A. H., Piatti, T., Van Doorn, A., Musgrave, A., Felix, G., Boller, T., et al. (2000). Elicitation of suspension-cultured tomato cells triggers the formation of phosphatidic acid and diacylglycerol pyrophosphate. *Plant Physiol.* 123, 1507–1516. doi: 10.1104/pp.123.4.1507
- Wang, X. (2004). Lipid signaling. *Curr. Opin. Plant Biol.* 7, 329–336. doi: 10.1016/j.pbi.2004.03.012
- Zabela, M. D., Fernandez-Delmond, I., Niittyala, T., Sanchez, P., and Grant, M. (2002). Differential expression of genes encoding *Arabidopsis* phospholipases after challenge with virulent or avirulent *Pseudomonas* isolates. *Mol. Plant Microbe Interact.* 15, 808–816. doi: 10.1094/MPMI.2002.15.8.808
- Zhao, J., Devaiah, S. P., Wang, C., Li, M., Welti, R., and Wang, X. (2013). *Arabidopsis* phospholipase D beta1 modulates defense responses to bacterial and fungal pathogens. *New Phytol.* 199, 228–240. doi: 10.1111/nph.12256

Conflict of Interest Statement: The authors declare that the research was conducted in the absence of any commercial or financial relationships that could be construed as a potential conflict of interest.

Received: 30 June 2014; accepted: 28 October 2014; published online: 13 November 2014.

Citation: Johansson ON, Fahlberg P, Karimi E, Nilsson AK, Ellerström M and Andersson MX (2014) Redundancy among phospholipase D isoforms in resistance triggered by recognition of the *Pseudomonas syringae* effector AvrRpm1 in *Arabidopsis thaliana*. *Front. Plant Sci.* 5:639. doi: 10.3389/fpls.2014.00639

This article was submitted to Plant Physiology, a section of the journal Frontiers in Plant Science.

Copyright © 2014 Johansson, Fahlberg, Karimi, Nilsson, Ellerström and Andersson. This is an open-access article distributed under the terms of the Creative Commons Attribution License (CC BY). The use, distribution or reproduction in other forums is permitted, provided the original author(s) or licensor are credited and that the original publication in this journal is cited, in accordance with accepted academic practice. No use, distribution or reproduction is permitted which does not comply with these terms.



Characterization of the inositol monophosphatase gene family in Arabidopsis

Aida Nourbakhsh¹, Eva Collakova² and Glenda E. Gillaspy^{3*}

¹ Department of Human and Molecular Genetics, Virginia Commonwealth University, Richmond, VA, USA

² Department of Plant Pathology, Physiology, and Weed Science, Virginia Polytechnic Institute and State University, Blacksburg, VA, USA

³ Department of Biochemistry, Virginia Polytechnic Institute and State University, Blacksburg, VA, USA

Edited by:

Eric Ruelland, Centre National de la Recherche Scientifique, France

Reviewed by:

Alain Zachowski, Université Pierre et Marie Curie, France

William Laing, Plant and Food Research, New Zealand

*Correspondence:

Glenda E. Gillaspy, Department of Biochemistry, Virginia Polytechnic Institute and State University, 542 Latham Hall, Blacksburg, VA 24061, USA
e-mail: gillaspy@vt.edu

Synthesis of *myo*-inositol is crucial in multicellular eukaryotes for production of phosphatidylinositol and inositol phosphate signaling molecules. The *myo*-inositol monophosphatase (IMP) enzyme is required for the synthesis of *myo*-inositol, breakdown of inositol (1,4,5)-trisphosphate, a second messenger involved in Ca^{2+} signaling, and synthesis of L-galactose, a precursor of ascorbic acid. Two *myo*-inositol monophosphatase-like (IMPL) genes in Arabidopsis encode chloroplast proteins with homology to the prokaryotic IMPs and one of these, IMPL2, can complement a bacterial histidinol 1-phosphate phosphatase mutant defective in histidine synthesis, indicating an important role for IMPL2 in amino acid synthesis. To delineate how this small gene family functions in inositol synthesis and metabolism, we sought to compare recombinant enzyme activities, expression patterns, and impact of genetic loss-of-function mutations for each. Our data show that purified IMPL2 protein is an active histidinol-phosphate phosphatase enzyme in contrast to the IMPL1 enzyme, which has the ability to hydrolyze D-galactose 1-phosphate, and D-*myo*-inositol 1-phosphate, a breakdown product of D-inositol (1,4,5) trisphosphate. Expression studies indicated that all three genes are expressed in multiple tissues, however, IMPL1 expression is restricted to above-ground tissues only. Identification and characterization of *impl1* and *impl2* mutants revealed no viable mutants for IMPL1, while two different *impl2* mutants were identified and shown to be severely compromised in growth, which can be rescued by histidine. Analyses of metabolite levels in *impl2* and complemented mutants reveals *impl2* mutant growth is impacted by alterations in the histidine biosynthesis pathway, but does not impact *myo*-inositol synthesis. Together, these data indicate that IMPL2 functions in the histidine biosynthetic pathway, while IMP and IMPL1 catalyze the hydrolysis of inositol- and galactose-phosphates in the plant cell.

Keywords: histidine, inositol, histidinol phosphatase, inositol monophosphatase, IMPL

INTRODUCTION

The *myo*-inositol (inositol) synthesis pathway is crucial in many multicellular eukaryotes for the production of lipid phosphatidylinositol phosphate signaling molecules (for review see Gillaspy, 2011). Inositol is also used in the synthesis of other important molecules in plants, including the glycerophosphoinositide membrane anchors, cell wall pectic non-cellulosic polysaccharides, and ascorbic acid (Loewus, 1969, 2006; Kroh et al., 1970; Chen and Loewus, 1977). Inositol monophosphatase (IMP) is a major enzyme required both for the *de novo* synthesis of inositol, and the breakdown of D-inositol (1,4,5) trisphosphate ($\text{Ins}(1,4,5)\text{P}_3$) (Loewus and Loewus, 1983), a second messenger involved in many plant physiological responses (for review see Boss and Im, 2012).

We previously characterized the single, canonical IMP gene from tomato (Gillaspy et al., 1995) and Arabidopsis (Torabinejad et al., 2009), encoded by the Vitamin C 4 (VTC4; At3g02870) gene (Conklin et al., 2006). The active site of IMP has been noted

to accommodate a variety of substrates, and seminal work has shown that the plant IMP can hydrolyze L-galactose 1-P (L-Gal 1-P), a precursor for ascorbic acid synthesis (Laing et al., 2004). Arabidopsis *imp* mutants have decreases in both ascorbic acid and inositol, underscoring the bifunctionality of this enzyme (Torabinejad et al., 2009). Surprisingly, *imp* mutants have only a 30% reduction in inositol content, which indicates the likely presence of other plant IMP enzymes (Torabinejad et al., 2009).

Indeed, all plants queried contain multiple IMP-like (IMPL) genes, which are closer in amino acid sequence identity to the prokaryote IMPs (Torabinejad and Gillaspy, 2006; Torabinejad et al., 2009). A preliminary characterization of the two Arabidopsis IMPL enzymes indicated these enzymes differ from IMP in their substrate specificity (Torabinejad et al., 2009). However, both enzymes were not stable and no kinetic characterization could be performed, precluding a definitive comparison of these enzymes to IMP (Torabinejad et al., 2009). Both IMPL1 and IMPL2 proteins have been localized to the chloroplast

(Sun et al., 2009; Petersen et al., 2010), and it has been shown that heterologous expression of IMPL2 (At4g39120) but not IMPL1 (At1g31190), is sufficient to rescue the histidine auxotrophy of a *Streptomyces coelicolor* hisN mutant, which is defective in L-histidinol 1-phosphate (His 1-P) phosphatase activity (Petersen et al., 2010). This work made an important contribution to not only identifying the last missing step in histidine biosynthesis in plants, but as well suggested that either the catalytic site of IMPL2 accommodated a different substrate (i.e., His 1-P) or that IMPL2 functioned in multiple pathways (i.e., both histidine and inositol synthesis) (Petersen et al., 2010; Ingle, 2011).

Since both *Arabidopsis* IMPL1 and IMPL2 genes are possible candidates for a redundant IMP function, we sought to purify and characterize these enzymes. Further, given the bifunctionality of the IMP enzyme, we wanted to examine the expression patterns and impact of a loss-of-function in these genes on both the inositol and histidine synthetic pathways. Since histidine is an essential amino acid utilized for protein synthesis, a complete blockage of histidine production causes lethality in plants and leads to elevated expression of genes in other amino acid biosynthetic pathways (Guyer et al., 1995). Probably because of this, very little is known about the role of histidine in plant development and physiology. This is also influenced by the difficulty in experimentally separating the metabolic and regulatory functions of this essential amino acid and the embryo lethality that results from loss-of-function mutants of genes in the pathway (Mo et al., 2006). Indeed, *impl2* mutants have been identified previously, however embryo lethality of homozygotes limited analysis of the impact of IMPL2 mutation on plant growth and development (Petersen et al., 2010).

In this work we demonstrate kinetic analysis of recombinant AtIMPL1 and AtIMPL2 proteins and show that AtIMPL2 is uniquely able to hydrolyze His 1-P *in vitro*, while AtIMPL1 hydrolyzes D-inositol 1-phosphate (D-Ins 1-P) and D-galactose 1-phosphate (D-Gal 1-P). We characterized and complemented an *impl2* mutant, and were able to grow this mutant to maturity. Thus, we were able to assess the impact of IMPL2 on histidine synthesis and show that it does not impact inositol synthesis. Interestingly, the *impl2* mutant has the described symptoms of previously reported histidine synthesis mutants such as the pale-green leaf phenotype of *agp10* (Noutoshi et al., 2005) and the root meristem defect of *hpa1* mutants (Mo et al., 2006). Thus, our biochemical and genetic data solidify the role of the IMPL2 gene in histidine synthesis in plants, and point to the IMPL1 gene as a likely candidate for regulating inositol recycling from inositol phosphate second messengers.

RESULTS

EXPRESSION OF RECOMBINANT IMPL1 AND IMPL2 PROTEINS

To examine the roles of IMPL1 and IMPL2 enzymes, we expressed and purified recombinant IMPL1 and IMPL2 proteins. Both genes encode putative chloroplast transit peptides, as predicted by alignment of IMPL amino acid sequences with those of non-chloroplastic IMPs. The open reading frames minus the putative chloroplastic transit peptide of the IMPL1 gene (At1g31190) and the IMPL2 gene (At4g39120) were cloned as glutathione s-transferase (GST) fusions and purified with

glutathione-sepharose to greater than 95% purity as observed by SDS-PAGE (data not shown). The molecular mass of the fusion proteins is estimated to be 65 kD for IMPL1 and 60 kD for IMPL2, which is slightly larger than expected given their predicted molecular masses of 55.5 and 55.4 kD, respectively.

Because it has been shown that Mg²⁺ is necessary for maximal activity of other IMP enzymes (Gumber et al., 1984; Laing et al., 2004; Islas-Flores and Villanueva, 2007; Torabinejad et al., 2009) we delineated the optimal Mg²⁺ and pH conditions for each enzyme (Supplemental Figure 1). IMPL2 had near maximal activation at 2 mM Mg²⁺ (Supplemental Figure 1) and the concentration of Mg²⁺ in the chloroplast has been measured to be approximately 0.5 mM and to increase to approximately 2 mM in the stroma upon illumination (Ishijima et al., 2003). Therefore, for IMPL2, we used 2 mM MgCl₂ as starting conditions to mimic the chloroplast environmental conditions during daylight. IMPL1 had slightly higher enzymatic activity at 3 mM Mg²⁺, therefore 3 mM MgCl₂ was used in activity assays performed with IMPL1. Since IMPL1 is most active at pH 9, and IMPL2 at pH 7.5, all kinetic assays were carried out at these pH values, respectively.

Arabidopsis IMP is a bifunctional enzyme hydrolyzing L-Gal 1-P and D-inositol 3-phosphate (D-Ins 3-P) (Conklin et al., 2000;

Table 1 | Substrates tested with IMPL1.

| Substrate | IMPL1 | IMP |
|-------------------------------------|--------|---------|
| | Rate % | Rate % |
| D-myoinositol 1-phosphate | 100 | 100 |
| D-Galactose 1-phosphate | 105.4 | 16.6 |
| β-Glycerophosphate (glycerol 2-P) | 39.7 | 52 |
| D-myoinositol 3-phosphate | 18.8 | 100 |
| D-myoinositol 2-phosphate | 17.8 | 0.94 |
| L-Galactose 1-phosphate | 7.6 | 166–240 |
| Adenosine 2'-phosphate | 3.6 | 9.6 |
| α-D-Glucose 1-phosphate | 2.8 | 19.3 |
| D-α-Glycerophosphate (glycerol 3-P) | 0.24 | 4.9 |
| α-D-Glucose 6-phosphate | 0 | 0.25 |
| D-Mannitol 1-phosphate | 0 | 10.5 |
| D-Sorbitol 1-phosphate | 0 | 1.7 |
| D-Fructose 1-phosphate | 0 | 2.3 |
| Fructose 1,6-bisphosphate | 0 | 0.30 |
| NADP | 0 | nd |
| NADPH | 0 | nd |
| PAP | 0 | nd |
| L-Histidinol 1-phosphate | 0 | nd |
| Inositol (1,4)P ₂ | 0 | nd |
| Inositol (4,5)P ₂ | 0 | nd |
| Inositol (1,4,5)P ₃ | 0 | nd |

IMPL1 activity was determined at pH 9 in the presence of 3 mM MgCl₂ using the phosphate release assay, 452 ng of IMPL1 enzyme, and 0.4 mM of the indicated substrate (substrate was present in excess amount as compared to the estimated Km value for D-myoinositol 1-phosphate). Reaction rates were compared with the rate of activity with 0.4 mM D-myoinositol 1-phosphate (units). The values for IMP enzyme were published in Torabinejad et al. (2009). nd, not determined.

Laing et al., 2004; Torabinejad et al., 2009). It has also been reported that heterologous expression of IMPL2 was sufficient to rescue the histidine auxotrophy of a *Streptomyces coelicolor* hisN mutant (Petersen et al., 2010). Therefore, to compare the substrate preferences of IMPL enzymes, we analyzed their abilities to utilize several related substrates (Table 1). For the IMPL2 enzyme, testing of different substrates validated that IMPL2 has high specificity for His 1-P and is not able to hydrolyze D-Ins 1-P, D-Ins 3-P, L-Gal 1-P, or fructose 1,6-bisphosphate (Fru 1,6-bisP). We conclude that the IMPL2 gene encodes an active histidinol 1-P phosphatase, and is unlikely to function in inositol phosphate hydrolysis. In reaction mixtures of pH 7.5, 2 mM MgCl₂ and 112 ng of enzyme, the K_m for histidinol 1-P is $180 \pm 5 \mu\text{M}$, the k_{cat} is $1.3 \pm 0.2 \text{ s}^{-1}$, and the k_{cat}/K_m is $7.9 \pm 0.2 \times 10^3 \text{ M}^{-1}\text{s}^{-1}$ (Figure 1 and Table 2).

For IMPL1, various substrates were tested (Table 1). D-Ins 1-P can be derived from Ins(1,4,5)P₃ second messenger breakdown, in contrast to D-Ins 3-P, which is an intermediate in *de novo* inositol synthesis. Interestingly, D-Gal 1-P is hydrolyzed by IMPL1 (Table 1), which is similar to the action of the human IMP which hydrolyzes D-Gal 1-P as effectively as D-Ins 1-P (Parthasarathy et al., 1997). β -Glycerophosphate can also be

hydrolyzed (39.7% of the D-Ins 1-P rate). Under these reaction conditions, D-Ins 3-P, D-Ins 2-P, L-Gal 1-P, adenosine 2'-monophosphate and D-Glc 1-P are hydrolyzed at a lower rate. In addition, glycerol 3-phosphate, D-glucose 6-P, D-mannitol 1-P, D-sorbitol 1-P, D-fructose 1-P and Fru 1,6-bisP, NADP, NADPH and PAP are not hydrolyzed at all by IMPL1. IMPL1 is also not able to hydrolyze the poly-phosphorylated inositol compounds (Table 1). Together, these data suggest that IMPL1 has distinct substrate specificity as compared to either IMPL2 or IMP, and might be involved in hydrolysis of D-Ins 1-P and/or D-Gal 1-P.

Catalytic properties of enzymes are important factors in determining substrate specificity of an enzyme. In reaction conditions of pH 9, 3 mM MgCl₂, and 452 ng of IMPL1 recombinant enzyme, the K_m for D-Ins 1-P was $180 \pm 3 \mu\text{M}$ (Figure 1) and that for D-Gal 1-P was approximated to be $450 \pm 60 \mu\text{M}$. Substrate inhibition occurred at concentrations greater than 1 mM of D-Ins 1-P. The k_{cat} -value for IMPL1 with D-Ins 1-P is $0.6 \pm 0.1 \text{ s}^{-1}$ and $2.4 \pm 1.3 \text{ s}^{-1}$ with D-Gal 1-P. Further, the ratio of k_{cat} to K_m provides a perspective on the catalytic efficiency of an enzyme with a specific substrate, and the calculated k_{cat}/K_m with D-Ins 1-P is $3.3 \pm 0.1 \times 10^3 \text{ M}^{-1}\text{s}^{-1}$, and $5.3 \pm 0.5 \times 10^3 \text{ M}^{-1}\text{s}^{-1}$ with D-Gal 1-P (Table 2).

Lithium and calcium (Ca²⁺) ions have an inhibitory effect on other IMPs (Leech et al., 1993; Parthasarathy et al., 1997; Torabinejad et al., 2009). IMPL1 and IMPL2 are both inhibited by Li⁺ or Ca²⁺ addition (Figure 2), albeit this inhibition occurs at a high level of substrate such that these ions may be inhibiting the enzymes by complexing with substrate and displacing Mg²⁺. Interestingly, these data suggest that Li⁺ contamination of soil could impact IMPL2 function and histidine biosynthesis in plants. Indeed, several incidents of lithium toxicity in field-grown citrus with lithium concentrations of 0.06–0.1 ppm in the irrigation water has been reported in the state of California (Bradford, 1963).

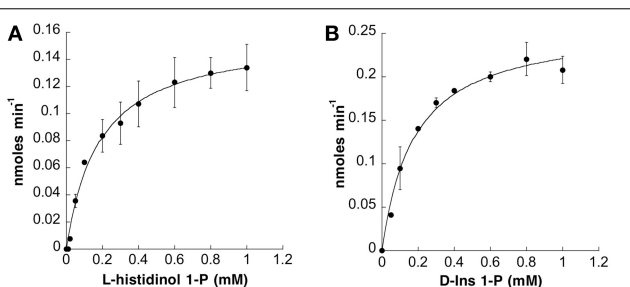


FIGURE 1 | Kinetic Analysis of IMPL1 with D-Ins 1-P and IMPL2 with Histidinol 1-P. Phosphatase activity vs. concentration of histidinol 1-P for IMPL2 in (A) and D-Ins 1-P for IMPL1 in (B) using the reaction conditions described in “Experimental Procedures.” Data (average of 3 independent replicates) were imported into Kaleidagraph (Synergy Software) and fit to a non-linear curve based on the Michaelis-Menten equation to calculate K_m and V_{max} . The error bars represent standard deviation of the independent replicates.

Table 2 | Kinetic parameters of IMPL1 and IMPL2 recombinant proteins.

| Enzyme (Substrate) | K_m (μM) | k_{cat} (s^{-1}) | k_{cat}/K_m ($\text{s}^{-1}\text{M}^{-1}$) |
|-----------------------------------|-------------------------|--------------------------------------|-------------------------------------------------------|
| IMPL2 (Histidinol 1-phosphate) | 180 ± 5 | 1.3 ± 0.2 | $7.9 \pm 0.2 \times 10^3$ |
| IMPL1 (D-myoinositol 1-phosphate) | 180 ± 3 | 0.6 ± 0.1 | $3.3 \pm 0.1 \times 10^3$ |
| IMPL1 (D-Galactose 1-phosphate) | 450 ± 60 | 2.4 ± 1.3 | $5.3 \pm 0.5 \times 10^3$ |

The initial rate for IMPL1 and IMPL2 activity was determined at 22°C (reaction conditions for IMPL1 and IMPL2 as described in Methods). The kinetic parameters were obtained from the initial velocity as described in Methods. The concentration of substrates was varied from 0 to 1 mM.

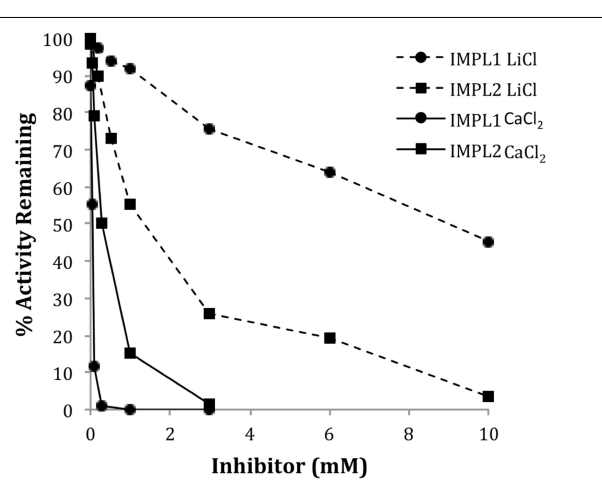


FIGURE 2 | Inhibition of IMPL1 and IMPL2 Activity by either LiCl or CaCl₂. IMPL1 activity was assayed with D-Ins 1-P (circles) and IMPL2 was assayed with histidinol 1-P (squares) in the presence of the indicated concentrations of CaCl₂ (solid lines) or LiCl (dashed lines).

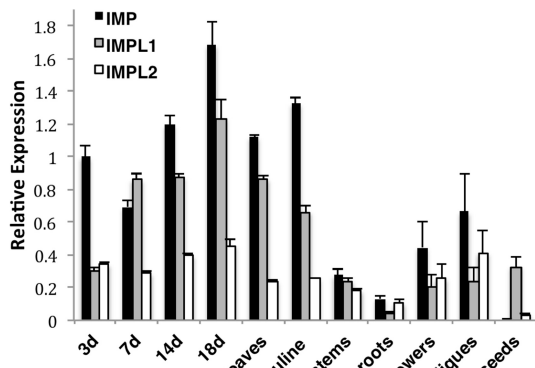


FIGURE 3 | Relative Expression of IMP and IMPL Genes as Determined by Real-time PCR. IMP, IMPL1, IMPL2 gene expression was measured in 3,714-d-old wild type seedlings grown on 0.5× MS plus 1% sucrose-soaked filter paper under 16-h-light conditions, soil-grown 18-d-old whole plants (18d), young rosette leaves (leaves), roots, caudine leaves (cauline), stems, flowers, and immature siliques from 35-d-old plants and seeds imbibed in water for 3 d at 4°C. Real-time PCR amplification curves of genes of interest were compared with PEX4 (peroxisomal ubiquitin4) amplification to generate relative expression levels. PEX4 was used as an endogenous control because it is expressed constitutively at all stages of development. Means of triplicate reactions of three biological replicates ± SE are presented.

IMP AND IMPL GENE EXPRESSION IS TEMPORALLY AND SPATIALLY REGULATED

To determine whether transcription of IMP and IMPL genes is differentially regulated, we performed quantitative PCR to compare relative expression of IMP, IMPL1, and IMPL2 in various tissues (Figure 3). We found that IMP is expressed in all tested tissues except seeds and levels are high in seedlings, leaves, and caudine leaves during early development. IMPL1 has a similar expression pattern as IMP, however it is expressed at slightly lower levels, and it is the only IMP gene abundantly expressed in seeds. IMPL2 expression is overall lower as compared to IMP and IMPL1, and IMPL2 appears to be expressed constitutively in all tissues except seeds. The results are similar to those reported from microarray data provided by Genevestigator database (Zimmermann et al., 2004) (Supplemental Figure 2).

To investigate the spatial pattern of regulation of the IMP and IMPL genes, we sought to generate transgenic plants expressing IMP, IMPL1, and IMPL2 promoters fused to the *uidA* gene, which encodes β-glucuronidase (GUS). Several independent transgenic lines for ProIMP-*uidA* and ProIMPL1-*uidA* constructs were analyzed and consistent patterns were detected in ProIMP-*uidA* 3-d-old seedlings, β-glucuronidase (GUS) activity was noted in the entire cotyledon, within the upper hypocotyl, leaf primordia, lateral root primordia, primary root tips, and guard cells (Figures 4A–D). ProIMPL1-*uidA* shows a similar pattern in 3-d-old seedlings, however IMPL1 is not expressed in root tissue (Figure 4E and not shown). In 7-d-old seedlings, IMP expression is prevalent in the vascular tissue in cotyledons, roots, and leaves, and trichomes (Figures 4F–H). At 7-d, IMPL1 expression is weakly maintained in the cotyledons but expression in leaf primordia is stronger (Figure 4I). In 14-d-old plants, IMP

expression is similar to 7-d seedlings with vascular expression in most leaves and within roots (Figures 4J,K). At 14-d, IMPL1 expression is highest in young sink leaves, and is restricted to vascular tissue within older, source leaves (Figure 4L). In 19-d-old plants, IMP expression is observed in all cells of young, sink leaves and becomes restricted to vascular tissue within older, source leaves (Figure 4M). The expression of IMP in 19-d-old roots remains the same as in the earlier stages of development (Figure 4K). At 19-d, the IMPL1 expression pattern is similar to that of IMP, however expression is restricted to the shoot (Figure 4N and not shown). Leaves from soil-grown plants indicate that IMP expression is restricted to the vascular tissue and IMPL1 is expressed throughout the leaf (Figures 4O,P). In flowers, IMP is expressed in the pistil while IMPL1 expression is present in vascular tissue in the sepals (Figures 4Q,R). Both genes are expressed in the mature embryo, however, once again, IMPL1 is restricted to the shoot portion of the embryo (Figures 4S,T). Within siliques, IMP is expressed in the tips and abscission zones of immature siliques (Figure 4U), while IMPL1 is restricted to the stem of the immature silique (Figure 4V). Together, these data indicate that the IMP and IMPL1 genes are developmentally and spatially regulated in a similar fashion. One exception to this is that IMPL1 expression is restricted to shoot tissues, while IMP is expressed in both shoots and roots.

We have analyzed multiple transgenic plant lines containing four different IMPL2 promoter:*uidA* constructs, and have been unsuccessful in obtaining lines that show expression in any tissue. For this work we examined 1628 bp, 1085 bp or 461 bp upstream of the start site of transcription and the entire genomic sequence. We therefore conclude that it is likely that sequences outside of the promoter are necessary for dictating IMPL2 expression.

THE IMP PROTEIN IS LOCATED IN THE CYTOSOL AND IMPL PROTEINS ARE LOCATED IN THE CHLOROPLAST

Both IMPL1 and IMPL2 have been localized to the chloroplast in transient expression assays and in proteomics analysis of chloroplasts (Sun et al., 2009; Petersen et al., 2010). To investigate the subcellular location of IMP and IMPL proteins in multiple tissues, we constructed transgenic plants expressing IMP:GFP, IMPL1:GFP or IMPL2:GFP under the control of the 35S cauliflower mosaic virus (CaMV) promoter (Figure 5). We analyzed homozygous progeny from two independent lines for each construct with confocal microscopy and found similar patterns. Western blot analysis confirmed that intact fusion proteins accumulate (Supplemental Figure 3). For IMP:GFP, GFP fluorescence was predominantly associated with the cytoplasm in 3-d-old light-grown seedling shoots and roots (roots are shown in Figure 5A). Plasmolysis with 800 mM NaCl confirmed the cytoplasmic location (Figure 5B).

As expected, we found that IMPL1:GFP and IMPL2:GFP localized to small organelles in root and shoot tissues (Figures 5C,F). In addition, co-localization of IMPL1:GFP and IMPL2:RFP fusion proteins from plants expressing both indicate that both are present in the same compartment (Figures 5C–E). To confirm this, we transformed IMPL2:GFP and IMPL1:GFP transgenic plants with a plastid-mcherry marker containing the signal peptide of the pea Rubisco small subunit (Nelson et al., 2007).

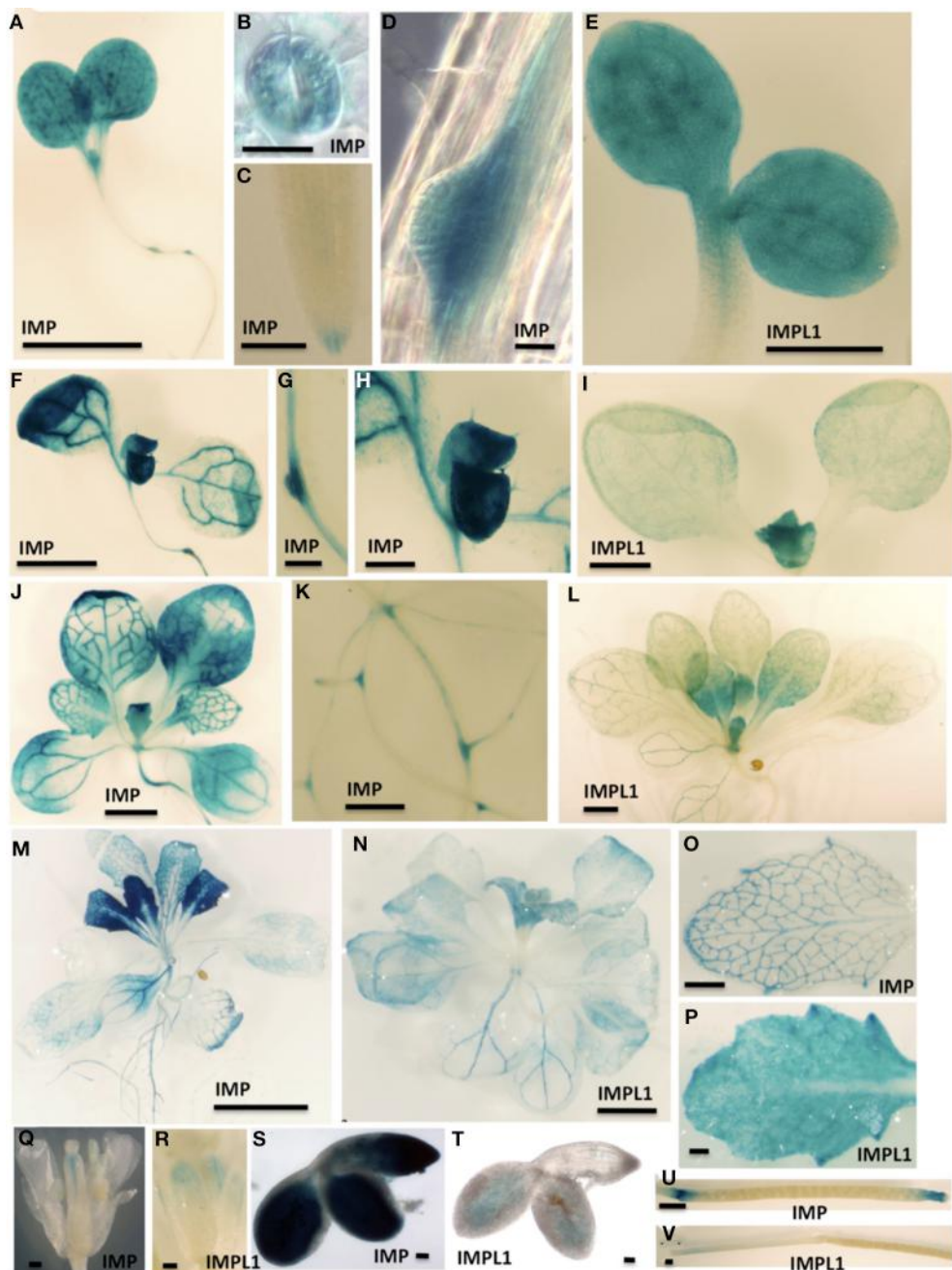


FIGURE 4 | Spatial Expression Patterns of IMP and IMPL1 Genes.

The promoters from IMP and IMPL1 were used to drive GUS expression in transgenic plants. (A–E) Three-day-old seedlings grown on 0.5× MS plus 1% sucrose. Bars = 1 mm in (A), 20 µm in (B,D), 200 µm in (C), and 500 µm in (E). (F–I) Seven-day-old seedlings grown on 0.5× MS plus 1% sucrose. Bars = 1.3 mm in (F), 200 µm in (G).

377 µm in (H), and 1 mm in (I). (J–L) Fourteen-day-old seedling grown on 0.5× MS plus 1% sucrose. Bars = 2 mm in (J,L), and 500 µm in (K). (M,N) Nineteen-day-old seedling grown on 0.5× MS plus 1% sucrose. Bars = 5 mm in (M) and 2 mm in (N). (O–V) Organs from soil-grown plants. (O,P) Leaves. Bars = 50 µm in (O), and 200 µm in (P). (Q,R) Flowers. Bars = 500 µm.

The data demonstrate that both IMPL1 and IMPL2 proteins are directed to plastids (Figures 5E–K).

IMPL1 and IMPL2 proteins have N-terminal extensions of 77 amino acids that are predicted to function as transit peptides and are not present in homologous IMP proteins. To

determine whether these predicted transit peptides are sufficient for organelle targeting, these N-terminal extensions were fused to GFP. The resulting constructs, Pro35S:NterIMPL1:GFP and Pro35S:NterIMPL2:GFP were stably transformed and the putative IMPL2 signal peptide directed plastid expression of GFP similar

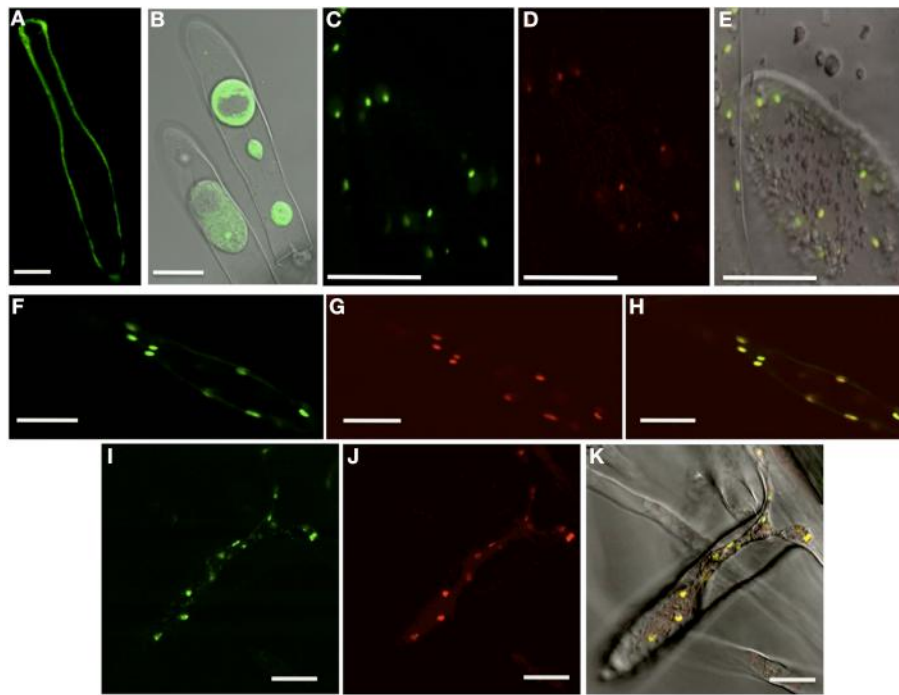


FIGURE 5 | Subcellular Location of IMP, IMPL1, and IMPL2 Proteins.

Single optical sections of transgenic plants expressing IMP:GFP (A,B), IMPL1:GFP (C), IMPL2:RFP (D), overlay of IMPL1:GFP/IMPL2:RFP (E), IMPL2:GFP (F), Plastid mcherry (G), overlay of IMPL2:GFP/plastid-mcherry

(H), IMPL1:GFP (I), Plastid mcherry (J), overlay of IMPL1:GFP/plastid-mcherry (K). All images were taken of root hairs with differential interference contrast (DIC) overlay of plasmolyzed cells (B), DIC overlay of co-localizations (E,K). Bars = 20 μ m.

to that seen with IMPL2:GFP localization (Supplemental Figure 4). The 77 amino acid putative transit peptide from IMPL1 also was sufficient for localization to plastids, however the intensity of expression was significantly reduced (Supplemental Figure 4). From these data, we conclude that the N-terminal 77 amino acids on both IMPL1 and IMPL2 are sufficient for localization to plastids.

CHARACTERIZATION OF *impl2* MUTANTS

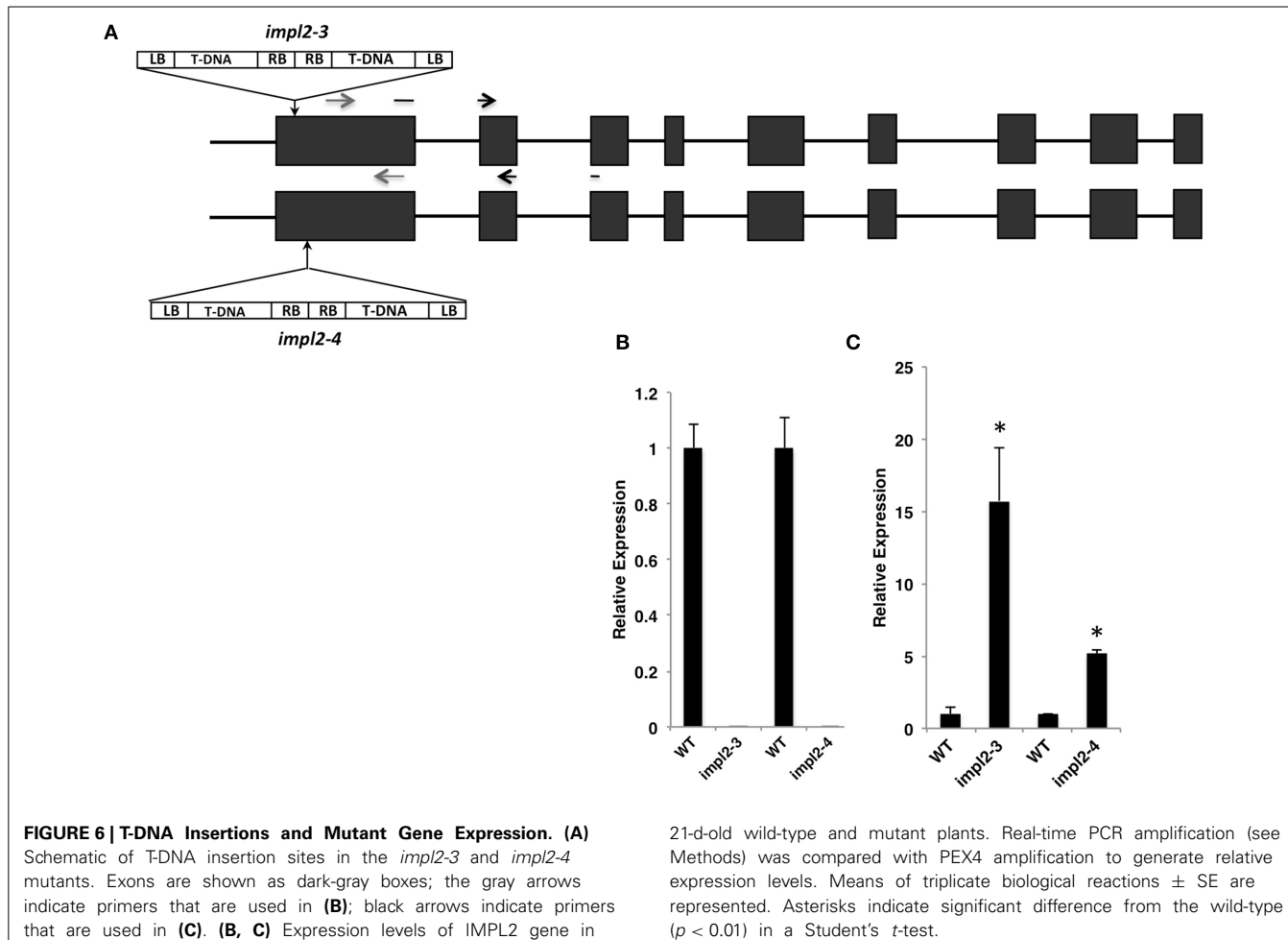
To determine how the IMPL2 gene impacts histidine synthesis and plant growth and development, T-DNA insertion mutants were obtained from the SALK T-DNA insertion collection (Alonso et al., 2003). Seeds for *impl2-3* (SAIL_35_A08) and *impl2-4* (SAIL_146_E09) were obtained, and homozygous mutants were verified by diagnostic PCR screening and DNA sequencing, as described in the experimental procedures. The *impl2-3* mutant contains two tandem T-DNA insertions occurring 24 nucleotides from the start of translation (Figure 6), and is the same line identified previously as an embryo-lethal (Petersen et al., 2010). The *impl2-4* mutant contains two tandem T-DNA insertions 66 nucleotides from the start of translation (Figure 6). Lack of full-length IMPL2 gene expression was verified in the mutants by qPCR (Figure 6). Interestingly, we detected an increased presence of truncated transcript in both mutants using primers downstream of exon one (Figure 6). Thus, there is a possibility that a functional or non-functional IMPL2 protein accumulates in the cytosol of these mutants.

THE *impl2* MUTANTS ARE ALTERED IN GROWTH AND DEVELOPMENT

Previous examination of *impl2-3* mutants indicated homozygosity leads to embryo lethality, and histidine application to heterozygous plants can rescue seed development (Petersen et al., 2010). However, we were able to obtain homozygous progeny of both *impl2-3* and *impl2-4* that produce viable seeds. We analyzed two other T-DNA insertion mutant lines, *impl2-1* and *impl2-2*, but were not able to recover homozygous progeny, strongly suggesting embryo lethality within these lines. Analysis of 30 siliques from wild-type and heterozygous *impl2-1* mutants revealed that approximately 25% of the *impl2-1* seeds were dark and shriveled, while less than 1% of wildtype seed had this appearance, suggesting embryo lethality of homozygous *impl2-1* seed.

The *impl2-3* and *impl2-4* mutant plants are severely compromised in growth and exhibit several main phenotypes, which are quantified in Table 3. These phenotypes include smaller size, reduced inflorescences and seed production (Figure 7). To ensure that these phenotypes result from an IMPL2 loss-of-function, we complemented *impl2-3* with a 35Spromoter: IMPL2:GFP transgene. These complemented plants (*impl2-3/IMPL2:GFP*) exhibited wild-type or near wild-type phenotypes in several different assays (Figures 7A,B). This, along with the finding of two separate mutant alleles (*impl2-3* and *impl2-4*), strongly supports alteration in IMPL2 function as the primary cause for our observed growth phenotypes.

Although both *impl2* mutant lines show very similar phenotypes throughout development, *impl2-3* has been the focus for our experiments. We analyzed the germination rate of mutant

**Table 3 | Overview of the *impl2-3* and *impl2-4* mutant phenotype.**

| | Wild type | <i>impl2-3</i> ^a | <i>impl2-3 + histidine</i> | <i>impl2-3 IMPL2:GFP</i> | <i>impl2-4</i> ^b |
|-------------------------------------------------|----------------|-----------------------------|----------------------------|--------------------------|-----------------------------|
| Rosette diameter (cm) | 4.87 ± 0.2 | $1.10 \pm 0.1^*$ | 4.14 ± 0.2 | 3.69 ± 0.2 | $1.6 \pm 0.1^*$ |
| Number of rosette leaves per plant | 18.3 ± 0.7 | $9.4 \pm 0.5^*$ | 17.1 ± 1.2 | 17.3 ± 0.9 | $12.1 \pm 0.6^*$ |
| Average rosette leaf surface (cm ²) | 2.03 ± 0.1 | $0.20 \pm 0.02^*$ | 2.03 ± 0.1 | 1.57 ± 0.1 | $0.28 \pm 0.02^*$ |
| Number of inflorescence stems per plant | 6.6 ± 0.5 | $1.9 \pm 0.3^*$ | 7.2 ± 0.8 | 4.6 ± 0.6 | $1.8 \pm 0.2^*$ |
| Weight of seeds per 6 plants (mg) | 226 ± 9 | $51.7 \pm 2^*$ | 247 ± 19 | 190 ± 3 | $65.3 \pm 4.1^*$ |

Rosettes and stems were measured 9 weeks after germination. Seeds were harvested, and weighed after they were dried. Data represents the means \pm SE; $n = 20$ for rosettes and stems; $n = 4$ for seeds. ^{a,b}Asterisks indicate values found to be significantly (Student's *t*-test) different from the wild type: * $p < 0.005$.

seeds and noted that only 75% of *impl2-3* seeds germinate, while 97.5% of WT seeds germinate (Figure 8A). After germination of *impl2-3* mutant seeds, we noted significant delay in seedling development as compared to wild-type seedlings, which continues throughout development. Homozygous *impl2* mutants are overall smaller than wild-type plants (Figure 7 and Table 3); *impl2* mutant roots do not grow well (Figures 8B,C), and most seedlings do not produce true leaves and die after a few days. The seedlings that develop beyond this stage are able to produce true leaves, however the leaves are a pale

green color (Figure 7B), and roots remain stunted. Mutant cotyledons and leaves were observed by microscopy; the overall structure of chloroplasts appeared similar to those in wild-type plants (data not shown). The *impl2* plants that survive to maturity produce very few siliques, and some viable seeds (Table 3).

To test whether histidine deficiency is responsible for the altered development of *impl2* mutants, we watered *impl2* mutants and wild-type plants with 1 mM histidine, with a control amino acid, glutamine (Figures 7, 8). The results show that continuous

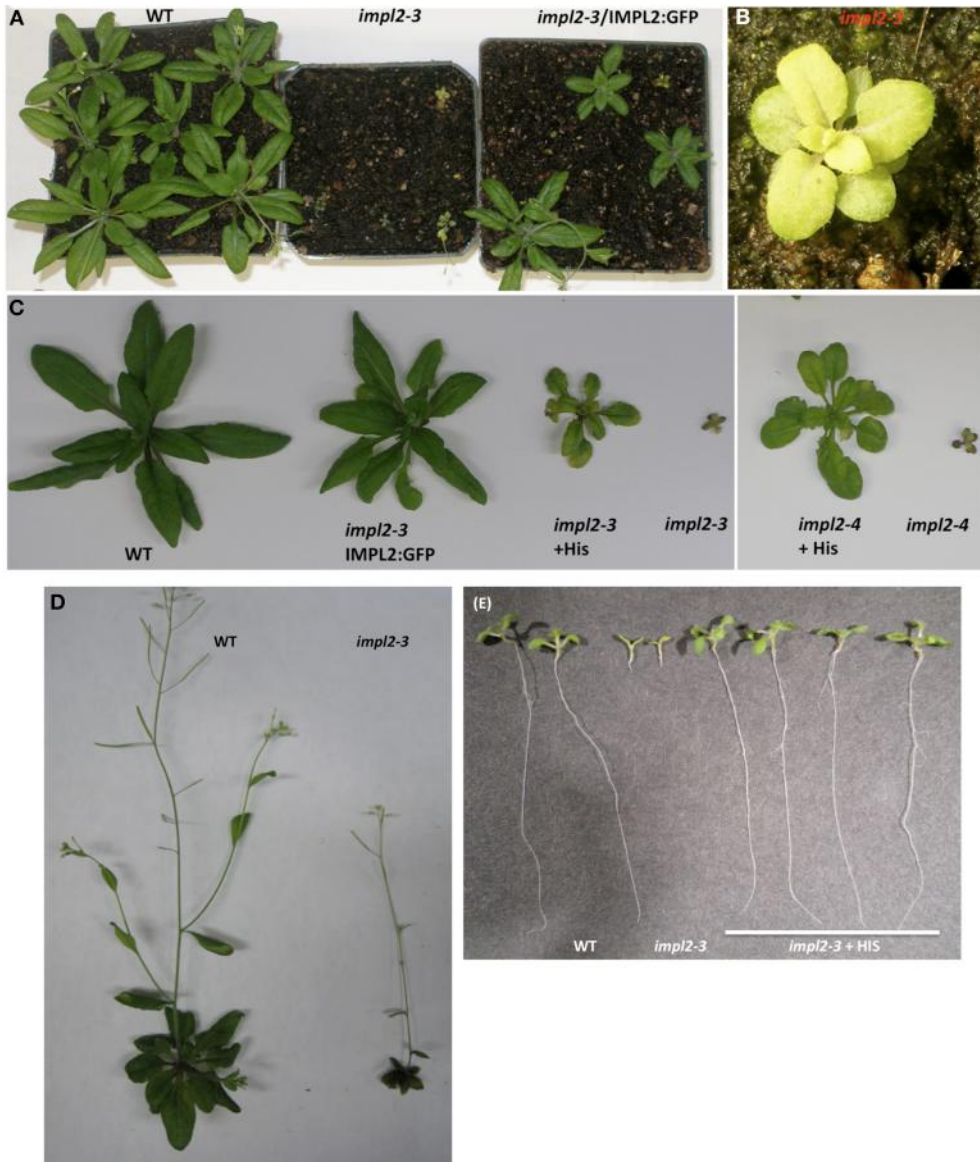


FIGURE 7 | Histidine or IMPL2-GFP Gene Complement the Stunted Stature of *impl2* Mutants. (A) Segregation of progeny from heterozygous *impl2-3* plants containing 35S promoter-IMPL2-GFP. (B) Image of *impl2-3* rosette exhibiting small, pale green leaves (C) Soil-grown *impl2-3*, *impl2-4*, wild-type (CS60000) and complemented

plants. Mutant plants were watered with 1 mM histidine. (D) Soil-grown wild-type and *impl2-3* plants. (E) Photos of 9-d-old wild-type and *impl2-3* seedlings grown on agar plates for root length studies. Root phenotype of *impl2-3* is complemented by the addition of 0.04 mM histidine.

watering with 1 mM histidine (Figures 7, 8) but not 1 mM glutamine (data not shown), alleviates much of the severe growth reduction in *impl2* mutants. To test whether histidine application could rescue *impl2* seed germination and seedling defects, we produced age-matched seed populations that had been harvested from plants grown at the same time. Control and mutant age-matched seeds were plated on Murashige and Skoog (MS) medium in the presence of various concentrations of histidine, glutamine and/or inositol. Our results indicate that *impl2-3* mutants germinate at the same rate in the presence or absence of histidine (Figure 8A). However, root growth of *impl2* mutants

is restored to wild-type levels in the presence of histidine, while neither glutamine nor inositol improves root growth of these mutant plants (Figure 8C). The optimal range for chemical complementation with exogenous histidine is 0.02–0.04 mM, and larger concentrations such as 0.4 or 0.8 mM of histidine have an inhibitory effect on root growth of both *impl2* mutant and wild-type plants grown on agar plates (Figure 8B). The fact that exogenous inositol added to medium was not able to alleviate the stunted root phenotype of *impl2* mutants (Figure 8), suggests that IMPL2 is not involved in inositol synthesis or inositol phosphate metabolism.

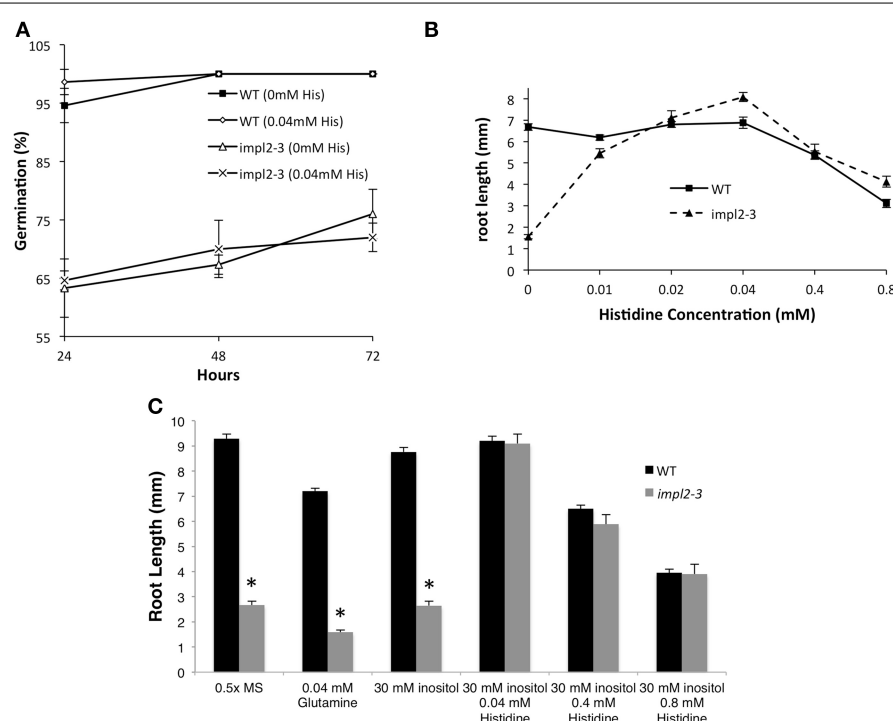


FIGURE 8 | Physiological Responses of *impl2-3* Mutants to Exogenous Histidine and Inositol. (A) Effects of histidine on germination of the wild-type and *impl2-3* mutants grown on agar plates. **(B)** Dose Response of 4-d-old wild-type and *impl2-3* mutant seedlings grown for root length studies on agar plates with the indicated histidine concentrations. **(C)** Effects of

glutamine, inositol and histidine on root length of wild-type and *impl2-3* mutants grown on agar plates. Presented are means \pm SE of three experiments of $n = 50$ (germination) and three experiments of $n = 30$ (root length). Asterisks indicate values found to be significantly (Student's *t*-test) different from the wild type: * $p < 0.005$.

IMPL2 IMPACTS HISTIDINE SYNTHESIS

To determine if a loss in IMPL2 function impacts histidine biosynthesis, we used LC-MS-MS to quantify histidine levels in wild-type and *impl2-3* mutants (Table 4). Amino acids were extracted using 1:1 chloroform: 10 mM HCl (v/v) and norvaline was used as internal standard. Standard curves and interpretation of MS data are described in the Supplemental Methods.

In 7-d-old seedlings, histidine levels are slightly increased in *impl2-3* mutants as compared to wild-type, and the levels are not rescued to wild-type levels in the complemented plants (Table 4). Histidine levels remain elevated in 18-d mutants as compared to wildtype plants. Interestingly, later in development (31 days), whole plants from *impl2-3* mutants show levels of free histidine equal to that found in wild-type, indicating that the amount of histidine is not altered in the *impl2* mutants at this time in development.

We also sought to measure histidinol 1-P, the substrate of IMPL2, and histidinol, the product of IMPL2 catalysis of histidinol 1-P. After numerous attempts, we found we could not detect histidinol 1-P in any plant extract. In contrast, although levels of histidinol were low in wild-type plants, we could reproducibly quantify this compound (Table 4). Since a common issue with metabolite extraction of phosphorylated compounds is hydrolysis of phosphates during sample extraction and derivatization, we tested whether the histidinol measured in our assays could result from the breakdown of histidinol 1-P during sample

preparation. We added 100 μ moles of purified histidinol 1-P to wild-type tissue during the extraction procedure along with the addition of internal standard, norvaline, and found that in wild-type extracts where no histidinol 1-P was added, histidinol levels are barely detectable ($0.001 \pm 0.002 \mu$ moles mg dried weight $^{-1}$). Conversely, in the wild-type extract with added 100 μ moles of histidinol 1-P, histidinol levels are increased by 100-fold to a concentration of $0.1 \pm 0.01 \mu$ moles mg dried weight $^{-1}$ (Supplemental Figure 5). Our conclusion is that our histidinol peak from LC-MS-MS analyses of plant extracts likely gives us information on the histidinol plus histidinol 1-P concentration in mutants and wild-type plants.

Using this methodology, we measured the histidinol plus histidinol 1-P in *impl2* mutants and wild-type plants. We found that *impl2-3* 7-d-old seedlings accumulated $0.33 \pm 0.01 \mu$ moles mg dried weight $^{-1}$ as compared to the barely detectable wild-type levels of $0.0092 \pm 0.0001 \mu$ moles mg dried weight $^{-1}$ (Table 4). This trend for higher levels was seen at 18-d and 31-d as well. This suggests that lack of histidinol 1-P hydrolysis in *impl2* mutants results in accumulation of precursors in the histidine pathway. Importantly, in IMPL2 complemented plants and IMPL2:GFP plants, histidinol plus histidinol 1-P levels at 7, 18, and 31 days are similar to those from wild-type plants (Table 4). Thus, the elevation of precursors in the histidine pathway correlates with the altered growth and development of *impl2* mutants.

Table 4 | Histidine and histidinol levels at different developmental stages.

| Tissue | WT ($\mu\text{moles mg DW}^{-1}$) | <i>impl2-3</i> ($\mu\text{moles mg DW}^{-1}$) | <i>impl2-3</i> IMPL2:GFP ($\mu\text{moles mg DW}^{-1}$) | IMPL2:GFP ($\mu\text{moles mg DW}^{-1}$) |
|-----------------|----------------------------------------|----------------------------------------------------|--------------------------------------------------------------|-----------------------------------------------|
| histidine 7-d | 0.15 ± 0.01 | 0.27 ± 0.01 | 0.28 ± 0.01 | 0.15 ± 0.01 |
| histidine 18-d | 0.25 ± 0.01 | 0.38 ± 0.01 | 0.37 ± 0.01 | 0.35 ± 0.02 |
| histidine 31-d | 0.35 ± 0.01 | 0.35 ± 0.01 | 0.36 ± 0.01 | 0.35 ± 0.01 |
| histidinol 7-d | 0.0092 ± 0.0001 | 0.33 ± 0.01* | 0.0010 ± 0.0001 | 0.0009 ± 0.0001 |
| histidinol 18-d | 0.0010 ± 0.0002 | 0.48 ± 0.01* | 0.0008 ± 0.0001 | 0.0008 ± 0.0001 |
| histidinol 31-d | 0.0007 ± 0.0001 | 0.34 ± 0.02* | 0.0009 ± 0.0002 | 0.0009 ± 0.0001 |
| histidine + | 1.87 ± 0.03 | 2.10 ± 0.02 | NM | NM |
| histidinol + | 0.54 ± 0.02 | 1.03 ± 0.02 | NM | NM |

Seedlings and plants were grown on 0.5x MS, pH 5.8, and 1% sucrose. Seedlings of 7-d-old, 18-d-old or whole rosette and roots of 31-d-old wild-type, *impl2-3*, *impl2-3* IMPL2:GFP, and IMPL2:GFP plants were harvested, and histidine and histidinol levels were quantified with LC-MS-MS as described in Methods. + histidine and histidinol levels were measured in 7-d-old seedlings that were grown on 0.8 mM histidinol (NM = not measured). Data represents the means ± SE; $n = 3$.

*Asterisks indicate values found to be significantly (Student's t-test) different from the wild type: * $p < 0.005$.

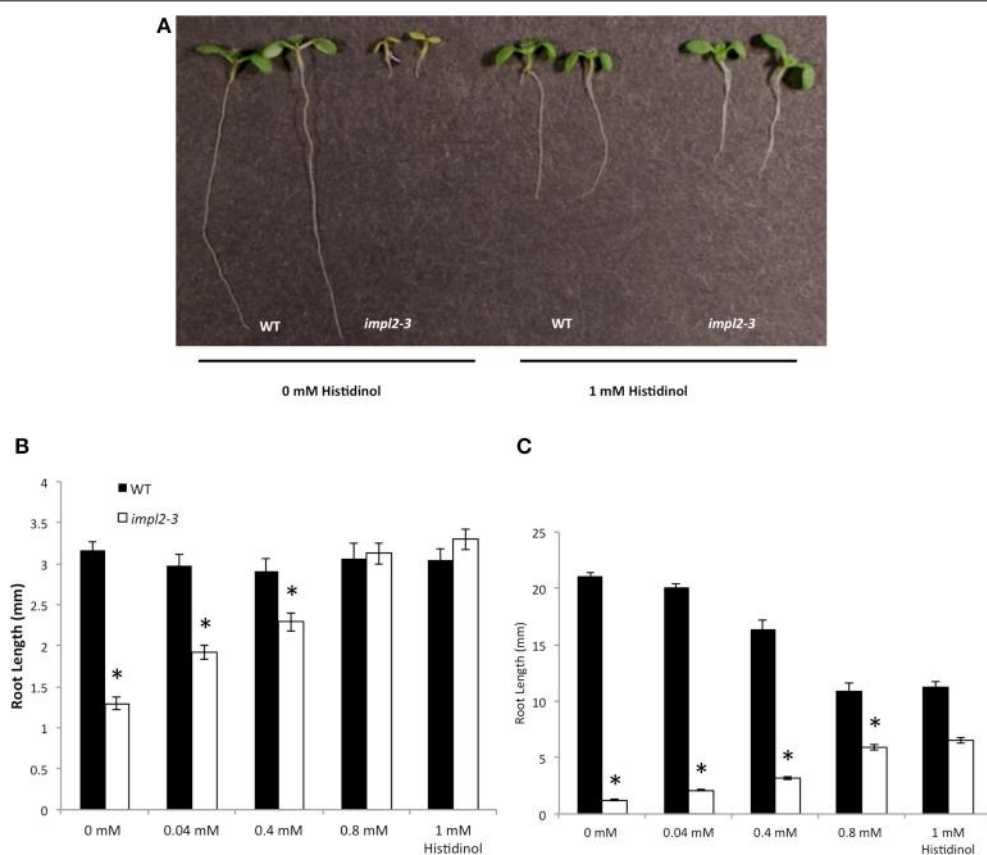


FIGURE 9 | Chemical Complementation of *impl2-3* Mutants with Exogenous Histidinol. (A) Photos of 8-d-old wild-type and *impl2-3* seedlings grown on agar plates for root length studies. Root phenotype of *impl2-3* is complemented by the addition of 0.8–1 mM

histidinol. **(B)** Dosage Response of 4-d-old **(C)** 8-d-old wild-type and *impl2-3* mutant seedlings grown for root length studies on agar plates with the indicated histidinol concentrations. Presented are means ± SE of $n = 40$, * $p < 0.05$.

To test whether *impl2* mutants can be rescued by histidinol, we grew *impl2-3* and wild-type seeds in the presence of varying concentrations of histidinol (Figure 9). The root length phenotype of *impl2-3* seedlings was complemented by 0.8–1 mM of

histidinol by day 4 and this amount was not toxic to the growth of wild-type seedlings. However, at 8 days the histidinol started to have an inhibitory effect on growth in both WT and *impl2-3* mutant plants. We conclude that exogenous histidinol can rescue

the growth of *impl2-3* mutants, however accumulation of high levels of histidinol can exhibit an inhibition in growth further in development. Thus, our developmental analysis and histidine metabolite data analyses firmly establish that *impl2* mutants have alterations in the histidine biosynthetic pathway that lead to severe growth alterations, and underscore the importance of this pathway in plant growth and development.

AN IMPL2 LOSS-OF-FUNCTION DOES NOT IMPACT MYO-INOSITOL LEVELS

Given the bifunctionality of several of the characterized IMPs, we wanted to rule out the possibility that IMPL2 can impact inositol levels by *in vivo* hydrolysis of D-Ins 1-P or D-Ins 3-P. We quantified inositol and six other metabolites, including ascorbic acid, a downstream product that can result from inositol catabolism. No difference in inositol levels was observed in *impl2-3* 7-d-old seedlings as compared to wild-type seedlings, however, fructose, ascorbic acid, glycerate, and xylose levels were altered in these mutants (Supplemental Figure 6). Given the substrate specificity of recombinant IMPL2-GST and the lack of inositol alterations in *impl2* mutants, we conclude that IMPL2 plays little to no role in inositol synthesis or recycling in the plant cell. We also examined IMPL1 overexpressing plants (Supplemental Figure 6). We found that inositol levels were not altered in these plants. However, as was true for the *impl2-3* mutants we found that overexpression of IMPL1:GFP resulted a small elevation of ascorbic acid (Supplemental Figure 6).

DISCUSSION

IMP enzymes have been a focus of study in plants since the pioneering work of Frank Loewus in the 1960s (Loewus and Kelly, 1962; Loewus et al., 1962; Loewus, 1964, 1965, 1969). Given that the canonical IMP in plants is bifunctional, hydrolyzing both inositol phosphates involved in *de novo* inositol synthesis and inositol signaling, and L-Gal 1-P, a precursor to ascorbic acid (Torabinejad et al., 2009), we wanted to address the functionality of the IMPL enzymes. We were guided by work from Petersen et al. that IMPL2, but not IMPL1, is sufficient to rescue the histidine auxotrophy of a *Streptomyces coelicolor* hisN mutant, which is defective in His 1-P phosphatase activity (Petersen et al., 2010). Our comparison of IMPL1 and IMPL2 recombinant protein activity using a variety of substrates, along with genetic characterization of metabolite levels in viable *impl2* mutants, solidifies the role of IMPL1 in inositol and/or galactose phosphate metabolism, and IMPL2 in the histidine synthesis pathway.

IMPL2 IS NOT A MOONLIGHTING ENZYME

The fact that IMPL2 can rescue histidine auxotrophy of a *Streptomyces coelicolor* hisN mutant (Petersen et al., 2010) suggested IMPL2 either functioned in both inositol and histidine synthesis (i.e., a moonlighting activity), or had diverged in its substrate specificity. Our biochemical examination shows that IMPL2 has specificity for His 1-P, and our genetic and metabolite analyses of viable *impl2* mutants shows the importance of this reaction in the histidine synthetic pathway, with no apparent role in the inositol metabolic pathway.

BIOCHEMICAL EVIDENCE FOR HISTIDINOL 1-PHOSPHATE PHOSPHATASE ACTIVITY

Key to our analysis of IMPL2 activity was the synthesis of the His 1-P substrate (provided by Robert White), which is not available commercially, and limits the ability of investigators to examine catalysis by these enzymes. We found that recombinant AtIMPL2 has a K_m value slightly higher than other monofunctional His 1-P phosphatases characterized previously. The catalytic efficiency we delineated for AtIMPL2 is lower than those from unicellular organisms (Millay and Houston, 1973; Lee et al., 2008). In contrast, the AtIMPL2 K_m value of 180 μM is slightly different than the only other reported value from a partially purified plant His 1-P phosphatase activity (from wheat) estimated to be 0.4 mM (Wiater et al., 1971). The lack of hydrolysis of inositol phosphates or related molecules by IMPL2 clearly allows us to make a definitive statement that the IMPL2 is indeed the last missing enzyme in the plant histidine pathway (Petersen et al., 2010), and it does not play a role in inositol metabolism or signaling.

THE IMPACT OF IMPL2 ON HISTIDINE SYNTHESIS AND PLANT GROWTH

The most common histidine-starvation phenotype in plants is embryo-lethal at the pre-globular stage (Muralla et al., 2007). In our search for a genetic loss of function mutant in IMPL2, we identified two embryo-lethals and two other viable, homozygous mutants, named *impl2-3* and *impl2-4*. Both mutant lines are greatly altered in growth and development, produce few seeds and can be rescued by exogenous histidine application. The *impl2-3* mutant has been previously reported to be embryo-lethal which can be rescued by exogenous histidine application. It is not obvious why we have been able to grow this same mutant and obtain progeny without histidine application, but one possible explanation is a difference in our growth conditions that may facilitate His 1-P breakdown in the mutants.

We complemented the *impl2-3* mutant with a 35S:IMPL2:GFP construct, which rescued the growth and production of histidine pathway precursors. It is interesting to note that our metabolite analyses indicated that *impl2-3* mutants, complemented mutants and IMPL2 overexpressors all had concomitant small changes in fructose, ascorbate, and xylose. We feel these changes are most likely resulting from our use of the 35S promoter, which clearly drives expression of IMPL2 to complement the growth of *impl2* mutants, but may not recapitulate the native pattern of IMPL2 expression. Thus, these metabolite differences may be linked to the decrease or relative increase in IMPL2 function in these plants.

FUNCTION OF IMPL1

Our biochemical experiments with recombinant IMPL1 indicate that it has no activity with His 1-P, as predicted from lack of genetic complementation in the Actinobacteria *histidine* auxotroph mutant (Petersen et al., 2010). From our kinetic studies, IMPL1 is most likely involved in hydrolyzing D-Ins 1-P and/or D-Gal 1-P. D-Ins 1-P is a breakdown product of D-Ins(1,4,5)P₃ second messenger, while no role is yet known for D-Gal 1-P in plants, although the mammalian IMP is capable of hydrolyzing D-Gal 1-P (Parthasarathy et al., 1997). The IMPL1 substrate specificity is thus different from that of the plant IMP, which

hydrolyzes D-Ins 1-P and D-Ins 3-P and L-Gal 1-P to similar degrees (Laing et al., 2004; Torabinejad et al., 2009). As we and others have provided evidence that IMPL1 is located in the chloroplast, this suggests that IMPL1 may be involved in recycling *myo*-inositol from InsP(1,4,5)P₃ or another D-inositol phosphate within the chloroplast. It is interesting to note that IMP and IMPL1 are regulated similarly at the spatial level, except for the lack of IMPL1 expression in roots. Thus, for most above-ground tissues, IMP and IMPL1 could be functionally redundant with respect to breakdown of D-inositol phosphates. The role of signaling inositol phosphates in the chloroplast, is at present, unknown, however there is evidence for inositol synthesis within the chloroplast (Parker et al., 1987; Johnson and Wang, 1996). It is currently unknown whether chloroplasts synthesizes higher inositol phosphates or phosphatidylinositol phosphates that could be acted on by phospholipase C, resulting in Ins(1,4,5)P₃. Interestingly, chloroplasts are capable of releasing Ca²⁺ (Johnson et al., 1995), and a chloroplast Ca²⁺ sensor has also been characterized (Weinl et al., 2008).

Without more definitive data, such as an IMPL1 genetic mutant, we cannot ascribe a clear function to IMPL1. It is of interest that no IMPL1 T-DNA insertion mutant lines have been identified, and our multiple attempts to produce IMPL1 RNAi lines have not been successful, suggesting that IMPL1 is an essential gene. An interesting clue to IMPL1 function comes from the *Chlamydomonas* IMPL1 homolog (called INM1), which is required for uniparental inheritance of chloroplast DNA in gametes, along with the key regulator for zygote development, *GSP1* (Nishimura et al., 2012). It has been shown that inactivation of the *Chlamydomonas* mating structure induces a rapid turnover of phosphatidylinositol(4,5)bisphosphate (Irvine et al., 1992; Musgrave et al., 1992), and it is speculated that this might drive Ins(1,4,5)P₃ synthesis, stimulating the Ca²⁺/cAMP signal transduction system needed for successful mating and zygote development (Nishimura et al., 2012). If so, then IMPL1 (INM1) may be required for recycling of Ins(1,4,5)P₃ in this system.

Given the similarity in sequence between IMP, IMPL1, and IMPL2, the difference in substrate specificity among these highly homologous enzymes is somewhat surprising.

Our work clearly delineates that the plant family of IMP and IMPL enzymes has evolved different substrate specificities, and that IMPL2 does not function in the inositol signaling pathway. In contrast, the IMPL1 enzyme appears to utilize similar substrates as the IMP enzyme, and the role of this chloroplast-localized IMPL1 enzyme awaits further investigation that could be greatly facilitated by a genetic mutant to examine accumulation of *in vivo* substrates and products.

EXPERIMENTAL PROCEDURES

PLANT MATERIAL AND GROWTH CONDITIONS

Arabidopsis thaliana ecotype Columbia plants were maintained in Sunshine Mix #1 soil at 22–24°C with 100–140 μmol m⁻² s⁻¹ light set for 16 h days. Mutant *impl2-3* and *impl2-4* plants were given exogenous histidine by watering with a 1 mM histidine solution every other day. Age-matched seeds after-ripened for 3 weeks at RT were used for all assays. Details of seed germination,

root growth, and mutant selection are described in Supplemental Methods.

EXPRESSION ANALYSES

RNA was purified from soil grown plants, 3-d-old, and 7-d-old seedlings grown on 0.5× MS/1% sucrose-soaked filter paper under 16 h of light, as described in Donahue et al. (2010). Mature seeds, imbibed with water for 3 days at 4°C, were freeze-dried, followed by initial RNA extraction and LiCl precipitation (Vicente-Carabajosa and Carbonero, 2005). cDNA was synthesized from 2 μg of RNA using Bio-Rad iScript cDNA synthesis kit, loaded into 96-well plates containing Sybr Green PCR MasterMix (Applied Biosystems) with gene-specific primers as described in Donahue et al. (2010).

CONSTRUCTS AND IMAGING

IMP/IMPL ORFs without stop codons were amplified by PCR from *Arabidopsis* CS60000 cDNA. IMPs were cloned into pENTR/D-TOPO vector (Invitrogen), confirmed by sequencing, and recombined via the Gateway system (Invitrogen) using the manufacturer's protocol into destination vector pK7FWG2 (Karimi et al., 2002). The resulting vectors, IMP:GFP, IMPL1:GFP and IMPL2:GFP contain *Egfp* fused to the 3' end of the cDNAs, under control of the 35S CaMV promoter, flanked by left border (LB), and right border (RB) and a plant Kanamycin resistance cassette. The constructs were transformed into *Agrobacterium tumefaciens* by cold shock and were used in stable transformation of wild-type plants and *impl2-3* and *impl2-4* mutant plants. Transformation of *Arabidopsis* was as described (Bechtold et al., 1993). Screening of plants and generation of transgenic plants for co-localization studies are described in Supplemental Methods online.

LC-MS/MS ANALYSIS OF HISTIDINE AND HISTIDINOL

Tissues were harvested and immediately flash frozen in liquid nitrogen and were ground to fine powder in liquid nitrogen and lyophilized. Five mg of lyophilized seedlings and tissue samples were disrupted with glass beads and extracted with chloroform:10 mM HCl 1:1 (v/v) (1 ml final volume) and 40 μM of norvaline was added to the aqueous phase as internal standard. The insoluble chloroform portion was removed by centrifugation. A portion of the (1:5 dilution) supernatant was dried and reconstituted in 200 μl of 65% (0.1% formic acid and water) and 35% acetonitrile. The LC-MS/MS method used for histidine and histidinol analysis has been described previously (Gu et al., 2007) and modifications are described in the Supplemental Methods.

EXPRESSION OF RECOMBINANT PROTEIN AND PHOSPHATASE ACTIVITY ASSAYS

Plasmids containing the genes IMPL1 (At1g31190) and IMPL2 (At4g39120), designated pAtIMPL1H and pAtIMPL2H, respectively, were constructed as described in Torabinejad et al. (2009). The His 1-P substrate for IMPL2 was synthesized according to previous methods (Fujimoto and Naruse, 1967; Yoshikawa et al., 1967). The purity of the substrate was determined by Mass Spectrometry. In addition the absence of free phosphates was confirmed by a Malachite Green phosphate release assay. Phosphatase activity was determined by the inorganic phosphate

quantification assay (Lanzetta et al., 1979) with minor modifications. Standard reaction conditions were 50 mM Tris-Cl, pH 7.5, 2 mM MgCl₂, 0.4 mM substrate, and 112 ng of purified enzyme in a total reaction volume of 50 μl for IMPL2. Reaction conditions were 50 mM Tris, pH 9, 3 mM MgCl₂, 0.4 mM substrate, and 452 ng of purified enzyme in a total reaction volume of 50 μl for IMPL1. Reactions were performed at room temperature (25°C) for 10 min, after which 800 μl of color reagent malachite green/ ammonium molybdate solution was added to terminate the reaction. The A₆₆₀ was determined by a spectrophotometer. Control reactions without enzyme or without substrate were used to determine background phosphate levels, which were subtracted from experimental values. Enzyme-specific activity units are in μmol of phosphate. Protein concentrations were determined as described by Bradford Assay with bovine serum albumin as the standard. Data from kinetic experiments were analyzed with Kaleidograph software (version Mac; Synergy Software). Data were fit to the Michaelis-Menten equation $v = V_{max} [S] / (K_m + [S])$.

ACKNOWLEDGMENTS

The authors are indebted to Robert White for synthesis of histidinol 1-phosphate. We acknowledge Keith Ray and Kim Harrick for assistance with LC-MS, and Janet Donahue for assistance with cloning. Funding from NSF (MCB# 1051646) and NIFA (2013-02277) to Glenda E. Gillaspy are gratefully acknowledged. This work was supported by an award from the NSF (MCB#1051646 to Glenda E. Gillaspy).

SUPPLEMENTARY MATERIAL

The Supplementary Material for this article can be found online at: <http://www.frontiersin.org/journal/10.3389/fpls.2014.00725/abstract>

REFERENCES

- Alonso, J. M., Stepanova, A. N., Leisse, T. J., Kim, C. J., Chen, H., Shinn, P., et al. (2003). Genome-wide insertional mutagenesis of *Arabidopsis thaliana*. *Science* 301, 653–657. doi: 10.1126/science.1086391
- Bechtold, N., Ellis, J., and Pelletier, G. (1993). In planta Agrobacterium mediated gene transfer by infiltration of adult *Arabidopsis thaliana* plants. *C. R. Acad. Sci. III-Vie* 316, 1194–1199.
- Boss, W. F., and Im, Y. J. (2012). Phosphoinositide signaling. *Annu. Rev. Plant Biol.* 63, 409–429. doi: 10.1146/annurev-arplant-042110-103840
- Bradford, G. R. (1963). Lithium survey of California's water resources. *Soil Sci.* 96, 77–81. doi: 10.1097/00010694-196308000-00001
- Chen, M., and Loewus, F. A. (1977). myo-inositol metabolism in *Lilium longiflorum* pollen: uptake and incorporation of myo-inositol-2-H. *Plant Physiol.* 59, 653–657. doi: 10.1104/pp.59.4.653
- Collakova, E., Goyer, A., Naponelli, V., Krassovskaya, I., Gregory, J. F. III., Hanson, A. D., et al. (2008). Arabidopsis 10-formyl tetrahydrofolate deformylases are essential for photorespiration. *Plant Cell* 20, 1818–1832. doi: 10.1105/tpc.108.058701
- Conklin, P. L., Gatzek, S., Wheeler, G. L., Dowdle, J., Raymond, M. J., Rolinski, S., et al. (2006). *Arabidopsis thaliana* VTC4 encodes L-galactose-1-P phosphatase, a plant ascorbic acid biosynthetic enzyme. *J. Biol. Chem.* 281, 15662–15670. doi: 10.1074/jbc.M61409200
- Conklin, P. L., Saracco, S. A., Norris, S. R., and Last, R. L. (2000). Identification of ascorbic acid-deficient *Arabidopsis thaliana* mutants. *Genetics* 154, 847–856.
- Donahue, J. L., Alford, S. R., Torabinejad, J., Kerwin, R. E., Nourbakhsh, A., Ray, W. K., et al. (2010). The *Arabidopsis thaliana* myo-inositol 1-phosphate synthase1 gene is required for myo-inositol synthesis and suppression of cell death. *Plant Cell* 22, 888–903. doi: 10.1105/tpc.109.071779
- Fujimoto, Y., and Naruse, M. (1967). [Synthesis of nucleotides. 3. Selective phosphorylation of ribonucleoside with phosphorus oxychloride]. *Yakugaku zasshi* 87, 270–274.
- Gillaspy, G. E. (2011). The cellular language of myo-inositol signaling. *New Phytol.* 192, 823–839. doi: 10.1111/j.1469-8137.2011.03939.x
- Gillaspy, G. E., Keddie, J. S., Oda, K., and Gruissem, W. (1995). Plant inositol monophosphatase is a lithium-sensitive enzyme encoded by a multigene family. *Plant Cell* 7, 2175–2185. doi: 10.1105/tpc.7.12.2175
- Goyer, A., Collakova, E., Diaz De La Garza, R., Quinlivan, E. P., Williamson, J., Gregory, J. F. III., et al. (2005). 5-Formyltetrahydrofolate is an inhibitory but well tolerated metabolite in *Arabidopsis* leaves. *J. Biol. Chem.* 280, 26137–26142. doi: 10.1074/jbc.M503106200
- Gu, L., Jones, A. D., and Last, R. L. (2007). LC-MS/MS assay for protein amino acids and metabolically related compounds for large-scale screening of metabolic phenotypes. *Anal. Chem.* 79, 8067–8075. doi: 10.1021/ac070938b
- Gumber, S. C., Loewus, M. W., and Loewus, F. A. (1984). Further Studies on myo-inositol-1-phosphatase from the pollen of *Lilium longiflorum* thunb. *Plant Physiol.* 76, 40–44. doi: 10.1104/pp.76.1.40
- Guyer, D., Patton, D., and Ward, E. (1995). Evidence for cross-pathway regulation of metabolic gene expression in plants. *Proc. Natl. Acad. Sci. U.S.A.* 92, 4997–5000. doi: 10.1073/pnas.92.11.4997
- Ingle, R. A. (2011). Histidine biosynthesis. *Arabidopsis Book* 9:e0141. doi: 10.1199/tab.0141
- Irvine, R. F., Letcher, A. J., Stephens, L. R., and Musgrave, A. (1992). Inositol polyphosphate metabolism and inositol lipids in a green alga, *Chlamydomonas eugametos*. *Biochem. J.* 281(Pt 1), 261–266.
- Ishijima, S., Uchibori, A., Takagi, H., Maki, R., and Ohnishi, M. (2003). Light-induced increase in free Mg²⁺ concentration in spinach chloroplasts: measurement of free Mg²⁺ by using a fluorescent probe and necessity of stromal alkalinization. *Arch. Biochem. Biophys.* 412, 126–132. doi: 10.1016/S0003-9861(03)00038-9
- Islas-Flores, I., and Villanueva, M. A. (2007). Inositol-1 (or 4)-monophosphatase from Glycine max embryo axes is a phosphatase with broad substrate specificity that includes phytate dephosphorylation. *Biochim. Biophys. Acta* 1770, 543–550. doi: 10.1016/j.bbagen.2006.12.001
- Jefferson, R. A. (1987). Assaying chimeric genes in plants: the GUS fusion system. *Plant Mol. Biol. Rep.* 5, 387–405. doi: 10.1007/BF02667740
- Johnson, C. H., Knight, M. R., Kondo, T., Masson, P., Sedbrook, J., Haley, A., et al. (1995). Circadian oscillations of cytosolic and chloroplastic free calcium in plants. *Science* 269, 1863–1865. doi: 10.1126/science.7569925
- Johnson, M. D., and Wang, X. (1996). Differentially expressed forms of 1-L-myo-inositol-1-phosphate synthase (EC 5.5.1.4) in *Phaseolus vulgaris*. *J. Biol. Chem.* 271, 17215–17218. doi: 10.1074/jbc.271.29.17215
- Karimi, M., Inze, D., and Depicker, A. (2002). GATEWAY vectors for Agrobacterium-mediated plant transformation. *Trends Plant Sci.* 7, 193–195. doi: 10.1016/S1360-1385(02)02251-3
- Kroh, M., Miki-Hirosige, H., Rosen, W., and Loewus, F. (1970). Inositol metabolism in plants. VII. Distribution and utilization of label from myo-inositol-U 14C and -2-3H by detached flowers and pistils of *Lilium longiflorum*. *Plant Physiol.* 45, 86–91. doi: 10.1104/pp.45.1.86
- Laing, W. A., Bulley, S., Wright, M., Cooney, J., Jensen, D., Barracough, D., et al. (2004). A highly specific L-galactose-1-phosphate phosphatase on the path to ascorbate biosynthesis. *Proc. Natl. Acad. Sci. U.S.A.* 101, 16976–16981. doi: 10.1073/pnas.0407453101
- Lanzetta, P. A., Alvarez, L. J., Reinach, P. S., and Candia, O. A. (1979). An improved assay for nanomole amounts of inorganic phosphate. *Anal. Biochem.* 100, 95–97. doi: 10.1016/0003-2697(79)90115-5
- Lee, H. S., Cho, Y., Lee, J. H., and Kang, S. G. (2008). Novel mono-functional histidinol-phosphate phosphatase of the DDDD superfamily of phosphohydrolases. *J. Bacteriol.* 190, 2629–2632. doi: 10.1128/JB.01722-07
- Leech, A. P., Baker, G. R., Shute, J. K., Cohen, M. A., and Gani, D. (1993). Chemical and kinetic mechanism of the inositol monophosphatase reaction and its inhibition by Li⁺. *Eur. J. Biochem.* 212, 693–704. doi: 10.1111/j.1432-1033.1993.tb17707.x
- Loewus, F. (1965). Inositol metabolism and cell wall formation in plants. *Fed. Proc.* 24, 855–862.
- Loewus, F. (1969). Metabolism of inositol in higher plants. *Ann. N. Y. Acad. Sci.* 165, 577–598.

- Loewus, F. A. (1964). Inositol metabolism in plants. II. The absolute configuration of D-Xylose-5-T derived metabolically from myo-inositol-2-T in the ripening strawberry. *Arch. Biochem. Biophys.* 105, 590–598. doi: 10.1016/0003-9861(64)90055-4
- Loewus, F. A. (2006). Inositol and plant cell wall polysaccharide biogenesis. *Subcell. Biochem.* 39, 21–45. doi: 10.1007/0-387-27600-9_2
- Loewus, F. A., and Kelly, S. (1962). Conversion of glucose to inositol in parsley leaves. *Biochem. Biophys. Res. Commun.* 7, 204–208. doi: 10.1016/0006-291X(62)90175-4
- Loewus, F. A., Kelly, S., and Neufeld, E. F. (1962). Metabolism of myo-inositol in plants: conversion to pectin, hemicellulose, D-Xylose, and sugar acids. *Proc. Natl. Acad. Sci. U.S.A.* 48, 421–425. doi: 10.1073/pnas.48.3.421
- Loewus, M. W., and Loewus, F. A. (1983). Myo-inositol-1-phosphatase from the pollen of *Lilium longiflorum* thunb. *Plant Physiol.* 70, 765–770. doi: 10.1104/pp.70.3.765
- Millay, R. H. Jr., and Houston, L. L. (1973). Purification and properties of yeast histidinol phosphate phosphatase. *Biochemistry* 12, 2591–2596. doi: 10.1021/bi00738a007
- Mo, X., Zhu, Q., Li, X., Li, J., Zeng, Q., Rong, H., et al. (2006). The hpa1 mutant of Arabidopsis reveals a crucial role of histidine homeostasis in root meristem maintenance. *Plant Physiol.* 141, 1425–1435. doi: 10.1104/pp.106.084178
- Muralla, R., Sweeney, C., Stepansky, A., Leustek, T., and Meinke, D. (2007). Genetic dissection of histidine biosynthesis in Arabidopsis. *Plant Physiol.* 144, 890–903. doi: 10.1104/pp.107.096511
- Musgrave, A., Kuin, H., Jongen, M., De Wildt, P., Schuring, F., Clerk, H., et al. (1992). Ethanol stimulates phospholipid turnover and inositol 1,4,5-trisphosphate production in Chlamydomonas eugametes gametes. *Planta* 186, 442–449. doi: 10.1007/BF00195326
- Nelson, B. K., Cai, X., and Nebenfuhr, A. (2007). A multicolored set of *in vivo* organelle markers for co-localization studies in Arabidopsis and other plants. *Plant J.* 51, 1126–1136. doi: 10.1111/j.1365-313X.2007.03212.x
- Nishimura, Y., Shikanai, T., Nakamura, S., Kawai-Yamada, M., and Uchimiya, H. (2012). Gsp1 triggers the sexual developmental program including inheritance of chloroplast DNA and mitochondrial DNA in *Chlamydomonas reinhardtii*. *Plant Cell* 24, 2401–2414. doi: 10.1105/tpc.112.097865
- Noutoshi, Y., Ito, T., and Shinozaki, K. (2005). ALBINO AND PALE GREEN 10 encodes BBMII isomerase involved in histidine biosynthesis in *Arabidopsis thaliana*. *Plant Cell Physiol.* 46, 1165–1172. doi: 10.1093/pcp/pci119
- Parker, H., Majumder, A. L., Bhaduri, T. J., Dasgupta, S., and Majumder, A. L. (1987). Chloroplast as a locale of L-myo-inositol-1-phosphate synthase. *Plant Physiol.* 85, 611–614. doi: 10.1104/pp.85.3.611
- Parthasarathy, R., Parthasarathy, L., and Vadnal, R. (1997). Brain inositol monophosphatase identified as a galactose 1-phosphatase. *Brain Res.* 778, 99–106. doi: 10.1016/S0006-8993(97)01042-1
- Petersen, L. N., Marineo, S., Mandala, S., Davids, F., Sewell, B. T., and Ingle, R. A. (2010). The missing link in plant histidine biosynthesis: Arabidopsis myo-inositol monophosphatase-like2 encodes a functional histidinol-phosphate phosphatase. *Plant Physiol.* 152, 1186–1196. doi: 10.1104/pp.109.150805
- Sessions, A., Burke, E., Presting, G., Aux, G., McElver, J., Patton, D., et al. (2002). A high-throughput Arabidopsis reverse genetics system. *Plant Cell* 14, 2985–2994. doi: 10.1105/tpc.004630
- Sun, Q., Zybalov, B., Majeran, W., Friso, G., Olinares, P. D., and Van Wijk, K. J. (2009). PPDB, the plant proteomics database at cornell. *Nucleic Acids Res.* 37, D969–D974. doi: 10.1093/nar/gkn654
- Torabinejad, J., Donahue, J. L., Gunesekera, B. N., Allen-Daniels, M. J., and Gillaspay, G. E. (2009). VTC4 is a bifunctional enzyme that affects myo-inositol and ascorbate biosynthesis in plants. *Plant Physiol.* 150, 951–961. doi: 10.1104/pp.108.135129
- Torabinejad, J., and Gillaspay, G. E. (2006). Functional genomics of inositol metabolism. *Subcell. Biochem.* 39, 47–70. doi: 10.1007/0-387-27600-9_3
- Vicente-Carbajosa, J., and Carbonero, P. (2005). Seed maturation: developing an intrusive phase to accomplish a quiescent state. *Int. J. Dev. Biol.* 49, 645–651. doi: 10.1387/ijdb.052046jc
- Weinl, S., Held, K., Schlücking, K., Steinhorst, L., Kuhlgert, S., Hippler, M., et al. (2008). A plastid protein crucial for Ca²⁺-regulated stomatal responses. *New Phytol.* 179, 675–686. doi: 10.1111/j.1469-8137.2008.02492.x
- Wiater, A., Krajewska-Grynkiewicz, K., and Klopotowski, T. (1971). Histidine biosynthesis and its regulation in higher plants. *Acta Biochim. Pol.* 18, 299–307.
- Yoshikawa, M., Kato, T., and Takenishi, T. (1967). A novel method for phosphorylation of nucleosides to 5'-nucleotides. *Tetrahedron Lett.* 50, 5065–5068. doi: 10.1016/S0040-4039(01)89915-9
- Zimmermann, P., Hirsch-Hoffmann, M., Hennig, L., and Gruisse, W. (2004). GENEVESTIGATOR. Arabidopsis microarray database and analysis toolbox. *Plant Physiol.* 136, 2621–2632. doi: 10.1104/pp.104.046367

Conflict of Interest Statement: The authors declare that the research was conducted in the absence of any commercial or financial relationships that could be construed as a potential conflict of interest.

Received: 15 September 2014; accepted: 01 December 2014; published online: 09 January 2015.

Citation: Nourbakhsh A, Collakova E and Gillaspay GE (2015) Characterization of the inositol monophosphatase gene family in Arabidopsis. *Front. Plant Sci.* 5:725. doi: 10.3389/fpls.2014.00725

This article was submitted to Plant Physiology, a section of the journal Frontiers in Plant Science.

Copyright © 2015 Nourbakhsh, Collakova and Gillaspay. This is an open-access article distributed under the terms of the Creative Commons Attribution License (CC BY). The use, distribution or reproduction in other forums is permitted, provided the original author(s) or licensor are credited and that the original publication in this journal is cited, in accordance with accepted academic practice. No use, distribution or reproduction is permitted which does not comply with these terms.



Involvement of Phosphatidylinositol 3-kinase in the regulation of proline catabolism in *Arabidopsis thaliana*

Anne-Sophie Leprince^{1,2*}, Nelly Magalhaes^{1,2}, Delphine De Vos^{1,2†}, Marianne Bordenave¹, Emilie Crialat¹, Gilles Clément², Christian Meyer², Teun Munnik³ and Arnould Savouré^{1*}

¹ Sorbonne Universités, Université Pierre et Marie Curie Univ Paris 06, Adaptation de Plantes aux Contraintes Environnementales, URF5, Paris, France

² INRA-AgroParisTech, Institut Jean-Pierre Bourgin, UMR 1318, ERL CNRS 3559, Saclay Plant Sciences, Versailles, France

³ Section Plant Physiology, Swammerdam Institute for Life Sciences, University of Amsterdam, Amsterdam, Netherlands

Edited by:

Eric Ruelland, Centre National de la Recherche Scientifique, France

Reviewed by:

Dietmar Funck, University of Konstanz, Germany

Maurizio Trovato, University of Rome Sapienza, Italy

***Correspondence:**

Anne-Sophie Leprince and Arnould Savouré, Sorbonne Universités, UPMC Univ Paris 06, APCE URF5, Case 156, 4 Place Jussieu, F-75252, Paris 05, France
e-mail: anne-sophie.leprince@upmc.fr; arnould.savoure@upmc.fr

†Present address:

Anne-Sophie Leprince and Delphine De Vos, INRA-AgroParisTech, Institut Jean-Pierre Bourgin, UMR 1318, ERL CNRS 3559, Saclay Plant Sciences, Versailles, France

Plant adaptation to abiotic stresses such as drought and salinity involves complex regulatory processes. Deciphering the signaling components that are involved in stress signal transduction and cellular responses is of importance to understand how plants cope with salt stress. Accumulation of osmolytes such as proline is considered to participate in the osmotic adjustment of plant cells to salinity. Proline accumulation results from a tight regulation between its biosynthesis and catabolism. Lipid signal components such as phospholipases C and D have previously been shown to be involved in the regulation of proline metabolism in *Arabidopsis thaliana*. In this study, we demonstrate that proline metabolism is also regulated by class-III Phosphatidylinositol 3-kinase (PI3K), VPS34, which catalyses the formation of phosphatidylinositol 3-phosphate (PI3P) from phosphatidylinositol. Using pharmacological and biochemical approaches, we show that the PI3K inhibitor, LY294002, affects PI3P levels *in vivo* and that it triggers a decrease in proline accumulation in response to salt treatment of *A. thaliana* seedlings. The lower proline accumulation is correlated with a lower transcript level of *Pyrroline-5-carboxylate synthetase 1* (*P5CS1*) biosynthetic enzyme and higher transcript and protein levels of *Proline dehydrogenase 1* (*ProDH1*), a key-enzyme in proline catabolism. We also found that the *ProDH1* expression is induced in a *pi3k*-hemizygous mutant, further demonstrating that PI3K is involved in the regulation of proline catabolism through transcriptional regulation of *ProDH1*. A broader metabolomic analysis indicates that LY294002 also reduced other metabolites, such as hydrophobic and aromatic amino acids and sugars like raffinose.

Keywords: *Arabidopsis thaliana*, lipid signaling, Phosphatidylinositol 3-kinase (PI3K), proline, proline dehydrogenase 1 (*ProDH1*), salt stress

INTRODUCTION

As sessile organisms, plants need to cope with adverse environmental stresses. Abiotic constraints such as drought and salinity have a major impact on plant development and crop productivity (Zhu, 2002). A common feature of drought and salt stress is the lower availability of water, due to decrease of soil water potential. In addition, salt generates an ionic stress due to the presence of Na^+ and Cl^- . Perception of drought and salt constraints triggers complex signaling networks, which then induce the adaptive response of plants. Among these networks, various molecular components are involved, including phytohormones, protein kinases and phosphatases, and second messengers like Ca^{2+} , ROS, and lipid signaling elements (Munnik and Vermeer, 2010; Huang et al., 2012; Deinlein et al., 2014; Golldack et al., 2014).

Phospholipids are important structural components of cellular membranes but can also play an essential role in the adaptation of plants to abiotic stress (Munnik and Testerink, 2009; Xue et al., 2009; Munnik and Vermeer, 2010; McLoughlin and Testerink, 2013). They are modified by enzymes such as phospholipase C

(PLC) and D (PLD), and by lipid-kinases, such as diacylglycerol kinase (DGK), PA kinase and various phosphoinositide kinases (Meijer and Munnik, 2003). These modifications produce important second messengers that regulate various plant responses.

Phosphatidylinositol 3-kinase (PI3K) phosphorylates the D-3 position of the inositol ring of phosphoinositides. In mammals, three distinct PI3K classes (I-III) can be distinguished, differing in gene structure, enzyme regulation, and substrate preference. Class III PI3Ks are homologous to the yeast VPS34, which uses PI as a sole substrate to produce PI3P (Backer, 2008). VPS34 promotes membrane fusion and vesicle trafficking by recruiting PI3P-binding proteins to membranes. VPS34 is associated with different proteins, forming distinct protein complexes, including the regulation of mTORC1 (Target of rapamycin complex 1) that monitors the nutritional status of the cell (Backer, 2008; Ktistakis et al., 2012; Robaglia et al., 2012).

Higher plants only contain VPS34-like PI3Ks (Lee et al., 2010). In *Arabidopsis*, PI3K activity is encoded by a single gene (*At1g60490*), which is important for pollen development

(Welters et al., 1994; Lee et al., 2010). Pollen grains harboring a *pi3k* KO allele display abnormal germination (Lee et al., 2008b; Gao and Zhang, 2012), preventing the acquirement of homozygous *pi3k* KO mutants. PI3P has been detected in vacuolar membranes and in late endosomal and pre-vacuolar compartments, indicating that, like in mammals and yeast, plant PI3K is involved in vesicle trafficking and membrane biogenesis (Voigt et al., 2005; Vermeer et al., 2006; Lee et al., 2010; Simon et al., 2014). PI3P is considered as a second messenger that recruits PI3P-binding proteins to membranes (Meijer and Munnik, 2003; Van Leeuwen et al., 2004; Wyrial and Singh, 2010). Numerous data indicate that PI3K and its product PI3P are involved in plant responses to drought and salt stress. PI3P participates in stomata closure in response to abscisic acid (ABA) and ROS production in guard cells (Jung et al., 2002; Park et al., 2003; Choi et al., 2008). Also NADPH oxidase endocytosis leading to ROS production upon ionic stress is triggered by PI3K via PI3P (Leshem et al., 2007).

In plants, PI3P can be further phosphorylated by PI3P-5 kinase (FAB) to produce PI(3,5)P₂ (Meijer et al., 1999; Munnik and Nielsen, 2011; Gao and Zhang, 2012).

Wortmannin (Acaro and Wymann, 1993) and LY294002 (Vlahos et al., 1994) are pharmacological PI3K inhibitors that have frequently been used to decipher the function of PI3Ks and their products in various mammalian and yeast systems. LY294002 is derived from the flavonoid quercetin and competes with ATP and binds to a Lys residue in the ATP-binding pocket of PI3Ks (Walker et al., 2000). As such, LY294002 has been described to inhibit PI3K-related kinases such as TOR (Target of rapamycin) and DNA-PK (DNA-dependent protein kinase; Brunn et al., 1996), but also other protein kinases, such as Casein Kinase 2 (Gharbi et al., 2007). Nevertheless LY294002 is considered to be a more selective PI3K inhibitor (Walker et al., 2000; Jung et al., 2002; Templeton and Moorhead, 2005).

In plants, Wortmannin and LY294002 have also been used to show the involvement PI3K and PI3P (Jung et al., 2002; Park et al., 2003; Jallais et al., 2006; Vermeer et al., 2006; Leshem et al., 2007; Choi et al., 2008; Lee et al., 2008a; Takáč et al., 2012, 2013). LY294002 was shown to inhibit stomatal closing induced by ABA, polar tip-growth of root hairs, and chloroplast accumulation in response to blue light (Jung et al., 2002; Lee et al., 2008a; Aggarwal et al., 2013). At the subcellular level, LY294002 blocks endocytosis and vacuolar trafficking and inhibits auxin-mediated ROS generation (Etxeberria et al., 2005; Joo et al., 2005). Despite LY294002's frequent use, only few reports have showed an effect on PI3K activity *in vitro* (Jung et al., 2002; Joo et al., 2005), yet none *in vivo*.

In response to water stress, plants accumulate organic osmolytes such as amino acids, sugars and polyamines, which play key roles in decreasing the cellular osmotic potential but also in preventing the aggregation and/or precipitation of macromolecules following the decrease of water availability (Slama et al., 2015). Among these organic osmolytes, free proline is well known to rapidly increase upon water constraints (Szabados and Savouré, 2010; Liang et al., 2013). Proline levels represent a delicate balance between biosynthesis and catabolism. Proline is synthesized from glutamate by a two-step reaction (Szabados and Savouré, 2010; Liang et al., 2013). First, glutamate is reduced to glutamyl-5-semialdehyde (GSA) by the bifunctional enzyme

pyrroline-5-carboxylate synthetase (P5CS). GSA is then spontaneously converted to P5C, which is then reduced to proline by P5C reductase (P5CR). The rate-limiting enzyme of the biosynthetic pathway is P5CS, which is encoded by two genes *P5CS1* and *P5CS2* in *A. thaliana*. These two isoforms play distinct roles during development and stress responses (Székely et al., 2008). Under normal growth conditions, proline biosynthesis occurs in the cytosol and is mainly under the control of *P5CS2*. *P5CS2* has been shown to be expressed in dividing cells, in meristematic and reproductive tissues (Strizhov et al., 1997; Székely et al., 2008; Mattioli et al., 2009). Upon salt stress and drought, proline accumulation is dependent of *P5CS1* expression (Savouré et al., 1995; Yoshioka et al., 1995). *P5CS1* has been shown to be localized in chloroplasts upon water stress by Székely et al. (2008).

Upon relief from stress, proline is rapidly oxidized in mitochondria by a two-step reaction. First, proline is oxidized by proline dehydrogenase (ProDH) to form P5C, which is then oxidized to glutamate by P5C dehydrogenase (P5CDH). ProDH is the rate-limiting enzyme for proline catabolism and is encoded in *Arabidopsis* by two genes, *ProDH1* (also named *ERD5*) and *ProDH2* (Servet et al., 2012). *ProDH1* is considered as the main isoform, *ProDH2* being weakly expressed (Kiyosue et al., 1996; Funck et al., 2010). Under either salt or drought stress, *ProDH1* expression is repressed allowing proline accumulation (Funck et al., 2010). On the opposite, when stress is relieved, *ProDH1* expression is triggered leading to proline degradation in mitochondria (Kiyosue et al., 1996; Verbruggen et al., 1996).

Proline accumulation in response to water stress is not only important for osmotic adjustment, but also as scavenger for reactive oxygen species (ROS) and molecular chaperone to stabilize proteins, antioxidant enzymes and membrane structures (Szabados and Savouré, 2010; Liang et al., 2013). Proline is also considered as a source of energy, which may be important upon stress recovery (Szabados and Savouré, 2010; Liang et al., 2013; Kavi Kishor and Sreenivasulu, 2014).

As proline accumulation and degradation result from a tight regulation of its metabolism, deciphering the signaling networks involved is of prime importance. Activation of proline biosynthesis is linked to both ABA mediated-signal transduction (Strizhov et al., 1997; Abrahám et al., 2003) and ABA-independent signaling (Savouré et al., 1997; Sharma and Verslues, 2010). *P5CS1* expression was also shown to be positively regulated by ROS, acting as intermediate in ABA-mediated proline accumulation, while ProDH activity was repressed (Yang et al., 2009).

In *Arabidopsis*, lipid signaling components are involved in the regulation of *P5CS1* expression. Under normal growth condition, PLD negatively regulates *P5CS1* expression, preventing proline accumulation (Thiery et al., 2004). Upon ionic but not osmotic stress, PLC triggers *P5CS1* expression leading to proline accumulation (Parre et al., 2007). *P5CS1* up-regulation by PLC involves Ca^{2+} as a second messenger, which acts as a molecular switch to trigger downstream signaling events (Parre et al., 2007). Expression of both *ProDH* genes is regulated by bZIP transcription factors (Weltmeier et al., 2006; Hanson et al., 2008). After dark treatment or in response to hypoosmolarity stress, *ProDH1* expression is induced by the heterodimer bZIP53/bZIP10 which recognizes the ACTCAT regulating sequence in *ProDH1* promoter

(Satoh et al., 2004; Weltmeier et al., 2006; Dietrich et al., 2011).

Here, the role of PI3K in the regulation of proline accumulation was investigated. Using a pharmacological and biochemical approach, we show that the decrease of PI3P by LY294002 treatment correlated with lower proline accumulation upon salt stress in *Arabidopsis* seedlings. The decrease of proline content was associated with both the reduction of *P5CS1* transcript and protein levels and the induction of *ProDH1* transcript and protein levels. In a reverse genetic approach, using a hemizygous *pi3k* mutant, a similar pattern of *ProDH1* expression was found as WT seedlings treated with LY294002. During normal growth condition, a strong expression of *ProDH1* is detected in WT seedlings treated with LY294002 as well as in *pi3k* hemizygous mutant. These data suggest that a signaling pathway involving PI3P participates to the regulation of proline metabolism in normal growth condition and in response to salt stress through the repression of proline catabolism. A detailed metabolite profiling analysis was conducted to search for other compounds regulated by PI3P. Interestingly, raffinose exhibited a similar pattern of accumulation as proline in the presence of LY294002. In addition, hydrophobic- and aromatic amino acid contents strongly increased in presence of LY294002.

MATERIALS AND METHODS

PLANT MATERIAL

Arabidopsis (*Arabidopsis thaliana*) Heynh, ecotype Columbia Col-0 as wild-type (WT) and *pi3k* hemizygous mutant from GABI library (GK_418H02-018138) were used. In the hemizygous *pi3k* mutant (*PI3K/pi3k*), T-DNA insertion is located in the fifth exon of one allele of the gene (Lee et al., 2008b). WT seeds were sown on 0.5× Murashige and Skoog (MS) solid medium (0.8% agar) in 14-cm-diameter Petri dishes as described previously (Parre et al., 2007). *pi3k* mutant seeds were sown on 0.5× MS solid medium supplemented with 19.2 μM sulfadiazine (dissolved in DMSO) in order to select hemizygous plants versus WT homozygous plants. After 16 h at 4°C to raise dormancy, seeds were germinated and grown under continuous light with an intensity of 90 μmole photons m⁻² s⁻¹ for 12 days at 22°C.

STRESS AND PHARMACOLOGICAL TREATMENTS

Twelve-days-old seedlings were removed from 0.5× MS agar plates and put onto liquid 0.5× MS medium (control) supplemented with either 200 mM NaCl or 400 mM mannitol. After different incubation times, seedlings were collected and immediately frozen in liquid nitrogen and stored at -80°C prior analysis.

For pharmacological treatments, seedlings were pre-treated for 1 h in 0.5× MS liquid medium with various concentrations of LY294002 dissolved in DMSO or with the same amount of DMSO as a control. Seedlings were thereafter transferred for 3 h or 24 h onto 0.5× MS liquid medium alone (control), or supplemented with either 200 mM NaCl or 400 mM mannitol and with the same amount of DMSO or LY294002 as for the pre-treatment.

PROLINE DETERMINATION

Free proline contents were measured using L-proline as a standard according to Bates et al. (1973).

PHOSPHOLIPIDS ANALYSIS

For practical reasons this experiment was performed on 3- to 5-days-old seedlings into a 2 mL Eppendorf tube containing 200 μL of 2.5 mM MES/KOH buffer (pH 5.7) and 1 mM KCl. In order to label phospholipids, 10 μCi of ³²P-inorganic phosphate were added in each tube and incubated overnight (Munnik and Zarza, 2013). Either 100 μM LY294002 or the same amount of DMSO for the control were then added for 1 h of pre-incubation. Then a volume of 2.5 mM MES/KOH buffer (pH 5.7), 1 mM KCl buffer with 400 mM NaCl was added into the tube to reach a final concentration of 200 mM NaCl. For control condition, an equivalent volume of MES/KCl buffer was added. Treatments were stopped just after the addition of NaCl (0 h), or after 30 min or 3 h, by adding perchloric acid (5% w/v, final concentration), and after 10 min shaking the total solvent was removed. To extract lipids from the seedlings, 400 μL CHCl₃/MeOH/HCl (50/100/1, v/v/v) was added and the mix was vortexed for 10 min. To induce the separation of two phases, 400 μL CHCl₃ and 200 μL 0.9% (w/v) NaCl were added, vortexed 10 s and then centrifuged for 1 min at 10,000 g. The organic lower phase was transferred to a new tube containing 400 μL CHCl₃/MeOH/1M HCl (3/48/47, v/v/v). After shaking and centrifugation, the upper phase was removed, and 20 μL isopropanol was added to the purified organic phase, which was then dried down in a vacuum centrifuge at 50°C. The residue was dissolved in 100 μL CHCl₃.

Phospholipids were separated as previously described (Munnik et al., 1994, 1995; Munnik and Zarza, 2013) by thin-layer chromatography (TLC) using heat-activated silica gel plates impregnated with a solution of 1% K-oxalate, 2 mM EDTA in MeOH/H₂O (2/3, v/v) and chromatographed with an alkaline solvent CHCl₃/MeOH/NH₄OH/H₂O (90/70/4/16, v/v/v/v). Radiolabeled phospholipids were visualized and quantified using a phosphoImager.

In order to separate PI3P and PI4P, spots corresponding to the PIP pool was scraped off from the TLC plate and deacylated with 800 μL of mono-methylamine reagent (25% mono-methylamine/MeOH/n-ButOH (42.8/45.7/11.5, v/v/v) at 53°C for 30 min as described in (Munnik et al., 1994, 1996; Munnik, 2013). Samples were centrifuged at 10,000 g for 2 min and the supernatant was collected and dried under a N₂ stream for 30 min and then by rotary evaporation. To remove the fatty-acyl groups, samples were dissolved in 500 μL H₂O and extracted twice with 600 μL n-ButOH/petroleum ether (40–60°)/ethyl formate (20/40/1, v/v/v). The aqueous lower phase that contains glycerophosphoinositides (GroPInsP) was dried by rotary evaporation, dissolved in 500 μL H₂O and filtered (0.22 μm).

GroPIns3P and GroPIns4P were separated by anion-exchange HPLC using a Partisil 10-SAX column and a discontinuous gradient of 1.25 M NaH₂PO₄ (pH 3.7) at a flow rate of 1 ml·min⁻¹ (Munnik, 2013). Fractions were collected every 30 s and measured for radioactivity by liquid-scintillation counting.

NORTHERN BLOTH ANALYSIS

Total RNAs were isolated from seedlings ground in liquid nitrogen using the guanidinium thiocyanate-CsCl purification method (Sambrook et al., 1989). RNAs were separated by electrophoresis in a 1.2% agarose-formaldehyde gel. After transfer to nylon membrane, RNAs were fixed by UV cross-linking. Membranes

were hybridized at 65°C with either specific 3'UTR region of *AtP5CS1* or with full length of *AtProDH1* according to Church and Gilbert (1984). The fragments were labeled with ^{32}P -dCTP using Ready-To-GoTM DNA labeling beads. Before hybridization, membranes were stained with methylene blue as a control for RNA loading and transfer. The hybridization signals were quantified using a PhosphorImager (Amersham Biosciences, USA).

QUANTITATIVE RT-qPCR ANALYSIS

Total RNAs were extracted following the protocol of the RNeasy Plant Mini Kit (Qiagen) from around 100 mg of powder obtained after grinding a pool of seedlings. After treatment with the RNase-free DNase (Fermentas), 1.5 μg of total RNA were reverse-transcribed by Revertaid™ Reverse Transcriptase (Fermentas) using 1 μM oligodT following the manufacturer instructions. The resulting first-strand cDNA was 20-fold diluted and used as the template for real-time quantitative PCR (RT-qPCR) amplification performed on a MasterCycler® ep realplex thermocycler (Eppendorf) with Maxima® SYBR Green/ROX qPCR Master Mix (Thermo Scientific) following the manufacturer protocol. Each reaction was performed with 5 μL diluted cDNA sample in a total reaction volume of 15 μL . The relative expression of *P5CS1* (*At2g39800*), *ProDH1* (*At3g30775*) and *PI3K* (*At1g60490*) genes were determined using specific primers (Supplementary Table 1). Expression levels of the different genes were standardized to *APT1* (*At1g27450*) used as a standard reference. The applied RT-qPCR program was 2 min at 95°C, 40 cycles with 15 s at 95°C, 30 s at 57°C and 30 s at 72°C followed by 15 s at 95°C, 15 s at 55°C, a gradual temperature rise of 20 min to 55°C at 95°C associated with a streaming of the plate, followed by 15 s at 95°C. The expression level of each gene was calculated using the following equation: $2^{(\text{Ct}_{\text{APT1}} - \text{Ct}_{\text{gene}})} \times 100$.

GEL ELECTROPHORESIS, ELECTRO-BLOTTING AND IMMUNOLOGICAL DETECTION

Proteins were extracted as described in Martínez-García et al. (1999) separated by SDS-PAGE (Laemmli, 1970) and transferred electrophoretically to a nitrocellulose membrane in a solution of 48 mM Tris, 39 mM glycine, 0.04% (w/v) SDS and 20% (v/v) ethanol at 50 mA for 1 h. For immunodetection, the nitrocellulose membrane was incubated in TBS with 0.05% (v/v) Tween 20 (TBS-T) and 5% non-fat dry milk for 1 h at 4°C and then in TBS-T with 0.1% (v/v) rabbit antiserum for 16 h at room temperature. Antisera were obtained by immunization of rabbits with either P5CS or ProDH recombinant proteins (Thiery et al., 2004). Blots were washed with TBS-T. Detection was performed with an ECL assay using horseradish peroxidase-conjugated secondary antibodies (GE Healthcare). Equal protein loading and integrity of protein samples were verified by Ponceau S red staining of the blot membrane.

METABOLITE PROFILING USING GC-MS AND METABOLOMICS DATA PROCESSING

Three independent samples of 12-days-old seedlings from each genotype treated during 24 h in different conditions were collected, and the equivalent of 50 mg of powder of each samples

were used to perform the extraction and further metabolomics analysis. Extraction, derivatization, analysis, and data processing were performed according to Fiehn (2006). Metabolites were analyzed by GC-MS 3 h after derivatization. One microliter of the derivatized samples was injected in splitless mode on an Agilent 7890A gas chromatograph coupled to an Agilent 5975C mass spectrometer. The column was an Rtx-5SilMS from Restek (30 m with 10-m Integra-Guard column). The liner (Restek 20994) was changed before each series of analyses, and 10 cm of column was removed. The oven temperature ramp was 70°C for 7 min then 10°C/min to 325°C for 4 min (run length 36.5 min). The helium constant flow was 1.5231 mL/min. Temperatures were as follows: injector, 250°C; transfer line, 290°C; source: 250°C; and quadripole, 150°C. Samples and blanks were randomized. Amino acid standards were injected at the beginning and end of the analysis to monitor the derivatization stability. An alkane mix (C10, C12, C15, C19, C22, C28, C32, and C36) was injected in the middle of the queue for external calibration. Five scans per second were acquired.

Metabolites were annotated, and their levels on a fresh weight basis were normalized with respect to the ribitol internal standard.

Raw Agilent data files were converted in NetCDF format and analyzed with AMDIS (<http://chemdata.nist.gov/mass-spc/amdis/>). A home retention index/mass spectra library built from the NIST, Golm, and Fiehn databases and standard compounds were used for metabolite identification. Peak areas were then determined using the Quanlynx software (Waters) after conversion of the NetCDF file to masslynx format. TMEV (<http://www.tm4.org/mev.html>) was used for all statistical analysis. Univariate analysis by permutation (One-Way and Two-Way ANOVA) was first used to select the significant metabolites. Multivariate analysis (hierarchical clustering and principal component analysis) was then performed on this subset.

RESULTS

LY294002 AFFECTS PROLINE ACCUMULATION ONLY IN RESPONSE TO SALT TREATMENT

To investigate whether PI3K is involved in the regulation of proline metabolism in response to ionic and/or hyperosmotic constraints, the effect of LY294002 on proline accumulation was assessed in 12-days-old *Arabidopsis* seedlings subjected to either 200 mM NaCl or 400 mM mannitol for 24 h. As shown in **Figure 1A**, typically a 5- to 6-fold accumulation of proline is observed in *Arabidopsis* seedlings treated with either NaCl or mannitol in comparison to the control seedlings. Interestingly, while LY294002 had no effect on the proline levels in control seedlings or seedlings stressed with mannitol (**Figure 1**), 40% less proline accumulated in the LY294002-treated seedlings upon salt stress. When increasing concentrations of LY294002 were applied, proline levels decreased in a dose-dependent manner in plants stressed with NaCl, with a maximum effect observed for 100 μM LY294002 (Supplementary Figure 1). In contrast, no effect on the proline levels of control or mannitol-stressed seedlings where found, whatever concentration of LY294002 (**Figure 1** and Supplementary Figure 1). These results show that LY294002 negatively regulates

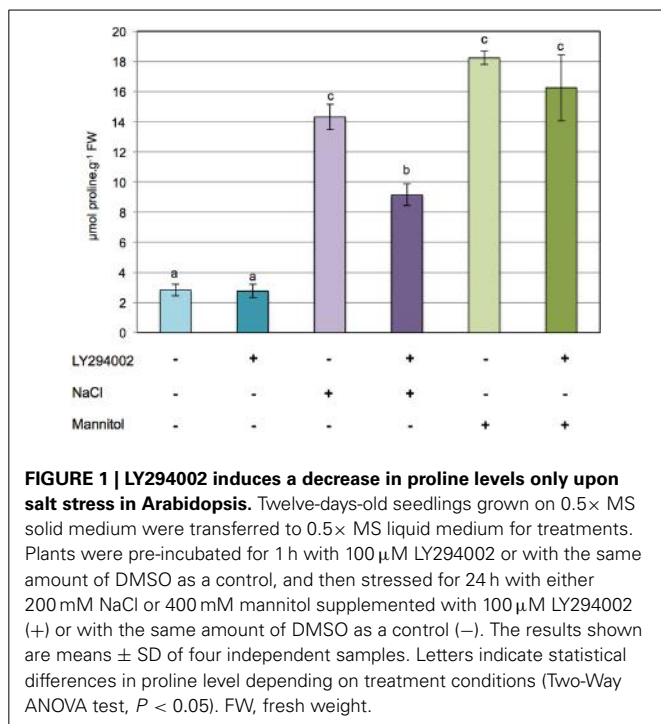


FIGURE 1 | LY294002 induces a decrease in proline levels only upon salt stress in *Arabidopsis*. Twelve-days-old seedlings grown on 0.5 × MS solid medium were transferred to 0.5 × MS liquid medium for treatments. Plants were pre-incubated for 1 h with 100 μM LY294002 or with the same amount of DMSO as a control, and then stressed for 24 h with either 200 mM NaCl or 400 mM mannitol supplemented with 100 μM LY294002 (+) or with the same amount of DMSO as a control (−). The results shown are means \pm SD of four independent samples. Letters indicate statistical differences in proline level depending on treatment conditions (Two-Way ANOVA test, $P < 0.05$). FW, fresh weight.

proline accumulation in response to salt stress but not to mannitol.

LY294002 REDUCES THE LEVEL OF PI3P

In order to characterize the inhibitory effect of LY294002 on PI3K activity, *in vivo* PI3P levels were measured. For practical reasons, 6-days-old seedlings were used. These seedlings accumulated slightly less proline than the 12-days-old seedlings after NaCl treatment but the results were consistent, indicating that the younger seedlings perceived and responded well to salt stress (data not shown).

Seedlings were $^{32}\text{P}_i$ -labeled overnight and the lipids extracted and separated by TLC (Supplementary Figure 2). Phosphoinositides (PI, PIP, and PIP₂) were quantified using PhosphoImaging (Figure 2A). PI, a structural phospholipid of membranes, represented 11–12 % of the total ^{32}P -labeled phospholipids, and its levels remained fairly constant throughout our experiments. PIP and PIP₂ are minor lipid constituents and accounted for 1–2% and 0.1–0.15% of the total phospholipids, respectively. PIP₂ progressively increased upon salt stress, reaching a 3-fold increase at 3 h compared to control seedlings, while no significant effects of salt stress were found for PIP levels. Interestingly, LY294002 treatment caused a slight but significant decrease in PIP₂ under control conditions as well as in response to salt stress.

In plants, the PIP pool is composed of 3 isomers, PI3P, PI4P, and PI5P (Munnik and Vermeer, 2010). PI4P is the most predominant PIP species (~80–90%), with PI3P and PI5P each accounting for ~5–10% of the PIP pool (Meijer et al., 2001). On TLC, the PIP isomers cannot be separated but by removing their fatty acids and analysing the resulting glycerophosphoinositolphosphates (GroPInsPs) by HPLC, it is relatively easy to

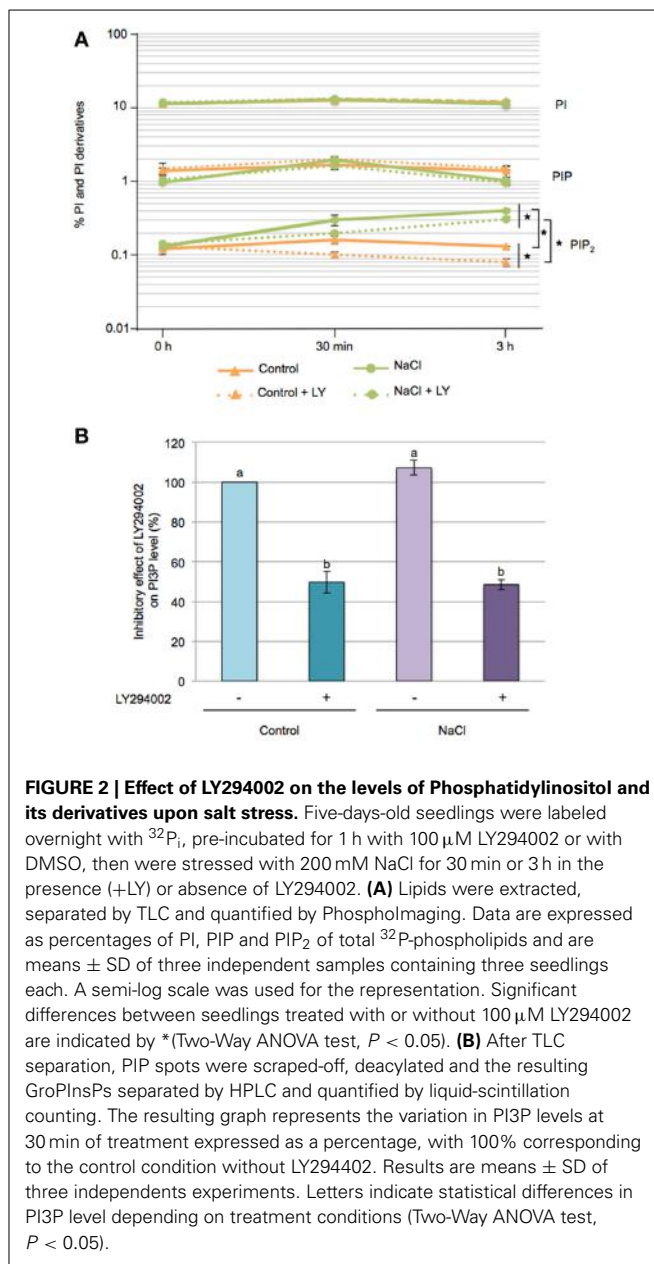


FIGURE 2 | Effect of LY294002 on the levels of Phosphatidylinositol and its derivatives upon salt stress. Five-days-old seedlings were labeled overnight with $^{32}\text{P}_i$, pre-incubated for 1 h with 100 μM LY294002 or with DMSO, then were stressed with 200 mM NaCl for 30 min or 3 h in the presence (+LY) or absence of LY294002. **(A)** Lipids were extracted, separated by TLC and quantified by PhosphoImaging. Data are expressed as percentages of PI, PIP and PIP₂ of total ^{32}P -phospholipids and are means \pm SD of three independent samples containing three seedlings each. A semi-log scale was used for the representation. Significant differences between seedlings treated with or without 100 μM LY294002 are indicated by * (Two-Way ANOVA test, $P < 0.05$). **(B)** After TLC separation, PIP spots were scraped-off, deacylated and the resulting GroPInsPs separated by HPLC and quantified by liquid-scintillation counting. The resulting graph represents the variation in PI3P levels at 30 min of treatment expressed as a percentage, with 100% corresponding to the control condition without LY294002. Results are means \pm SD of three independent experiments. Letters indicate statistical differences in PI3P level depending on treatment conditions (Two-Way ANOVA test, $P < 0.05$).

distinguish and quantify the GroPIns3P from the GroPIns4P and GroPIns5P. The latter two are rather difficult to separate (Meijer et al., 2001).

So to determine the PI3P levels under our conditions, TLC-separated ^{32}P -labeled PIP spots from 30 min treated seedlings were scraped off, deacylated and separated by anion-exchange HPLC. At control and salt conditions, PI3P was found to account for ~5% of the PIP pool. Addition of 100 μM LY294002, however, induced a 50% decrease of PI3P, whatever control or stress condition (Figure 2B). These results, and the inhibitory effect of LY294002 on proline accumulation in response to salt stress, are consistent with the involvement of PI3P as a lipid mediator on the regulation of proline metabolism.

LY294002 IMPACTS THE EXPRESSION OF GENES INVOLVED IN PROLINE METABOLISM

Proline accumulation is the consequence of a tight regulation of gene expression (Szabadó and Savouré, 2010; Liang et al., 2013). We investigated transcript accumulation of two genes involved in proline metabolism, *P5CS1* and *ProDH1* that encode key enzymes regulating proline biosynthesis and catabolism, respectively. RT-qPCR analysis showed a 17-fold higher *AtP5CS1* transcript accumulation in seedlings upon 3 h salt stress than in control ones (Supplementary Figure 3), which lower to 3-fold at 24 h salt stress. In addition, salt stress induced a slight accumulation of *AtProDH1* transcript but only after 24 h (Supplementary Figure 3).

The role of PI3K on key genes and enzymes involved in proline metabolism was investigated using LY294002. Northern and western blot analysis revealed that LY294002 affected mRNA and protein accumulation in all tested conditions. After 3 h LY294002 treatment, a modest increase of *P5CS1* mRNA was observed in control condition while *ProDH1* transcripts were not detectable (Figure 3A). A dramatic effect of LY294002 on both *P5CS1* and *ProDH1* expression compared to non-treated seedlings was observed at 24 h salt stress. In salt stress seedlings treated with LY294002, *P5CS1* steady state transcript level was lower than in non-treated ones while *ProDH1* transcript level was higher (Figure 3A). In salt stress seedlings treated with LY294002, *P5CS1* transcript accumulation decreased by 60% (Figure 3C) compared to non-treated seedlings. RT-qPCR analysis confirmed the higher *ProDH1* transcript accumulation in presence of LY294002 whatever the growth conditions (Figure 3C). Using western blots, LY294002 triggered P5CS accumulation in control seedlings while P5CS level diminished in salt-treated plantlets. In contrast, LY294002 strongly enhanced ProDH accumulation in both control and salt-treated seedlings (Figure 3B).

The lower proline accumulation observed in response to salt stress with LY294002 is correlated with a down-regulation of *P5CS1* and up-regulation of *ProDH1* at both transcript and protein levels. As LY294002 reduced PI3P levels, our data suggest that PI3K is involved in the regulation of proline metabolism.

ProDH1 EXPRESSION IS INDUCED IN *pi3k* MUTANT

To further unravel the role of PI3K in the regulation of proline metabolism, we aimed for *Arabidopsis pi3k* KO mutants. Unfortunately, however, homozygous *pi3k* mutants are not viable (Lee et al., 2008b; Gao and Zhang, 2012). To partly resolve this issue, we selected sulfadiazine-resistant seedlings to get hemizygous *pi3k* mutant (Leshem et al., 2007; Lee et al., 2008a,b). Segregation analysis indicated a 1:1 ratio in sulfadiazine resistant and sensitive seedlings, respectively (data not shown), due to the male gametophytic defect (Lee et al., 2008b). Therefore *PI3K/pi3k* hemizygous mutants were selected and further analyzed (Figure 4A). PCR-based genotyping of GABI_418H02 *pi3k* mutants confirmed that no homozygous mutants were obtained from this selection (data not shown).

Expression analysis by RT-qPCR revealed a 25% decrease of steady-state *PI3K* transcript level in *pi3k* hemizygous mutants compared to WT (Figure 4B). In this mutant, *ProDH1* transcript level was almost 5-fold higher than in WT seedlings in normal growth condition. On the contrary, no difference in *P5CS1*

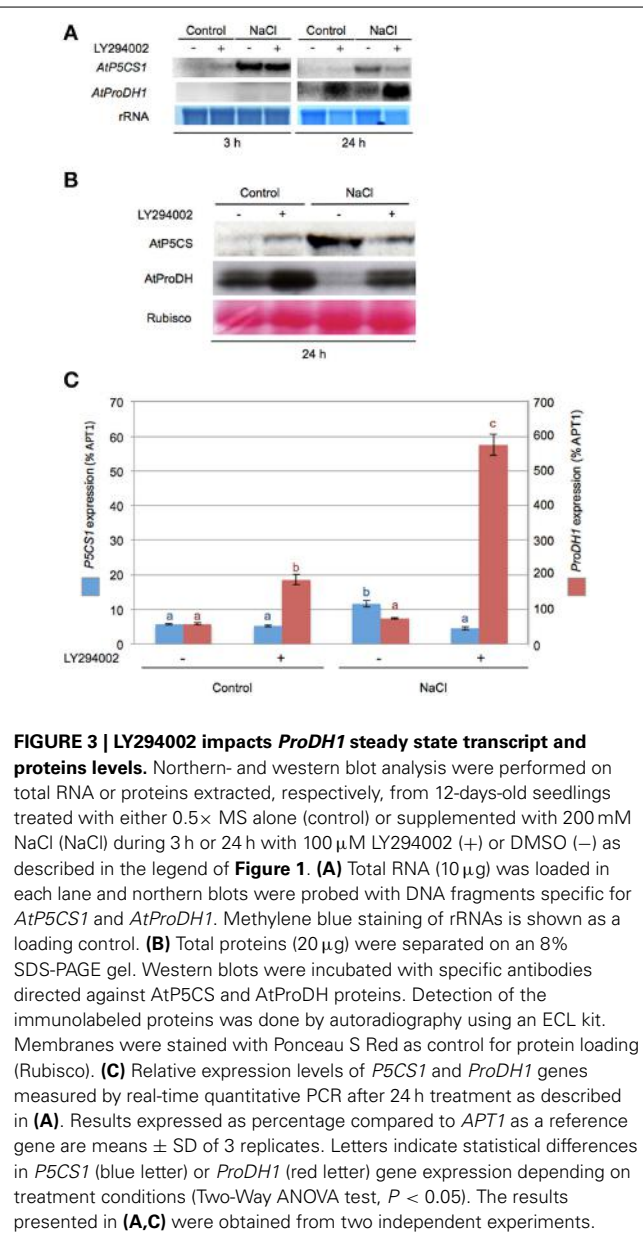


FIGURE 3 | LY294002 impacts *ProDH1* steady state transcript and protein levels. Northern- and western blot analysis were performed on total RNA or proteins extracted, respectively, from 12-days-old seedlings treated with either 0.5x MS alone (control) or supplemented with 200 mM NaCl (NaCl) during 3 h or 24 h with 100 μ M LY294002 (+) or DMSO (-) as described in the legend of Figure 1. (A) Total RNA (10 μ g) was loaded in each lane and northern blots were probed with DNA fragments specific for *AtP5CS1* and *AtProDH1*. Methylene blue staining of rRNAs is shown as a loading control. (B) Total proteins (20 μ g) were separated on an 8% SDS-PAGE gel. Western blots were incubated with specific antibodies directed against AtP5CS and AtProDH proteins. Detection of the immunolabeled proteins was done by autoradiography using an ECL kit. Membranes were stained with Ponceau S Red as control for protein loading (Rubisco). (C) Relative expression levels of *P5CS1* and *ProDH1* genes measured by real-time quantitative PCR after 24 h treatment as described in (A). Results expressed as percentage compared to *APT1* as a reference gene are means \pm SD of 3 replicates. Letters indicate statistical differences in *P5CS1* (blue letter) or *ProDH1* (red letter) gene expression depending on treatment conditions (Two-Way ANOVA test, $P < 0.05$). The results presented in (A,C) were obtained from two independent experiments.

transcript level was observed between WT and *pi3k* hemizygous mutant.

When WT and *pi3k* hemizygous mutant were subjected to 200 mM NaCl for 24 h, they showed a higher proline accumulation of 18-fold and 11.5-fold, respectively (Figure 5A). *pi3k* hemizygous mutant showed a lower proline accumulation in response to NaCl. However the proline accumulation was not significantly different from WT seedlings, probably due to the remaining *PI3K* wild-type allele.

P5CS1 and *ProDH1* transcript levels were investigated in *pi3k* hemizygous seedlings in response to 3 and 24 h of salt stress (Figure 5B). *P5CS1* mRNA accumulation was similar in WT and *pi3k* hemizygous in response to salt stress. An equivalent increase of *P5CS1* transcripts was observed at 3 h of stress and a decrease at 24 h of stress. Higher *ProDH1* transcript levels than WT were

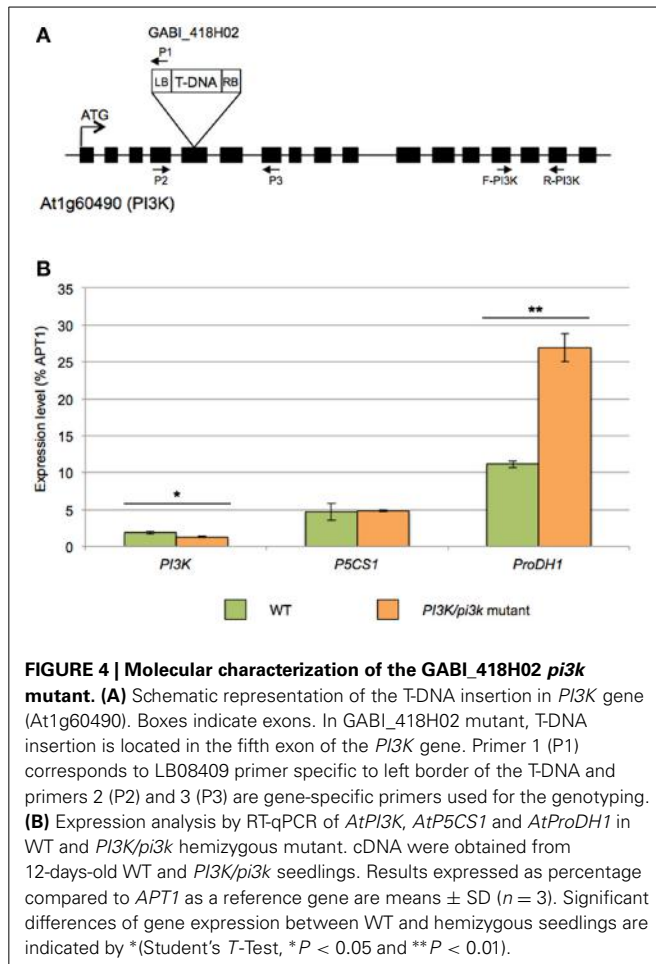


FIGURE 4 | Molecular characterization of the GABI_418H02 *pi3k* mutant. (A) Schematic representation of the T-DNA insertion in *PI3K* gene (At1g60490). Boxes indicate exons. In GABI_418H02 mutant, T-DNA insertion is located in the fifth exon of the *PI3K* gene. Primer 1 (P1) corresponds to LB08409 primer specific to left border of the T-DNA and primers 2 (P2) and 3 (P3) are gene-specific primers used for the genotyping. **(B)** Expression analysis by RT-qPCR of *AtPI3K*, *AtP5CS1* and *AtProDH1* in WT and *PI3K/pi3k* hemizygous mutant. cDNA were obtained from 12-days-old WT and *PI3K/pi3k* seedlings. Results expressed as percentage compared to *APT1* as a reference gene are means \pm SD ($n = 3$). Significant differences of gene expression between WT and hemizygous seedlings are indicated by *(Student's *T*-Test, * $P < 0.05$ and ** $P < 0.01$).

observed in *pi3k* mutant in all tested conditions whether the seedlings were subjected to salt stress or not (Figure 5B). In *pi3k* hemizygous mutant, ProDH protein levels were stronger than in WT at both 3 and 24 h salt stress (Figure 5C). These results indicate that *pi3k* hemizygous seedlings are able to respond to salt stress, triggering *P5CS1* gene expression and proline accumulation, although the transcript level of *ProDH1* gene is increased. Alltogether, our data indicate that the higher level of *ProDH1* transcripts is correlated with higher ProDH amount in *pi3k* mutant. These data are consistent with those obtained with LY294002 treatment (Figure 3), where LY294002 induced higher *ProDH1* transcripts and proteins. These results further strengthen the participation of a PI3K-mediated pathway regulating proline catabolism.

LY294002 AFFECTS SEEDLING METABOLOME

To investigate other changes induced by LY294002, we compared the metabolite profiles of 12-days old WT seedlings treated with LY294002 or DMSO upon control and salt stress conditions. Hierarchic clustering analysis indicated that DMSO did not have any significant effect on the relative metabolites contents, indicating that the difference in the metabolite patterns obtained with LY294002 is an effect of the inhibitor (Figure 6). Treatment for 24 h of salt stress significantly modified the amounts of several

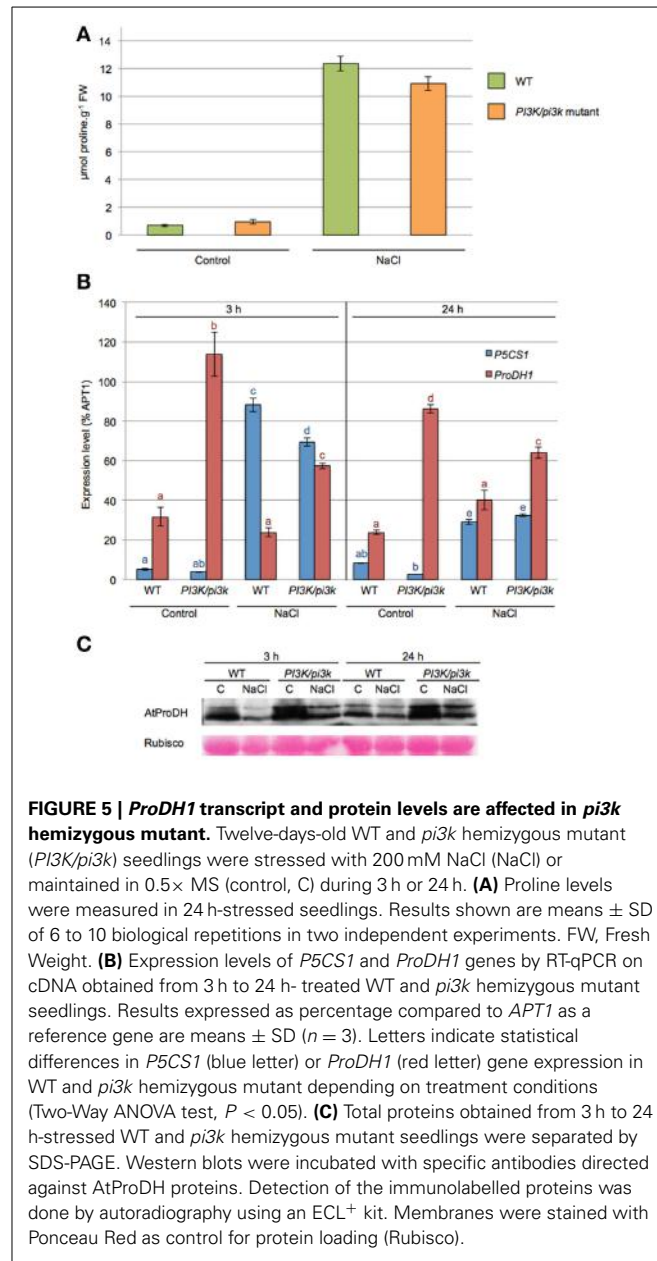
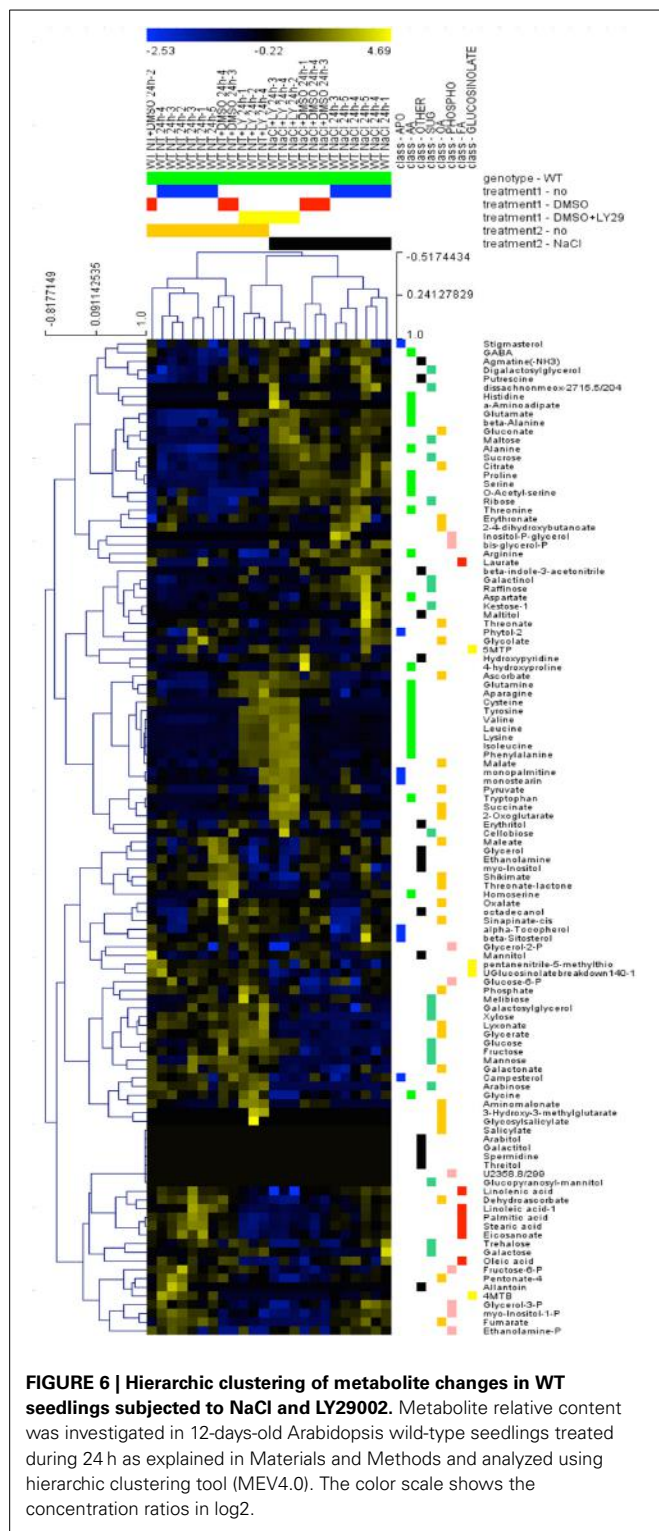
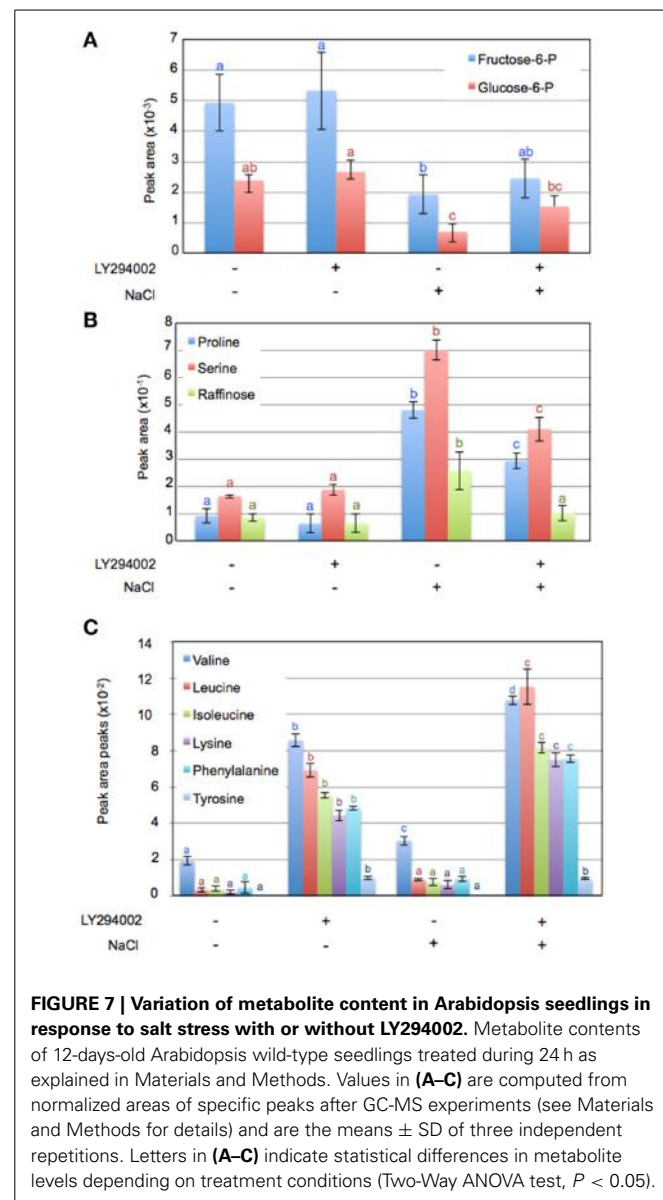


FIGURE 5 | *ProDH1* transcript and protein levels are affected in *pi3k* hemizygous mutant. Twelve-days-old WT and *pi3k* hemizygous mutant (*PI3K/pi3k*) seedlings were stressed with 200 mM NaCl (NaCl) or maintained in 0.5× MS (control, C) during 3 h or 24 h. **(A)** Proline levels were measured in 24-h-stressed seedlings. Results shown are means \pm SD of 6 to 10 biological repetitions in two independent experiments. FW, Fresh Weight. **(B)** Expression levels of *P5CS1* and *ProDH1* genes by RT-qPCR on cDNA obtained from 3 h to 24 h-treated WT and *pi3k* hemizygous mutant seedlings. Results expressed as percentage compared to *APT1* as a reference gene are means \pm SD ($n = 3$). Letters indicate statistical differences in *P5CS1* (blue letter) or *ProDH1* (red letter) gene expression in WT and *pi3k* hemizygous mutant depending on treatment conditions (Two-Way ANOVA test, $P < 0.05$). **(C)** Total proteins obtained from 3 h to 24 h-stressed WT and *pi3k* hemizygous mutant seedlings were separated by SDS-PAGE. Western blots were incubated with specific antibodies directed against AtProDH proteins. Detection of the immunolabelled proteins was done by autoradiography using an ECL⁺ kit. Membranes were stained with Ponceau Red as control for protein loading (Rubisco).

metabolites. Relative amounts of sucrose, ribose and maltose as well as proline, serine and raffinose increased in response to salt stress (Figures 6, 7B). On the contrary, the amounts of some other sugars, like galactose, mannose, trehalose and xylose (Figure 6) and glucose-6-phosphate (Glucose-6-P) and fructose-6-phosphate (Fructose-6-P) decreased in response to salt stress (Figure 7A). LY294002 reduced the level of proline content almost by half (Figure 7B), in accordance with our previous results (Figure 1 and Supplementary Figure 1). Interestingly, two other compatible osmolytes, serine and raffinose, exhibited an accumulation pattern similar to that of proline, i.e., higher accumulation in response to salt stress and lower when LY294002 is added (Figure 7B). Surprisingly, LY294002 addition had a strong impact on some amino-acid levels whatever the treatment. The



most dramatic effect being for tyrosine with an almost 100-fold increase in the presence of LY294002, in either control condition or NaCl stress (Figure 7C). Similarly, a 10–20-fold increase was observed for lysine, leucine, isoleucine and phenylalanine and a 4-fold increase for valine in response to LY294002.



Thus, the strong increase of those aliphatic and aromatic amino acids in presence of LY294002 suggests that PI3K, and/or its product PI3P, negatively regulates their metabolism through inhibition of their synthesis and/or promotion of their catabolism.

DISCUSSION

In this paper, we investigated the effect of the PI3K inhibitor, LY294002, on the response of Arabidopsis seedlings to salt stress. LY294002 was found to reduce PI3P levels by 50% and to dramatically decrease the accumulation of proline upon salt stress. The latter was a consequence of lower transcript- and protein levels for P5CS1 and higher transcript and protein levels for ProDH1. In the *pi3k* hemizygous mutant line, as also observed for WT seedlings treated with LY294002, an up-regulation of *ProDH1* expression was found, suggesting that PI3K and its product PI3P are involved

in a pathway repressing *ProDH1* expression. Metabolomic profiling of *Arabidopsis* seedlings in response to salt stress showed that LY294002 reduced the amount of raffinose, another compatible osmolyte, and strongly increased the amount of free aliphatic and aromatic amino acids.

NaCl STRESS MODIFIED PHOSPHOINOSITIDE COMPOSITION

PI is not only a structural phospholipid of membranes, but also a precursor of several signaling phosphoinositides that are produced by distinct kinases and phosphatases, which add and remove phosphates at different positions of the inositol ring (Mueller-Roeber and Pical, 2002; Xue et al., 2009; Munnik and Vermeer, 2010; Munnik and Nielsen, 2011). Characterization of the phospholipid composition of overnight ^{32}P -labeled *Arabidopsis* seedlings showed that salt stress mostly affected the PIP_2 pool. This latter is predominantly composed of the PI(4,5)P₂ isomer (Munnik, 2013). Some plant systems, in particular *Chlamydomonas*, have reported on increased PI(3,5)P₂ levels (Meijer et al., 1999), but we did not observe this here for *Arabidopsis* seedlings. Increased PIP_2 levels in response to salt and/or osmotic stress have been reported for several plant systems (Pical et al., 1999; DeWald et al., 2001; Zonia and Munnik, 2004; Darwish et al., 2009; Munnik and Zarza, 2013). Part of this PI(4,5)P₂ response occurs at the plasma membrane (Van Leeuwen et al., 2007; König et al., 2008), where it is considered to be an important signaling molecule (Munnik and Nielsen, 2011), potentially through initiation of vesicle budding via its interaction with clathrin-adapter proteins. The subsequent formation of clathrin-coated vesicles during salt stress could be a mechanism for the cell to modify the plasma membrane according to water/ion movement (König et al., 2008). E.g., PI(4,5)P₂ has been suggested to modulate stomatal aperture in response to water stress by regulating K⁺-efflux channel (Lee and Lee, 2008). Alternatively, PI(4,5)P₂ can be hydrolysed by PLC to form inositol trisphosphate (IP₃) and DAG, which can both be rapidly metabolized into other signaling molecules, e.g., IP₆ and phosphatidic acid (Munnik and Vermeer, 2010). PLC has been implicated in salt stress signaling (Drøbak and Watkins, 2000; Tasma et al., 2008; Xue et al., 2009; Munnik and Vermeer, 2010). In addition, Parre et al. (2007) have demonstrated that proline biosynthesis in response to salt stress is regulated by a Ca²⁺-signature depending on PLC activity.

LY294002 addition had a small effect on the PIP_2 pool. Theoretically, as an ATP analog, LY294002 could inhibit other enzymes (Davies et al., 2000; Walker et al., 2000; Gharbi et al., 2007), but to our knowledge there is no report regarding such an effect on PIP 5-kinases. Another explanation could be that vesicles containing the LY294002-sensitive PI3P pool require the downstream synthesis of PIP_2 , for example, to fuse with or pinch-off from membranes.

Minor changes in PIP levels were measured in *Arabidopsis* seedlings upon salt stress. This pool is a mixture of 3 isomers, i.e., PI3P, PI4P, and PI5P. The latter isomer is thought to result from PI(3,5)P₂ dephosphorylation and is, like its precursor, present at very low concentrations (Meijer et al., 2001; Munnik, 2013). Since the PIP isomers cannot be separated by TLC, we removed the fatty acids by chemical deacylation and analyzed the resulting

GroPInsP isomers by anion-exchange chromatography. As such, we found that only 5% of the PIP pool accounted for PI3P. The majority of the pool was composed of PI4P pool (>90%). PI5P levels were not determined as they were extremely difficult to separate from the 4-isomer (Meijer et al., 2001). LY294002 caused the PI3P pool to be reduced by 50%. No variation was observed in response to salt stress. Earlier, Meijer et al. (2001) reported an increase in PI3P after 5 min of 300 mM NaCl but this was in *Chlamydomonas*, which seems to exhibit a big difference in PI3P- and PI(3,5)P₂ metabolism compared to higher plants. To our knowledge, there is no other data available on the effect of salt on PI3P levels. Nevertheless, several studies have indicated a role for PI3P in the plant's response to salt or water stress on the basis of PI3K inhibitors. As such, PI3P has been implicated in the regulation of stomatal closure in response to ABA (Jung et al., 2002). Leshem et al. (2007) have demonstrated that PI3P triggers the endocytosis of NADPH oxidase located at the plasma membrane under salt stress and this was implicated in the formation of ROS, which are important signaling molecules for plants to cope with salt stress (Leshem et al., 2006; Ben Rejeb et al., 2014). Phosphoinositides recruit proteins through specific phosphoinositide-binding domains to particular membranes (Van Leeuwen et al., 2004; Banerjee et al., 2010; Munnik and Nielsen, 2011). As such, the interaction between PI3P and the immunophilin ROF1 could participate in the plant's response to salt stress too (Karali et al., 2012). In addition, PI3P can participate in the regulation of vesicular trafficking and vacuole formation by recruiting proteins such as VTI11 and EPSIN that are involved in membrane fusion (Lee and Lee, 2008; Lee et al., 2010; Zheng et al., 2014a,b).

PI3P IS INVOLVED IN THE REPRESSION OF PROLINE CATABOLISM

Proline accumulation is a well-known plant response to salt, and more generally, to water stress (Szabadó and Savouré, 2010; Gupta and Huang, 2014). We found that LY294002 reduced the proline accumulation in response to salt stress. This could be explained by repression of proline biosynthesis and induction of proline catabolism genes both at the RNA and protein levels. The strong induction of *ProDH1* expression and the accumulation of the corresponding protein were correlated with the inhibitory effect of LY294002 on PI3P levels in both control and stress conditions, suggesting a role of PI3P on the inhibition of proline catabolism whatever the conditions. This hypothesis was confirmed by studies on *pi3k* mutant. *ProDH1* expression was higher in *pi3k* mutant than in the WT upon salt stress but also in normal growth condition. On the contrary, *P5CS1* expression while being diminished by LY294002 was not affected in *pi3k* mutant, suggesting that LY294002 may also act on other protein kinase activity involved in signaling pathway regulating *P5CS1* expression. We previously found evidence that *P5CS1* expression in response to salt stress fell under the regulation of PLC activity (Parre et al., 2007). Here, seedlings treated with LY294002 had a lower PIP_2 response with salt. Maybe the lower availability of PIP_2 as PLC substrate contributes to the reduced *P5CS1* expression. The comparison between seedlings treated with LY and *pi3k* mutant showed differences in *P5CS* expression in contrast to *ProDH* expression. This may be due to the fact that LY294002 could

have additional effects like inhibiting other kinases. Another possibility is that adaptation to long-term decrease in PI3K activity could occur in the hemizygous *pi3k* mutant whereas the effect of LY294002 is more sudden and could change some of the plant stress responses.

Lee et al. (2008b) indicated that the *pi3k* mutant is strongly impaired in its pollen development, leading to the inability to obtain homozygous mutant. Our segregation analysis also showed a gametophytic defect in *pi3k* mutant, which explained why only *pi3k* hemizygous mutant could be obtained. *pi3k* mutant showed a reduced expression of the complete gene, in agreement with Leshem et al. (2007) and to the lethal phenotype of the reported antisense transformation (Welters et al., 1994). Consequently, genetic and biochemical analyses of PI3K are very difficult to assess. The development of promoter inducible lines may be useful to further investigate the role of PI3K in plant stress adaptation.

ProDH1 expression is under the control of bZIP10 and bZIP53 transcription factors (Satoh et al., 2004; Weltmeier et al., 2006; Dietrich et al., 2011; Veerabagu et al., 2014). Their expression and activity is regulated by various abiotic constraints, and also by the nutrient status of the plant (Weltmeier et al., 2009). In mammals, nutrient deficiency induces *ProDH* gene expression as a consequence of mTOR complex inactivation (Liao et al., 2008). VPS34 has been shown to participate in the regulation of mTOR upon nutrient stress (Backer, 2008). TOR is a protein kinase that possesses a catalytic domain with strong homology to the kinase domain of PI3K, and has also been shown to be sensitive to LY294002 (Brunn et al., 1996). In *Arabidopsis*, it is therefore possible that LY294002 inhibits TOR kinase too and as a result ProDH. Nevertheless, the fact that the *ProDH1* increase is also observed in the *pi3k* hemizygous mutant background supports a direct involvement of the PI3K pathway in repressing *ProDH1*. TOR could even be a downstream component of PI3K and as such participate in the regulation of *ProDH* expression. This has already been observed in other eukaryotes (Liao et al., 2008).

BESIDES PROLINE ACCUMULATION, LY294002 AFFECTS PLANT METABOLISM

Salt stress affects several metabolites, among them sugars such as hexose-phosphates, disaccharides and raffinose family oligosaccharides (RFO). Sucrose, maltose and raffinose accumulated in response to salt stress, whereas Glu-6-P and Fru-6-P decreased. Variations of these sugar contents are well-conserved responses among various plant species upon salt stress (Kempa et al., 2008; Sanchez et al., 2008). These sugars are derived from photosynthesis activity. They have a key role in osmoprotection, in ROS scavenging and as a source of carbon storage (Keunen et al., 2013; Gupta and Huang, 2014). Sugar could also be considered as signaling molecules regulating gene expression and triggering specific responses to abiotic stress (Keunen et al., 2013). Raffinose is the only sugar whose accumulation was reduced by 50% in salt-stressed *Arabidopsis* seedlings treated with LY294002. Similar to proline, raffinose is also considered as a compatible solute for plant cells (Valluru and Van den Ende, 2011; Van den Ende, 2013). In order to determine whether the biosynthesis of raffinose upon salt stress is dependent of the same signaling pathway

as proline, it will be of interest to investigate the regulation of raffinose metabolism in *pi3k* mutant background.

The accumulation of several amino acids other than proline was observed upon salt stress. Aliphatic (Val, Leu, Ileu) and aromatic (Phe, Tyr) amino acids increased in response to salt stress (our study; Kempa et al., 2008; Sanchez et al., 2008), but also after an extended period of darkness (Usadel et al., 2008). These authors suggested that these might be due to induction of protein catabolism and/or remobilization of nitrogen sources. Surprisingly, a dramatic increase of these amino acids was observed in seedlings treated with LY294002 grown in normal conditions. Further experiments will be required to determine the role of PI3K signaling in the regulation of amino acid metabolism.

In conclusion, our results strongly indicate that a signaling pathway involving PI3K and its product PI3P is involved in the repression of proline catabolism upon salt stress. Identifying specific PI3P targets will allow to decipher whether TOR is an intermediate signaling component in the regulation of ProDH in plants.

ACKNOWLEDGMENTS

We thank L. Thiery and E. Parre for their early participation to this work. Part of this work got financial support from COST program FA0605 STSM. We also thank Prof. Pierre Carol for critical reading of the manuscript. The COST action FA0901 “Putting Halophytes to Work – From Genes to Ecosystems” is acknowledged for its financial support. This work was supported by UPMC.

SUPPLEMENTARY MATERIAL

The Supplementary Material for this article can be found online at: <http://www.frontiersin.org/Journal/10.3389/fpls.2014.00772/abstract>

REFERENCES

- Abrahám, E., Rigó, G., Székely, G., Nagy, R., Koncz, C., and Szabados, L. (2003). Light-dependent induction of proline biosynthesis by abscisic acid and salt stress is inhibited by brassinosteroid in *Arabidopsis*. *Plant Mol. Biol.* 51, 363–372. doi: 10.1023/A:1022043000516
- Acaro, A., and Wymann, M. P. (1993). Wortmannin is a potent phosphatidylinositol 3-kinase inhibitor: the role of phosphatidylinositol 3,4,5-triphosphate in neutrophil responses. *Biochem. J.* 296, 297–301.
- Aggarwal, C., Labuz, J., and Gabryś, H. (2013). Phosphoinositides play differential roles in regulating phototropin1- and phototropin2-mediated chloroplast movements in *Arabidopsis*. *PLoS ONE* 8:e55393. doi: 10.1371/journal.pone.0055393
- Backer, J. M. (2008). The regulation and function of Class III PI3Ks: novel roles for Vps34. *Biochem. J.* 410, 1–17. doi: 10.1042/BJ20071427
- Banerjee, S., Basu, S., and Sarkar, S. (2010). Comparative genomics reveals selective distribution and domain organization of FYVE and PX domain proteins across eukaryotic lineages. *BMC Genomics* 11:83. doi: 10.1186/1471-2164-11-83
- Bates, L. S., Waldren, R. P., and Teare, I. D. (1973). Rapid determination of free proline for water-stress studies. *Plant Soil* 39, 205–207. doi: 10.1007/BF00018060
- Ben Rejeb, K., Abdelly, C., and Savouré, A. (2014). How reactive oxygen species and proline face stress together. *Plant Physiol. Biochem.* 80, 278–284. doi: 10.1016/j.plaphy.2014.04.007
- Brunn, G. J., Williams, J., Sabers, C., Wiederrecht, G., Lawrence, J. C. Jr., and Abraham, R. T. (1996). Direct inhibition of the signaling functions of the mammalian target of rapamycin by the phosphoinositide 3-kinase inhibitors, wortmannin and LY294002. *EMBO J.* 15, 5256–5267.

- Choi, Y., Lee, Y., Jeon, B. W., Staiger, C. J., and Lee, Y. (2008). Phosphatidylinositol 3- and 4-phosphate modulate actin filament reorganization in guard cells of day flower. *Plant Cell Environ.* 31, 366–377. doi: 10.1111/j.1365-3040.2007.01769.x
- Church, G. M., and Gilbert, W. (1984). Genomic sequencing. *Proc. Natl. Acad. Sci. U.S.A.* 81, 1991–1995. doi: 10.1073/pnas.81.7.1991
- Darwish, E., Testerink, C., Khalil, M., El-Shihy, O., and Munnik, T. (2009). Phospholipid signaling responses in salt-stressed rice leaves. *Plant Cell Physiol.* 50, 986–997. doi: 10.1093/pcp/pcp051
- Davies, S. P., Reddy, H., Caivano, M., and Cohen, P. (2000). Specificity and mechanism of action of some commonly used protein kinase inhibitors. *Biochem. J.* 351, 95–105. doi: 10.1042/0264-6021:3510095
- Deinlein, U., Stephan, A. B., Horie, T., Luo, W., Xu, G., and Schroeder, J. I. (2014). Plant salt-tolerance mechanisms. *Trends Plant Sci.* 19, 371–379. doi: 10.1016/j.tplants.2014.02.001
- DeWald, D. B., Torabinejad, J., Jones, C. A., Shope, J. C., Cangelosi, A. R., Thompson, J. E., et al. (2001). Rapid accumulation of phosphatidylinositol 4,5-bisphosphate and inositol 1,4,5-trisphosphate correlates with calcium mobilization in salt-stressed arabidopsis. *Plant Physiol.* 126, 759–769. doi: 10.1104/pp.126.2.759
- Dietrich, K., Weltmeier, F., Ehlert, A., Weiste, C., Stahl, M., Harter, K., et al. (2011). Heterodimers of the Arabidopsis transcription factors bZIP1 and bZIP53 reprogram amino acid metabolism during low energy stress. *Plant Cell* 23, 381–395. doi: 10.1105/tpc.110.075390
- Dröbak, B. K., and Watkins, P. A. (2000). Inositol(1,4,5)trisphosphate production in plant cells: an early response to salinity and hyperosmotic stress. *FEBS Lett.* 481, 240–244. doi: 10.1016/S0014-5793(00)01941-4
- Etxeberria, E., Baroja-Fernandez, E., Muñoz, F. J., and Pozueta-Romero, J. (2005). Sucrose-inducible endocytosis as a mechanism for nutrient uptake in heterotrophic plant cells. *Plant Cell Physiol.* 46, 474–481. doi: 10.1093/pcp/pci044
- Fiehn, O. (2006). Metabolite profiling in Arabidopsis. *Methods Mol. Biol.* 323, 439–447. doi: 10.1385/1-59745-003-0:439
- Funck, D., Eckard, S., and Müller, G. (2010). Non-redundant functions of two proline dehydrogenase isoforms in Arabidopsis. *BMC Plant Biol.* 10:70. doi: 10.1186/1471-2229-10-70
- Gao, X.-Q., and Zhang, X. S. (2012). Metabolism and roles of phosphatidylinositol 3-phosphate in pollen development and pollen tube growth in Arabidopsis. *Plant Signal. Behav.* 7, 165–169. doi: 10.4161/psb.18743
- Gharbi, S. I., Zvelebil, M. J., Shuttleworth, S. J., Hancox, T., Saghir, N., Timms, J. F., et al. (2007). Exploring the specificity of the PI3K family inhibitor LY294002. *Biochem. J.* 404, 15–21. doi: 10.1042/BJ20061489
- Golldack, D., Li, C., Mohan, H., and Probst, N. (2014). Tolerance to drought and salt stress in plants: unraveling the signaling networks. *Front. Plant Sci.* 5:151. doi: 10.3389/fpls.2014.00151
- Gupta, B., and Huang, B. (2014). Mechanism of salinity tolerance in plants: physiological, biochemical, and molecular characterization. *Int. J. Genomics* 2014:701596. doi: 10.1155/2014/701596
- Hanson, J., Hanssen, M., Wiese, A., Hendriks, M. M., and Smeekens, S. (2008). The sucrose regulated transcription factor bZIP11 affects amino acid metabolism by regulating the expression of ASPARAGINE SYNTHETASE1 and PROLINE DEHYDROGENASE2. *Plant J.* 53, 935–949. doi: 10.1111/j.1365-313X.2007.03385.x
- Huang, G.-T., Ma, S.-L., Bai, L.-P., Zhang, L., Ma, H., Jia, P., et al. (2012). Signal transduction during cold, salt, and drought stresses in plants. *Mol. Biol. Rep.* 39, 969–987. doi: 10.1007/s11033-011-0823-1
- Jallais, Y., Fobis-Loisy, I., Miège, C., and Gaudé, T. (2006). AtSNX1 defines an endosome for auxin-carrier trafficking in Arabidopsis. *Nature* 443, 106–109. doi: 10.1038/nature05046
- Joo, J. H., Yoo, H. J., Hwang, I., Lee, J. S., Nam, K. H., and Bae, Y. S. (2005). Auxin-induced reactive oxygen species production requires the activation of phosphatidylinositol 3-kinase. *FEBS Lett.* 579, 1243–1248. doi: 10.1016/j.febslet.2005.01.018
- Jung, J.-Y., Kim, Y.-W., Kwak, J. M., Hwang, J.-U., Young, J., Schroeder, J. I., et al. (2002). Phosphatidylinositol 3- and 4-phosphate are required for normal stomatal movements. *Plant Cell* 14, 2399–2412. doi: 10.1105/tpc.004143
- Karali, D., Oxley, D., Runions, J., Ktistakis, N., and Farmaki, T. (2012). The *Arabidopsis thaliana* immunophilin ROF1 directly interacts with PI(3)P and PI(3,5)P₂ and affects germination under osmotic stress. *PLoS ONE* 7:e48241. doi: 10.1371/journal.pone.0048241
- Kavi Kishor, P. B., and Sreenivasulu, N. (2014). Is proline accumulation *per se* correlated with stress tolerance or is proline homeostasis a more critical issue? *Plant Cell Environ.* 37, 300–311. doi: 10.1111/pce.12157
- Kempa, S., Krasensky, J., Dal Santo, S., Kopka, J., and Jonak, C. (2008). A central role of abscisic acid in stress-regulated carbohydrate metabolism. *PLoS ONE* 3:e3935. doi: 10.1371/journal.pone.0003935
- Keunen, E., Peshev, D., Vangronsveld, J., Van den Ende, W., and Cuypers, A. (2013). Plant sugars are crucial players in the oxidative challenge during abiotic stress: extending the traditional concept. *Plant Cell Environ.* 36, 1242–1255. doi: 10.1111/pce.12061
- Kiyosue, T., Yoshioka, Y., Yamaguchi-Shinozaki, K., and Shinozaki, K. (1996). A nuclear gene encoding mitochondrial proline dehydrogenase, an enzyme involved in proline metabolism, is upregulated by proline but downregulated by dehydration in Arabidopsis. *Plant Cell* 8, 1323–1335. doi: 10.1105/tpc.8.8.1323
- König, S., Ischebeck, T., Lerche, J., Stenzel, I., and Heilmann, I. (2008). Salt-stress-induced association of phosphatidylinositol 4,5-bisphosphate with clathrin-coated vesicles in plants. *Biochem. J.* 415, 387–399. doi: 10.1042/BJ20081306
- Ktistakis, N. T., Manifava, M., Schoenfelder, P., and Rotondo, S. (2012). How phosphoinositide 3-phosphate controls growth downstream of amino acids and autophagy downstream of amino acid withdrawal. *Biochem. Soc. Trans.* 40, 37–43. doi: 10.1042/BST20110684
- Laemmli, U. K. (1970). Cleavage of structural proteins during the assembly of the head of bacteriophage T4. *Nature* 227, 680–685. doi: 10.1038/227680a0
- Lee, Y., Bak, G., Choi, Y., Chuang, W.-I., Cho, H.-T., and Lee, Y. (2008a). Roles of phosphatidylinositol 3-kinase in root hair growth. *Plant Physiol.* 147, 624–635. doi: 10.1104/pp.108.117341
- Lee, Y., Kim, E.-S., Choi, Y., Hwang, I., Staiger, C. J., Chung, Y.-Y., et al. (2008b). The Arabidopsis phosphatidylinositol 3-kinase is important for pollen development. *Plant Physiol.* 147, 1886–1897. doi: 10.1104/pp.108.121590
- Lee, Y., and Lee, Y. (2008). Roles of phosphoinositides in regulation of stomatal movements. *Plant Signal. Behav.* 3, 211–213. doi: 10.4161/psb.3.4.5557
- Lee, Y., Munnik, T., and Lee, Y. (2010). “Plant phosphatidylinositol 3-kinase,” in *Lipid Signaling in Plants*, ed T. Munnik (Berlin; Heidelberg: Springer Verlag), 95–106.
- Leshem, Y., Melamed-Book, N., Cagnac, O., Ronen, G., Nishri, Y., Solomon, M., et al. (2006). Suppression of Arabidopsis vesicle-SNARE expression inhibited fusion of H2O₂-containing vesicles with tonoplast and increased salt tolerance. *Proc. Natl. Acad. Sci. U.S.A.* 103, 18008–18013. doi: 10.1073/pnas.0604421103
- Leshem, Y., Seri, L., and Levine, A. (2007). Induction of phosphatidylinositol 3-kinase-mediated endocytosis by salt stress leads to intracellular production of reactive oxygen species and salt tolerance. *Plant J.* 51, 185–197. doi: 10.1111/j.1365-313X.2007.03134.x
- Liang, X., Zhang, L., Natarajan, S. K., and Becker, D. F. (2013). Proline mechanisms of stress survival. *Antioxid. Redox Signal.* 19, 998–1011. doi: 10.1089/ars.2012.5074
- Liao, X.-H., Majithia, A., Huang, X., and Kimmel, A. R. (2008). Growth control via TOR kinase signaling, an intracellular sensor of amino acid and energy availability, with crosstalk potential to proline metabolism. *Amino Acids* 35, 761–770. doi: 10.1007/s00726-008-0100-3
- Martínez-García, J. F., Monte, E., and Quail, P. H. (1999). A simple, rapid and quantitative method for preparing Arabidopsis protein extracts for immunoblot analysis. *Plant J.* 20, 251–257. doi: 10.1046/j.1365-313X.1999.00579.x
- Mattioli, R., Falasca, G., Sabatini, S., Altamura, M. M., Costantino, P., and Trovato, M. (2009). The proline biosynthetic genes *P5CS1* and *P5CS2* play overlapping roles in Arabidopsis flower transition but not in embryo development. *Physiol. Plant.* 137, 72–85. doi: 10.1111/j.1399-3054.2009.01261.x
- McLoughlin, F., and Testerink, C. (2013). Phosphatidic acid, a versatile water-stress signal in roots. *Front. Plant Sci.* 4:525. doi: 10.3389/fpls.2013.00525
- Meijer, H. J., Berrie, C. P., Iurisci, C., Divecha, N., Musgrave, A., and Munnik, T. (2001). Identification of a new polyphosphoinositide in plants, phosphatidylinositol 5-monophosphate (PtdIns5P), and its accumulation upon osmotic stress. *Biochem. J.* 360, 491–498. doi: 10.1042/0264-6021:3600491
- Meijer, H. J., Divecha, N., Van den Ende, H., Musgrave, A., and Munnik, T. (1999). Hyperosmotic stress induces rapid synthesis of phosphatidyl-D-inositol 3,5-bisphosphate in plant cells. *Planta* 208, 294–298. doi: 10.1007/s004250050561
- Meijer, H. J. G., and Munnik, T. (2003). Phospholipid-based signaling in plants. *Annu. Rev. Plant Biol.* 54, 265–306. doi: 10.1146/annurev.applant.54.031902.134748

- Mueller-Roeber, B., and Pical, C. (2002). Inositol phospholipid metabolism in Arabidopsis. Characterized and putative isoforms of inositol phospholipid kinase and phosphoinositide-specific phospholipase C. *Plant Physiol.* 130, 22–46. doi: 10.1104/pp.004770
- Munnik, T. (2013). Analysis of D3-,4-,5-phosphorylated phosphoinositides using HPLC. *Methods Mol. Biol.* 1009, 17–24. doi: 10.1007/978-1-62703-401-2_2
- Munnik, T., Arisz, S. A., De Vrije, T., and Musgrave, A. (1995). G Protein activation stimulates phospholipase D signaling in plants. *Plant Cell* 7, 2197–2210. doi: 10.1105/tpc.7.12.2197
- Munnik, T., De Vrije, T., Irvine, R. F., and Musgrave, A. (1996). Identification of diacylglycerol pyrophosphate as a novel metabolic product of phosphatidic acid during G-protein activation in plants. *J. Biol. Chem.* 271, 15708–15715. doi: 10.1074/jbc.271.26.15708
- Munnik, T., Irvine, R. F., and Musgrave, A. (1994). Rapid turnover of phosphatidylinositol 3-phosphate in the green alga Chlamydomonas eugametos: signs of a phosphatidylinositide 3-kinase signalling pathway in lower plants? *Biochem. J.* 298, 269–273.
- Munnik, T., and Nielsen, E. (2011). Green light for polyphosphoinositide signals in plants. *Curr. Opin. Plant Biol.* 14, 489–497. doi: 10.1016/j.pbi.2011.06.007
- Munnik, T., and Testerink, C. (2009). Plant phospholipid signaling: “in a nutshell.” *J. Lipid Res.* 50(Suppl.), S260–S265. doi: 10.1194/jlr.R800098-JLR200
- Munnik, T., and Vermeer, J. E. M. (2010). Osmotic stress-induced phosphoinositide and inositol phosphate signalling in plants. *Plant Cell Environ.* 33, 655–669. doi: 10.1111/j.1365-3040.2009.02097.x
- Munnik, T., and Zarza, X. (2013). Analyzing plant signaling phospholipids through 32Pi-labeling and TLC. *Methods Mol. Biol.* 1009, 3–15. doi: 10.1007/978-1-62703-401-2_1
- Park, K.-Y., Jung, J.-Y., Park, J., Hwang, J.-U., Kim, Y.-W., Hwang, I., et al. (2003). A role for phosphatidylinositol 3-phosphate in abscisic acid-induced reactive oxygen species generation in guard cells. *Plant Physiol.* 132, 92–98. doi: 10.1104/pp.102.016964
- Parre, E., Ghars, M. A., Leprince, A.-S., Thiery, L., Lefebvre, D., Bordenave, M., et al. (2007). Calcium signaling via phospholipase C is essential for proline accumulation upon ionic but not nonionic hyperosmotic stresses in Arabidopsis. *Plant Physiol.* 144, 503–512. doi: 10.1104/pp.106.095281
- Pical, C., Westergren, T., Dove, S. K., Larsson, C., and Sommarin, M. (1999). Salinity and hyperosmotic stress induce rapid increases in phosphatidylinositol 4,5-bisphosphate, diacylglycerol pyrophosphate, and phosphatidylcholine in *Arabidopsis thaliana* cells. *J. Biol. Chem.* 274, 38232–38240. doi: 10.1074/jbc.274.53.38232
- Robaglia, C., Thomas, M., and Meyer, C. (2012). Sensing nutrient and energy status by SnRK1 and TOR kinases. *Curr. Opin. Plant Biol.* 15, 301–307. doi: 10.1016/j.pbi.2012.01.012
- Sambrook, J., Fritsch, E. F., and Maniatis, T. (1989). *Molecular Cloning: A Laboratory Manual*. New York, NY: Laboratory Press.
- Sanchez, D. H., Siahpoosh, M. R., Roessner, U., Udvardi, M., and Kopka, J. (2008). Plant metabolomics reveals conserved and divergent metabolic responses to salinity. *Physiol. Plant.* 132, 209–219. doi: 10.1111/j.1399-3054.2007.00993.x
- Satoh, R., Fujita, Y., Nakashima, K., Shinozaki, K., and Yamaguchi-Shinozaki, K. (2004). A novel subgroup of bZIP proteins functions as transcriptional activators in hypoosmolarity-responsive expression of the ProDH gene in Arabidopsis. *Plant Cell Physiol.* 45, 309–317. doi: 10.1093/pcp/pch036
- Savouré, A., Hua, X. J., Bertauché, N., Van Montagu, M., and Verbruggen, N. (1997). Abscisic acid-independent and abscisic acid-dependent regulation of proline biosynthesis following cold and osmotic stresses in *Arabidopsis thaliana*. *Mol. Gen. Genet.* 254, 104–109. doi: 10.1007/s004380050397
- Savouré, A., Jaoua, S., Hua, X. J., Ardiles, W., Van Montagu, M., and Verbruggen, N. (1995). Isolation, characterization, and chromosomal location of a gene encoding the delta 1-pyrroline-5-carboxylate synthetase in *Arabidopsis thaliana*. *FEBS Lett.* 372, 13–19. doi: 10.1016/0014-5793(95)00935-3
- Servet, C., Ghelis, T., Richard, L., Zilberman, A., and Savoure, A. (2012). Proline dehydrogenase: a key enzyme in controlling cellular homeostasis. *Front. Biosci. (Landmark Ed.)* 17, 607–620. doi: 10.2741/3947
- Sharma, S., and Verslues, P. E. (2010). Mechanisms independent of abscisic acid (ABA) or proline feedback have a predominant role in transcriptional regulation of proline metabolism during low water potential and stress recovery. *Plant Cell Environ.* 33, 1838–1851. doi: 10.1111/j.1365-3040.2010.02188.x
- Simon, M., Platret, M., Assil, S., van Wijk, R., Chen, W. Y., Chory, J., et al. (2014). A multi-colour/multi-affinity marker set to visualize phosphoinositide dynamics in Arabidopsis. *Plant J.* 77, 322–337. doi: 10.1111/tpj.12358
- Slama, I., Abdelly, C., Bouchereau, A., Flowers, T., and Savouré, A. (2015). Diversity, distribution and roles of osmoprotective compounds accumulated in halophytes under abiotic stress. *Ann. Bot.* doi: 10.1093/aob/mcu239
- Strizhov, N., Abrahám, E., Okrész, L., Blickling, S., Zilberman, A., Schell, J., et al. (1997). Differential expression of two P5CS genes controlling proline accumulation during salt-stress requires ABA and is regulated by ABA1, ABI1 and AXR2 in Arabidopsis. *Plant J.* 12, 557–569. doi: 10.1046/j.1365-313X.1997.00557.x
- Szabados, L., and Savouré, A. (2010). Proline: a multifunctional amino acid. *Trends Plant Sci.* 15, 89–97. doi: 10.1016/j.tplants.2009.11.009
- Székely, G., Abrahám, E., Cséplő, A., Rigó, G., Zsigmond, L., Csiszár, J., et al. (2008). Duplicated P5CS genes of Arabidopsis play distinct roles in stress regulation and developmental control of proline biosynthesis. *Plant J.* 53, 11–28. doi: 10.1111/j.1365-313X.2007.03318.x
- Takáč, T., Pechan, T., Samajová, O., Ovečka, M., Richter, H., Eck, C., et al. (2012). Wortmannin treatment induces changes in Arabidopsis root proteome and post-Golgi compartments. *J. Proteome Res.* 11, 3127–3142. doi: 10.1021/pr201111n
- Takáč, T., Pechan, T., Samajová, O., and Samaj, J. (2013). Vesicular trafficking and stress response coupled to PI3K inhibition by LY294002 as revealed by proteomic and cell biological analysis. *J. Proteome Res.* 12, 4435–4448. doi: 10.1021/pr400466x
- Tasma, I. M., Brendel, V., Whitham, S. A., and Bhattacharyya, M. K. (2008). Expression and evolution of the phosphoinositide-specific phospholipase C gene family in *Arabidopsis thaliana*. *Plant Physiol. Biochem.* 46, 627–637. doi: 10.1016/j.plaphy.2008.04.015
- Templeton, G. W., and Moorhead, G. B. G. (2005). The phosphoinositide-3-OH-kinase-related kinases of *Arabidopsis thaliana*. *EMBO Rep.* 6, 723–728. doi: 10.1038/sj.embo.7400479
- Thiery, L., Leprince, A.-S., Lefebvre, D., Ghars, M. A., Debarbieux, E., and Savouré, A. (2004). Phospholipase D is a negative regulator of proline biosynthesis in *Arabidopsis thaliana*. *J. Biol. Chem.* 279, 14812–14818. doi: 10.1074/jbc.M308456200
- Usadel, B., Bläsing, O. E., Gibon, Y., Retzlaff, K., Höhne, M., Günther, M., et al. (2008). Global transcript levels respond to small changes of the carbon status during progressive exhaustion of carbohydrates in Arabidopsis rosettes. *Plant Physiol.* 146, 1834–1861. doi: 10.1104/pp.107.115592
- Valluru, R., and Van den Ende, W. (2011). Myo-inositol and beyond—emerging networks under stress. *Plant Sci.* 181, 387–400. doi: 10.1016/j.plantsci.2011.07.009
- Van den Ende, W. (2013). Multifunctional fructans and raffinose family oligosaccharides. *Front. Plant Sci.* 4:247. doi: 10.3389/fpls.2013.00247
- Van Leeuwen, W., Okrész, L., Bögör, L., and Munnik, T. (2004). Learning the lipid language of plant signalling. *Trends Plant Sci.* 9, 378–384. doi: 10.1016/j.tplants.2004.06.008
- Van Leeuwen, W., Vermeer, J. E. M., Gadella, T. W. J., and Munnik, T. (2007). Visualization of phosphatidylinositol 4,5-bisphosphate in the plasma membrane of suspension-cultured tobacco BY-2 cells and whole Arabidopsis seedlings. *Plant J.* 52, 1014–1026. doi: 10.1111/j.1365-313X.2007.03292.x
- Veerabagu, M., Kirchler, T., Elgass, K., Stadelhofer, B., Stahl, M., Harter, K., et al. (2014). The interaction of the arabidopsis response regulator arr18 with bzip63 mediates the regulation of PROLINE DEHYDROGENASE expression. *Mol. Plant* 7, 1560–1577. doi: 10.1093/mp/ssu074
- Verbruggen, N., Hua, X. J., May, M., and Van Montagu, M. (1996). Environmental and developmental signals modulate proline homeostasis: evidence for a negative transcriptional regulator. *Proc. Natl. Acad. Sci. U.S.A.* 93, 8787–8791. doi: 10.1073/pnas.93.16.8787
- Vermeer, J. E. M., van Leeuwen, W., Tobeña-Santamaría, R., Laxalt, A. M., Jones, D. R., Divecha, N., et al. (2006). Visualization of PtdIns3P dynamics in living plant cells. *Plant J.* 47, 687–700. doi: 10.1111/j.1365-313X.2006.02830.x
- Vlahos, C., Matter, W., Hui, K., and Brown, R. (1994). A specific inhibitor of phosphatidylinositol 3-kinase, 2-(4-morpholinyl)-8-phenyl-4H-1-benzopyran-4-one (LY294002). *J. Biol. Chem.* 269, 5241–5248.
- Voigt, B., Timmers, A. C. J., Samaj, J., Hlavacka, A., Ueda, T., Preuss, M., et al. (2005). Actin-based motility of endosomes is linked to the polar tip growth of root hairs. *Eur. J. Cell Biol.* 84, 609–621. doi: 10.1016/j.ejcb.2004.12.029

- Walker, E. H., Pacold, M. E., Perisic, O., Stephens, L., Hawkins, P. T., Wymann, M. P., et al. (2000). Structural determinants of phosphoinositide 3-kinase inhibition by wortmannin, LY294002, quercetin, myricetin, and staurosporine. *Mol. Cell* 6, 909–919. doi: 10.1016/S1097-2765(05)00089-4
- Welters, P., Takegawa, K., Emr, S. D., and Chrispeels, M. J. (1994). AtVPS34, a phosphatidylinositol 3-kinase of *Arabidopsis thaliana*, is an essential protein with homology to a calcium-dependent lipid binding domain. *Proc. Natl. Acad. Sci. U.S.A.* 91, 11398–11402. doi: 10.1073/pnas.91.24.11398
- Weltmeier, F., Ehlert, A., Mayer, C. S., Dietrich, K., Wang, X., Schütze, K., et al. (2006). Combinatorial control of *Arabidopsis* proline dehydrogenase transcription by specific heterodimerisation of bZIP transcription factors. *EMBO J.* 25, 3133–3143. doi: 10.1038/sj.emboj.7601206
- Weltmeier, F., Rahmani, F., Ehlert, A., Dietrich, K., Schütze, K., Wang, X., et al. (2009). Expression patterns within the *Arabidopsis* C/S1 bZIP transcription factor network: availability of heterodimerization partners controls gene expression during stress response and development. *Plant Mol. Biol.* 69, 107–119. doi: 10.1007/s11103-008-9410-9
- Wywial, E., and Singh, S. M. (2010). Identification and structural characterization of FYVE domain-containing proteins of *Arabidopsis thaliana*. *BMC Plant Biol.* 10:157. doi: 10.1186/1471-2229-10-157
- Xue, H.-W., Chen, X., and Mei, Y. (2009). Function and regulation of phospholipid signalling in plants. *Biochem. J.* 421, 145–156. doi: 10.1042/BJ20090300
- Yang, S.-L., Lan, S.-S., and Gong, M. (2009). Hydrogen peroxide-induced proline and metabolic pathway of its accumulation in maize seedlings. *J. Plant Physiol.* 166, 1694–1699. doi: 10.1016/j.jplph.2009.04.006
- Yoshiba, Y., Kiyosue, T., Katagiri, T., Ueda, H., Mizoguchi, T., Yamaguchi-Shinozaki, K., et al. (1995). Correlation between the induction of a gene for delta 1-pyrroline-5-carboxylate synthetase and the accumulation of proline in *Arabidopsis thaliana* under osmotic stress. *Plant J.* 7, 751–760. doi: 10.1046/j.1365-313X.1995.07050751.x
- Zheng, J., Han, S. W., Rodriguez-Welsh, M. F., and Rojas-Pierce, M. (2014a). Homotypic vacuole fusion requires VTI11 ans is regulated by phosphoinositides. *Mol. Plant* 7, 1026–1040. doi: 10.1093/mp/ssp019
- Zheng, J., Won Han, S., Munnik, T., and Rojas-Pierce, M. (2014b). Multiple vacuoles in impaired tonoplast trafficking3 mutants are independent organelles. *Plant Signal. Behav.* 9:e29783. doi: 10.4161/psb.29783
- Zhu, J. K. (2002). Salt and drought stress signal transduction in plants. *Annu. Rev. Plant Biol.* 53, 247–273. doi: 10.1146/annurev.arplant.53.091401.143329
- Zonia, L., and Munnik, T. (2004). Osmotically induced cell swelling versus cell shrinking elicits specific changes in phospholipid signals in tobacco pollen tubes. *Plant Physiol.* 134, 813–823. doi: 10.1104/pp.103.029454

Conflict of Interest Statement: The authors declare that the research was conducted in the absence of any commercial or financial relationships that could be construed as a potential conflict of interest.

Received: 15 September 2014; accepted: 15 December 2014; published online: 12 January 2015.

Citation: Leprince A-S, Magalhaes N, De Vos D, Bordenave M, Crilat E, Clément G, Meyer C, Munnik T and Savouré A (2015) Involvement of Phosphatidylinositol 3-kinase in the regulation of proline catabolism in *Arabidopsis thaliana*. *Front. Plant Sci.* 5:772. doi: 10.3389/fpls.2014.00772

This article was submitted to Plant Physiology, a section of the journal *Frontiers in Plant Science*.

Copyright © 2015 Leprince, Magalhaes, De Vos, Bordenave, Crilat, Clément, Meyer, Munnik and Savouré. This is an open-access article distributed under the terms of the Creative Commons Attribution License (CC BY). The use, distribution or reproduction in other forums is permitted, provided the original author(s) or licensor are credited and that the original publication in this journal is cited, in accordance with accepted academic practice. No use, distribution or reproduction is permitted which does not comply with these terms.



Ion and lipid signaling in apical growth—a dynamic machinery responding to extracellular cues

OPEN ACCESS

Edited by:

Eric Ruelland,
Centre National de la Recherche
Scientifique, France

Reviewed by:

Imara Y. Perera,
North Carolina State University, USA

Haitao Shi,
Hainan University, China

*Correspondence:

Rui Malhó and Reiaz Ul-Rehman,
BiolSI – Biosystems & Integrative
Sciences Institute, Faculdade
de Ciências, Universidade de Lisboa,
Campo Grande, 1749-016 Lisboa,
Portugal
r.malho@fc.ul.pt
reiazrehman@yahoo.co.in

†Present address:

Laura Saavedra,
Cátedra de Fisiología Vegetal,
Facultad de Ciencias Exactas, Físicas
y Naturales, Universidad Nacional
de Córdoba, Córdoba, Argentina;
Reiaz Ul-Rehman,
Department of Bioresources,
University of Kashmir, Hazratbal,
Srinagar 190006, India

Specialty section:

This article was submitted to
Plant Physiology,
a section of the journal
Frontiers in Plant Science

Received: 30 June 2015

Accepted: 18 September 2015

Published: 06 October 2015

Citation:

Malahó R, Serrazina S, Saavedra L,
Dias FV and Rehman RU (2015)
Ion and lipid signaling in apical
growth—a dynamic machinery
responding to extracellular cues.
Front. Plant Sci. 6:816.
doi: 10.3389/fpls.2015.00816

Rui Malhó*, Susana Serrazina, Laura Saavedra†, Fernando V. Dias and Reiaz Ul-Rehman*†

BiolSI – Biosystems & Integrative Sciences Institute, Faculdade de Ciências, Universidade de Lisboa, Lisboa, Portugal

Apical cell growth seems to have independently evolved throughout the major lineages of life. To a certain extent, so does our body of knowledge on the mechanisms regulating this morphogenetic process. Studies on pollen tubes, root hairs, rhizoids, fungal hyphae, even nerve cells, have highlighted tissue and cell specificities but also common regulatory characteristics (e.g., ions, proteins, phospholipids) that our focused research sometimes failed to grasp. The working hypothesis to test how apical cell growth is established and maintained have thus been shaped by the model organism under study and the type of methods used to study them. The current picture is one of a dynamic and adaptative process, based on a spatial segregation of components that network to achieve growth and respond to environmental (extracellular) cues. Here, we explore some examples of our live imaging research, namely on cyclic nucleotide gated ion channels, lipid kinases and syntaxins involved in exocytosis. We discuss how their spatial distribution, activity and concentration suggest that the players regulating apical cell growth may display more mobility than previously thought. Furthermore, we speculate on the implications of such perspective in our understanding of the mechanisms regulating apical cell growth and their responses to extracellular cues.

Keywords: Ca^{2+} , cyclic nucleotides, syntaxins, phosphoinositides, signaling, tip growth

Introduction

Apical tip growth is a form of cell extension common in all eukaryotes from rhizoids, pollen tubes, fungal hyphae to nerve cells. This growth form serves as a paradigm for cell polarity because cell extension is restricted to a narrow zone at the apex (Cheung and Wu, 2008). These cells are recognizably excellent models for cell research, particularly suitable for investigations on polarization, signal transduction, channel and ion flux activity, gene expression, cytoskeleton and wall structure, membrane dynamics and even cell-cell communication (Malahó et al., 2000; Onelli and Moscatelli, 2013; Sekereš et al., 2015).

As in any topic in science, advances in knowledge are dictated by current state of technology, the models under study and pre-existing ideas (typically represented in static diagrams such as the one represented in Figure 1). In the case of apical growth in plants, the outstanding technological advance registered in the past two decades, caused a perspective change from a morphological/structural approach to a dynamic/functional approach. When cell biology tools were predominantly used, researchers focused on larger cells that would grow straight and fast under *in vitro* conditions and would tolerate more harsh experimental conditions (e.g., microinjection, synthetic dyes, use of antibodies, and fixation methods). *Lilium longiflorum* was the paradigmatic example and underlying most experimental design was the hypothesis that if a molecule was important for tip growth, then

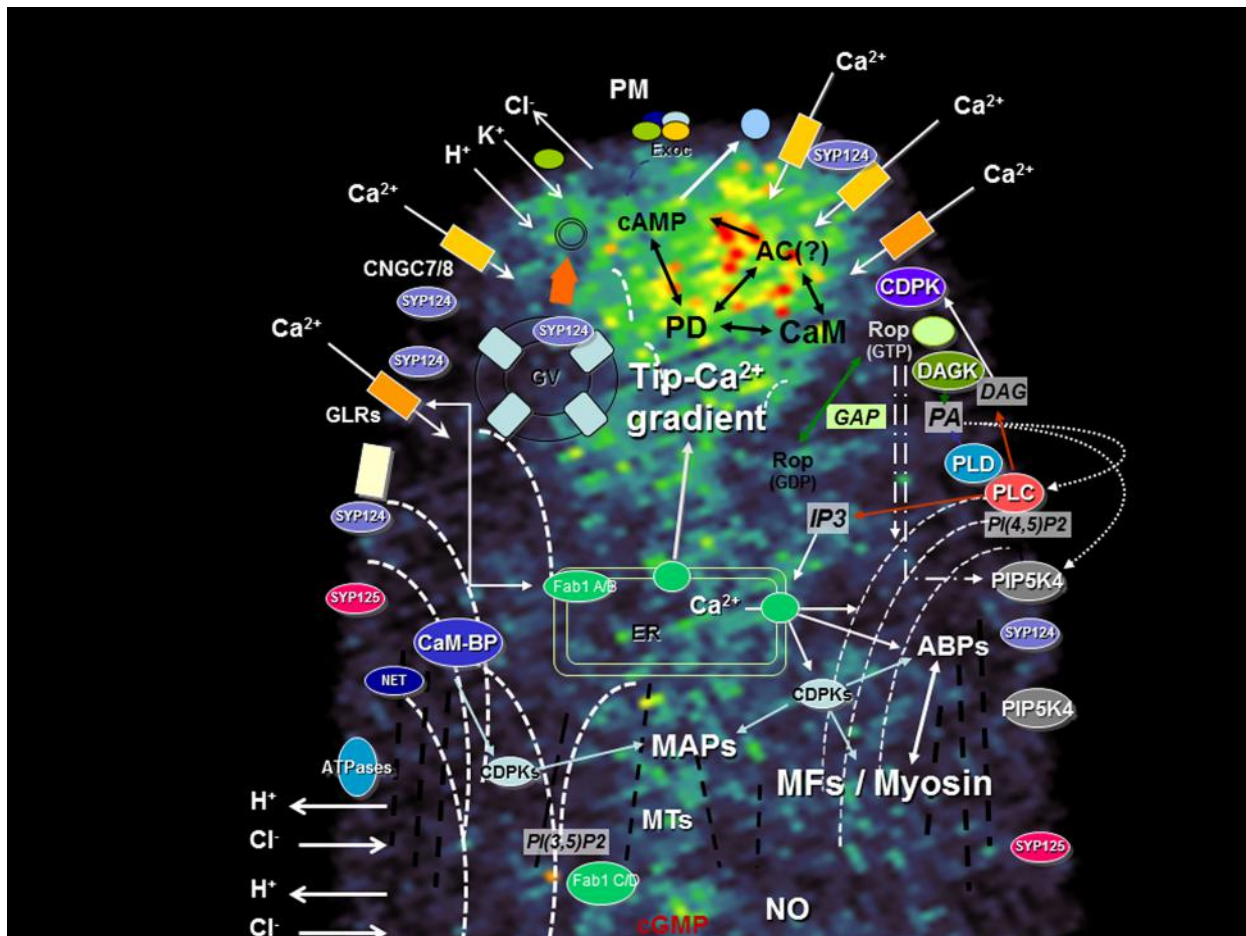


FIGURE 1 | Apical region of a growing pollen tube depicting the main signaling transduction pathways and their components. A network between the different signaling pathways foresees the existence of a highly dynamic mechanism capable to interpret simultaneous extracellular cues and maintain polarity. The diagram is superimposed on a confocal image of a growing tobacco pollen tube loaded with FM1-43, a probe for endo-exocytosis [for methods see Camacho and Malhó (2003)]. ABPs, actin-binding proteins; AC, Adenyl cyclase; CaM-BP, Calmodulin-binding protein; CDPK, Ca^{2+} dependent protein kinase; CNGC, cyclic nucleotide gated channel; DAG, diacylglycerol; DAGK, DAG kinase; Exoc, Exocyst; Fab1, PIKfyve/Fab1 kinase; GAP, Rop GTPase activating protein; GLR, Glutamate-like receptor; GV, Golgi vesicle; IP3, Inositol 1,4,5 triphosphate; MAPs, microtubule-associated protein; MFs, microfilaments (dashed white bars); MTs, microtubules (dashed black bars); NET, plant-specific Networked protein; NO, nitric oxide; PA, phosphatidic acid; PD, Phosphodiesterase; PI(3,5)P2, phosphatidylinositol-(3,5)-bis phosphate; PI(4,5)P2, phosphatidylinositol-(4,5)-bis phosphate; PIPK, phosphatidylinositol kinase; PLC, phospholipase C; PLD, phospholipase D; PM, plasma membrane; PMEs, pectin-methyl-esterases; R, IP3 receptor; SYP, syntaxin. Barbed arrows (\nearrow) indicate direction of flux; Triangle arrows (Δ) indicate potential cross-regulatory effects. The curved MFs lines represent the actin fringe with larger cables extending to the sub-apex (and connecting to the plasma membrane) but not to the apical zone. The microtubules, where a fringe is not so visible, are represented as straight lines.

its concentration should be higher in the apex (Malhó et al., 2000). The development of molecular tools in parallel with non-invasive methods to study live cells, made *Arabidopsis thaliana* a more accessible model and diversified tip growth studies. With the burst of genomics, a wider range of species (e.g., *Physcomitrella patens*) became also more prone to functional studies. Simple traits like *fast growth rate* or *straight growth direction* no longer hold as “universal” physiological controls and data interpretation must consider cellular and tissue variability.

The diversity of species and characteristics of cells under study naturally generated a diversity of results (e.g., the natural growing environment of an *Arabidopsis* pollen tube is different from one of lily, from a root hair or from a moss rhizoid). Distinct asymmetric localization of components of the apical growth machinery

(summarized in the diagram of Figure 1) were reported as part of new studies or reassessment of previous data. This, in turn, generated discrepancies, challenged old ideas and opened new perspectives. The architecture of the actin cytoskeleton (Vidalí et al., 2009) and the secretory activity (Zonia and Munnik, 2008) are just two examples that challenged the “all-in-the-tip” concept and highlighted the importance of dynamics at the sub-apical region (Cheung and Wu, 2008; Sekereš et al., 2015). Here we explore the example of four different types of proteins recently studied by our group and which were found to be important for tip growth. In all four cases, we found that changes in growth pattern (e.g., redirection of growth axis, transient loss of polarity and recovery, oscillatory growth rates) were accompanied by protein delocalization. We discuss the implications of such findings

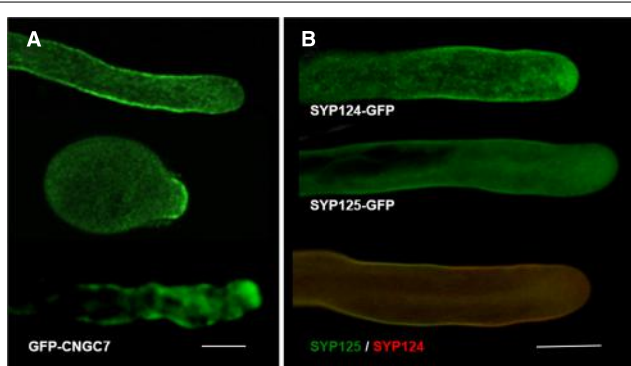


FIGURE 2 | Confocal Imaging of GFP constructs of CNGC7, SYP124 and SYP125. **(A)** Arabidopsis pollen tubes expressing GFP-CNGC7, in different growth phases—straight growth; upon germination; wiggling growth. For methods see Tunc-Ozdemir et al. (2013). Bar = 10 μ m. **(B)** Tobacco pollen tubes expressing SYP124-GFP (upper image), SYP125-GFP (middle image), and co-expressing both constructs (lower image; SYP124 signal in red and SYP125 signal in green). For methods see Ul-Rehman et al. (2011). Bar = 10 μ m.

and outline hypothesis to interpret the mechanisms underlying this complex machinery and their responses to extracellular stimuli.

Cyclic Nucleotide Gated Channels—Mobile and Flexible Ion Influx

Ca^{2+} signaling plays a key role in all aspects of plant development including apical growth. Namely, a tip-high gradient of cytosolic free ($[\text{Ca}^{2+}]_c$) resulting from influx of extracellular Ca^{2+} seems crucial to establish polarity (Hepler et al., 2012). Evidence from pharmacological and genetic approaches indicate this influx occurs through at least two different types of Ca^{2+} -permeable channels—glutamate receptor-like proteins (GLRs) and cyclic nucleotide gated channels (CNGCs; Michard et al., 2011; Tunc-Ozdemir et al., 2013). CNGCs are cation channels with varying degrees of ion conduction selectivity harboring a cyclic nucleotide-binding domain and a calmodulin binding domain (Zelman et al., 2012). They can therefore integrate signals from distinct transduction pathways and could be functioning in a way that indirectly triggers a Ca^{2+} release from an internal store (Spalding and Harper, 2011). CNGCs were shown to be essential in tip-growing cells (Frietsch et al., 2007; Tunc-Ozdemir et al., 2013) and, in straight growing pollen tubes, GFP-CNGC7 was found to preferentially localize to the plasma membrane at the flanks of the growing tip (Figure 2A, top image). But at the onset of germination, perhaps the phase where apical Ca^{2+} influx is more relevant to establish a growth axis, the GFP-CNGC7 signal was higher at the apex (Figure 2A, middle image). Similar observations were made in pollen tubes recovering and/or reorienting the growth axis (Figure 2A, lower image) suggesting that cells regulate the fine tuning of protein localization in response to extracellular cues. FRAP experiments of GFP fused to RLK (Receptor-Like-Kinase; Lee et al., 2008) showing apical fluorescence recovery support such hypothesis.

Tip growing cells not only have to frequently adjust direction of growth axis but they also experience oscillations in growth rates. Several types of growth fluctuations (of asymmetric periodicity and intensity) have been observed and they seem to vary according to species and cell type. Whether these oscillations have any special physiological meaning or whether they are just a “built-in” characteristic is not clear. $[\text{Ca}^{2+}]_c$ exhibits changes that correlated to such fluctuations of growth rates and reorientation of growth axis (Castanho Coelho and Malhó, 2006) so it is highly plausible that other components of the polarity mechanism (e.g., lipids and membrane-associated proteins) also exhibit changes in activity and/or localization. The timing of our observations (and the inherent physiological status of the cells) may thus influence our reports and help to explain some apparent discrepancies that exist in the literature.

PIP Kinases—Versatile and Key Transducers of “Signal to Form”

In the last years PtdIns(4,5)P₂ and its synthesizing enzyme, phosphatidylinositol phosphate kinase (PIP), have been intensively studied in plant cells, revealing a key role in the control of polar tip growth. Using fluorescence markers fused to the pleckstrin homology (PH) domain of the human PLC δ 1, PtdIns(4,5)P₂ was found to accumulate at the tip of growing apical cells (Kost et al., 1999; Dowd et al., 2006; Helling et al., 2006; Ischebeck et al., 2008; Sousa et al., 2008). Analysis of the PIPK members from *Arabidopsis thaliana*, *Oryza sativa*, and *Physcomitrella patens* showed that they share some regulatory features with animal PIPKs but also exert plant-specific modes of regulation (Saavedra et al., 2012). Deletion or overexpression of these lipid kinases were found to cause distinct phenotypes and perturbations in cellular processes such as cell wall deposition, endocytosis, and actin bundling (Ischebeck et al., 2008, 2010; Kusano et al., 2008; Sousa et al., 2008; Stenzel et al., 2008; Zhao et al., 2010; Saavedra et al., 2011). Interestingly, in actively growing pollen tubes, all the six PIPK isoforms (*AtPIP5K10*, *AtPIP5K11*, *AtPIP5K2*, *AtPIP5K4*, *AtPIP5K5*, and *AtPIP5K6*) were found to localize preferentially at the flanks of the tube apex and not superimposed with the highest PtdIns(4,5)P₂ concentration. However, it was also observed that the region displaying the highest protein fluorescent signal would change according to speed of growth and reorientation of the growth axis—slower growth resulting in delocalization from the flanks to the apex (e.g., Figure 6 of Ischebeck et al., 2008; Sousa et al., 2008). It has been suggested that distinct localization patterns of proteins may be the consequence of interactions with specific partners, which recruit them to different functional microdomains (Ischebeck et al., 2010). For example, PtdIns(4,5)P₂ could be channeled to targets via specific interactions PIPK-downstream effectors (Heilmann and Heilmann, 2015) resulting in differential cellular responses and phenotypes as observed upon deletion of AtPIP5Ks (Ischebeck et al., 2008, 2010; Kusano et al., 2008; Sousa et al., 2008).

Phosphatidylinositol phosphate kinases have membrane occupation and recognition nexus (MORN) motifs which are thought to be the plasma membrane localizing module (Kusano

et al., 2008) but other modules were shown to be important for correct subcellular localization (Mikami et al., 2010; Stenzel et al., 2012). E.g., AtPIP5K5 and NtPIP5K6-1 require non-conserved linker (LIM) domain for correct localization in pollen tubes, as the deletion of the N-terminal and MORN domain did not affect their apical plasma membrane localization (Stenzel et al., 2012). It is thus possible that protein modules responsible for plasma membrane localization are distinct in each PIPK allowing a fine tuning that depends on differences in physiological and/or developmental status of cells, such as polarized and non-polarized. Full comprehension of the localization mechanisms will probably involve comparison of the function of the MORN, LIM, and kinase domains of every PIPKs in cells exhibiting the same stage in development.

Syntaxins—Spatial Targeting of Secretion and Membrane Recycling

Apical growth occurs by continuous vesicle secretion and delivery of new wall material. Therefore, the exact sub-cellular location of endocytic and exocytic domains is essential to determine cellular responses and reshape form. In pollen tubes, it was previously assumed that exocytosis events occur mostly at the extreme apex, where $[Ca^{2+}]_c$ is higher, while membrane recycling (endocytosis) would take place further back from the tip, at the flanks of the apex and/or at sub-apical regions (Picton and Steer, 1981; Castanho Coelho and Malhó, 2006). Recent data questioned this paradigm suggesting that the preferential location for fusion is on a limited membrane domain at the sub-apical flanks and not at the extreme apex (Bove et al., 2008; Zonia and Munnik, 2008). Similar observations have been made in root hairs (Ovecka et al., 2005). The hypothesis of two endocytic modes co-existing according to the growth conditions—a clathrin-dependent and an independent one—was raised (Camacho and Malhó, 2003; Monteiro et al., 2005) and experimental evidence to support it was obtained by Moscatelli et al. (2007) and McKenna et al. (2009). We have also obtained evidence that two pollen-specific SNAREs (for soluble N-ethylmaleimide sensitive factor attachment protein receptor), syntaxins SYP125 and SYP124 (Silva et al., 2010; Ul-Rehman et al., 2011) have a complementary, not fully overlapping, dynamic distribution (**Figure 2B**). Similarly to PIPK proteins, the observed changes in protein accumulation at the plasma membrane might reflect specific interactions with unidentified targets (e.g., PIP2 and phosphatidic acid) which, under natural growth conditions of pollen tubes, could translate into discrete asymmetric secretory events and relate to the two endocytic modes. Indirect support for such hypothesis derives from our observations that in pollen tubes, $[Ca^{2+}]_c$ and membrane fusion exhibit frequent non-linear changes correlated to growth rates and reorientation of growth axis (Castanho Coelho and Malhó, 2006). Over-expression of PIP5K4 or Rab GTPases was also found to perturb SYP124 localization (Silva et al., 2010). The changes in SYP124 and SYP125 distribution observed upon growth modulation are thus likely to reflect membrane dynamics and a repositioning of the vesicle's docking machinery upon intra- and extracellular cues. In nerve cells, syntaxins were reported to be involved in rapid and slow endocytosis (Xu et al., 2013)

and could thus act as regulators of both endo- and exocytosis. VAMP726, another member of the SNARES family, was also shown to mediate fusion of endo- and exocytic compartments in pollen tube tip growth (Guo and McCubbin, 2012). A similar role has just been proposed for the exocyst (Jose et al., 2015), a complex known to be present in tip growing cells (Zárský et al., 2013).

Similarly to our CNGC observations, these findings highlight the importance of syntaxins in secretion and tip growth but must be interpreted considering that the localization reported reflects protein accumulation and not necessarily activity.

FAB Kinases- Dynamics in the Secretory Pathway

Most of the data now available relating apical polarity and growth focused on the role of plasma membrane (integral or associated) events. The plasma membrane and its links to the cell wall and the cytoskeleton are the obvious main targets for perceiving and transducing both intra- and extracellular cues. Notwithstanding, we have recently obtained data suggesting that PIKfyve/Fab1 kinases localized to the endomembrane compartment are also involved in the regulation of plasma membrane recycling events and thus in the maintenance of polarity (Serrazina et al., 2014).

In plants, the Fab1 phosphatidylinositol-3-monophosphate 5-kinases produce phosphatidylinositol (3,5)-bisphosphate [PtdIns(3,5)P₂], a phosphoinositide implicated in endomembrane trafficking and pH control in the vacuole (Dove et al., 2009; Bak et al., 2013). In pollen tubes, we found that AtFAB1B-GFP had a highly mobile reticulate-like distribution, distinct from γ -TIP (Serrazina et al., 2014) and decorating the sub-apical region in a manner similar to the actin cytoskeleton—a sort of V-shaped collar that adjusts and “accompanies” the reorientation of the growth axis (Vidali et al., 2009). This suggests that the protein is localized in protein storage vacuoles, endoplasmic reticulum and possibly trans-Golgi network mediating transport to and from the plasma membrane (Gary et al., 1998; Wang et al., 2011). Additionally, we found that FAB1 deletion resulted in lower internalization rates and perturbed secretion and deposition of new wall material (Serrazina et al., 2014). Analogous observations were made in root hairs (Hirano et al., 2011). FAB1 deletion was also found to impair acidification of the endomembrane compartment and to cause abnormal pollen tube diameter (Serrazina et al., 2014). The perturbation of proton gradients across membranes was reported to affect membrane curvature and vesicularization (Hope et al., 1989), protein sorting (Hurtado-Lorenzo et al., 2006), and ion fluxes, all of which are processes essential for tip growth.

These results confirm that apical polarity is not solely dependent on a positive feedback mechanism based on a single protein or ion influx localization but rather on an orchestrated network of signals. Gui et al. (2014) have recently found that overexpression of LePRK1, a pollen-specific and plasma membrane-localized receptor-like kinase, dramatically affects tube morphology in a process that can be counterbalanced by an actin bundling protein (PLIM2a) in a Ca^{2+} -responsive manner.

Conclusion and Perspectives

The establishment and maintenance of apical polarity relies on a dynamic, mobile network of signaling mechanisms. Currently, our conceptual models focus mostly on apical and sub-apical localization (of ions, proteins, lipids), particularly at the plasma membrane (or associated with). Here we provided examples of four classes of proteins related to ion and lipid signaling which indicates that a careful analysis of localization, activity and mobility is required in order to fully assign their role in apical growth. This rationale can probably be extended to other equally relevant signaling components identified in these cells (e.g., Rop GTPases, Ca^{2+} -dependent protein kinases, actin and actin-binding proteins, etc; **Figure 1**; for a review see Onelli and Moscatelli, 2013). The results obtained with FAB kinases further suggest the importance of plasma membrane—endomembrane signaling raising new perspectives in the study of apical growth mechanisms. Signaling to other organelles and compartments is also likely to play key roles in the establishment of polarity.

We have discussed the hypothesis that, in nature, and upon a myriad of environmental (extracellular) cues, cellular responses

involve flexible positioning of proteins, lipids and ion fluxes. Such dynamics may go partly unnoticed in the set-ups we devise for our experimental planning which are conditioned by the species under study, the technical approach, the pre-existing knowledge and, most importantly, by the requirements to test individual stimuli. Thus, transient gradients or peaks of activity/localization may or not be recorded (even dismissed) depending on the experimental set-up, cellular conditions and our biased previous background. Large single cell analysis and settings mimicking (or bearing in mind) the natural environment where cells develop, are required but may be difficult to implement. To compare and interpret results obtained with different experimental as well as plant systems will be a challenge, but one that must be tackled.

Acknowledgments

This work was supported by Fundação Ciência e Tecnologia (FCT/MCTES/PIDDAC, Portugal) with post-doc fellowship to LS (SFRH/BPD/63619/2009), FD (SFRH/BPD/81635/2011), and research funds to RM (PEst-OE/BIA/UI4046/2014; UID/MULTI/04046/2013).

References

- Bak, G., Lee, E.-J., Lee, Y., Kato, M., Segami, S., Sze, H., et al. (2013). Rapid structural changes and acidification of guard cell vacuoles during stomatal closure require phosphatidylinositol 3,5-bisphosphate. *Plant Cell* 25, 2202–2216. doi: 10.1105/tpc.113.110411
- Bove, J., Vaillancourt, B., Kroeger, J., Hepler, P. K., Wiseman, P. W., and Geitmann, A. (2008). Magnitude and direction of vesicle dynamics in growing pollen tubes using spatiotemporal image correlation spectroscopy and fluorescence recovery after photobleaching. *Plant Physiol.* 147, 1646–1658. doi: 10.1104/pp.108.120212
- Camacho, L., and Malhó, R. (2003). Endo-exocytosis in the pollen tube apex is differentially regulated by Ca^{2+} and GTPases. *J. Exp. Bot.* 54, 83–92. doi: 10.1093/jxb/erg043
- Castanho Coelho, P., and Malhó, R. (2006). Correlative analysis of apical secretion and $[\text{Ca}^{2+}]_c$ in pollen tube growth and reorientation. *Plant Signal. Behav.* 1, 152–157. doi: 10.4161/psb.1.3.2999
- Cheung, A., and Wu, H. M. (2008). Structural and signaling networks for the polar cell growth machinery in pollen tubes. *Annu. Rev. Plant Biol.* 59, 547–572. doi: 10.1146/annurev.arplant.59.032607.092921
- Dove, S. K., Dong, K., Kobayashi, T., Williams, F. K., and Michell, R. H. (2009). Phosphatidylinositol 3,5-bisphosphate and Fab1p/PIKfyve under PPIn endolysosome function. *Biochem. J.* 419, 1–13. doi: 10.1042/BJ20081950
- Dowd, P. E., Courso, S., Skirpan, A. L., Kao, T.-H., and Gilroy, S. (2006). Petunia phospholipase C1 is involved in pollen tube growth. *Plant Cell* 18, 1438–1453. doi: 10.1105/tpc.106.041582
- Frietsch, S., Wang, Y.-F., Sladek, C., Poulsen, L. R., Romanowsky, S. M., Schroeder, J. I., et al. (2007). A cyclic nucleotide-gated channel is essential for polarized tip growth of pollen. *Proc. Natl. Acad. Sci. U.S.A.* 104, 14531–14536. doi: 10.1073/pnas.0701781104
- Gary, J. D., Wurmser, A. E., Bonangelino, C. J., Weisman, L. S., and Emr, S. D. (1998). Fab1p is essential for PtdIns(3)P 5-kinase activity and the maintenance of vacuolar size and membrane homeostasis. *J. Cell Biol.* 143, 65–79. doi: 10.1083/jcb.143.1.65
- Gui, C. P., Dong, X., Liu, H. K., Huang, W. J., Zhang, D., Wang, S. J., et al. (2014). Overexpression of the tomato pollen receptor kinase LePRK1 rewires pollen tube growth to a blebbing mode. *Plant Cell* 26, 3538–3555. doi: 10.1105/tpc.114.127381
- Guo, F., and McCubbin, A. (2012). The pollen-specific R-SNARE/longin PiVAMP726 mediates fusion of endo- and exocytic compartments in pollen tube tip growth. *J. Exp. Bot.* 63, 3083–3095. doi: 10.1093/jxb/ers023
- Heilmann, M., and Heilmann, I. (2015). Plant phosphoinositides-complex networks controlling growth and adaptation. *Biochim. Biophys. Acta* 1851, 759–769. doi: 10.1016/j.bbalip.2014.09.018
- Helling, D., Possart, A., Cottier, S., Klahre, U., and Kost, B. (2006). Pollen tube tip growth depends on plasma membrane polarization mediated by tobacco PLC3 activity and endocytic membrane recycling. *Plant Cell* 18, 3519–3534. doi: 10.1105/tpc.106.047373
- Hepler, P. K., Kunkel, J. G., Rounds, C. M., and Winship, L. J. (2012). Calcium entry into pollen tubes. *Trends Plant Sci.* 17, 32–38. doi: 10.1016/j.tplants.2011.10.007
- Hirano, T., Matsuzawa, T., Takegawa, K., and Sato, M. H. (2011). Loss-of-function and gain-of-function mutations in FAB1A/B impair endomembrane homeostasis, conferring pleiotropic developmental abnormalities in *Arabidopsis*. *Plant Physiol.* 155, 797–807. doi: 10.1104/pp.110.167981
- Hope, M. J., Redelmeier, T. E., Wong, K. F., Rodriguez, W., and Cullis, P. R. (1989). Phospholipid asymmetry in large unilamellar vesicles induced by transmembrane pH gradients. *Biochemistry* 28, 4181–4187. doi: 10.1021/bi00436a009
- Hurtado-Lorenzo, A., Skinner, M., El Annan, J., Futai, M., Sun-Wada, G. H., Bourgois, S., et al. (2006). V-ATPase interacts with ARNO and Arf6 in early endosomes and regulates the protein degradative pathway. *Nat. Cell Biol.* 8, 124–136. doi: 10.1038/ncb1348
- Ischebeck, T., Stenzel, I., and Heilmann, I. (2008). Type B phosphatidylinositol-4-phosphate 5-kinases mediate *Arabidopsis* and *Nicotiana tabacum* pollen tube growth by regulating apical pectin secretion. *Plant Cell* 20, 3312–3330. doi: 10.1105/tpc.108.059568
- Ischebeck, T., Stenzel, I., Hempel, F., Jin, X., Mosblech, A., and Heilmann, I. (2010). Phosphatidylinositol-4,5-bisphosphate influences Nt-Rac5-mediated cell expansion in pollen tubes of *Nicotiana tabacum*. *Plant J.* 65, 453–468. doi: 10.1111/j.1365-313X.2010.04435.x
- Jose, M., Tollis, S., Nair, D., Mitteau, R., Velours, C., Massoni-Laporte, A., et al. (2015). A quantitative imaging-based screen reveals the exocyst as a network hub connecting endocytosis and exocytosis. *Mol. Biol. Cell* 26, 2519–2534. doi: 10.1091/mbc.E14-11-1527
- Kost, B., Lemichez, E., Spielhofer, P., Hong, Y., Tolias, K., Carpenter, C., et al. (1999). Rac homologues and compartmentalized phosphatidylinositol 4,5-bisphosphate act in a common pathway to regulate polar pollen tube growth. *J. Cell Biol.* 145, 317–330. doi: 10.1083/jcb.145.2.317
- Kusano, H., Testerink, C., Vermeer, J. E., Tsuge, T., Shimada, H., Oka, A., et al. (2008). The *Arabidopsis* phosphatidylinositol phosphate 5-kinase PIP5K3 is a key regulator of root hair tip growth. *Plant Cell* 20, 367–380. doi: 10.1105/tpc.107.056119

- Lee, Y. J., Szumlanski, A., Nielsen, E., and Yang, Z. (2008). Rho-GTPase-dependent filamentous actin dynamics coordinate vesicle targeting and exocytosis during tip growth. *J. Cell Biol.* 181, 1155–1168. doi: 10.1083/jcb.200801086
- Malhó, R., Camacho, L., and Moutinho, A. (2000). Signaling pathways in pollen tube growth and reorientation. *Ann. Bot.* 85(Suppl. A), 59–68. doi: 10.1006/anbo.1999.0991
- McKenna, S. T., Kunkel, J. G., Bosch, M., Rounds, C. M., Vidali, L., Winship, L. J. et al. (2009). Exocytosis precedes and predicts the increase in growth in oscillating pollen tubes. *Plant Cell* 21, 3026–3040. doi: 10.1105/tpc.109.069260
- Richard, E., Lima, P. T., Borges, F., Silva, A. C., Portes, M. T., Carvalho, J. E., et al. (2011). Glutamate receptor-like genes form Ca^{2+} channels in pollen tubes and are regulated by pistil D-serine. *Science* 332, 434–437. doi: 10.1126/science.1201101
- Mikami, K., Saavedra, L., Hiwatashi, Y., Uji, T., Hasebe, M., and Sommarin, M. (2010). A dibasic amino acid pair conserved in the activation loop directs plasma membrane localization and is necessary for activity of plant type I/II phosphatidylinositol phosphate kinase. *Plant Physiol.* 153, 1004–1015. doi: 10.1104/pp.109.152686
- Monteiro, D., Liu, Q., Lisboa, S., Scherer, G. E. F., Quader, H., and Malhó, R. (2005). Phosphoinositides and phosphatidic acid regulate pollen tube growth and reorientation through modulation of $[\text{Ca}^{2+}]_c$ and membrane secretion. *J. Exp. Bot.* 56, 1665–1674. doi: 10.1093/jxb/eri163
- Moscatelli, A., Ciampolini, F., Rodighiero, S., Onelli, E., Cresti, M., Santo, N., et al. (2007). Distinct endocytic pathways identified in tobacco pollen tubes using charged nanogold. *J. Cell Sci.* 120, 3804–3819. doi: 10.1242/jcs.012138
- Onelli, E., and Moscatelli, A. (2013). Endocytic pathways and recycling in growing pollen tubes. *Plants* 2, 211–229. doi: 10.3390/plants2020211
- Ovecka, M., Lang, I., Baluška, F., Ismail, A., Illes, P., and Lichtscheidl, I. (2005). Endocytosis and vesicle trafficking during tip growth of root hairs. *Protoplasma* 226, 39–54. doi: 10.1007/s00709-005-0103-9
- Picton, J. M., and Steer, M. W. (1981). Determination of secretory vesicle production rates by dictyosomes in pollen tubes of *Tradescantia* using cytochalasin D. *J. Cell Sci.* 49, 261–272.
- Saavedra, L., Balbi, V., Lerche, J., Mikami, K., Heilmann, I., and Sommarin, M. (2011). PIPKs are essential for rhizoid elongation and caulinodal cell development in the moss *Physcomitrella patens*. *Plant J.* 67, 635–647. doi: 10.1111/j.1365-313X.2011.04623.x
- Saavedra, L., Mikami, K., Malhó, R., and Sommarin, M. (2012). PIP kinases and their role in plant tip growing cells. *Plant Signal. Behav.* 7, 1302–1305. doi: 10.4161/psb.21547
- Sekereš, J., Pleskot, R., Pejchar, P., Žáráský, V., and Potocký, M. (2015). The song of lipids and proteins: dynamic lipid–protein interfaces in the regulation of plant cell polarity at different scales. *J. Exp. Bot.* 66, 1587–1598. doi: 10.1093/jxb/erv052
- Serrazina, S., Vaz Dias, F., and Malhó, R. (2014). Characterization of FAB1 phosphatidylinositol kinases in *Arabidopsis* pollen tube growth and fertilization. *New Phytol.* 203, 784–793. doi: 10.1111/nph.12836
- Silva, P., Rehman, R., Rato, C., Di Sansebastiano, G.-P., and Malhó, R. (2010). Asymmetric localization of *Arabidopsis* syntaxins at the pollen tube apical and sub-apical zones is involved in tip growth. *BMC Plant Biol.* 10:179. doi: 10.1186/1471-2229-10-179
- Sousa, E., Kost, B., and Malhó, R. (2008). *Arabidopsis* phosphatidylinositol-4-monophosphate 5-kinase 4 regulates pollen tube growth and polarity by modulating membrane recycling. *Plant Cell* 20, 3050–3064. doi: 10.1105/tpc.108.058826
- Spalding, E. P., and Harper, J. F. (2011). The ins and outs of cellular Ca^{2+} transport. *Curr. Opin. Plant Biol.* 14, 715–720. doi: 10.1016/j.pbi.2011.08.001
- Stenzel, I., Ischebeck, T., Konig, S., Holubowska, A., Sporysz, M., Hause, B., et al. (2008). The type B phosphatidylinositol-4-phosphate 5-kinase 3 is essential for root hair formation in *Arabidopsis thaliana*. *Plant Cell* 20, 124–141. doi: 10.1105/tpc.107.052852
- Stenzel, I., Ischebeck, T., Quint, M., and Heilmann, I. (2012). Variable regions of PI4P 5-kinases direct PtdIns(4,5)P₂ towards alternative regulatory functions in tobacco pollen tubes. *Front. Plant Sci.* 2:114. doi: 10.3389/fpls.2011.00114
- Tunc-Ozdemir, M., Rato, C., Brown, E., Rogers, S., Mooneyham, A., Frietsch, S., et al. (2013). Cyclic nucleotide gated channels 7 and 8 are essential for male reproductive fertility. *PLoS ONE* 8:e55277. doi: 10.1371/journal.pone.0055277
- Ul-Rehman, R., Silva, P., and Malhó, R. (2011). Localization of *Arabidopsis* SYP125 syntaxin in the plasma membrane sub-apical and distal zones of growing pollen tubes. *Plant Signal. Behav.* 6, 665–670. doi: 10.4161/psb.6.5.14423
- Vidali, L., Rounds, C. M., Hepler, P. K., and Bezanilla, M. (2009). Lifeact-mEGFP reveals a dynamic apical F-Actin network in tip growing plant cells. *PLoS ONE* 4:e5744. doi: 10.1371/journal.pone.0005744
- Wang, H., Zhuang, X. H., Hillmer, S., Robinson, D. G., and Jiang, L. W. (2011). Vacuolar sorting receptor (VSR) proteins reach the plasma membrane in germinating pollen tubes. *Mol. Plant* 4, 845–853. doi: 10.1093/mp/ssr011
- Xu, J., Luo, F., Zhang, Z., Xue, L., Wu, X.-S., Chiang, H.-C., et al. (2013). SNARE proteins synaptobrevin, SNAP-25, and syntaxin are involved in rapid and slow endocytosis at synapses. *Cell Rep.* 3, 1414–1421. doi: 10.1016/j.celrep.2013.03.010
- Záráský, V., Kulich, I., Fendrych, M., and Pečenková, T. (2013). Exocyst complexes multiple functions in plant cells secretory pathways. *Curr. Opin. Plant Biol.* 16, 726–733. doi: 10.1016/j.pbi.2013.10.013
- Zelman, A. K., Dawe, A., Gehring, C., and Berkowitz, G. A. (2012). Evolutionary and structural perspectives of plant cyclic nucleotide-gated cation channel. *Front. Plant Sci.* 3:95. doi: 10.3389/fpls.2012.00095
- Zhao, Y., Yan, A., Feijó, J. A., Furutani, M., Takenawa, T., Hwang, I., et al. (2010). Phosphoinositides regulate clathrin-dependent endocytosis at the tip of pollen tubes in *Arabidopsis* and tobacco. *Plant Cell* 22, 4031–4044. doi: 10.1105/tpc.110.076760
- Zonia, L., and Munnik, T. (2008). Vesicle trafficking dynamics and visualization of zones of exocytosis and endocytosis in tobacco pollen tubes. *J. Exp. Bot.* 59, 861–873. doi: 10.1093/jxb/ern007

Conflict of Interest Statement: The authors declare that the research was conducted in the absence of any commercial or financial relationships that could be construed as a potential conflict of interest.

Copyright © 2015 Malhó, Serrazina, Saavedra, Dias and Rehman. This is an open-access article distributed under the terms of the Creative Commons Attribution License (CC BY). The use, distribution or reproduction in other forums is permitted, provided the original author(s) or licensor are credited and that the original publication in this journal is cited, in accordance with accepted academic practice. No use, distribution or reproduction is permitted which does not comply with these terms.



Non-specific phospholipase C4 mediates response to aluminum toxicity in *Arabidopsis thaliana*

Přemysl Pejchar*, Martin Potocký, Zuzana Krčková, Jitka Brouzdová, Michal Daněk and Jan Martinec

Institute of Experimental Botany, Academy of Sciences of the Czech Republic, Prague, Czech Republic

Edited by:

Eric Ruelland, Centre National de la Recherche Scientifique, France

Reviewed by:

Frantisek Baluska, University of Bonn, Germany

Alain Zachowski, Université Pierre et Marie Curie, France

***Correspondence:**

Přemysl Pejchar, Laboratory of Signal Transduction, Institute of Experimental Botany, Academy of Sciences of the Czech Republic, v. v. i., Rozvojová 263, 16502 Prague 6 – Lysolaje, Czech Republic
e-mail: pejchar@ueb.cas.cz

Aluminum ions (Al) have been recognized as a major toxic factor for crop production in acidic soils. The first indication of the Al toxicity in plants is the cessation of root growth, but the mechanism of root growth inhibition is largely unknown. Here we examined the impact of Al on the expression, activity, and function of the non-specific phospholipase C4 (NPC4), a plasma membrane-bound isoform of NPC, a member of the plant phospholipase family, in *Arabidopsis thaliana*. We observed a lower expression of *NPC4* using β -glucuronidase assay and a decreased formation of labeled diacylglycerol, product of NPC activity, using fluorescently labeled phosphatidylcholine as a phospholipase substrate in *Arabidopsis* WT seedlings treated with $AlCl_3$ for 2 h. The effect on *in situ* NPC activity persisted for longer Al treatment periods (8, 14 h). Interestingly, in seedlings overexpressing *NPC4*, the Al-mediated NPC-inhibiting effect was alleviated at 14 h. However, *in vitro* activity and localization of NPC4 were not affected by Al, thus excluding direct inhibition by Al ions or possible translocation of NPC4 as the mechanisms involved in NPC-inhibiting effect. Furthermore, the growth of tobacco pollen tubes rapidly arrested by Al was partially rescued by the overexpression of *AtNPC4* while *Arabidopsis npc4* knockout lines were found to be more sensitive to Al stress during long-term exposure of Al at low phosphate conditions. Our observations suggest that NPC4 plays a role in both early and long-term responses to Al stress.

Keywords: aluminum toxicity, *Arabidopsis*, diacylglycerol, non-specific phospholipase C, plasma membrane, pollen tube, signaling, tobacco

INTRODUCTION

Aluminum (Al) toxicity represents a major growth-limiting factor for the regions with acid soils. Low pH of soil enables the release of toxic Al ions from its insoluble forms fixed in soil minerals. Prolonged exposure to Al ions leads to changes in root morphology, e.g., root thickening, bursting, changes in the cell wall architecture, and even cell death. However, the first indication of the Al toxicity in plants is rapid cessation of root growth. The root tip has been found to be the most Al-responsive part of roots (Panda et al., 2009). Although molecular mechanisms of the prompt Al-mediated root growth inhibition are largely unclear, research on the targets of Al action in plants has demonstrated that Al enters and binds to the apoplast (Wissemeier and Horst, 1995) and changes the properties of the PM. A number of physiologically important processes connected with PM are affected by Al. Well documented early consequences of Al toxicity are lipid peroxidation (Boscolo et al., 2003), the disruption of ion fluxes (Matsumoto, 2000), the disruption of calcium homeostasis (Rengel and Zhang, 2003), the inhibition of nitric oxide synthase (Tian

et al., 2007), effects on the cytoskeleton (Sivaguru et al., 1999, 2003; Schwarzerová et al., 2002), and the depolarization of the PM (Sivaguru et al., 2003; Illéš et al., 2006). It has been found that rapid Al-mediated inhibition of root growth is related to the loss of PM fluidity and the inhibition of endocytosis (Illéš et al., 2006; Krčková et al., 2012) and it is controlled through local auxin biosynthesis and signaling (Shen et al., 2008; Yang et al., 2014). The rapid response of root growth suggests that signaling pathways are a part of the mechanism participating in Al toxicity.

Phospholipid-signaling pathway is now considered to be one of the important plant signaling mechanisms involved in many different reactions of plants to environmental factors such as drought, cold, salinity, or pathogen attack [for review see Munnik (2010) and Wang (2014)]. Al has been shown to affect the phospholipid-signaling pathway as well. Changes of phospholipase A₂ activity *in vitro* (Jones and Kochian, 1997), PLD activity (Pejchar et al., 2008; Zhao et al., 2011), and PI-PLC activity (Jones and Kochian, 1995; Martínez-Estevez et al., 2003; Ramos-Díaz et al., 2007) after Al treatment were demonstrated. In addition to PI-PLC, NPC, an enzyme that is able to hydrolyze phosphatidylcholine (PC) instead of PIP₂, was characterized in plants (Nakamura et al., 2005) in relation with phospholipid-to-galactosyl DAG exchange (Andersson et al., 2005; Nakamura et al., 2005; Gaude et al., 2008; Tjellström et al., 2008), elicitor signaling (Scherer et al., 2002), root development (Wimalasekera et al., 2010), hormone signaling (Peters et al.,

Abbreviations: BODIPY, 4,4-difluoro-4-bora-3a,4a-diaza-s-indacene; BY-2, bright yellow 2; DAG, diacylglycerol; GUS, β -glucuronidase; HP-TLC, high-performance thin-layer chromatography; MS, Murashige-Skoog; NPC, non-specific phospholipase C; PA, phosphatidic acid; PIP₂, phosphatidylinositol 4,5-bisphosphate; PI-PLC, phosphatidylinositol-specific phospholipase C; PLD, phospholipase D; PM, plasma membrane

2010; Wimalasekera et al., 2010), salt stress (Kocourková et al., 2011; Peters et al., 2014), and Al stress (Pejchar et al., 2010).

Arabidopsis NPC gene family consists of six members, denoted *NPC1–NPC6*, exhibiting differences in their localization and in their biochemical properties [for review see Pokotylo et al. (2013)]. Briefly, experimentally non-characterized NPC1, NPC2, and NPC6 were supposed to contain putative N-terminal signal peptide with predicted localization in endomembranes and specific organelles (Pokotylo et al., 2013). NPC3 was described to lack the ability to hydrolyze PC (Reddy et al., 2010), NPC4 to be PM-bound protein (Nakamura et al., 2005), NPC5 to be cytosolic-localized enzyme expressed only in floral organs under normal conditions (Gaude et al., 2008; Pokotylo et al., 2013). NPC4 and NPC5 were able to hydrolyze PC, however, NPC5 possessed 40-fold lower hydrolytic activity than NPC4 (Gaude et al., 2008).

We previously demonstrated that Al ions inhibit the formation of DAG generated by NPC in tobacco BY-2 cell line and pollen tubes, inhibit the growth of tobacco pollen tubes and that this growth, arrested by Al, can be rescued by an externally added DAG (Pejchar et al., 2010). This raises the following question: which NPC isoform is Al-targeted and what is the role of DAG in aluminum toxicity?

Here we report our findings that Al ions inhibit the expression of *NPC4* and decrease its enzymatic activity. However, the latter effect is caused neither by the direct *NPC4* inhibition by Al ions nor by *NPC4* translocation. Moreover, the overexpression of *AtNPC4* rapidly alleviated Al-mediated retardation of tobacco pollen tubes while *Arabidopsis* *npc4* knockout lines were found to be more sensitive to Al stress during long-term exposure of Al at low phosphate (P) conditions.

MATERIALS AND METHODS

PLANT MATERIAL

Arabidopsis thaliana Columbia (Col-0) seeds were obtained from Lehle seeds and used as wild-type (WT) controls. The T-DNA insertion line *npc4* (SALK_046713) used in our experiments was characterized earlier (Wimalasekera et al., 2010). *Arabidopsis* plants were grown on agar plates containing 2.2 g l^{-1} 1/2 MS basal salts and 1% (w/v) agar (pH 5.8). Seeds were surface sterilized with 30% (v/v) bleach solution for 10 min and rinsed five times with sterile water. To synchronize seed germination, the agar plates were kept for 3 days in a dark at 4°C. The plants were grown in the vertical position in a growth chamber at 22°C under long day conditions (16/8 h light/dark cycle). Tobacco (*Nicotiana tabacum* cv. Samsun) pollen grains germinated on simple sucrose medium (Peskot et al., 2012) containing 10% (w/v) sucrose and 0.01% (w/v) boric acid solidified by 0.5% (w/v) agar were used for biostatic transformation.

ASSAYING NON-SPECIFIC PHOSPHOLIPASE C ACTIVITY *IN SITU* AND *IN VITRO*

The NPC activity in *Arabidopsis* seedlings was measured according to Kocourková et al. (2011). Seven-day-old *Arabidopsis* seedlings (five seedlings for each sample) were transferred from liquid MS solution to 1/8 MS medium containing 10 μM AlCl₃, pH 4 and labeled with 0.66 μg ml⁻¹ of fluorescent PC (BODIPY-PC, D-3771, Invitrogen, USA). Seedlings were incubated on an orbital

shaker at 23°C for 2 h. NPC activity *in vitro* was measured according to Pejchar et al. (2013) using β-BODIPY-PC (D-3792, Invitrogen, USA). The identification of a BODIPY-DAG corresponding spot was based on a comparison with the BODIPY-DAG standard prepared as described earlier (Pejchar et al., 2010).

HISTOCHEMICAL β-GLUCURONIDASE STAINING

The construction of promoter:GUS plants was described previously (Wimalasekera et al., 2010). Seeds of *pNPC4:GUS* were grown on agar plates under the same conditions as described in Section “Plant Material.” Ten-day-old seedlings were transferred to a 24-well plate containing 1 ml of 1/8 MS solution with or without 100 μM AlCl₃, pH 4 for 24 h. The histochemical GUS assay (Jefferson et al., 1987) was carried out according to Kocourková et al. (2011).

MOLECULAR CLONING, TRANSFORMATIONS, ISOLATION

His:AtNPC4. The AtNPC4 coding sequence was amplified from *Arabidopsis* Col-0 cDNA with the specific forward primer 5'-CGCGAATTCTATGATCGAGACGACCAAA-3' and the reverse primer 5'-GCCCTCGAGTCATCATGGCGAATAAG-3' by PCR using Phusion DNA polymerase (Finnzymes), digested with XhoI and EcoRI enzymes and cloned into the pET30a(+) vector (Novagen). The expression vector was transformed into the *Escherichia coli* strain BL21 and cells were grown overnight at 37°C. After subculturing into fresh medium, the cells were grown at 16°C to an OD₆₀₀ of approximately 0.4, then induced overnight with 0.1 mM isopropyl thio-β-D-galactoside. The cells were harvested by centrifugation (5000 × g, 10 min), resuspended in an assay buffer (50 mM Tris-HCl; pH 7.3, 50 mM NaCl, 5% glycerol; Nakamura et al., 2005), and sonicated after 10 min treatment with lysozyme (1 mg ml⁻¹). The lysed cell suspension was centrifuged (10000 × g, 10 min) and supernatant was used for an enzyme activity assay. The western blot analysis was performed under reducing and denaturation conditions with SDS electrophoresis. 6x His tag was detected with Anti-His HRP Conjugate (Qiagen).

35S::AtNPC4/35S::GFP:AtNPC4. AtNPC4 cloned into the pENTR 223.1 entry vector (Gateway™ clone G12733, *Arabidopsis* Biological Resource Center) was recombined by LR reaction into the Gateway binary vector pGWB2 (35S::AtNPC4) or pGWB6 (35S::GFP::AtNPC4) under the control of the CaMV 35S promoter (Nakagawa et al., 2007). Constructs were transferred into *Agrobacterium tumefaciens* strain GV2260 and used to transform *Arabidopsis* Col-0 WT plants by the floral dip method (Clough and Bent, 1998). Transformants were selected on agar plates containing 50 μg ml⁻¹ kanamycin and 50 μg ml⁻¹ hygromycin B. Expression levels of *NPC4* in 10-day-old T3 seedlings of homozygous lines were measured using the quantitative RT-PCR. Lines with the highest expression levels of *NPC4* were used in experiments.

Lat52::AtNPC4:YFP. The AtNPC4 coding sequence flanked by NgoMIV and ApaI sites was generated by PCR with Phusion DNA polymerase (Finnzymes) using the specific forward primer 5'-ATAGCCGCATGATCGAGACGACCAAA-3' and the reverse primer 5'-TATGGGCCATCATGGCGAATAAGCA-3'. An amplified product was introduced into the multiple cloning sites of the pollen expression vector pHD32. The pHD32 vector

(Lat52::MCS::GA5::YFP::NOS; Klahre et al., 2006) was kindly provided by Prof. Benedikt Kost (University of Erlangen-Nuremberg, Erlangen, Germany). This construct allowed the pollen-specific expression and visualization of AtNPC4 protein fusions controlled by the *Lat52* promoter (Twell et al., 1991). The expression vector was transferred into tobacco pollen grains germinating on solid culture medium by particle bombardment using a helium-driven particle delivery system (PDS-1000/He; Bio-Rad, Hercules, CA, USA) as previously described (Kost et al., 1998). Particles were coated with 1 µg DNA.

MICROSCOPY

For live-cell imaging, a Zeiss LSM 5 DUO confocal laser scanning microscope with a 940 Zeiss C-Apochromat 340/1.2 water-corrected objective was used. For YFP/GFP imaging, singletrack acquisitions with 514 nm excitation, a 458/514 nm dichroic mirror, a 530–600 nm emission filter (YFP) and 488 nm excitation, a 488 nm dichroic mirror, a 505–550 emission filter (GFP) were used.

EVALUATION OF AL EFFECT

To analyze root length, five-day-old seedlings grown on agar (for details see Plant Material) were transferred on agar plates containing 1/8 MS, pH 4 supplemented with 200 µM AlCl₃. After 9 day incubation, plates were scanned (Canon CanoScan 8800F) and the root growth was measured using the JMicroVision 1.2.7 software.

To measure pollen tubes length, tobacco pollen was transiently transformed with *AtNPC4:YFP* by particle bombardment. After 6 h of germination in dark, pollen tubes were incubated in liquid simple sucrose medium (pH 5) with or without 50 µM AlCl₃ for additional 2 h. Mean growth rate of pollen tubes expressing *AtNPC4:YFP* and vector-only control was evaluated using the fluorescence microscope Olympus BX-51.

To determine survival rate, 7-day-old seedlings grown on agar (for details see Plant Material) were transferred to 6-well plates with liquid 1/8 Hoagland's (Kocourková et al., 2011) solution (pH 4) with 100 µM AlCl₃ for 22 days. Plates pictures were taken by Nikon SMZ 1500 zoom stereoscopic microscope coupled to a Nikon DS-5M digital camera. The survival rate was calculated as a number of viable true leaves.

RESULTS

Aluminum ions were described to inhibit the formation of DAG generated by NPC in tobacco cell line BY-2 and in tobacco pollen tubes (Pejchar et al., 2010). In order to find an NPC isoform that is responsible for the decrease of DAG formation during Al stress, described biochemical properties and localizations of all NPC isoforms were taken into account (see Introduction for details). Altogether, NPC4 was the first candidate to be investigated.

EXPRESSION OF NPC4 IN ROOT TIPS IS DECREASED DURING AL STRESS

Considering all available data about the NPC gene family and given that the root and PM are the main targets of Al toxicity, we chose NPC4 to study its role in Al stress. Although *NPC4* is not the most abundant *NPC* gene expressed in roots (Peters et al., 2010; Wimalasekera et al., 2010; Pokotylo et al., 2013)

it was described as the isoform with the strongest response to abiotic stress in plants (Kocourková et al., 2011). In our previous studies, we have shown that the expression of *NPC4*, investigated using *pNPC4:GUS* plants, was largely localized in the root tip (Wimalasekera et al., 2010; Kocourková et al., 2011). In this study, we performed histochemical analysis of *Arabidopsis pNPC4:GUS* seedlings treated with AlCl₃ to observe changes in the expression pattern of *NPC4* during Al stress. GUS staining in both control and Al-treated seedlings was found in the apical meristem and partly in the elongation zone of main and lateral root but the intensity of GUS staining signal was lower in Al-treated seedlings (Figure 1). These observations suggest that the *NPC4* expression is decreased during Al stress in *Arabidopsis* seedlings.

AL-INDUCED INHIBITION OF DIACYLGLYCEROL FORMATION IS ALLEVIATED IN *NPC4*-OVEREXPRESSING SEEDLINGS

The involvement of NPC4 in Al stress was also examined in the level of its activity. Because we used a different plant model organism than in our previous work (Pejchar et al., 2010), we first tested the reaction of *Arabidopsis* seedlings to Al stress. To study changes in the DAG pattern under Al stress, we used the fluorescent derivative of PC (BODIPY-PC) as a phospholipase substrate. When seven-day-old seedlings were treated with different concentrations of AlCl₃ in the presence of BODIPY-PC for 2 h, a concentration-dependent inhibiting effect of Al on BODIPY-DAG formation was observed (Pejchar, unpublished), revealing 10 µM AlCl₃ as a working concentration for *in situ* activity measurement (Figure 2).

Consequently, we tested the hypothesis that NPC4 is also the targeted isoform at activity level during Al stress and it is responsible for the inhibition of DAG formation. Therefore, a stable *Arabidopsis* line overexpressing *NPC4* under the control of 35S promoter (*NPC4-OE*) was prepared and was monitored to

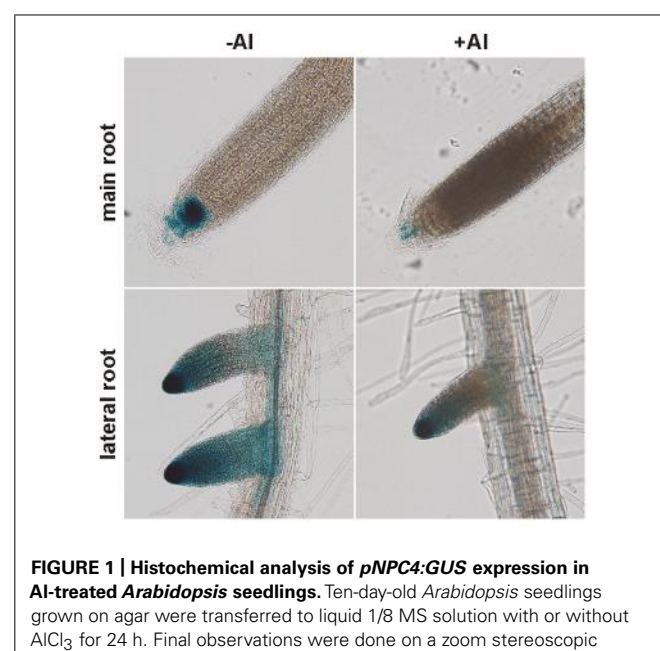


FIGURE 1 | Histochemical analysis of *pNPC4:GUS* expression in Al-treated *Arabidopsis* seedlings. Ten-day-old *Arabidopsis* seedlings grown on agar were transferred to liquid 1/8 MS solution with or without AlCl₃ for 24 h. Final observations were done on a zoom stereoscopic microscope. This experiment was repeated twice with similar results.

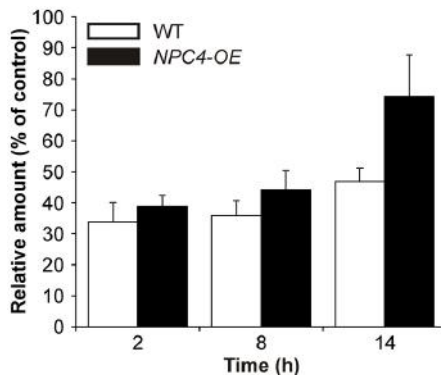


FIGURE 2 | BODIPY-diacylglycerol (DAG) production in *Arabidopsis* seedlings treated with Al for different times. Seven-day-old WT and *NPC4*-overexpressing seedlings were treated with 10 μ M AlCl₃ for different time intervals (0, 6, and 12 h) and then incubated with BODIPY-phosphatidylcholine (PC) for 2 h. Lipids were extracted at the time intervals indicated, separated by high-performance thin layer chromatography and quantified. Each value is related to the control non-treated cells (100%). The plotted values are the means + SEM from three independent experiments with parallel samples. NPC, non-specific phospholipase C.

BODIPY-DAG formation after Al treatment and compared to Al-treated WT seedlings. First, our HP-TLC analysis of the labeled products showed that the trend of the Al-induced BODIPY-DAG inhibition (~35% of control, non-treated seedlings) in WT seedlings was similar also for prolonged treatments with 10 μ M AlCl₃ (**Figure 2**) with a slightly diminished effect of Al after 14 h of treatment (~47% of control). *NPC4*-OE seedlings were slightly less sensitive to Al compared to WT when treated for 2 and 8 h. Intriguingly, the overexpression of *NPC4* resulted in a more pronounced difference (~74% compared to ~47% of control) after 14 h Al treatment. This suggests that *NPC4* is an Al-sensitive NPC isoform on activity level during Al stress, as well.

THE EFFECT OF AL ON NPC4 IS NEITHER DUE TO DIRECT INHIBITION OF NPC4 ENZYME NOR DUE TO NPC4 TRANSLOCATION

To test possible mechanisms that influenced NPC4 activity in Al stress, a heterologously expressed NPC4 protein was prepared (**Figure 3A**) and incubated with Al *in vitro* to detect possible direct inhibition of NPC4 by Al. However, β -BODIPY-DAG formation in Al-treated samples was not affected compared to non-treated samples (**Figure 3B**) indicating that NPC4 is not directly inhibited by Al.

Given that PM is well-documented cellular target of Al and that NPC4 was described as a PM-localized protein (Nakamura et al., 2005), we studied possible translocation of NPC4 from PM during Al treatment, which should cause a decrease in the DAG formation. The protein translocation under stress conditions was previously described in plants for another phospholipase type, PLD (Wang et al., 2000; Bargmann et al., 2006). To check this mechanism, stable *Arabidopsis* transformants harboring fusion protein GFP:NPC4 were prepared. Seven-day-old seedlings were transferred to 1% (w/v) sucrose (pH 4.3) solution containing 50 μ M AlCl₃ and the localization of GFP:NPC4 in roots was investigated

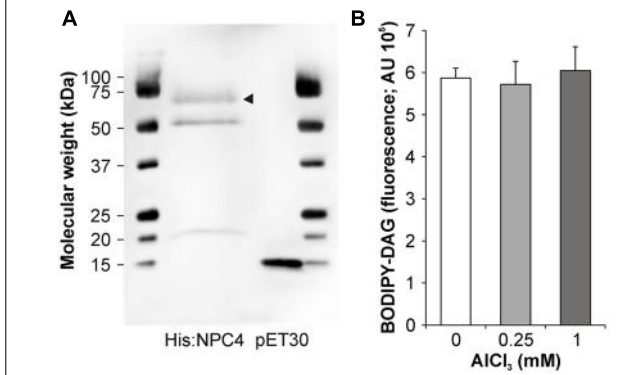


FIGURE 3 | In vitro activity of NPC4 is not altered by Al. (A) Western blot of His:NPC4 and vector control was probed with Anti-His HRP Conjugate (Qiagen). Arrow head indicates His:NPC4 protein. (B) NPC activity was determined *in vitro* using fluorescent substrate β -BODIPY-PC in the presence of AlCl₃. The plotted values are the means + SD from two independent experiments performed in duplicates ($n = 4$). DAG, diacylglycerol.

with a laser scanning confocal microscope. In control, non-treated seedlings, the PM localization of GFP:NPC4 was detected confirming previously published results (Nakamura et al., 2005). The localization of GFP:NPC4 remained unchanged in Al-treated seedlings (**Figure 4**, upper panels). The same results were obtained for transiently transformed tobacco pollen tubes expressing AtNPC4:YFP under the control of pollen specific *Lat52* promoter (**Figure 4**, lower panels), another plant model organism used in this study. These results provide evidence that NPC4 translocation is not a mechanism that induces DAG decrease during Al stress.

OVEREXPRESSION OF AtNPC4 PARTIALLY RESTORED GROWTH OF TOBACCO POLLEN TUBES UNDER AL STRESS

Next, a root growth phenotype under Al stress was investigated in *Arabidopsis* WT, *npc4* knockout line and *NPC4*-OE. Five-day-old seedlings grown on agar MS medium were transferred on agar 1/8 MS medium containing 200 μ M AlCl₃. The growth of the main root of all lines tested was retarded in the presence of Al. However, the root growth ratio between Al-treated and non-treated seedlings was not different for examined lines (**Figure 5**).

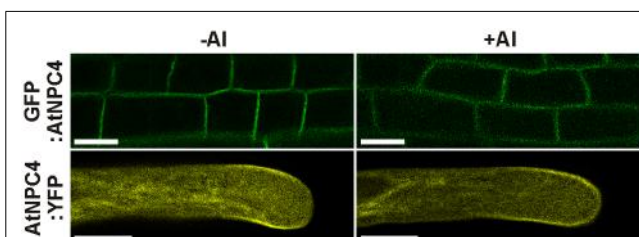


FIGURE 4 | Localization of NPC4 is not changed by Al treatment. Influence of AlCl₃ on localization of AtNPC4 was observed in 7-day-old stable *Arabidopsis* transformants (GFP:AtNPC4, upper panels) and transiently transformed tobacco pollen tubes (AtNPC4:YFP, lower panels) by confocal laser scanning microscopy. Bars, 10 μ m. NPC, non-specific phospholipase C.

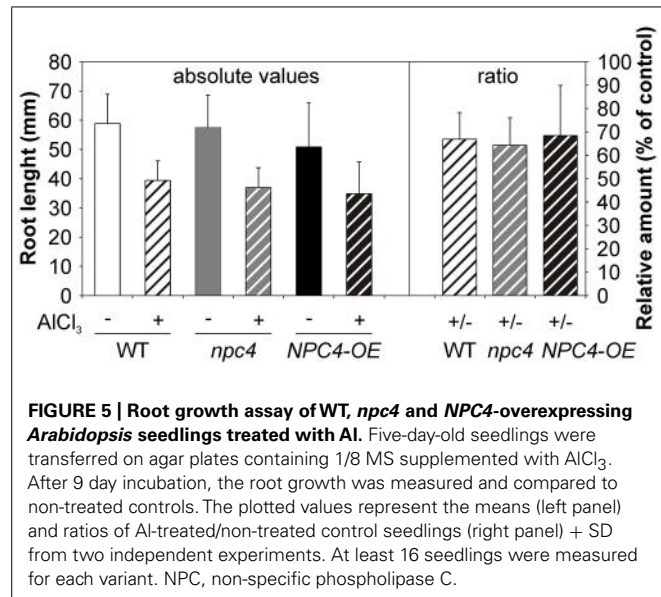


FIGURE 5 | Root growth assay of WT, *npc4* and *NPC4*-overexpressing *Arabidopsis* seedlings treated with Al. Five-day-old seedlings were transferred on agar plates containing 1/8 MS supplemented with AlCl₃. After 9 day incubation, the root growth was measured and compared to non-treated controls. The plotted values represent the means (left panel) and ratios of Al-treated/non-treated control seedlings (right panel) + SD from two independent experiments. At least 16 seedlings were measured for each variant. NPC, non-specific phospholipase C.

This could be explained by possible compensation of NPC4 function in stable transformants by another member of lipid signaling enzyme network. To bypass this, we employed transient transformation in heterologous system of tobacco pollen. Moreover, in our previously published study (Pejchar et al., 2010), DAG was shown to restore growth inhibition caused by Al treatment in tobacco pollen tubes. To test the possible role of NPC4 in this DAG function, tobacco pollen tubes were transiently transformed with *AtNPC4:YFP* under the control of pollen specific *Lat52* promoter and the length of pollen tubes overexpressing *AtNPC4:YFP* was determined in the presence of Al. In the control pollen tubes overexpressing YFP alone, the cytoplasmic YFP localization was found (data not shown) and the mean growth rate was $2.36 \pm 0.12 \mu\text{m min}^{-1}$ (Figure 6). Al-treatment caused the inhibition of control pollen tubes growth to approximately 15% ($0.34 \pm 0.03 \mu\text{m min}^{-1}$) of non-treated cells. Control pollen tubes overexpressing *AtNPC4:YFP* showed a slightly decreased mean growth rate ($2.17 \pm 0.09 \mu\text{m min}^{-1}$) compared to YFP only. However, in the presence of Al the mean growth of pollen tubes overexpressing *AtNPC4:YFP* ($1.01 \pm 0.05 \mu\text{m min}^{-1}$) was higher compared to Al-treated vector-only control (Figure 6). Taken together, these results clearly demonstrate that the role of DAG as a growth activator in Al stress is mediated by NPC4 activity.

***Arabidopsis* *npc4* SEEDLINGS ARE MORE SENSITIVE TO AL STRESS IN PHOSPHATE DEFICIENCY**

Based on the results concerning the role of NPC4 activity in longer time period of Al treatment (Figure 2), a long-term survival experiment was also performed. Seven-day-old seedlings grown on agar were transferred to liquid 1/8 Hoagland's solution with AlCl₃ for 22 days. However, all tested lines (WT, *npc4*, *NPC4-OE*) showed no difference in their survival rate (data not shown). Since NPC4 play a role in P starvation (Nakamura et al., 2005) and aluminum stress and P deficiency co-exist in acid soils (Ruiz-Herrera and López-Bucio, 2013), the same experiment was repeated under P deficiency conditions. Differences in both root abundance (Figure 7A) and

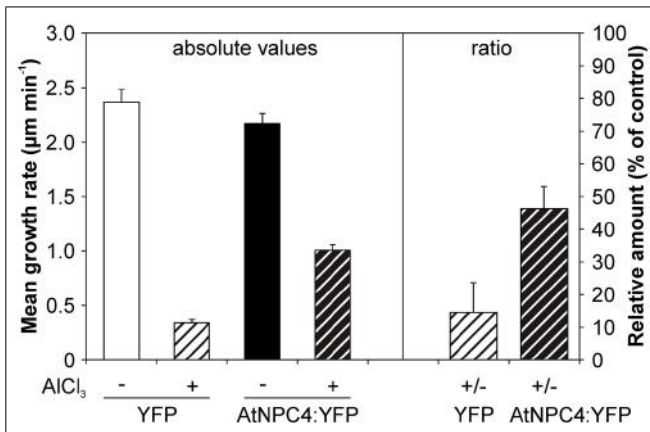


FIGURE 6 | Effect of Al on the growth rate of tobacco pollen tubes transiently expressing *AtNPC4:YFP*. Tobacco pollen was sown on solid germination medium and transiently transformed with *AtNPC4:YFP* by particle bombardment. After 6 h of germination, pollen tubes were incubated with $50 \mu\text{M}$ AlCl₃ for additional 2 h. Mean growth rate of pollen tubes expressing *AtNPC4:YFP* or vector-only control was evaluated using a fluorescence microscope. Data shown are from two independent experiments and represent means + SEM. At least 21 pollen tubes were measured for each variant. NPC, non-specific phospholipase C.

survival rate (Figures 7A,B) were found between WT and *npc4* seedlings after Al treatment. Seedlings of *npc4* were able to form only a weaker root system and significantly (*t*-test, $p < 0.0001$) less true leaves comparing to WT. This suggests that *npc4* seedlings are more sensitive to Al stress at low P conditions. In contrast to this finding, we also saw that *NPC4-OE* seedlings formed a more abundant root system compared to WT (Figure 7A). However, only a minimal increase of survival rate was found for *NPC4-OE* (Figures 7A,B). Collectively, these data strongly

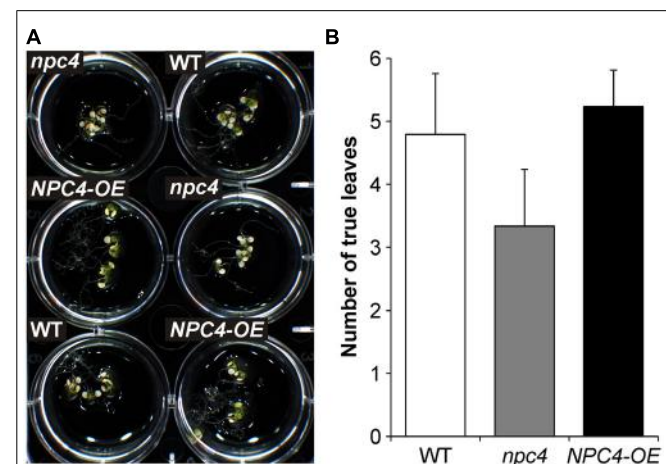


FIGURE 7 | Effect of Al on the survival of WT, *npc4*, and *NPC4*-overexpressing *Arabidopsis* seedlings under phosphate deficiency. (A) Seven-day-old seedlings grown on agar were transferred to liquid 1/8 Hoagland's solution with AlCl₃ for 22 days. (B) Quantitative analysis of survival rate calculated as a number of viable true leaves. The plotted values are the means + SD from two independent experiments ($n = 50$). NPC, non-specific phospholipase C.

support the involvement of NPC4 in response to long-term Al exposure.

DISCUSSION

Several physiologically important cellular processes are affected by Al, the major growth-limiting factor for the regions with acid soils. However, time sequence and the exact mechanism of processes involved in Al stress are still under investigation. Phospholipases, namely PI-PLC and PLD, have been shown to be affected within minutes as well as in longer time periods after Al treatment (Martínez-Estévez et al., 2003; Ramos-Díaz et al., 2007; Pejchar et al., 2008; Zhao et al., 2011). We previously described that the formation of DAG generated by NPC is rapidly inhibited by Al in tobacco cell line BY-2 and in tobacco pollen tubes and that Al inhibits growth of tobacco pollen tubes. These results, together with the fact that Al-mediated growth arrest can be rescued by an externally added DAG (Pejchar et al., 2010), raised a question which NPC isoform is Al-targeted in aluminum toxicity. Here we showed that NPC isoform NPC4 is involved in the response of *A. thaliana* to Al exposure.

We selected *Arabidopsis* NPC4 as the primary candidate gene based on the expression and localization criteria (see above). The expression analysis using *pNPC4:GUS* assay showed that the localization and the intensity of *NPC4* expression in the non-treated main root was the same as published previously (Wimalasekera et al., 2010). However, we found stronger GUS staining in non-treated lateral roots (Figure 1). This difference could be explained by different experimental conditions used as a control for Al treatments (pH 4) or by small variation of seedling age used for GUS assay. More importantly, Al treatment caused reduction in GUS staining in both main and lateral roots suggesting that the *NPC4* expression is decreased during Al treatment. In addition, *pNPC4:GUS* expression was confined mainly to the root tip (Figure 1), a plant tissue that was found to be the most Al-responsive part of roots (Panda et al., 2009).

Although we confirmed the generally accepted symptom of Al toxicity, root growth inhibition, and we observed diminished *NPC4* expression after Al treatment, we were not able to determine differences between Al-treated WT, *npc4*, and *NPC4-OE* *Arabidopsis* seedlings (Figure 5). We have two hypotheses regarding the lack of the differences. First, it is possible that no differences were found because NPC4 is involved in other aspects of the response to Al stress than in the studied root growth phenotype. Alternatively, the lack of the differences is caused by the positive or negative compensatory effect of another NPC isoform (or other lipid signaling genes) that may be up- or down-regulated in *npc4* knockout or stable *NPC4-OE* line, respectively. Similar observations were indeed described for studies dealing with other lipid signaling genes, such as PLD (Bargmann et al., 2009; Johansson et al., 2014) or phospholipase A (Rietz et al., 2010). All six NPC sequences are highly conserved with four invariable motives, however, the C-termini form the most divergent part of NPC sequences, with distinct lengths and sequence conservation among NPC subfamilies. This may be the part of the molecule responsible for the functional differences of various NPC isoforms through facilitating interactions with other proteins or defining protein localization (Pokotylo et al., 2014)

(et al., 2013). Interestingly, while NPC3-5 are found in triplicate in *Arabidopsis* genome and members of this subfamily can also be found in other monocot and dicot species, it seems to be missing in gymnosperms and it is also absent in *Solanaceae* (Potocký, unpublished). Taking advantage of this, we employed a strategy of studying the effect of Al in tobacco pollen tubes heterologously overexpressing *AtNPC4:YFP* under the control of strong pollen specific *Lat52* promoter. The growth of tobacco pollen tubes was rapidly arrested by Al, supporting our previous results (Pejchar et al., 2010), and was partially rescued by the overexpression of *AtNPC4:YFP* (Figure 6). Together with Al-mediated pollen growth inhibition rescue by exogenously added DAG (Pejchar et al., 2010), this strongly suggests that NPC4-generated DAG plays a role in the response to the Al-mediated toxicity.

Because a different plant model organism than in our previous work was used, we next tested the reaction of *Arabidopsis* seedlings to Al stress in the view of NPC activity. We utilized the same fluorescent derivative of PC as a phospholipase substrate and found a similar Al-mediated NPC-inhibiting effect (Figure 2) as for the tobacco cell line BY-2 and pollen tubes (Pejchar et al., 2010) suggesting that this phenomenon could be conserved across the plant kingdom. Interestingly, effects on *pNPC4:GUS* expression and NPC activity in Al-treated plants were in the opposite way than described for another abiotic stress that targets root, salt treatment (Kocourková et al., 2011). To test the hypothesis whether NPC4 is responsible for inhibition of DAG formation during Al stress, we prepared the stable *Arabidopsis* lines over-expressing *NPC4* and we compared the ratio of NPC activity in Al-treated/non-treated seedlings to WT seedlings. The differences between WT and *NPC4-OE* seedlings were slowly pronounced in time with the most evident change obtained for the seedlings treated with Al for 14 h (Figure 2) indicating that NPC4 activity is altered by Al gradually. Two possible mechanisms that could be responsible for the decrease of NPC activity were examined. The inhibition of phospholipase activity *in vitro* in cellular fractions is well documented for different toxic metals (Pokotylo et al., 2014) and for Al as well (Martínez-Estévez et al., 2003; Pejchar et al., 2008). Here, the direct inhibition of heterologously expressed NPC4 enzyme by Al was tested with no alteration in activity detected even for high AlCl₃ concentrations (Figure 3). The second possible mechanism, enzyme translocation, was previously described in plants under stress conditions for another phospholipase type, PLD (Wang et al., 2000; Bargmann et al., 2006). However, Al treatment had no effect on NPC4 localization neither in *Arabidopsis* seedlings nor tobacco pollen tubes (Figure 4).

Moreover, AtNPC4:YFP was found on PM in subapical region of growing pollen tube (Figure 4) and thus partially co-localize with Cys1:YFP that was used as a DAG marker in tobacco pollen tubes (Potocký et al., 2014). DAG is an important signaling phospholipid in animals but its signaling role in plant cells is still under debate. Meijer and Munnik (2003) reported that DAG as a product of PIP₂ hydrolysis is rapidly phosphorylated by DAG kinase to PA, which plays an active role in the plant signaling processes. However, a number of studies imply that DAG is likely to act as a signaling molecule in some plant systems including *Arabidopsis* seedlings and tobacco pollen tubes

[reviewed in Dong et al. (2012)]. DAG is also known to be important in the structure and dynamics of biological membranes, where it can influence membrane curvature and induce unstable, asymmetric regions in membrane bilayers important for membrane fusion processes (Carrasco and Mérida, 2007; Haucke and Di Paolo, 2007), events that occur in many physiological processes, such as exocytosis, endocytosis, membrane biogenesis, and cell division. Moreover Al-mediated inhibition of root growth was found to be connected with the inhibition of endocytosis (Illéš et al., 2006; Krtyková et al., 2012) and controlled through local auxin biosynthesis and signaling (Shen et al., 2008; Yang et al., 2014). Not curiously, expression of *NPC4* was increased and *npc4* seedlings exhibit shorter primary root and smaller density of lateral roots after auxin treatment (Wimalasekera et al., 2010). Thus, it is worthwhile to note that the inhibition of DAG formation during Al stress might affect the mentioned processes and rapidly inhibit growth. On the other hand, our long-term experiment revealed that *npc4* seedlings were more sensitive to Al stress while *NPC4-OE* seedlings formed a more abundant root system (**Figure 7**). This suggests that NPC4/DAG functions differently, more likely participating in lipid turnover and membrane remodeling, respectively.

In summary, our results suggest that the previously described involvement of NPC in response to Al stress is mediated by NPC4 in *A. thaliana*.

ACKNOWLEDGMENTS

This work was supported by the Czech Science Foundation (GACR) grant no. P501/12/P950 to P.P. The authors thank Daniela Kocourková and Kateřina Raková for their excellent technical assistance.

REFERENCES

- Andersson, M. X., Larsson, K. E., Tjellström, H., Liljenberg, C., and Sandelius, A. S. (2005). Phosphate-limited oat. The plasma membrane and the tonoplast as major targets for phospholipid-to-glycolipid replacement and stimulation of phospholipases in the plasma membrane. *J. Biol. Chem.* 280, 27578–27586. doi: 10.1074/jbc.M503273200
- Bargmann, B. O. R., Laxalt, A. M., Ter Riet, B., Schouten, E., van Leeuwen, W., Dekker, H. L., et al. (2006). LePLD β 1 activation and relocalization in suspension-cultured tomato cells treated with xylanase. *Plant J.* 45, 358–368. doi: 10.1111/j.1365-313X.2005.02631.x
- Bargmann, B. O. R., Laxalt, A. M., Ter Riet, B., van Schooten, B., Merquiol, E., Testerink, C., et al. (2009). Multiple PLDs required for high salinity and water deficit tolerance in plants. *Plant Cell Physiol.* 50, 78–89. doi: 10.1093/pcp/pcn173
- Boscolo, P. R. S., Menossi, M., and Jorge, R. A. (2003). Aluminum-induced oxidative stress in maize. *Phytochemistry* 62, 181–189. doi: 10.1016/S0031-9422(02)00491-0
- Carrasco, S., and Mérida, I. (2007). Diacylglycerol, when simplicity becomes complex. *Trends Biochem. Sci.* 32, 27–36. doi: 10.1016/j.tibs.2006.11.004
- Clough, S. J., and Bent, A. F. (1998). Floral dip: a simplified method for *Agrobacterium*-mediated transformation of *Arabidopsis thaliana*. *Plant J.* 16, 735–743. doi: 10.1046/j.1365-313X.1998.00343.x
- Dong, W., Lv, H., Xia, G., and Wang, M. (2012). Does diacylglycerol serve as a signaling molecule in plants? *Plant Signal. Behav.* 7, 1–4. doi: 10.4161/psb.19644
- Gaudé, N., Nakamura, Y., Scheible, W. R., Ohta, H., and Dormann, P. (2008). Phospholipase C5 (NPC5) is involved in galactolipid accumulation during phosphate limitation in leaves of *Arabidopsis*. *Plant J.* 56, 28–39. doi: 10.1111/j.1365-313X.2008.03582.x
- Haucke, V., and Di Paolo, G. (2007). Lipids and lipid modifications in the regulation of membrane. *Curr. Opin. Cell Biol.* 19, 426–435. doi: 10.1016/j.ceb.2007.06.003
- Illéš, P., Schlicht, M., Pavlovkin, J., Lichtscheidl, I., Baluška, F., and Ovečka, M. (2006). Aluminium toxicity in plants: internalization of aluminium into cells of the transition zone in *Arabidopsis* root apices related to changes in plasma membrane potential, endosomal behaviour, and nitric oxide production. *J. Exp. Bot.* 57, 4201–4213. doi: 10.1093/jxb/erl197
- Jefferson, R. A., Kavanagh, T. A., and Bevan, M. W. (1987). GUS fusions: β -glucuronidase as a sensitive and versatile gene fusion marker in higher plants. *EMBO J.* 6, 3901–3907.
- Johansson, O. N., Fahlberg, P., Karimi, E., Nilsson, A. K., Ellerström, M., and Andersson, M. X. (2014). Redundancy among phospholipase D isoforms in resistance triggered by recognition of the *Pseudomonas syringae* effector AvrRpm1 in *Arabidopsis thaliana*. *Front. Plant Sci.* 5:639. doi: 10.3389/fpls.2014.00639
- Jones, D. L., and Kochian, L. V. (1995). Aluminium inhibition of the inositol 1,4,5-trisphosphate signal transduction pathway in wheat roots: a role in aluminium toxicity? *Plant Cell* 7, 1913–1922. doi: 10.1105/tpc.7.11.1913
- Jones, D. L., and Kochian, L. V. (1997). Aluminum interaction with plasma membrane lipids and enzyme metal binding sites and its potential role in Al cytotoxicity. *FEBS Lett.* 400, 51–57. doi: 10.1016/S0014-5793(96)01319-1
- Klahre, U., Becker, C., Schmitt, A. C., and Kost, B. (2006). Nt-RhoGDI2 regulates Rac/Rop signaling and polar cell growth in tobacco pollen tubes. *Plant J.* 46, 1018–1031. doi: 10.1111/j.1365-313X.2006.02757.x
- Kocourková, D., Krčková, Z., Pejchar, P., Veselková, Š., Valentová, O., Wimalasekera, R., et al. (2011). The phosphatidylcholine-hydrolyzing phospholipase C NPC4 plays a role in response of *Arabidopsis* roots to salt stress. *J. Exp. Bot.* 62, 3753–3763. doi: 10.1093/jxb/err039
- Kost, B., Spielhofer, P., and Chua, N.-H. (1998). A GFP-mouse talin fusion protein labels plant actin filaments in vivo and visualizes the actin cytoskeleton in growing pollen tubes. *Plant J.* 16, 393–401. doi: 10.1046/j.1365-313X.1998.00304.x
- Krtková, J., Havelková, L., Krepelová, A., Fišer, R., Vosolobě, S., Novotná, Z., et al. (2012). Loss of membrane fluidity and endocytosis inhibition are involved in rapid aluminum-induced root growth cessation in *Arabidopsis thaliana*. *Plant Physiol. Biochem.* 60, 88–97. doi: 10.1016/j.plaphy.2012.07.030
- Martínez-Estevez, M., Racagni-Di Palma, G., Muñoz-Sánchez, J. A., Brito-Argáez, L., Loyola-Vargas, V. M., and Hernández-Sotomayor, S. M. T. (2003). Aluminium differentially modifies lipid metabolism from the phosphoinositide pathway in *Coffea arabica* cells. *J. Plant Physiol.* 160, 1297–1303. doi: 10.1078/0176-1617-1168
- Matsumoto, H. (2000). Cell biology of aluminum toxicity and tolerance in higher plants. *Int. Rev. Cytol.* 200, 1–46. doi: 10.1016/S0074-7696(00)00001-2
- Meijer, H. J. G., and Munnik, T. (2003). Phospholipid-based signaling in plants. *Annu. Rev. Plant Biol.* 54, 265–306. doi: 10.1146/annurev.evol.54.031902.134748
- Munnik, T. (ed.). (2010). *Lipid Signaling in Plants*. Berlin: Springer. doi: 10.1007/978-3-642-03873-0
- Nakagawa, T., Kurose, T., Hino, T., Tanaka, K., Kawamukai, M., Niwa, Y., et al. (2007). Development of series of gateway binary vectors, pGWBs, for realizing efficient construction of fusion genes for plant transformation. *J. Biosci. Bioeng.* 104, 34–41. doi: 10.1263/jbb.104.34
- Nakamura, Y., Awai, K., Masuda, T., Yoshioka, Y., Takamiya, K., and Ohta, H. (2005). A novel phosphatidylcholine-hydrolyzing phospholipase C induced by phosphate starvation in *Arabidopsis*. *J. Biol. Chem.* 280, 7469–7476. doi: 10.1074/jbc.M408799200
- Panda, S. K., Baluška, F., and Matsumoto, H. (2009). Aluminum stress signaling in plants. *Plant Signal. Behav.* 4, 592–597. doi: 10.4161/psb.4.7.8903
- Pejchar, P., Pleskot, R., Schwarzerová, K., Martinec, J., Valentová, O., and Novotná, Z. (2008). Aluminum ions inhibit phospholipase D in a microtubule-dependent manner. *Cell Biol. Int.* 32, 554–556. doi: 10.1016/j.cbi.2007.11.008
- Pejchar, P., Potocký, M., Novotná, Z., Veselková, Š., Kocourková, D., Valentová, O., et al. (2010). Aluminium ions inhibit formation of diacylglycerol generated by phosphatidylcholine-hydrolysing phospholipase C in tobacco cells. *New Phytol.* 188, 150–160. doi: 10.1111/j.1469-8137.2010.03349.x
- Pejchar, P., Scherer, G. F. E., and Martinec, J. (2013). Assaying nonspecific phospholipase C activity. *Methods Mol. Biol.* 1009, 193–203. doi: 10.1007/978-1-62703-401-2_18
- Peters, C., Kim, S.-C., Devaiah, S., Li, M., and Wang, X. (2014). Non-specific phospholipase C5 and diacylglycerol promote lateral root development under mild salt stress in *Arabidopsis*. *Plant Cell Environ.* 37, 2002–2013. doi: 10.1111/pce.12334

- Peters, C., Li, M. Y., Narasimhan, R., Roth, M., Welti, R., and Wang, X. M. (2010). Nonspecific phospholipase C NPC4 promotes responses to abscisic acid and tolerance to hyperosmotic stress in *Arabidopsis*. *Plant Cell* 22, 2642–2659. doi: 10.1105/tpc.109.071720
- Pleskot, R., Pejchar, P., Bezdova, R., Lichtscheidl, I. K., Wolters-Arts, M., Marc, J., et al. (2012). Turnover of phosphatidic acid through distinct signalling pathways affects multiple aspects of tobacco pollen tube tip growth. *Front. Plant Sci.* 3:54. doi: 10.3389/fpls.2012.00054
- Pokotylo, I., Kolesnikov, Y., Kravets, V., Zachowski, A., and Ruelland, E. (2014). Plant phosphoinositide-dependent phospholipases C: variations around a canonical theme. *Biochimie* 96, 144–157. doi: 10.1016/j.biochi.2013.07.004
- Pokotylo, I., Pejchar, P., Potocký, M., Kocourková, D., Krčková, Z., Ruelland, E., et al. (2013). The plant non-specific phospholipase C gene family. Novel competitors in lipid signalling. *Prog. Lipid Res.* 52, 62–79. doi: 10.1016/j.plipres.2012.09.001
- Potocký, M., Pleskot, R., Pejchar, P., Vitale, N., Kost, B., and Žářský, V. (2014). Live-cell imaging of phosphatidic acid dynamics in pollen tubes visualized by Spo20p-derived biosensor. *New Phytol.* 203, 483–494. doi: 10.1111/nph.12814
- Ramos-Díaz, A., Brito-Argáez, L., Munnik, T., and Hernández-Sotomayor, S. (2007). Aluminum inhibits phosphatidic acid formation by blocking the phospholipase C pathway. *Planta* 225, 393–401. doi: 10.1007/s00425-006-0348-3
- Reddy, V. S., Rao, D. K. V., and Rajasekharan, R. (2010). Functional characterization of lysophosphatidic acid phosphatase from *Arabidopsis thaliana*. *Biochim. Biophys. Acta* 1801, 455–461. doi: 10.1016/j.bbapap.2009.12.005
- Rengel, Z., and Zhang, W. H. (2003). Role of dynamics of intracellular calcium in aluminium-toxicity syndrome. *New Phytol.* 159, 295–314. doi: 10.1046/j.1469-8137.2003.00821.x
- Rietz, S., Dermedjiev, G., Oppermann, E., Tafesse, F. G., Effendi, Y., Holk, A., et al. (2010). Roles of *Arabidopsis* patatin-related phospholipases A in root development are related to auxin responses and phosphate deficiency. *Mol. Plant* 3, 524–538. doi: 10.1093/mp/ssp109
- Ruiz-Herrera, L.-F., and López-Bucio, J. (2013). Aluminum induces low phosphate adaptive responses and modulates primary and lateral root growth by differentially affecting auxin signaling in *Arabidopsis* seedlings. *Plant Soil* 371, 593–609. doi: 10.1007/s11104-013-1722-0
- Scherer, G. F. E., Paul, R. U., Holk, A., and Martinec, J. (2002). Down-regulation by elicitors of phosphatidylcholine-hydrolyzing phospholipase C and up-regulation of phospholipase A in plant cells. *Biochem. Biophys. Res. Commun.* 293, 766–770. doi: 10.1016/S0006-291X(02)00292-9
- Schwarzerová, K., Zelenková, S., Nick, P., and Opatrný, Z. (2002). Aluminum-induced rapid changes in the microtubular cytoskeleton of tobacco cell lines. *Plant Cell Physiol.* 43, 207–216. doi: 10.1093/pcp/pcf028
- Shen, H., Hou, N., Schlicht, M., Wan, Y., Mancuso, S., and Baluška, F. (2008). Aluminium toxicity targets PIN2 in *Arabidopsis* root apices: effects on PIN2 endocytosis, vesicular recycling, and polar auxin transport. *Chin. Sci. Bull.* 53, 2480–2487. doi: 10.1007/s11434-008-0332-3
- Sivaguru, M., Baluška, F., Volkmann, D., Felle, H. H., and Horst, W. J. (1999). Impacts of aluminum on the cytoskeleton of the maize root apex. Short-term effects on the distal part of the transition zone. *Plant Physiol.* 119, 1073–1082. doi: 10.1104/pp.119.3.1073
- Sivaguru, M., Pike, S., Gassmann, W., and Baskin, T. I. (2003). Aluminum rapidly depolymerizes cortical microtubules and depolarizes the plasma membrane: evidence that these responses are mediated by a glutamate receptor. *Plant Cell Physiol.* 44, 667–675. doi: 10.1093/pcp/pcg094
- Tian, Q.-Y., Sun, D.-H., Zhao, M.-G., and Zhang, W.-H. (2007). Inhibition of nitric oxide synthase (NOS) underlies aluminum-induced inhibition of root elongation in *Hibiscus moscheutos*. *New Phytol.* 174, 322–331. doi: 10.1111/j.1469-8137.2007.02005.x
- Tjellström, H., Andersson, M. X., Larsson, K. L., and Sandelin, A. S. (2008). Membrane phospholipids as a phosphate reserve: the dynamic nature of phospholipid-to-digalactosyl diacylglycerol exchange in higher plants. *Plant Cell Environ.* 31, 1388–1398. doi: 10.1111/j.1365-3040.2008.01851.x
- Twell, D., Yamaguchi, J., Wing, R. A., Ushiba, J., and McCormick, S. (1991). Promoter analysis of genes that are coordinately expressed during pollen development reveals pollen-specific enhancer sequences and shared regulatory elements. *Genes Dev.* 5, 496–507. doi: 10.1101/gad.5.3.496
- Wang, C., Zien, C. A., Afiflile, M., Welti, R., Hildebrand, D. F., and Wang, X. (2000). Involvement of phospholipase D in wound-induced accumulation of jasmonic acid in *Arabidopsis*. *Plant Cell* 12, 2237–2246. doi: 10.1105/tpc.12.11.2237
- Wang, X. (ed.). (2014). *Phospholipases in Plant Signaling*. Berlin: Springer-Verlag. doi: 10.1007/978-3-642-42011-5
- Wimalasekera, R., Pejchar, P., Holk, A., Martinec, J., and Scherer, G. F. E. (2010). Plant phosphatidylcholine-hydrolyzing phospholipases C NPC3 and NPC4 with roles in root development and brassinolide signalling in *Arabidopsis thaliana*. *Mol. Plant* 3, 610–625. doi: 10.1093/mp/ssp005
- Wissemeier, A. H., and Horst, W. J. (1995). Effect of calcium supply on aluminium-induced callose formation, its distribution and persistence in roots of soybean (*Glycine max* (L.) Merr.). *J. Plant Physiol.* 145, 470–476. doi: 10.1016/S0176-1617(11)81773-6
- Yang, Z. B., Geng, X., He, C., Zhang, F., Wang, R., Horst, W. J., et al. (2014). TAA1-regulated local auxin biosynthesis in the root-apex transition zone mediates the aluminum-induced inhibition of root growth in *Arabidopsis*. *Plant Cell* 26, 2889–2904. doi: 10.1105/tpc.114.127993
- Zhao, J., Wang, C., Bedair, M., Welti, R. W., Sumner, L., Baxter, I., et al. (2011). Suppression of phospholipase Dys confers increased aluminum resistance in *Arabidopsis thaliana*. *PLoS ONE* 6:e28086. doi: 10.1371/journal.pone.0028086

Conflict of Interest Statement: The authors declare that the research was conducted in the absence of any commercial or financial relationships that could be construed as a potential conflict of interest.

Received: 22 December 2014; accepted: 26 January 2015; published online: 16 February 2015.

Citation: Pejchar P, Potocký M, Krčková Z, Brouzdová J, Daněk M and Martinec J (2015) Non-specific phospholipase C4 mediates response to aluminum toxicity in *Arabidopsis thaliana*. *Front. Plant Sci.* 6:66. doi: 10.3389/fpls.2015.00066

This article was submitted to Plant Physiology, a section of the journal Frontiers in Plant Science.

Copyright © 2015 Pejchar, Potocký, Krčková, Brouzdová, Daněk and Martinec. This is an open-access article distributed under the terms of the Creative Commons Attribution License (CC BY). The use, distribution or reproduction in other forums is permitted, provided the original author(s) or licensor are credited and that the original publication in this journal is cited, in accordance with accepted academic practice. No use, distribution or reproduction is permitted which does not comply with these terms.



Salicylic acid modulates levels of phosphoinositide dependent-phospholipase C substrates and products to remodel the *Arabidopsis* suspension cell transcriptome

Eric Ruelland^{1,2*}, Igor Pokotylo³, Nabila Djafi^{1,2}, Catherine Cantrel^{1,2}, Anne Repellin^{1,2} and Alain Zachowski^{1,2}

¹ Université Paris-Est Créteil, Institut d'Ecologie et des Sciences de l'Environnement de Paris, Créteil, France

² Centre National de la Recherche Scientifique, Unité Mixte de Recherche 7618, Institut d'Ecologie et des Sciences de l'Environnement de Paris, Créteil, France

³ Molecular Mechanisms of Plant Cell Regulation, Institute of Bioorganic Chemistry and Petrochemistry, National Academy of Sciences, Kyiv, Ukraine

Edited by:

Zuhua He, Chinese Academy of Sciences, China

Reviewed by:

Ruth Welti, Kansas State University, USA

Wenxian Sun, China Agricultural University, China

***Correspondence:**

Eric Ruelland, Centre National de la Recherche Scientifique, Unité Mixte de Recherche 7618, Institut d'Ecologie et des Sciences de l'Environnement de Paris, Université Paris-Est Créteil, Faculté des Sciences, 61 Avenue du Général de Gaulle, 94010 Créteil, France
e-mail: eric.ruelland@upec.fr

Basal phosphoinositide-dependent phospholipase C (PI-PLC) activity controls gene expression in *Arabidopsis* suspension cells and seedlings. PI-PLC catalyzes the production of phosphorylated inositol and diacylglycerol (DAG) from phosphoinositides. It is not known how PI-PLC regulates the transcriptome although the action of DAG-kinase (DGK) on DAG immediately downstream from PI-PLC is responsible for some of the regulation. We previously established a list of genes whose expression is affected in the presence of PI-PLC inhibitors. Here this list of genes was used as a signature in similarity searches of curated plant hormone response transcriptome data. The strongest correlations obtained with the inhibited PI-PLC signature were with salicylic acid (SA) treatments. We confirm here that in *Arabidopsis* suspension cells SA treatment leads to an increase in phosphoinositides, then demonstrate that SA leads to a significant 20% decrease in phosphatidic acid, indicative of a decrease in PI-PLC products. Previous sets of microarray data were re-assessed. The SA response of one set of genes was dependent on phosphoinositides. Alterations in the levels of a second set of genes, mostly SA-repressed genes, could be related to decreases in PI-PLC products that occur in response to SA action. Together, the two groups of genes comprise at least 40% of all SA-responsive genes. Overall these two groups of genes are distinct in the functional categories of the proteins they encode, their promoter *cis*-elements and their regulation by DGK or phospholipase D. SA-regulated genes dependent on phosphoinositides are typical SA response genes while those with an SA response that is possibly dependent on PI-PLC products are less SA-specific. We propose a model in which SA inhibits PI-PLC activity and alters levels of PI-PLC products and substrates, thereby regulating gene expression divergently.

Keywords: lipid signaling, salicylic acid, hormone transduction, *Arabidopsis*, phospholipase C, diacylglycerol kinase, transcriptomic

INTRODUCTION

Phospholipids are secondary messengers in plant signal transduction pathways that start with stimulus perception and lead to changes in gene expression that alter the growth, development and/or physiology of cells (Janda et al., 2013). *Arabidopsis thaliana* cell suspension cultures (ACSC) are an amenable, simplified model in which to study specific signaling mechanisms that would be too complex in plant tissues or organs. For instance, ACSC were recently used to study sugar signaling (Kunz et al., 2014), MAPK kinase and phosphatase signaling (Schweighofer et al., 2014), chitosan and galacturonide elicitor signaling (Ledoux et al., 2014), photooxidative damage (Gutiérrez et al., 2014), auxin transmembrane transport (Seifertová et al., 2014) and ion channel activity (Haapalainen et al., 2012). ACSC are easily labeled which is convenient for studying metabolic fluxes (Tjellström

et al., 2012) like those in lipid phospholipid signaling. ACSC were used in this way to show that a drop in temperature activates both phospholipase C (PLC) and phospholipase D (PLD) pathways (Ruelland et al., 2002), while abscisic acid only activated PLD (Hallouin et al., 2002). We were also showed that stimulation of ACSC with the phytohormone salicylic acid (SA) leads to the rapid activation of PLD and to the production of phosphatidic acid (PA) (Krinke et al., 2009; Rainteau et al., 2012). When PLD-catalyzed PA production is inhibited in the presence of primary alcohols SA-induced gene expression is strongly disrupted, showing that PLD activity is needed to control SA-triggered transcriptome changes (Krinke et al., 2009). *PATHOGENESIS RELATED-1* (*PR-1*), a SA response marker gene related to SA's role in establishing systemic acquired resistance against a broad spectrum of pathogens (Malamy et al., 1990; Metraux et al., 1990;

Durrant and Dong, 2004), is one of these PLD-dependent genes. Treating plants with SA also increases either the PA level or the PLD activity in *A. thaliana*, *Brassica napus*, and *Glycine max* (Profotova et al., 2006; Kalachova et al., 2012), so the signaling information gained from ASCS, although an artificial system, is directly relevant to whole plant physiology.

Phosphoinositide-dependent phospholipase C (PI-PLC) catalyses the hydrolysis of phosphoinositides into soluble phosphorylated inositol and into diacylglycerol (DAG) (Pokotylo et al., 2014). In *Arabidopsis*, PI-PLC enzymes are encoded by 9 genes. Some isoforms are more markedly expressed in response to drought, cold or salt stress (Pokotylo et al., 2014). PI-PLC are involved in plant adaptation to drought, heat, and cold conditions, as shown by pharmacological or reverse genetic approaches (Pokotylo et al., 2014; Ruelland et al., in press). Recently, we showed that a basal level of PI-PLC activity controlled the expression of a number of genes in ACSC (Djafi et al., 2013). In the same ACSC model, two phosphoinositide substrates of PI-PLC, phosphatidylinositol-4-phosphate (PI4P) and phosphatidylinositol-4,5-bisphosphate (PI-4,5-P₂), are formed when a type-III phosphatidylinositol-4-kinase (PI4K) is activated by SA (Krinke et al., 2007). Mechanistically, it is not known how PI-PLC has a downstream effect on gene expression in ACSC.

Here our aim was to clarify the position of PI-PLC in the phospholipidic and genetic control of the ACSC transcriptome in the context of plant hormone responses, and more specifically the SA response. In our previous pharmacological approach, we applied edelfosine and U73122 to inhibit PI-PLC in ACSC and used microarrays to establish which genes were up or down regulated. Here we used this list of PI-PLC controlled genes as a signature in similarity searches against archived microarray data. No additional microarray data was generated here, but data mining and bioinformatics analysis of the inhibited PI-PLC signature allowed us to reassess and extend previous correlations between transcriptome changes and levels of PI-PLC substrates or products triggered by SA. The detection of two SA-regulated pools of genes, distinct in their promoters, regulations and functions, allows us to propose a new working model of the role of PI-PLC and phospholipid signaling in SA transduction, in which both PI-PLC products and substrates participate in SA-triggered transcriptome remodeling.

RESULTS

TRANSCRIPTOME CHANGES CONTROLLED BY EDELFOSENINE, A PI-PLC INHIBITOR, RESEMBLE THOSE CONTROLLED BY SA

We had previously identified genes whose basal expression is dependent on PI-PLC activity. Briefly, by microarray analysis, we monitored transcript levels in ACSC treated or not treated for 4 h with a PI-PLC inhibitor called edelfosine (Djafi et al., 2013). We defined the list of genes altered in response to edelfosine as a “signature.” The Genevestigator interface compares the transcript expression levels from an experiment of interest, the signature, to a subset of other microarray data and returns microarray experiments with similar gene responses. For each comparison, a correlation factor is calculated.

From a subset of 734 microarray experiments categorized as dealing with phytohormone responses, the edelfosine-induced

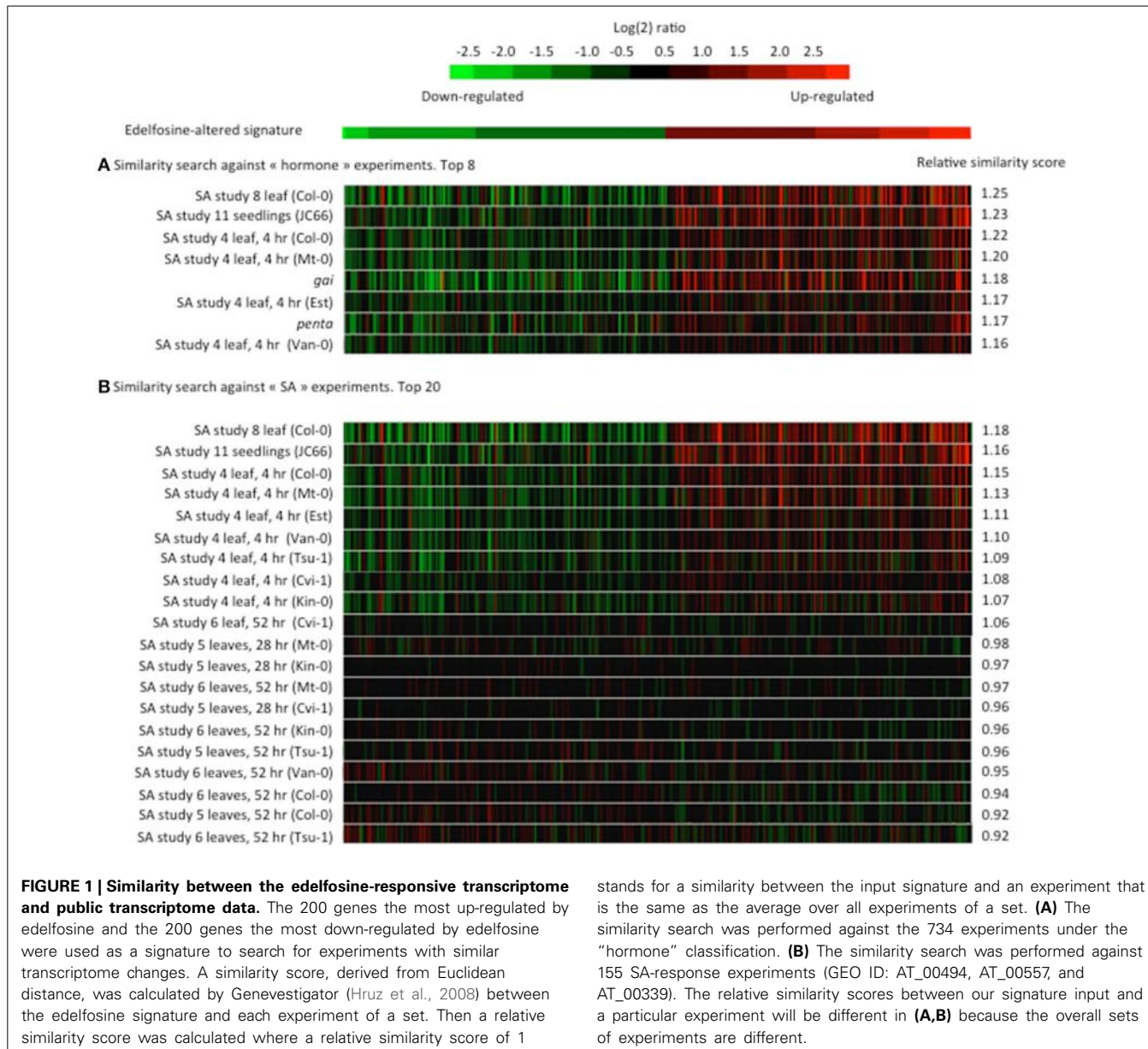
transcriptome changes in ACSC correlated most with changes caused by SA or by the *gai* and *penta* mutations (Figure 1A). SA is a major phytohormone well known for its action in plant responses to biotic stresses (Janda and Ruelland, in press). SA has other roles in plant responses to many abiotic stresses such as chilling, heat, heavy metal toxicity, drought, osmotic stress, and salinity (Horvath et al., 2007; Vicente and Plasencia, 2011). The *penta* mutant is mutated in genes encoding DELLA proteins, while *gai* is a constitutively active dominant DELLA mutant. DELLA proteins are central regulators of growth responses in gibberellin and light signaling pathways (Achard and Genschik, 2008). Interestingly, it was shown that DELLAs promote susceptibility to virulent biotrophs and resistance to necrotrophs, partly by altering the relative strength of SA and jasmonic acid signaling (Navarro et al., 2008). Even though we cannot rule out a direct crosstalk between edelfosine and DELLAs, most, if not all, of the top ranked transcriptome experiments have some link to SA signaling.

As the strongest and most frequent correlations were with the SA response, we performed a second signature similarity search, this time restricting the query database to experiments specifically dealing with SA responses (Figure 1B). The similarity between the edelfosine response and the SA gene response is found in several independent SA experiments on whole seedlings or leaves and in many *Arabidopsis* cultivars. We noted that the edelfosine data correlates more with the early SA response (4 h) than with later responses (28 or 52 h).

IDENTIFICATION OF GENES SIMILARLY CONTROLLED BY TWO PI-PLC INHIBITORS AND SA IN ACSC

In the past, we had analyzed the early SA-triggered transcriptome response in the same ACSC model as the one used for our more recent edelfosine experiments. The list of genes whose expression is altered after 4 h of incubation with SA is given in Table S1A (Krinke et al., 2007). We built a contingency table summarizing the results of the edelfosine and SA experiments by categorizing the responses of each individual gene. A gene may be up-regulated, down-regulated, or not affected by SA. Equally, a gene may be up-regulated, down-regulated, or not affected by edelfosine. An individual gene will therefore have one of nine possible response modes to SA and edelfosine (Table 1). From the microarray experiments, the response modes of 20556 genes were known and these observations were tabulated (Table 1).

To investigate the observed response modes of genes, we first supposed that the effects of SA and edelfosine were independent. Knowing the total number of genes tested on the microarrays, and the total number of genes up-regulated, down-regulated, or unchanged by each treatment separately, it is possible to calculate how many genes would theoretically belong to each of the 9 response modes if they were sorted randomly. We calculated the ratios between the observed number of genes per response mode and the theoretical one (Table 1). We identified 89 genes that are induced both by SA and edelfosine treatment, and 156 genes that are repressed by both treatments. This is not a random distribution as there are 10-fold more genes induced by SA and edelfosine (separately) than would be expected in a random distribution, while 20-fold more were repressed by both treatments



than would be expected. On the contrary, the genes on which SA and edelfosine have opposite effects are not over-represented.

To demonstrate that the relationship between PI-PLC inhibition and SA action was not due to non-specific effects of edelfosine, we used another PI-PLC inhibitor, U73122, which is chemically different from edelfosine (Djafri et al., 2013). We made another contingency table cross-categorizing the list of SA-responsive genes with the list of U73122-responsive genes (Table S2). Again a statistical over-representation of genes similarly regulated by SA and U73122 was observed. Genes induced separately by both SA and U73122 are 7-fold more frequent than would be expected for a random distribution, while those repressed separately by both SA and U73122 are 12-fold more frequent. The genes that respond in the same way to SA and edelfosine are listed in Table S1B and those that respond in the same way to SA and U73122 are listed in Table S1C.

We built a third contingency table categorizing the separate effects of edelfosine and U73122 with their nine possible gene response modes, relative to the three possible SA response modes, giving 27 possible response modes in total (Table 2). The genes that are induced by U73122 and by edelfosine are statistically more likely to be SA-inducible than would be expected if the effects were independent. The genes that are induced by edelfosine but unaffected by U73122, and the genes that are induced by U73122 but unaffected by edelfosine are also more likely to be SA inducible. The over-representation effect is more marked for genes induced by both inhibitors (12.8-fold) than for genes induced by only one inhibitor (i.e., 4.1-fold for U73122-induced and 7.7-fold for edelfosine-induced genes). On the contrary, SA-inhibited genes are less common than expected among the genes that are induced by either one of the two PI-PLC inhibitors. The genes that are repressed by U73122 and by edelfosine are

Table 1 | Contingency table summarizing the gene expression response of *Arabidopsis* cells to edelfosine or SA treatments.

| Number of transcripts per response mode | SA > control | SA = control | SA < control | Total |
|-----------------------------------------|----------------|----------------------|----------------|--------|
| Edelfosine > control | 89 (8.9) | 301 (377.9) | 3 (6.1) | 393 |
| | 10 | 0.8 | 0.5 | |
| Edelfosine = control | 365 (450.1) | 19,197 (18,980.8) | 175 (306.1) | 19,737 |
| | 0.8 | 1.0 | 0.6 | |
| Edelfosine < control | 15 (9.9) | 280 (419.3) | 141 (6.8) | 436 |
| | 1.5 | 0.7 | 21 | |
| Total | 469 | 19,778 | 319 | 20,556 |

For each response mode, the number of genes previously reported to be up-regulated (>), down-regulated (<) or unaffected (=) by a treatment were included. Assuming that edelfosine and SA act independently on gene expression, the number of genes predicted to be found for each response mode (given in brackets) was calculated as the product of the corresponding row and column totals divided by the total number of genes tested. The ratio of the “observed number of genes” to “theoretical number of genes” is given in bold.

statistically more likely to be SA-repressed than would be expected if the effects were independent. The genes that are repressed only by edelfosine and the genes that are repressed only by U73122 are also more likely to be SA-repressed. The over-representation effect is more marked for genes repressed by both inhibitors (29.6-fold) than for genes repressed by only one of them (3.5-fold for U73122-induced genes and 9.3-fold for edelfosine-induced genes). The list of genes that respond in the same way to SA, edelfosine and U73122 is in Table S1D.

SA INHIBITS BASAL PI-PLC ACTIVITY IN ACSC

The fact that SA treatment can be in part mimicked by inhibitors of PI-PLC might indicate that part of the SA signal is transduced via PI-PLC inhibition. To investigate whether PI-PLC is inhibited in ACSC, we used radioactive ^{33}Pi orthophosphate labeling to visualize phosphorylated lipids. PI-PLCs use phosphoinositides PI4P and/or PI-4,5-P₂ as substrates and release phosphorylated inositol and DAG, which can be further phosphorylated into PA by DGKs. Inhibition of PI-PLC would be expected to lead to an increase in substrates and a decrease in products (and of any derivatives). We added 250 μM SA to ACSC and extracted lipids 20 and 45 min later, labeling cells 15 min before the lipid extraction. When short labeling times are used, labeled PA is almost exclusively due to DGK activity (Vaultier et al., 2006; Djafi et al., 2013). As already reported (Krinke et al., 2007), SA induced an increase in phosphoinositides (Figure 2A). Furthermore, SA led to a small but significant decrease in PA (Figure 2B). This suggests that PI-PLC activity is inhibited as early as 20 min after SA stimulation, resulting in an increase in phosphoinositides and a decrease in DAG, PA and phosphorylated inositol.

Table 2 | Contingency table summarizing the gene expression response of *Arabidopsis* cells to edelfosine, U73122 or SA treatments.

| Number of transcripts per response mode | SA > control | SA = control | SA < control | Total |
|-----------------------------------------|---------------|--------------------|---------------|-------|
| Edelfosine > control | 60 (4.7) | 147 (200.1) | 1 (3.2) | 208 |
| | 12.8 | 0.7 | 0.31 | |
| Edelfosine = control | 119 (28.9) | 1238 (1309.2) | 4 (21.1) | 1361 |
| | 4.1 | 0.9 | 0.19 | |
| Edelfosine < control | 28 (3.6) | 131 (154.9) | 2 (2.5) | 161 |
| | 7.7 | 0.8 | 0.8 | |
| Edelfosine > control | 2 (0.13) | 4 (5.8) | 0 (0.1) | 6 |
| | 14.8 | 0.7 | 0 | |
| Edelfosine = control | 227 (380) | 16558 (16232.2) | 89 (261.8) | 16874 |
| | 0.6 | 1.02 | 0.34 | |
| Edelfosine > control | 0 (0.04) | 2 (1.9) | 0 (0.03) | 2 |
| | 0 | 1.03 | 0 | |
| Edelfosine = control | 14 (33.7) | 1401 (1440.1) | 82 (23.2) | 1497 |
| | 0.4 | 1.0 | 3.5 | |
| Edelfosine < control | 8 (4.7) | 171 (201.1) | 30 (3.2) | 209 |
| | 1.7 | 0.9 | 9.3 | |
| Edelfosine < control | 5 (5.45) | 126 (232.8) | 111 (3.8) | 242 |
| | 0.91 | 0.54 | 29.6 | |
| Total | 463 | 19778 | 319 | 20560 |

For each response mode, the number of genes previously reported to be up-regulated (>), down-regulated (<) or unaffected (=) by a treatment were included. Assuming that edelfosine and U73122 act independently of SA, the number of genes predicted to be found for each response mode (given in brackets) was calculated as the product of the corresponding row and column totals divided by the total number of genes tested. The ratio of the “observed number of genes” to the “theoretical number of genes” is given in bold.

ARE ANY SA-REGULATED GENES REGULATED THROUGH PI-PLC INHIBITION AND MODULATIONS IN THE LEVELS OF ITS SUBSTRATES OR PRODUCTS?

We can hypothesize that PI-PLC substrates positively or negatively regulate the basal expression of clusters of genes in resting cells, named clusters A and D respectively in Figure 3.

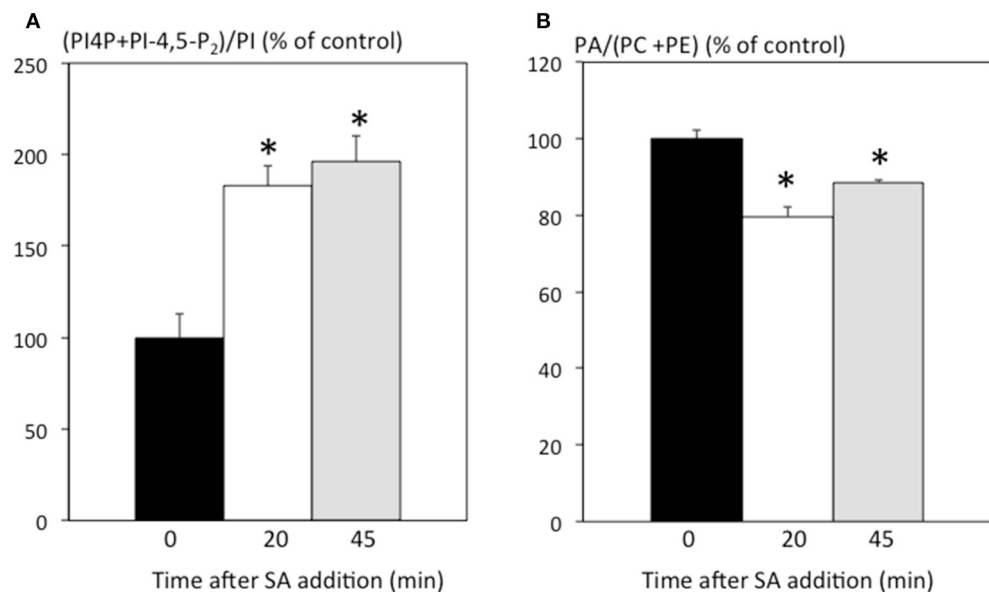


FIGURE 2 | SA effects on radioactively labeled phospholipids. Cells were treated with 250 μ M SA. Labeling was initiated 15 min before lipid extraction. Lipids were extracted and separated by TLC. **(A)** Amount of radioactivity incorporated into phosphoinositides relative to PI expressed

as % of the control without SA. **(B)** Amount of radioactivity incorporated into PA relative to the sum of PC and PE expressed as % of the control without SA. *Indicates a value statistically different from time 0 (*t*-test, *p*-value < 0.05).

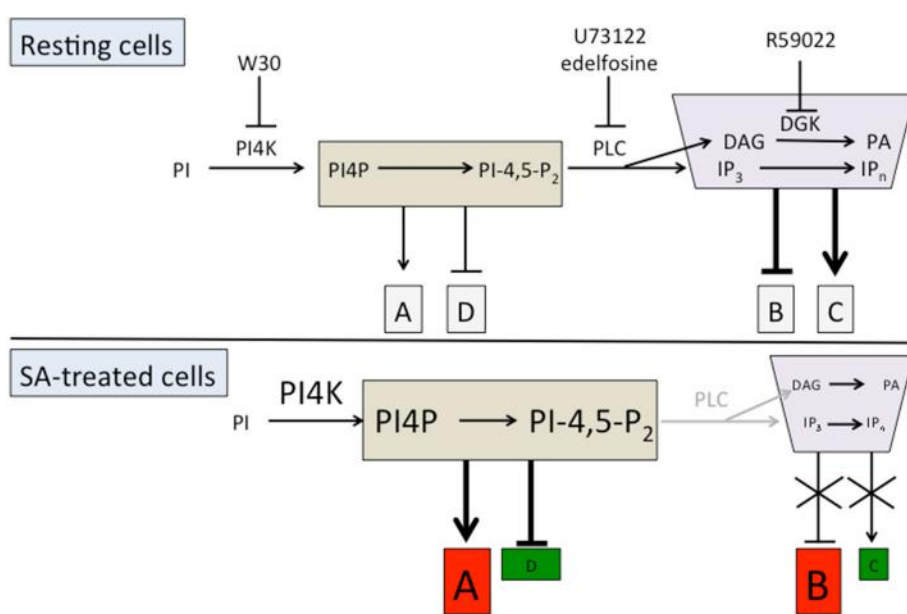


FIGURE 3 | Working model of the action of PI-PLC substrates and products on SA-triggered gene expression. The action of PI-PLC substrates and products on gene expression is represented either by an

arrow (positive action) or a line with a bar (negative action). The clusters of genes induced after SA treatment are represented in red and those inhibited in green.

Similarly, PI-PLC products could negatively or positively regulate the expression of some genes, respectively clusters B and C (Figure 3). When SA inhibits PI-PLC activity, the resulting increase in substrates leads to an enhancement of their basal action on gene expression. Cluster A genes would be induced by

SA and cluster D genes repressed by SA in a phosphoinositide-dependent manner. On the other hand, PI-PLC inhibition would alleviate the effects of its products on gene expression. Thus, cluster B genes would be induced and cluster C genes repressed compared to the resting state.

Is it possible to identify these hypothetical gene clusters? We have previously done a microarray experiment to find genes that are regulated by wortmannin. Type III-PI4Ks responsible for phosphoinositide formation are inhibited by 30 μ M wortmannin (W30), but not 1 μ M wortmannin (W1). These PI4Ks act immediately upstream of basal PI-PLC activity (Figure 3; Delage et al., 2012). For the genes that are regulated by basal PI-PLC products, W30 and edelfosine should have the same effects as both reduce the quantity of PI-PLC products. On the contrary, for the genes that are regulated by PI-PLC substrates, W30 and edelfosine should have opposite effects. W30 will diminish the level of phosphoinositides, while inhibiting PI-PLC with edelfosine will increase it.

To identify SA responsive genes regulated by PI-PLC inhibition, that is through substrate increase or product decrease, we can categorize the genes according to how they are regulated by SA, by edelfosine, by W30, or by SA in the presence of W30.

From the 463 SA-induced genes in ACSC, we first discounted the 141 genes that were unaffected by treatments with edelfosine or W30 (Figure 4A). SA induction of cluster A genes is inhibited by W30 and not by W1, so they must be among the subset that is down-regulated in the SAW30 (SAW, SA + wortmannin) condition compared to the SAW1 condition. The basal level of regulation by PI-PLC substrates is already in place in resting cells, with SA-dependent PI-PLC inhibition only enhancing it. This basal regulation must be of the same nature and cannot be opposite to regulation in the presence of SA. The genes must be expressed at a lower level in W30 than in W1, so we can eliminate the 6 genes that are more expressed in W30 than in W1. The subset of 12 genes that are repressed by edelfosine is excluded, as this would not be compatible with basal PI-PLC substrates having a positive role. The remaining 114 genes thus form cluster A (Figure 4A). Cluster B genes are induced by an alleviation of repression via PI-PLC products. These genes must be induced by edelfosine and by W30, as both molecules inhibit the basal PI-PLC pathway. The effect of W30 in the presence of SA is either neutral or additive, so the 2 genes that are repressed by SAW30 compared to SAW1 can be excluded. Therefore, 51 genes have the characteristics of cluster B genes.

The same step-wise analysis can be made for SA-repressed genes (Figure 4B). Discounting 67 genes that show no alteration in expression with any treatment, 247 genes remain. Cluster D genes are repressed by SA through the action of PI-PLC substrates. They have higher expression in SAW30 than in SAW1. This regulation may be in place in the absence of SA, but cannot be oppositely regulated. We can thus identify 26 genes that have the characteristics of cluster D. A final important point is that the genes of cluster C are already regulated in resting cells as they are induced by a basal PI-PLC activity through its products. Edelfosine should repress their expression (149 remaining genes), and so should W30. The remaining 118 genes have the characteristics of cluster C genes. Genes in clusters A, B, C, and D are listed in Table S3.

The expression characteristics of the genes in these newly defined clusters can be visualized graphically in Figure 5. Cluster A genes are SA-induced genes that can or cannot be induced independently by edelfosine. Importantly, the induction by SA of these

genes is repressed by W30. This inhibiting effect of W30 can also be detected on the basal expression without SA. Cluster B gene expression is induced by SA through the alleviation of a basal repression by PI-PLC products. These genes are induced independently by edelfosine and W30. For SA-repressed genes, the repression of cluster D genes is inhibited by W30, and inhibition by W30 can also, but not necessarily, be observed in resting cells. Cluster C genes are repressed by SA through alleviation of induction by PI-PLC products. W30 and edelfosine can repress cluster C expression in the absence of SA.

To pinpoint the effects of PI-PLC inhibition, we compared the effect of U73122 on gene expression to the effect of edelfosine to see if the same genes were assigned to each cluster despite using inhibitors with different biochemical modes of action (Figure 6). To continue the analysis, only the genes that were common to a cluster in both the edelfosine and the U73122 analyses were considered. In these *stringent* clusters A, B, C, and D, there are 105, 39, 97, and 23 genes, respectively (Table S4).

As all the data were from microarray experiments, the regulation of expression of some genes was confirmed by quantifying transcripts by qPCR. In fact, cluster A and cluster D gene expression had already been “confirmed” by Krinke et al. (2007). We therefore focused on two SA inhibited genes representative of the 118 genes in cluster C, the largest non-stringent cluster (Figure 7).

The SA responsive genes form two pools, one corresponding to genes dependent on PI-PLC substrates for their SA response, and the other corresponding to genes dependent on PI-PLC products for their SA response.

CLUSTERS INCLUDE GENES FROM SPECIFIC FUNCTIONAL CLASSES

The stringent clusters of genes are selected subsets of genes induced or repressed by SA. Some of the gene names from the four clusters are listed in Figure 7 with more precise details of their individual expression profiles. The genes of the different stringent clusters were classified according to gene ontology (GO) classes of “Biological processes,” “Molecular function,” and “Cellular component.” The results were normalized to the frequency of each class over the entire genome (Figure 8).

When compared to all SA-induced genes, cluster A is poor in genes involved in “response to abiotic or biotic stress” biological processes and has less “structural molecule activity” but more “nucleic acid binding” molecular functions. Cluster B is enriched in genes involved in “response to stress,” “response to abiotic and biotic stress” and “signal transduction” biological processes. Cluster B is also depleted in “nucleotide binding” and “transcription factor activity” but is enriched in “protein binding” molecular functions. Cluster B is enriched in “endoplasmic reticulum” and “Golgi” cellular components but depleted in “cell wall,” “extracellular” and “ribosome” cellular components (Figure 8).

When compared to all SA-repressed genes in ACSC, cluster C is depleted in genes involved in “developmental” and “electron transport” biological processes and in “nucleotide binding” and “transcription factor activity” molecular functions. Cluster C is enriched in genes encoding “cell wall” and “extracellular” components but is depleted in “plastid” components. Cluster D is depleted in genes involved in “cell organization,” “responses to

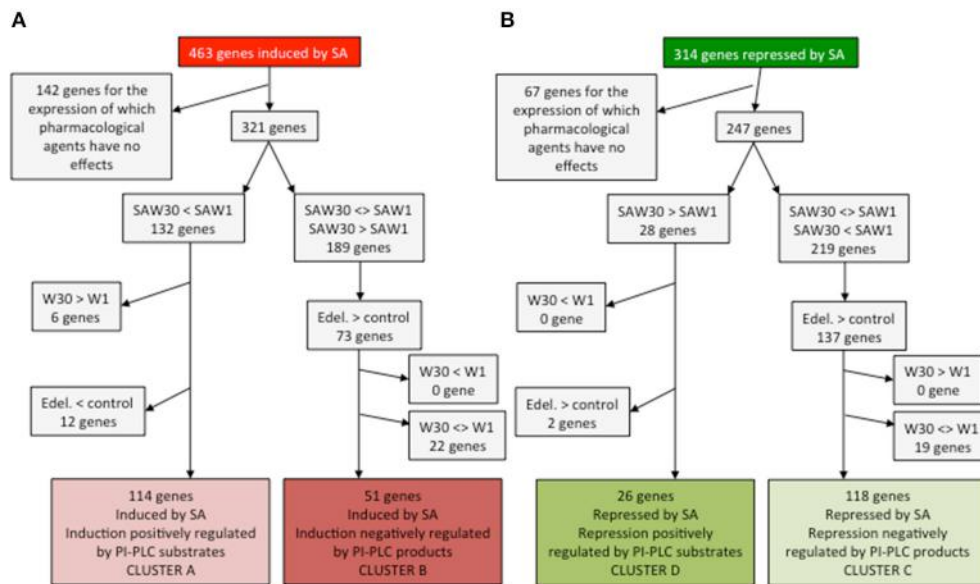


FIGURE 4 | Identification of genes whose expression characteristics are consistent with the clusters defined in Figure 3. Cluster A and B genes are SA-induced genes (A) while clusters C and D genes are SA-repressed genes (B).

abiotic and biotic stresses,” “DNA or RNA metabolism,” “protein metabolism” and “electron transport” biological processes. Cluster D is also depleted in “receptor binding activity” and “hydrolase activity” molecular functions and in “plasma membrane” and “extracellular” cellular components (Figure 9).

SPECIFIC PROMOTER CIS-ELEMENTS ARE OVER-REPRESENTED IN THE DIFFERENT CLUSTERS

The transcriptome responses to SA and to PI-PLC inhibition are rapid. We compared the promoters of the genes in *stringent* clusters A, B, C, and D by scanning for motifs. Some motifs are over-represented in the genes of the clusters relative to the whole genome dataset (Figure 10). Some of the motifs identified in clusters A and B and in clusters C and D are also over-represented when the motif scan compared all SA-induced and SA-repressed genes against the whole genome data set. This is not surprising since these clusters together include most of the SA-sensitive genes of Arabidopsis. In cluster A promoters, the W box is over-represented compared to the whole set of SA induced genes. In cluster B promoters, the T-box motif is over-represented when compared to the whole set of SA-induced genes. Not all the sequence motifs found are known as regulatory elements.

THE GENES OF THE DIFFERENT CLUSTERS DIFFER IN THEIR SA SPECIFICITY

More signature similarity searches were carried out with the genes of each of the different clusters. Which conditions lead to a similar shift in gene expression as the expression of each cluster in response to SA (Figure 11)?

For the signature SA response of cluster A, the top 10 most similar perturbations all relate to biotic stress and/or SA. For example, similar transcriptomes include Arabidopsis treated

with: *Hyeloperonospora arabidopsis* (the oomycete causal agent of downy mildew of Arabidopsis); bleomycin, an iron chelator (iron chelation is known to cause an increase in SA, Dellagi et al., 2009); pep2, an Arabidopsis derived active peptide elicitor that facilitates immune signaling and pathogen defense responses (Ross et al., 2014); or SA. Other similar transcriptomes were found in comparisons of *cpr5* (Bowling et al., 1994, 1997), and a *camta* triple mutant (Kim et al., 2013), mutants with constitutively high endogenous SA, to wild type plants. The signature of the cluster B response to SA does not match the same gene expression profiles as cluster A except for experiments dealing with treatment with SA. The top 10 most similar physiological perturbations of Arabidopsis include: inoculation with *Pseudomonas syringae*, a biotic stress that induces SA; treatment with fenchlorim (4,6-dichloro-2-phenylpyrimidine), a safener that increases tolerance of chloroacetanilide herbicides in rice by enhancing the expression of detoxifying glutathione S-transferases (Brazier-Hicks et al., 2008; Skipsey et al., 2011); osmotic stress; and drought. Genetic perturbations with similar gene expression effects are *flu1* or *arf7arf19* compared to wild type plants. *FLU1* encodes a coiled-coil, TPR domain-containing protein that is localized to the chloroplast membrane and is involved in chlorophyll biosynthesis. *flu1* plants accumulate protochlorophyllide, an intermediate in the chlorophyll biosynthesis pathway and release singlet oxygen in plastids upon a dark/light shift (Laloi et al., 2006). *arf7arf19* is a loss-of-function mutant of the auxin response factors ARF7 and ARF19 (Narise et al., 2010). Therefore, the genes of cluster B, while responding to SA, appear to be less characteristic of a typical SA response, and might correspond to a more general stress response like the oxidative stress response.

The response of cluster C genes to SA is similar to other SA or biotic stress experiments, but also to responses of plants treated with: salt; fenchlorim; phytoprostane A1,



FIGURE 5 | Representation of genes of cluster A, B, C, and D according to their expression in response to SA, to edelfosine, to W30 and to W30 in the presence of SA (SAW30). Red blocks indicate relative higher transcript levels in the condition written in red at the top of the table (versus that written in green); green blocks indicate higher transcript levels in the conditions written green at the top of the table (versus that written in red) and black blocks indicate no significant difference in transcript levels between both conditions. Note that clusters

B^E and C^E and clusters B^{W30} and C^{W30} are also represented here. Clusters B^E and B^{W30} are the genes that would belong to cluster B if we had considered that a basal inhibiting effect of either edelfosine or W30 respectively was sufficient for a gene to be classed as cluster B. Clusters C^E and C^{W30} are the genes that would belong to cluster B if we had considered that a basal inhibiting effect of either edelfosine or W30 respectively was sufficient for a gene to be classed as cluster C. These clusters are mentioned in Discussion.

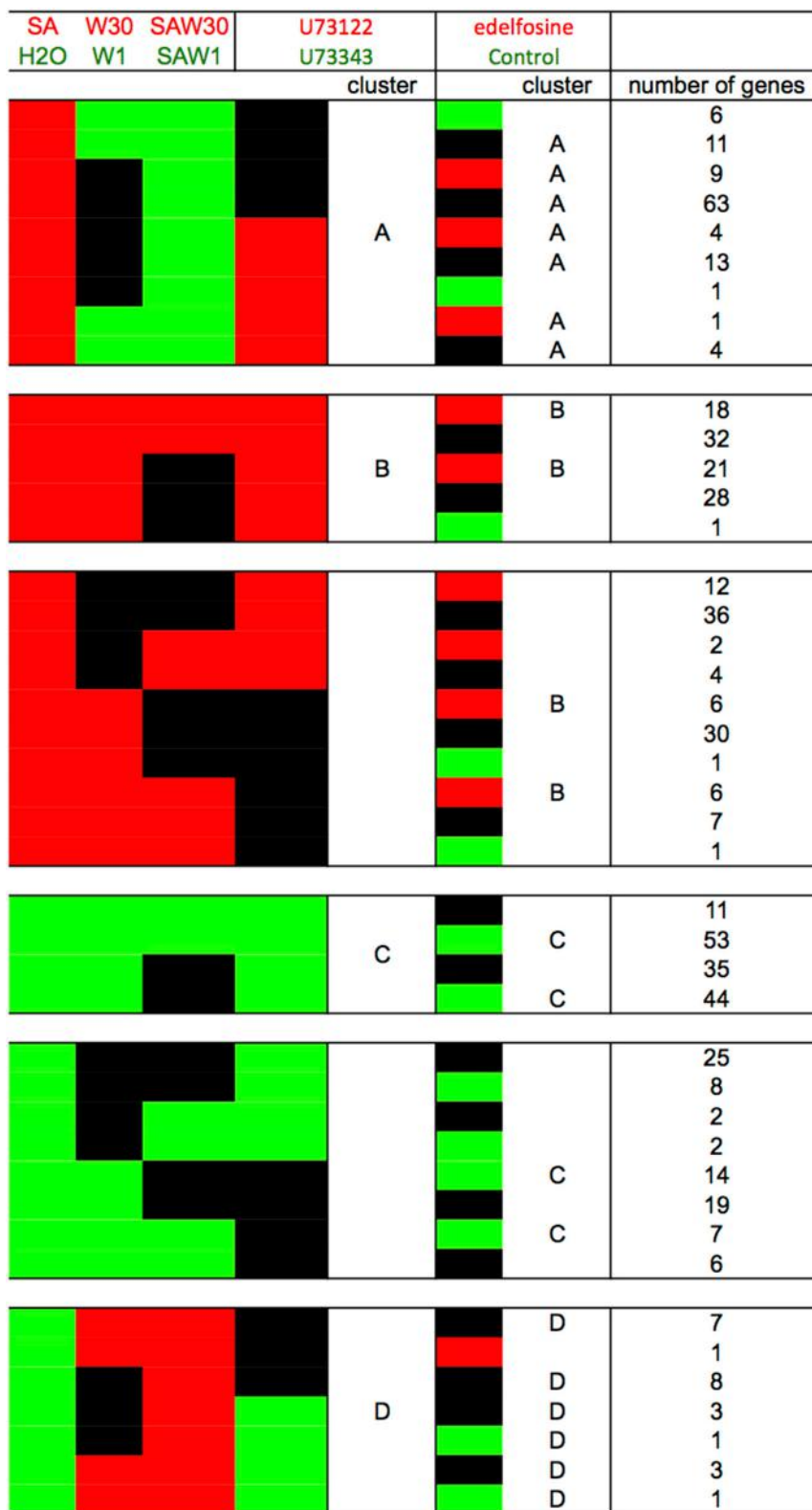


FIGURE 6 | Comparison of the clustering result according to the use of edelfosine or U73122 as the PI-PLC inhibitor. Red blocks indicate relative higher transcript levels in the condition written in red at the top of the table (versus that written in green); green blocks indicate higher transcript

levels in the conditions written green at the top of the table (versus that written in red) and black blocks indicate no significant difference in transcript levels between both conditions. Stringent clusters were defined from this analysis.

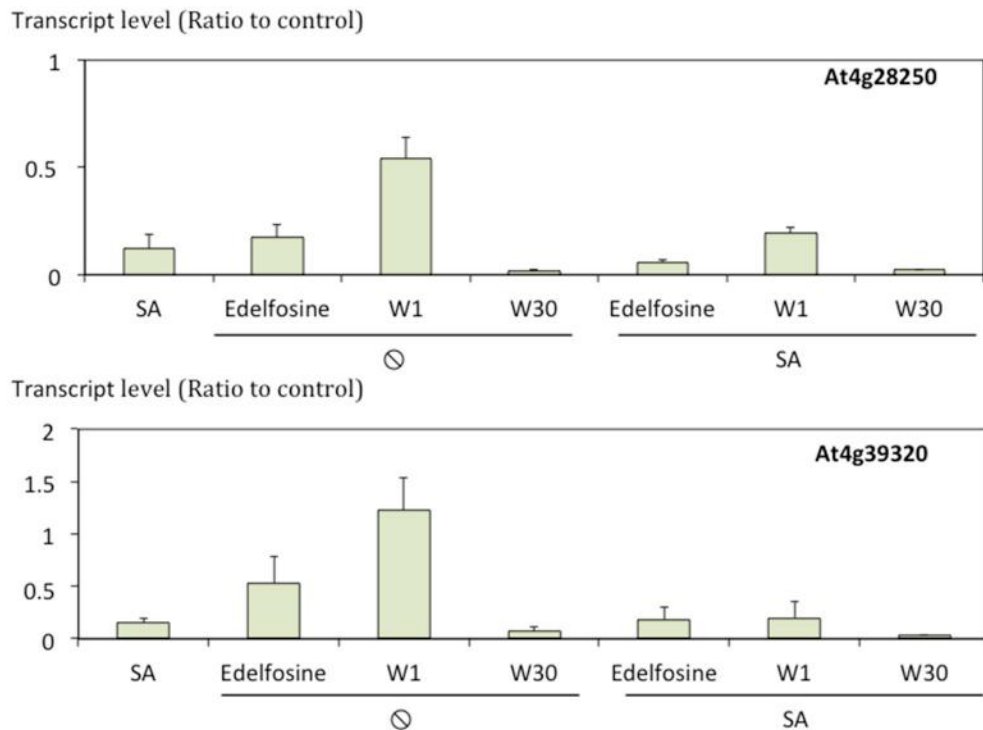


FIGURE 7 | Transcript levels of At4g28250 and At4g39320 in response to SA and/or lipid signaling inhibitors. Transcript levels were quantified by qPCR, normalized to actine transcript level and expressed relative to levels in control cells. $n = 3$.

which is a cyclopentenone oxylipin (Stotz et al., 2013); and DFPM ([5-(3,4-dichlorophenyl)furan-2-yl]-piperidine-1-ylmethanethione), a small molecule that rapidly down-regulates ABA-dependent gene expression (Kim et al., 2011). Here again, the gene response signature seems not to be specific to SA. For the cluster D response to SA, most of the similarities are to gene expression profiles in plants treated with SA or having high endogenous amounts of SA.

It is intriguing to find that the response to SA of genes of cluster B (SA-induced) and cluster C (SA-repressed) retrieve some of the same experiments in the signature searches. We therefore built an artificial list of genes merging clusters B and C. The response to SA of these genes was used as a signature in a similarity search and again SA experiments were the most similar, confirming that using either induced or repressed genes alone does not distort the accuracy of signature searches.

SA RESPONSES OF THE CLUSTERS DIFFER IN THEIR DEPENDENCY ON PLD

We have previously shown that SA activates PLD activity in ACSC (Krinke et al., 2009). We wanted to know if any genes of the different clusters depend on PLD for their response to SA. PLD can use primary alcohols as a substrate, producing phosphatidyl-alcohol instead of PA. It is therefore possible to identify which genes are dependent on PLD for their expression by studying the effect of primary alcohol (e.g., *n*-butanol, *n*-ButOH) and comparing it to the effect of a non-substrate alcohol (*tertiary*-butanol, *tert*-ButOH) (Krinke et al., 2009). We thus showed that for some genes

their response to SA could be inhibited by *n*-butanol, suggesting that the SA response is dependent on PLD activity.

The genes of the *stringent* clusters A, B, C, and D were sorted according to the effect of *n*-ButOH compared to *tert*-ButOH in the presence or absence of SA (Figure 12). If we first consider the SA-induced genes, we see a marked difference between clusters A and B. In cluster A, the SA induction of many more genes is repressed by *n*-ButOH rather than enhanced. There is a 14-fold over-representation in *stringent* cluster A of genes whose induction by SA is repressed by *n*-ButOH compared to *tert*-ButOH. On the contrary, for *stringent* cluster B genes, there is an over-representation of genes for which *n*-ButOH enhances the induction by SA. The effect of *n*-ButOH is seen even on the basal expression of cluster B genes. For genes inhibited by SA, in both *stringent* clusters C and D, the differences in the effect of *n*-ButOH or *tert*-ButOH on SA was not as marked as for cluster A genes.

GENES OF THE DIFFERENT CLUSTERS DIFFER IN THEIR RESPONSE TO R59022, A DGK INHIBITOR

The effect of basal PI-PLC can be partially attributed to a secondary effect on basal DGK, as seen by the action of DGK inhibitor R59022 (Djafri et al., 2013). Each gene of the different stringent clusters was sorted according to its expression in response to R59022 (Figure 13). Knowing that in the total group of genes 181 genes were repressed, 19705 genes were unaffected, and 261 genes were induced by R59022, we calculated the theoretical number of genes that should be present in each cluster

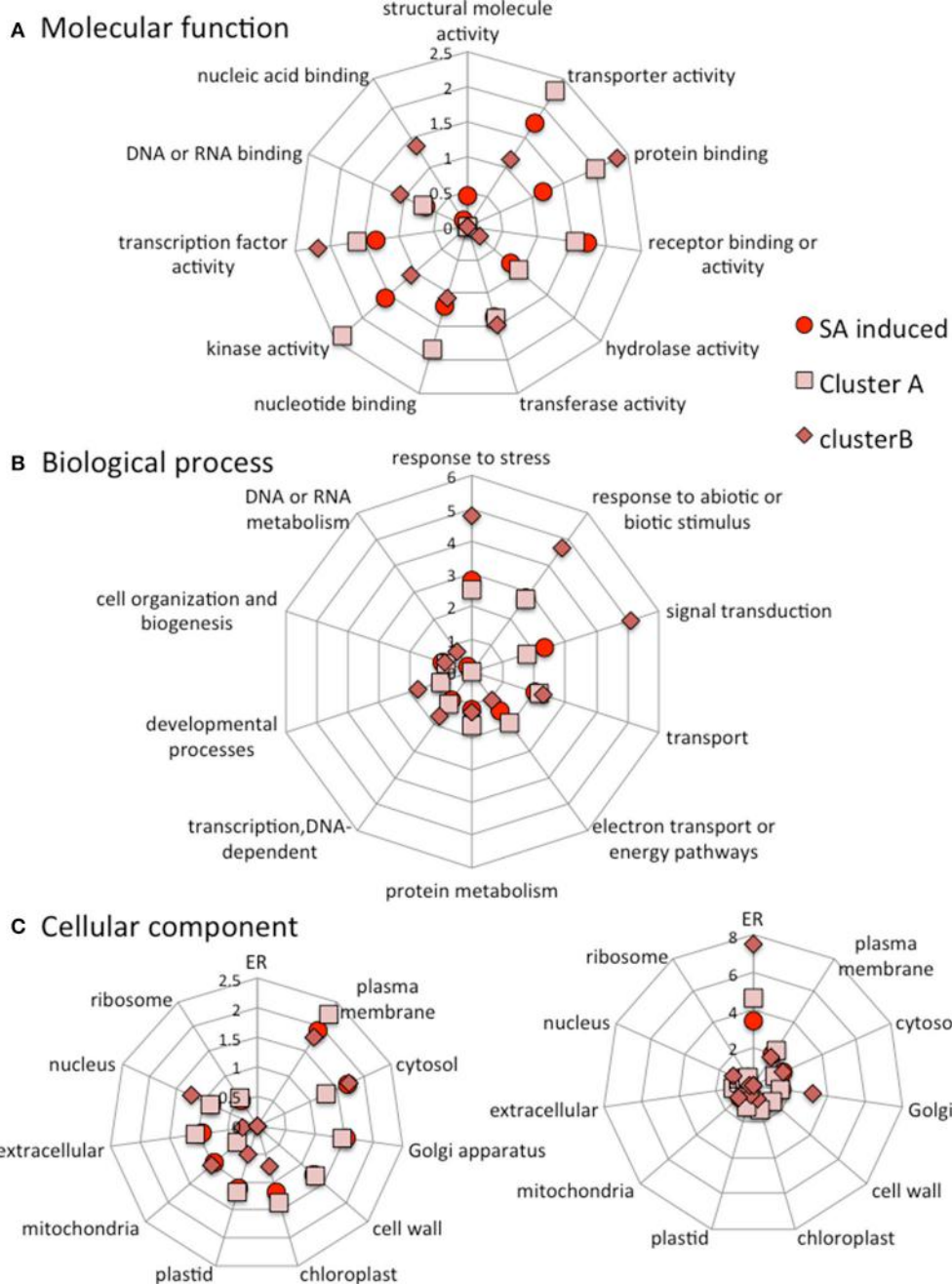


FIGURE 8 | Categorization of all SA-induced genes, cluster A genes and cluster B genes according to the molecular functions (A), Biological processes (B) and Cellular components (C) they are associated with. The

data are normalized to category frequencies in the *Arabidopsis* genome dataset. The mean and SD for 100 bootstraps of the input were calculated. For cellular component analysis, two scales are used for clarity.

if the gene expression was independent from the other cluster criteria.

Amongst cluster B genes, there is a 36-fold over-representation of genes that are induced by R59022. The basal level of these genes is negatively regulated by DGK. Conversely, amongst cluster C genes, there is a 31-fold over-representation of genes that are repressed by R59022. The basal level of those genes is positively regulated by DGK.

DISCUSSION

In a previous work we detected basal PI-PLC activity *in vivo* by assaying the DGK activity that is most likely coupled to this PI-PLC. PI-PLC was active in ACSC and this activity controlled the expression of some genes. To draw up the list of genes controlled by the basal PI-PLC activity, edelfosine, and U73122 were used separately to inhibit PI-PLC activity. The limitations of such a pharmacological approach were already discussed in

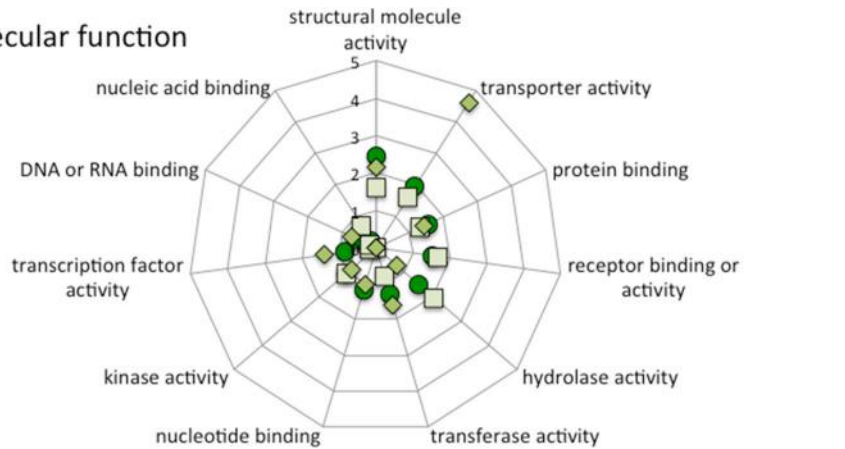
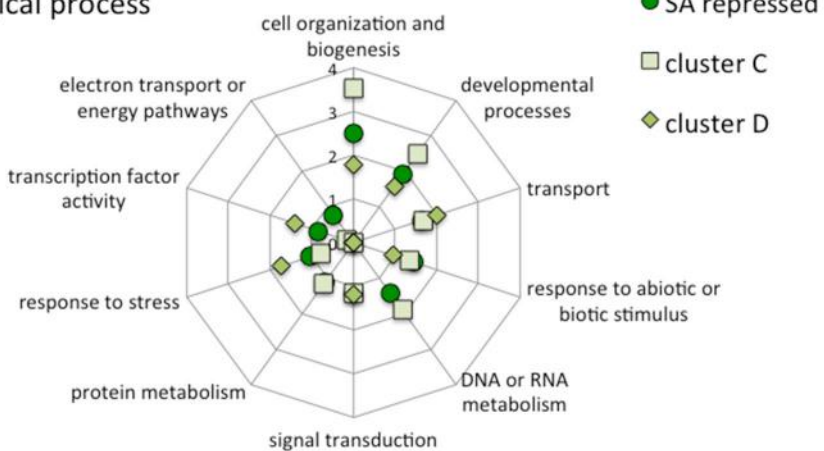
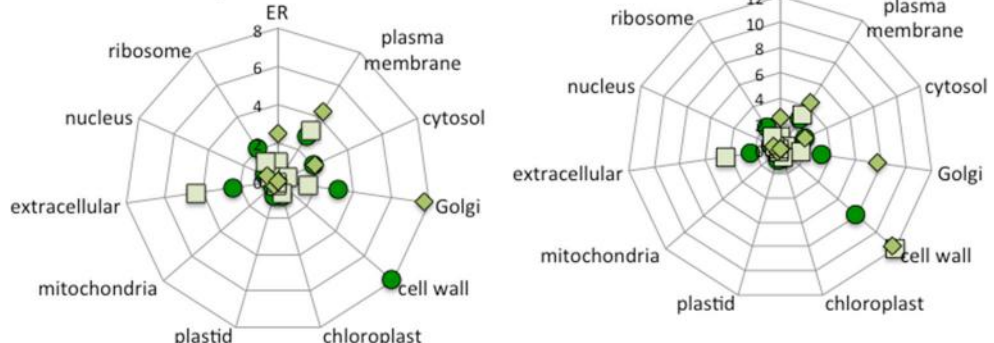
A Molecular function**B Biological process****C Cellular component**

FIGURE 9 | Categorization of all SA-repressed genes, cluster C genes and cluster D genes according to the molecular functions (A), Biological processes (B) and Cellular components (C) they are associated with. The

data are normalized to category frequencies in the *Arabidopsis* genome dataset. The mean and SD for 100 bootstraps of the input were calculated. For cellular component analysis, two scales are used for clarity.

depth (Djafi et al., 2013), but need to be taken into account here. Briefly, U73122, the most commonly used PI-PLC inhibitor, might have side effects. It is thought to be an alkylating agent and certain side effects might be attributable to general protein alkylation (Mogami et al., 1997; Horowitz et al., 2005). We previously demonstrated that edelfosine inhibits PI-PLC activation by cold shock in ACSC (Ruelland et al., 2002). Edelfosine does not have the structure of an alkylating agent and does not have

the same side effects as U73122 (Powis et al., 1992; Horowitz et al., 2005; Wong et al., 2007; Kelm et al., 2010). It could have other side effects, since its lyso-alkyl-phosphatidylcholine structure makes it an inhibitor of CTP:phosphocholine cytidylyltransferase (Boggs et al., 1995). However, we have shown that these two unrelated molecules have similar inhibitory effects on the same enzyme in a pathway leading to the same changes in gene expression.

| clusterA | | motif | | |
|----------|--|------------------------------------------------------|--------------------------------------------------------|------------------------------------------------|
| * | | W-box (TTGAC) | Over-represented in SA -induced vs. whole genome set | Over-represented in cluster A vs. SA - induced |
| * | | Circadian clock associated 1 binding site (AAMAATCT) | Over-represented in SA -induced vs. whole genome set | |
| * | | Dof proteins binding site core sequence (AAAG) | Over-represented in SA -induced vs. whole genome set | |
| * | | Non described | | |
| * | | Non described | | |
| * | | Non described | Over-represented in SA -induced vs. whole genome set | |
| clusterB | | | | |
| * | | T-box (ACTTG) | Over-represented in SA -induced vs. whole genome set | Over-represented in cluster B vs. SA - induced |
| clusterC | | | | |
| | | Mesophyll expression module 1 (YACT) | Over-represented in SA -repressed vs. whole genome set | |
| | | BELL homeodomain factor binding site (TGTCA) | | |
| | | Heat shock element (CCAAT) | Over-represented in SA -repressed vs. whole genome set | |
| | | Non described | | |
| clusterD | | | | |
| | | Low temperature responsive element (ACCGACA) | Over-represented in SA -repressed vs. whole genome set | |
| | | Non described | | |

FIGURE 10 | Motifs over-represented in clusters A, B and C, D compared to whole genome promoter set. Sequences of promoter regions were analyzed for 4- to 10-bp motifs over-represented in genes of the cluster vs. the whole genome set (p -value $< 10^{-5}$; Chi-squared test). Among the motifs thus obtained a search for described *cis*-acting

elements was performed. *, *cis*-acting element is located on reverse strand; M, A or C; Y, C or T. *Cis*-acting element is over-represented compared to the bulk list of SA-induced genes. The sizes of the nucleotide symbols indicate their frequency in the corresponding sequence.

Similarity searches for gene expression signatures provide preliminary indications that edelfosine and U73122 trigger transcriptome changes similar to those induced by SA in whole seedlings, leaves and ACSC (Krinke et al., 2007). More genes

are regulated, whether repressed or induced, in the same way by SA and PI-PLC inhibitors than would be expected if the effects were independent. Interestingly, Chou et al. (2004) identified a few genes for which inhibition of PI-PLC by U73122 mimics

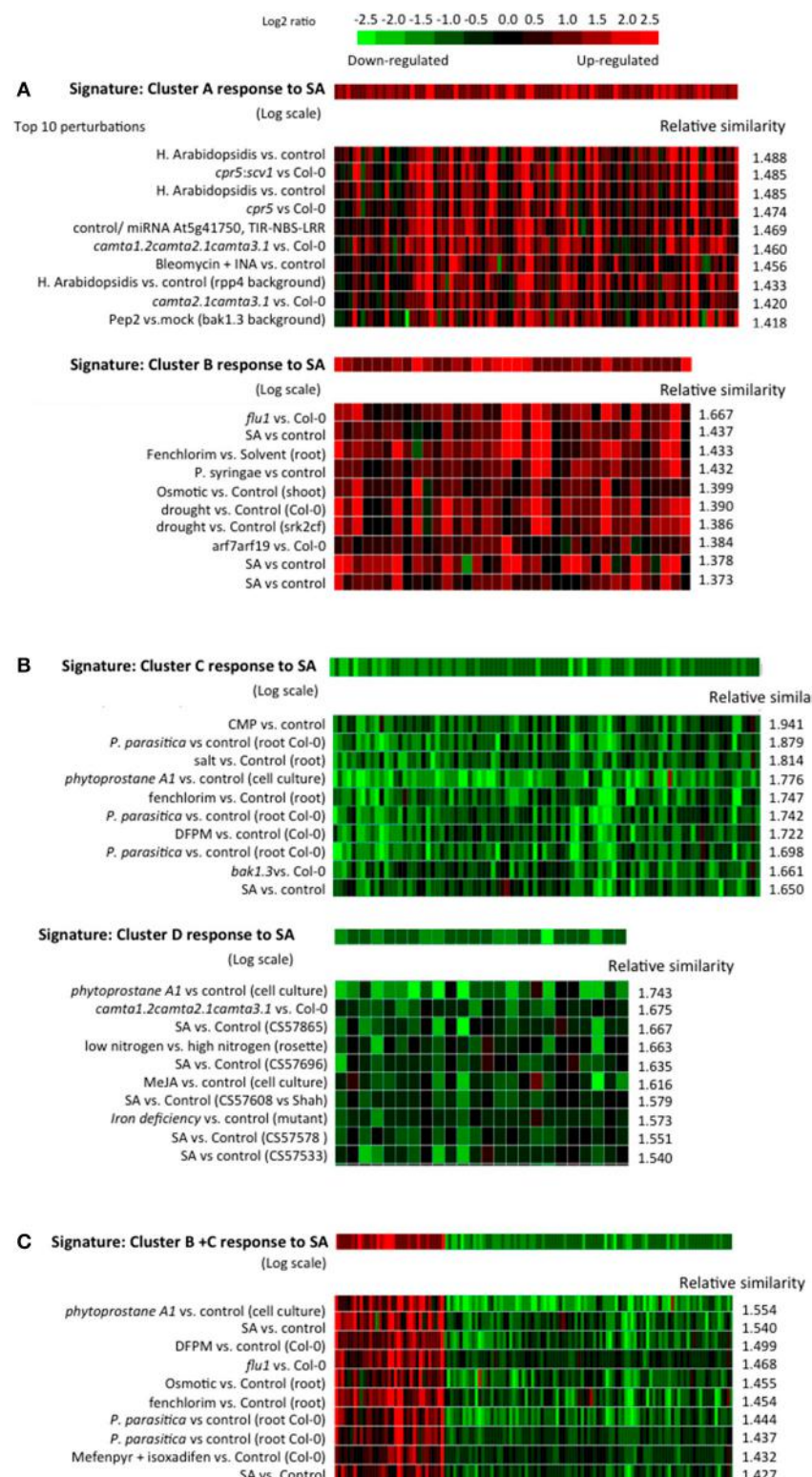


FIGURE 11 | Similarity between the SA responses of cluster A, B, C, and D and archived *Arabidopsis* transcriptomes in public databases. (A) Top 10 similar experiments retrieved using the response to SA of cluster A or cluster B genes as a signature. **(B)** Top 10 similar experiments retrieved using the response to SA of cluster C or cluster D genes as a signature. **(C)** Top 10 similar experiments retrieved using, as a signature, the response to SA of a list

of genes composed of cluster B and C. The similarity search was performed using the Genevestigator signature module. An Euclidean distance-derived similarity score was calculated between our signature and each experiment of a set. A relative similarity score was calculated where a relative similarity score of 1 stands for a similarity between the input signature and an experiment that is the same as the average over all experiments of the set.

| cluster | n-ButOH+SA t-ButOH+SA | number of genes | | ratio | n-ButOH t-ButOH | number of genes |
|-----------------------|--------------------------|-----------------|-------------|-------|----------------------------------------------|-----------------|
| | | observed | theoretical | | | |
| A | | 52 | 3.68 | 14.12 | 10 41 1 3 32 9 0 0 5 | |
| | | 44 | 93.50 | 0.47 | | |
| | | 5 | 3.82 | 1.31 | | |
| total number of genes | | 101 | | | | |
| B | | 2 | 1.42 | 1.41 | 1 1 0 0 16 8 0 3 10 | |
| | | 24 | 36.10 | 0.66 | | |
| | | 13 | 1.47 | 8.82 | | |
| total number of genes | | 39 | | | | |
| C | | 23 | 3.54 | 6.50 | 21 2 0 23 37 1 0 6 7 | |
| | | 61 | 89.80 | 0.68 | | |
| | | 13 | 3.66 | 3.55 | | |
| total number of genes | | 97 | | | | |
| D | | 2 | 0.88 | 2.28 | 1 1 0 4 12 0 1 3 2 | |
| | | 16 | 22.22 | 0.72 | | |
| | | 6 | 0.91 | 6.62 | | |
| total number of genes | | 24 | | | | |

FIGURE 12 | Crosstalk in gene expression in response to SA and PI-PLC dependency as defined by the clusters and dependency on PLD activity. The analysis was performed using stringent clusters as defined in the main text. Red blocks indicate relative higher transcript levels in the condition

written in red at the top of the table (versus that written in green); green blocks indicate higher transcript levels in the conditions written green at the top of the table (versus that written in red) and black blocks indicate no significant difference in transcript levels between both conditions.

infection by *Pseudomonas syringae*. Their conclusion that inhibition of PI-PLC results in the induction of pathogenesis-related genes is validated by our results (Chou et al., 2004).

Using archived microarray data from our model system of ACSC treated with or without SA and applying stringent criteria, we defined four gene clusters. Clusters A and B are SA-induced and clusters C and D are SA-repressed. Clusters A and D define

a pool of genes dependent on phosphoinositides for their SA response, while clusters B and C define a pool of genes dependent on PI-PLC products for their SA response. The clusters are not random subsets of the complete sets of SA-induced and SA-repressed genes. Based on their promoter sequences and GO classifications they represent distinct subsets, particularly clusters B and C. For instance, the GO “cell wall” term within the

| cluster | R59022 control | number of genes | | ratio |
|-----------------------|-----------------------------------------------------------------------------------|-----------------|-------------|-------|
| | | observed | theoretical | |
| A |  | 5 | 0.94 | 5.30 |
| | | 94 | 103.00 | 0.92 |
| | | 6 | 1.40 | 4.40 |
| Total number of genes | | 105 | | |
| B |  | 0 | 0.35 | 0.00 |
| | | 21 | 38.14 | 0.55 |
| | | 18 | 0.51 | 35.63 |
| Total number of genes | | 39 | | |
| C |  | 40 | 0.86 | 46.38 |
| | | 56 | 93.89 | 0.60 |
| | | 0 | 1.24 | 0.00 |
| Total number of genes | | 96 | | |
| D |  | 1 | 0.22 | 4.64 |
| | | 23 | 23.47 | 0.98 |
| | | 0 | 0.31 | 0.00 |
| Total number of genes | | 24 | | |

FIGURE 13 | Classification of the genes of the different clusters according to their response to DGK inhibitor R59022. The analysis was performed using stringent clusters as defined in the main text. Red blocks indicate relative higher transcript levels in the condition written in red at the

top of the table (versus that written in green); green blocks indicate higher transcript levels in the conditions written green at the top of the table (versus that written in red) and black blocks indicate no significant difference in transcript levels between both conditions.

cellular component category is 12-fold more frequent in clusters C and D than in the whole genome, but only 8-fold more frequent in the SA-repressed genes. By contrast the “cell wall” term does not appear at all in cluster B gene descriptions. For the biological processes, “cell organization and biogenesis” and “developmental process” are enriched in cluster C, SA-repressed and cluster D genes (in that order), but not in cluster A, cluster B or SA-induced genes. On the other hand, while SA-induced genes and cluster A genes are similarly enriched in genes involved in “response to stress,” “response to abiotic or biotic stimulus” and “signal transduction,” cluster B includes roughly twice as many genes from these categories. So clearly, the downstream cellular processes controlled by each gene cluster are distinct.

When the SA responses of genes in the different clusters were used in similarity searches, the genes of clusters A and D define different signatures than those of clusters B and C. The gene responses of clusters A and D are quite SA-specific. This is well characterized by the presence of *PR-1*, the most studied SA responsive gene, in cluster A (Krinke et al., 2007). Clusters B and C form a common pool of genes because their responses to SA are mimicked by edelfosine, by U73122, by wortmannin and to a certain extent by R59022. The responses of genes in clusters B and C are not only characteristic of SA treatment, as expected, but also of treatments with herbicide safeners, or to osmotic stress.

When the genes of clusters B and C are merged into a single list, the same microarray experiments with similar gene responses are retrieved, showing that these two clusters define a specific pool of SA responsive genes. The specificities of the pools hold true for the crosstalk between PLD and DGK. Genes for which the effect of DGK inhibitor is similar to the effect of SA (and incidentally of W30 and inhibitors of PI-PLC) are over-represented in clusters B and C. For clusters A and D, no such distortion is seen in the DGK inhibitor effect.

Clusters A and B represent 23 and 8% of SA-induced genes, respectively, while clusters C and D represent 31 and 7% of SA-repressed genes. However, the sizes of these clusters are certainly underestimated. Due to the transcriptome analysis thresholds used, it is likely that some genes have not been classified as being induced or repressed by a particular treatment, even though they were induced or repressed. For clustering, the more criteria are considered, the more genes are mistakenly discounted. This is especially true for cluster B and C genes, which were scored as being responsive to at least four molecules (SA, W30, U73122, and edelfosine). It is possible to define looser clusters by considering that a gene belongs to a cluster if it is affected by only one of the two PI-PLC inhibitors. This returns 121, 113, 164, and 27 genes for loose clusters A, B, C, and D, respectively (see Table S5). In this case, clusters A and B represent 26 and 24% of SA-induced genes, respectively, while clusters C and D represent 52 and 9%

of SA-repressed genes. It is perhaps important to note that cluster C represents most of the SA-repressed transcriptome. In **Figure 5** we defined clusters B^E and B^{W30} as the genes that would belong to cluster B if we had considered that a basal inhibiting effect of either edelfosine or W30, respectively, was sufficient for a gene to be classified as cluster B (see **Figure 5**). Similarly, we defined cluster C^E and C^{W30} as genes that have the same characteristics as cluster C genes, but are repressed by only edelfosine or W30, respectively. Genes in clusters B^E and B^{W30} and in C^E and C^{W30} might be sorted as B and C respectively if slightly different threshold criteria were used for microarray analysis. If the genes of clusters B^E , B^{W30} , C^E , and C^{W30} were considered in this way, the percentage of B and C cluster genes among SA-induced or SA-repressed genes would be even higher. The effect of SA inhibition of PI-PLC on gene expression appears to be a major event in the SA response.

What is the significance of the pool of genes in clusters B and C? What is the SA-triggered signaling event controlling expression of this pool? From a lipid signaling point of view it is tempting to consider that these genes are regulated in resting cells by PI-PLC pathway products. However, correlation alone is not proof. For clusters B and C we have only described correlations between different datasets showing that (i) challenging cells with SA induces *in vivo* PI-PLC inhibition, and (ii) inhibiting PI-PLC by different drugs alters the expression of a set of genes that is also affected when SA was added. We cannot rule out the possibility that the common effect of SA, wortmannin, and PI-PLC inhibitors on the same gene is due to another mechanism. To date, the inhibition of the PI-PLC pathway proposed in our working model seems the most obvious mechanism (**Figure 3**). Molecular events need to be pinpointed more precisely to make a firmer conclusion. Experimentally, one possibility would be to inhibit the PI-PLC inhibition by over-expressing PI-PLC. However, even over-expressed PI-PLC activity might be subject to the inhibition. We can be more confident that PI-PLC activity regulates expression of genes of clusters A and D, as these genes were specifically selected because their response to SA is inhibited when W30 blocks the accumulation of phosphoinositide.

Where does PI-PLC fit in SA signaling *in planta*? In radiolabeled ACSC, we showed that SA induces an increase in phosphoinositides, the substrates of PI-PLC, and a decrease in PA, a derivative of PI-PLC product. This is indeed what is expected if SA inhibits PI-PLC *in vivo*. We showed previously that the phosphoinositide increase required active type-III PI4K, which can be inhibited with wortmannin (Krinke et al., 2007). The type-III PI4Ks are the very ones that provide PI-PLC with substrates in response to cold (Delage et al., 2012). The basal PI-PLC activity is also fed with substrates formed by wortmannin-sensitive PI4K (Djafri et al., 2013). Therefore, the fact that SA activates a PI4K is compatible with it also inhibiting PI-PLC. It is likely that to monitor the phosphoinositide increase, it will be necessary to stimulate type-III PI4K activity and inhibit PI-PLC. Expressing human phosphatidylinositol phosphate kinase in tobacco resulted in a 40-fold increase in basal InsP_3 , while PI4P remained constant and $\text{PI}(4,5)\text{P}_2$ increased 7-fold (Im et al., 2007). This suggests that if basal PI-PLC is not inhibited, an increase in the formation of its substrates would directly lead to more products,

which is not what we observe. Finally it is important to note that independent data suggests that SA can inhibit PI-PLC. In *Capsicum chinense* J. cells, treatment with SA led to inhibition of PI-PLC but increased lipid kinase activities measured *in vitro* (Altuzar-Molina et al., 2011), which is consistent with our observed data. How could SA inhibit PI-PLC? The effect of SA on phosphoinositide increase can be detected as early as 15 min after its addition to cell culture medium, so the action of SA is probably not due to transcriptional control. Besides, using the microarray data we can see that after 4 h of SA incubation, PI-PLC genes are not repressed by the hormone (PLC10 is slightly induced) and type III-PI4K and DGK genes are not affected by it (data not shown). Structurally, it is difficult to conceive how SA could act on PI-PLC directly. Plant PI-PLCs are structurally similar to the simplest mammal PI-PLC, but the way they are regulated is not documented (Pokotylo et al., 2014). It is conceivable that they are subject to post-translational modifications as some phosphorylation sites have been detected (Janda et al., 2013).

CONCLUSION

We show that SA induces an increase in phosphoinositides with no increase in PA, the phosphorylated derivative of DAG, a PI-PLC product. This is likely to reflect an *in vivo* inhibition of PI-PLC by SA. We identified two pools of SA-responsive genes, one regulated by an increase in phosphoinositides and the other possibly by a decrease in PI-PLC products. Inhibition of PI-PLC by SA is likely to be a major step in the gene response to SA, especially in regulation of SA-inhibited genes, at least in ACSC. At a time when a great deal of omics data are being generated, this study illustrates that fine data mining using pertinent tools can reveal important processes.

MATERIALS AND METHODS

CELL CULTURE, LABELING, AND LIPID ANALYSIS

Arabidopsis thaliana Col-0 suspension cells were cultivated as described by Krinke et al. (2009). Experiments were performed on 5-day-old cultures. Suspension cells were labeled with $^{33}\text{P}_i$ according to the procedure previously described by Krinke et al. (2007). Total lipids were extracted and separated by thin layer chromatography (TLC). Structural phospholipids and PA were separated in the acid solvent system composed of chloroform-acetone-acetic acid-methanol-water (10:4:2:2:1, v/v/v/v) (Lepage, 1967). Phosphoinositides were separated in the alkaline solvent system composed of chloroform-methanol-5% (w/v) ammonia solution (9:7:2, v/v/v), where the TLC plates were soaked in potassium oxalate solution before heat activation (Munnik et al., 1994). Radiolabeled spots were quantified by autoradiography using a Storm Phosphorimager (Amersham Biosciences). Separated phospholipids were identified by co-migration with authentic non-labeled standards visualized by primuline staining (under UV light) or by phosphate staining.

TRANSCRIPTOMIC DATA

No new transcriptomic data were generated for this study. The microarray data used for this article are deposited in Gene Expression Omnibus (<http://www.ncbi.nlm.nih.gov/geo/>;

accession no. GSE7495, GSE9695, GSE19850 and GSE 35872) and CATdb (<http://urgv.evry.inra.fr/CATdb/>; Projects: RS05-04, AU07-01, RS09-04, and AU10-12).

RNA EXTRACTION AND TRANSCRIPT LEVEL

The extraction of RNA and the detection and quantification of transcripts were performed as in Djafi et al. (2013).

MOTIF ANALYSIS

Promoters (up to -1000 bp upstream of the transcription start site, without overlaps with other genes, and excluding 5'UTRs) of genes were extracted from the database of The Arabidopsis Information Resource (TAIR; Rhee et al., 2003). Sequences were used to search for over-represented motifs ranging from 4 to 10 bp using SIFT software (Hudson and Quail, 2003). The list of genes used as reference was either the list of promoters from the whole genome (33,062 promoters) or from all SA-induced genes or SA-repressed genes, as indicated. The motifs we defined were then compared with the ones in the PLACE database (Higo et al., 1999) to search for related *cis*-elements and similar motifs.

SUPPLEMENTARY MATERIAL

The Supplementary Material for this article can be found online at: <http://www.frontiersin.org/journal/10.3389/fpls.2014.00608/abstract>

REFERENCES

- Achard, P., and Genschik, P. (2008). Releasing the brakes of plant growth: how GAs shutdown DELLA proteins. *J. Exp. Bot.* 60, 1085–1092. doi: 10.1093/jxb/ern301
- Altzler-Molina, A. R., Armando Munoz-Sanchez, J., Vazquez-Flota, F., Monforte-Gonzalez, M., Racagni-Di Palma, G., and Teresa Hernandez-Sotomayor, S. M. (2011). Phospholipidic signaling and vanillin production in response to salicylic acid and methyl jasmonate in Capsicum chinense. *Plant Physiol. Biochem.* 49, 151–158. doi: 10.1016/j.plaphy.2010.11.005
- Boggs, K. P., Rock, C. O., and Jackowski, S. (1995). Lysophosphatidylcholine and 1-O-octadecyl-2-O-methyl-rac-glycero-3-phosphocholine inhibit the CDP-choline pathway of phosphatidylcholine synthesis at the CTP:phosphocholine cytidylyltransferase step. *J. Biol. Chem.* 270, 7757–7764.
- Bowling, S. A., Clarke, J. D., Liu, Y., Klessig, D. F., and Dong, X. (1997). The cpr5 mutant of Arabidopsis expresses both NPR1-dependent and NPR1-independent resistance. *Plant Cell* 9, 1573–1584.
- Bowling, S. A., Guo, A., Cao, H., Gordon, A. S., Klessig, D. F., and Dong, X. I. (1994). A mutation in arabidopsis that leads to constitutive expression of systemic acquired-resistance. *Plant Cell* 6, 1845–1857.
- Brazier-Hicks, M., Evans, K. M., Cunningham, O. D., Hodgson, D. R. W., Steel, P. G., and Edwards, R. (2008). Catabolism of glutathione conjugates in *Arabidopsis thaliana*. Role in metabolic reactivation of the herbicide safener fenclorim. *J. Biol. Chem.* 283, 21102–21112. doi: 10.1074/jbc.M801998200
- Chou, W.-M., Shigaki, T., Dammann, C., Liu, Y.-Q., and Bhattacharyya, M. K. (2004). Inhibition of phosphoinositide-specific phospholipase C results in the induction of pathogenesis-related genes in soybean. *Plant Biol. (Stuttg.)* 6, 664–672. doi: 10.1055/s-2004-830351
- Delage, E., Ruellan, E., Guillais, I., Zachowski, A., and Puyaubert, J. (2012). Arabidopsis Type-III Phosphatidylinositol 4-Kinases $\beta 1$ and $\beta 2$ are upstream of the phospholipase C pathway triggered by cold exposure. *Plant Cell Physiol.* 53, 565–576. doi: 10.1093/pcp/pcs011
- Dellagi, A., Segond, D., Rigault, M., Fagard, M., Simon, C., Saindrenan, P., et al. (2009). Microbial siderophores exert a subtle role in Arabidopsis during infection by manipulating the immune response and the iron status. *Plant Physiol.* 150, 1687–1696. doi: 10.1104/pp.109.138636
- Djafi, N., Vergnolle, C., Cantrel, C., Wietrzyński, W., Delage, E., Cochet, F., et al. (2013). The Arabidopsis DREB2 genetic pathway is constitutively repressed by basal phosphoinositide-dependent phospholipase C coupled to diacylglycerol kinase. *Front. Plant Sci.* 4:307. doi: 10.3389/fpls.2013.00307
- Durrant, W. E., and Dong, X. (2004). Systemic acquired resistance. *Annu. Rev. Phytopathol.* 42, 185–209. doi: 10.1146/annurev.phyto.42.040803.140421
- Gutiérrez, J., González-Pérez, S., García-García, F., Daly, C. T., Lorenzo, O., Revuelta, J. L., et al. (2014). Programmed cell death activated by Rose Bengal in *Arabidopsis thaliana* cell suspension cultures requires functional chloroplasts. *J. Exp. Bot.* 65, 3081–3095. doi: 10.1093/jxb/eru151
- Haapalainen, M., Dauphin, A., Li, C.-M., Bailly, G., Tran, D., Briand, J., et al. (2012). HrpZ harpins from different *Pseudomonas syringae* pathovars differ in molecular interactions and in induction of anion channel responses in *Arabidopsis thaliana* suspension cells. *Plant Physiol. Biochem.* 51, 168–174. doi: 10.1016/j.plaphy.2011.10.022
- Hallouin, M., Ghelis, T., Brault, M., Bardat, F., Cornel, D., Miginiac, E., et al. (2002). Plasmalemma abscisic acid perception leads to RAB18 expression via phospholipase D activation in Arabidopsis suspension cells. *Plant Physiol.* 130, 265–272. doi: 10.1104/pp.004168
- Higo, K., Ugawa, Y., Iwamoto, M., and Korenaga, T. (1999). Plant cis-acting regulatory DNA elements (PLACE) database: 1999. *Nucleic Acids Res.* 27, 297–300.
- Horowitz, L. F., Hirdes, W., Suh, B.-C., Hilgemann, D. W., Mackie, K., and Hille, B. (2005). Phospholipase C in living cells activation, inhibition, Ca²⁺ requirement, and regulation of M current. *J. Gen. Physiol.* 126, 243–262. doi: 10.1085/jgp.200509309
- Horvath, E., Szalai, G., and Janda, T. (2007). Induction of abiotic stress tolerance by salicylic acid signaling. *J. Plant Growth Regul.* 26, 290–300. doi: 10.1007/s00344-007-9017-4
- Hruz, T., Laule, O., Szabo, G., Wessendorp, F., Bleuler, S., Oertle, L., et al. (2008). Genevestigator v3: a reference expression database for the meta-analysis of transcriptomes. *Adv. Bioinformatics* 2008:420747. doi: 10.1155/2008/420747
- Hudson, M. E., and Quail, P. H. (2003). Identification of promoter motifs involved in the network of phytochrome A-Regulated gene expression by combined analysis of genomic sequence and microarray data. *Plant Physiol.* 133, 1605–1616. doi: 10.1104/pp.103.030437
- Im, Y. J., Perera, I. Y., Brglez, I., Davis, A. J., Stevenson-Paulik, J., Phillippe, B. Q., et al. (2007). Increasing plasma membrane phosphatidylinositol(4,5)bisphosphate biosynthesis increases phosphoinositide metabolism in *Nicotiana tabacum*. *Plant Cell* 19, 1603–1616. doi: 10.1105/tpc.107.051367
- Janda, M., Planchais, S., Djafi, N., Martinec, J., Burketo, L., Valentova, O., et al. (2013). Phosphoglycerolipids are master players in plant hormone signal transduction. *Plant Cell Rep.* 32, 839–851. doi: 10.1007/s00299-013-1399-0
- Janda, M., and Ruellan, E. (in press). Magical mystery tour: salicylic acid signalling. *Environ. Exp. Bot.* doi: 10.1016/j.enexpbot.2014.07.003
- Kalachova, T. A., Iakovenko, O. M., Kretinin, S. V., and Kravets, V. S. (2012). Effects of salicylic and jasmonic acid on phospholipase D activity and the level of active oxygen species in soybean seedlings. *Biol. Membrany* 29, 169–176. doi: 10.1134/S1990747812030099
- Kelm, M. K., Weinberg, R. J., Criswell, H. E., and Breese, G. R. (2010). The PLC/IP3R/PKC pathway is required for ethanol-enhanced GABA release. *Neuropharmacology* 58, 1179–1186. doi: 10.1016/j.neuropharm.2010.02.018
- Kim, T. H., Hauser, F., Ha, T., Xue, S., Böhmer, M., Nishimura, N., et al. (2011). Chemical genetics reveals negative regulation of abscisic acid signaling by a plant immune response pathway. *Curr. Biol.* 21, 990–997. doi: 10.1016/j.cub.2011.04.045
- Kim, Y., Park, S., Gilmour, S. J., and Thomashow, M. F. (2013). Roles of CAMTA transcription factors and salicylic acid in configuring the low-temperature transcriptome and freezing tolerance of Arabidopsis. *Plant. J.* 75, 364–376. doi: 10.1111/tpj.12205
- Krinke, O., Flemr, M., Vergnolle, C., Collin, S., Renou, J.-P., Taconnat, L., et al. (2009). Phospholipase D activation is an early component of the salicylic acid signaling pathway in Arabidopsis cell suspensions. *Plant Physiol.* 150, 424–436. doi: 10.1104/pp.108.133595
- Krinke, O., Ruellan, E., Valentová, O., Vergnolle, C., Renou, J.-P., Taconnat, L., et al. (2007). Phosphatidylinositol 4-kinase activation is an early response to salicylic acid in Arabidopsis suspension cells. *Plant Physiol.* 144, 1347–1359. doi: 10.1104/pp.107.100842
- Kunz, S., Pesquet, E., and Kleczkowski, L. A. (2014). Functional dissection of sugar signals affecting gene expression in *Arabidopsis thaliana*. *PLoS ONE* 9:e100312. doi: 10.1371/journal.pone.0100312
- Laloi, M., Perret, A.-M., Chatre, L., Melser, S., Cantrel, C., Vaultier, M.-N., et al. (2006). Insights into the role of specific lipids in the formation and delivery of

- lipid microdomains to the plasma membrane of plant cells. *Plant Physiol.* 143, 461–472. doi: 10.1104/pp.106.091496
- Ledoux, Q., Van Cutsem, P., Markó, I. E., and Veys, P. (2014). Specific localization and measurement of hydrogen peroxide in *Arabidopsis thaliana* cell suspensions and protoplasts elicited by COS-OGA. *Plant Signal. Behav.* 9:e28824. doi: 10.4161/pls.28824
- Lepage, M. (1967). Identification and composition of turnip root lipids. *Lipids* 2, 244–250.
- Malamy, J., Carr, J. P., Klessig, D. F., and Raskin, I. (1990). Salicylic-acid – a likely endogenous signal in the resistance response of tobacco to viral-infection. *Science* 250, 1002–1004. doi: 10.1126/science.250.4983.1002
- Metraux, J. P., Signer, H., Ryals, J., Ward, E., Wyssbenz, M., Gaudin, J., et al. (1990). Increase in salicylic-acid at the onset of systemic acquired-resistance in cucumber. *Science* 250, 1004–1006. doi: 10.1126/science.250.4983.1004
- Mogami, H., Lloyd Mills, C., and Gallacher, D. V. (1997). Phospholipase C inhibitor, U73122, releases intracellular Ca^{2+} , potentiates Ins(1,4,5)P3-mediated Ca^{2+} release and directly activates ion channels in mouse pancreatic acinar cells. *Biochem. J.* 324, 645–651.
- Munnik, T., Irvine, R., and Musgrave, A. (1994). Rapid turnover of phosphatidylinositol 3-phosphate in the green-alga chlamydomonas-eugametos - signs of a phosphatidylinositide 3-kinase signalling pathway in lower plants. *Biochem. J.* 298, 269–273.
- Narise, T., Kobayashi, K., Baba, S., Shimojima, M., Masuda, S., Fukaki, H., et al. (2010). Involvement of auxin signaling mediated by IAA14 and ARF7/19 in membrane lipid remodeling during phosphate starvation. *Plant Mol. Biol.* 72, 533–544. doi: 10.1007/s11103-009-9589-4
- Navarro, L., Bari, R., Achard, P., Lisón, P., Nemri, A., Harberd, N. P., et al. (2008). DELLA control plant immune responses by modulating the balance of jasmonic acid and salicylic acid signaling. *Curr. Biol.* 18, 650–655. doi: 10.1016/j.cub.2008.03.060
- Pokotylo, I., Kolesnikov, Y., Kravets, V., Zachowski, A., and Ruelland, E. (2014). Plant phosphoinositide-dependent phospholipases C: variations around a canonical theme. *Biochimie* 96, 144–157. doi: 10.1016/j.biochi.2013.07.004
- Powis, G., Seewald, M. J., Gratas, C., Melder, D., Riebow, J., and Modest, E. J. (1992). Selective inhibition of phosphatidylinositol phospholipase C by cytotoxic ether lipid analogues. *Cancer Res.* 52, 2835–2840.
- Profotova, B., Burkertova, L., Novotna, Z., Martinec, J., and Valentova, O. (2006). Involvement of phospholipases C and D in early response to SAR and ISR inducers in *Brassica napus* plants. *Plant Physiol. Biochem.* 44, 143–151. doi: 10.1016/j.plaphy.2006.02.003
- Rainteau, D., Humbert, L., Delage, E., Vergnolle, C., Cantrel, C., Maubert, M.-A., et al. (2012). Acyl chains of Phospholipase D transphosphatidylation products in *Arabidopsis* cells: a study using multiple reaction monitoring mass spectrometry. *PLoS ONE* 7:e41985. doi: 10.1371/journal.pone.0041985
- Rhee, S.-Y., Beavis, W., Berardini, T. Z., Chen, G., Dixon, D., Doyle, A., et al. (2003). The *Arabidopsis* Information Resource (TAIR): a model organism database providing a centralized, curated gateway to *Arabidopsis* biology, research materials and community. *Nucleic Acids Res.* 31, 224–228. doi: 10.1093/nar/gkg076
- Ross, A., Yamada, K., Hiruma, K., Yamashita-Yamada, M., Lu, X., Takano, Y., et al. (2014). The *Arabidopsis* PEPR pathway couples local and systemic plant immunity. *EMBO J.* 33, 62–75. doi: 10.1002/embj.201284303
- Ruelland, E., Cantrel, C., Gawer, M., Kader, J.-C., and Zachowski, A. (2002). Activation of phospholipases C and D is an early response to a cold exposure in *Arabidopsis* suspension cells. *Plant Physiol.* 130, 999–1007. doi: 10.1104/pp.006080
- Ruelland, E., Kravets, V., Derevyanchuk, M., Martinec, J., Zachowski, A. I., and Pokotylo, I. (in press). Role of phospholipid signalling in plant environmental responses. *Envir. Exp. Bot.* doi: 10.1016/j.envexpbot.2014.08.009
- Schweighofer, A., Shubchynskyy, V., Kazanaviciute, V., Djamei, A., and Meskiene, I. (2014). Bimolecular fluorescent complementation (BiFC) by MAP kinases and MAPK phosphatases. *Methods Mol. Biol.* 1171, 147–158. doi: 10.1007/978-1-4939-0922-3_12
- Seifertová, D., Skúpa, P., Rychtář, J., Lašková, M., Pařezová, M., Dobrev, P. I., et al. (2014). Characterization of transmembrane auxin transport in *Arabidopsis* suspension-cultured cells. *J. Plant Physiol.* 171, 429–437. doi: 10.1016/j.jplph.2013.09.026
- Skipsey, M., Knight, K. M., Brazier-Hicks, M., Dixon, D. P., Steel, P. G., and Edwards, R. (2011). Xenobiotic responsiveness of *Arabidopsis thaliana* to a chemical series derived from a herbicide safener. *J. Biol. Chem.* 286, 32268–32276. doi: 10.1074/jbc.M111.252726
- Stotz, H. U., Mueller, S., Zoeller, M., Mueller, M. J., and Berger, S. (2013). TGA transcription factors and jasmonate-independent COI1 signalling regulate specific plant responses to reactive oxylipins. *J. Exp. Bot.* 64, 963–975. doi: 10.1093/jxb/ers389
- Tjellström, H., Yang, Z., Allen, D. K., and Ohlrogge, J. B. (2012). Rapid kinetic labeling of *Arabidopsis* cell suspension cultures: implications for models of lipid export from plastids. *Plant Physiol.* 158, 601–611. doi: 10.1104/pp.111.186122
- Vaultier, M.-N., Cantrel, C., Vergnolle, C., Justin, A.-M., Demandre, C., Benhassaine-Kesri, G., et al. (2006). Desaturase mutants reveal that membrane rigidification acts as a cold perception mechanism upstream of the diacylglycerol kinase pathway in *Arabidopsis* cells. *FEBS Lett.* 580, 4218–4223. doi: 10.1016/j.febslet.2006.06.083
- Vicente, M. R. S., and Plasencia, J. (2011). Salicylic acid beyond defence: its role in plant growth and development. *J. Exp. Bot.* 62, 3321–3338. doi: 10.1093/jxb/err031
- Wong, R., Fabian, L., Forer, A., and Brill, J. A. (2007). Phospholipase C and myosin light chain kinase inhibition define a common step in actin regulation during cytokinesis. *BMC Cell Biol.* 8:15. doi: 10.1186/1471-2121-8-15
- Conflict of Interest Statement:** The authors declare that the research was conducted in the absence of any commercial or financial relationships that could be construed as a potential conflict of interest.

Received: 20 August 2014; accepted: 19 October 2014; published online: 11 November 2014.

Citation: Ruelland E, Pokotylo I, Djafi N, Cantrel C, Repellin A and Zachowski A (2014) Salicylic acid modulates levels of phosphoinositide dependent-phospholipase C substrates and products to remodel the *Arabidopsis* suspension cell transcriptome. *Front. Plant Sci.* 5:608. doi: 10.3389/fpls.2014.00608

This article was submitted to Plant Physiology, a section of the journal *Frontiers in Plant Science*.

Copyright © 2014 Ruelland, Pokotylo, Djafi, Cantrel, Repellin and Zachowski. This is an open-access article distributed under the terms of the Creative Commons Attribution License (CC BY). The use, distribution or reproduction in other forums is permitted, provided the original author(s) or licensor are credited and that the original publication in this journal is cited, in accordance with accepted academic practice. No use, distribution or reproduction is permitted which does not comply with these terms.



Corrigendum: Salicylic acid modulates levels of phosphoinositide dependent-phospholipase C substrates and products to remodel the *Arabidopsis* suspension cell transcriptome

OPEN ACCESS

Edited by:

Zuhua He,
Chinese Academy of Sciences, China

Reviewed by:

Golam Jalal Ahammed,
Zhejiang University, China

*Correspondence:

Eric Ruelland
eric.ruelland@upmc.fr

Specialty section:

This article was submitted to
Plant Physiology,
a section of the journal
Frontiers in Plant Science

Received: 08 November 2015

Accepted: 11 January 2016

Published: 28 January 2016

Citation:

Ruelland E, Pokotylo I, Djafi N, Cantrel C, Repellin A and Zachowski A (2016) Corrigendum: Salicylic acid modulates levels of phosphoinositide dependent-phospholipase C substrates and products to remodel the *Arabidopsis* suspension cell transcriptome. *Front. Plant Sci.* 7:36. doi: 10.3389/fpls.2016.00036

Eric Ruelland^{1,2*}, Igor Pokotylo³, Nabila Djafi^{1,2}, Catherine Cantrel^{1,2}, Anne Repellin^{1,2} and Alain Zachowski^{1,2}

¹ Université Paris-Est Créteil, Institut d'Ecologie et des Sciences de l'Environnement de Paris, Créteil, France, ² Centre National de la Recherche Scientifique, Unité Mixte de Recherche 7618, Institut d'Ecologie et des Sciences de l'Environnement de Paris, Créteil, France, ³ Molecular Mechanisms of Plant Cell Regulation, Institute of Bioorganic Chemistry and Petrochemistry, National Academy of Sciences, Kyiv, Ukraine

Keywords: *Arabidopsis*, diacylglycerol kinase, transcriptomic, lipid Signaling, hormone transduction, salicylic acid, phospholipase C

A corrigendum on

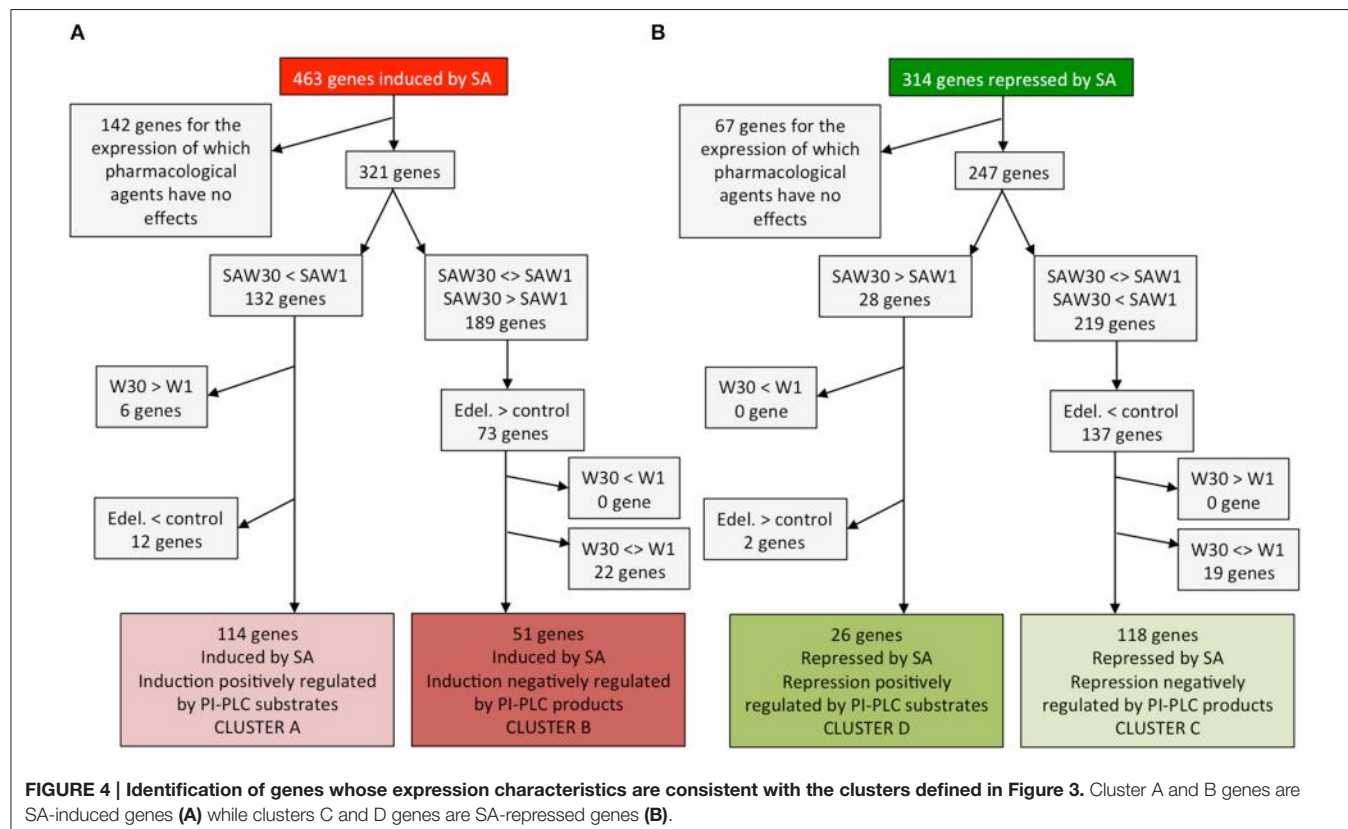
Salicylic acid modulates levels of phosphoinositide dependent-phospholipase C substrates and products to remodel the *Arabidopsis* suspension cell transcriptome

by Ruelland, E., Pokotylo, I., Djafi, N., Cantrel, C., Repellin, A., and Zachowski, A. (2014). *Front. Plant Sci.* 5:608. doi: 10.3389/fpls.2014.00608

In **Figure 4** of the original article, an error was noticed. For the path leading to cluster C genes, wrong symbol “>” was used instead of “<.” One should read “Edel. < control; 137 genes.” Readers are referred to the Figure of this corrigendum, that replace the previous **Figure 4**.

Conflict of Interest Statement: The authors declare that the research was conducted in the absence of any commercial or financial relationships that could be construed as a potential conflict of interest.

Copyright © 2016 Ruelland, Pokotylo, Djafi, Cantrel, Repellin and Zachowski. This is an open-access article distributed under the terms of the Creative Commons Attribution License (CC BY). The use, distribution or reproduction in other forums is permitted, provided the original author(s) or licensor are credited and that the original publication in this journal is cited, in accordance with accepted academic practice. No use, distribution or reproduction is permitted which does not comply with these terms.





Biosynthesis and possible functions of inositol pyrophosphates in plants

Sarah P. Williams¹, Glenda E. Gillaspy¹ and Imara Y. Perera^{2*}

¹ Biochemistry, Virginia Polytechnic and State University, Blacksburg, VA, USA

² Plant and Microbial Biology, North Carolina State University, Raleigh, NC, USA

Edited by:

Eric Ruelland, Centre National de la Recherche Scientifique, France

Reviewed by:

Tzyy-Jen Chiou, Academia Sinica, Taiwan

Ingo Heilmann,
Martin-Luther-University
Halle-Wittenberg, Germany

***Correspondence:**

Imara Y. Perera, Plant and Microbial Biology, North Carolina State University, Campus Box 7612, Raleigh, NC, USA
e-mail: imara_perera@ncsu.edu

Inositol phosphates (InsPs) are intricately tied to lipid signaling, as at least one portion of the inositol phosphate signaling pool is derived from hydrolysis of the lipid precursor, phosphatidyl inositol (4,5) bisphosphate. The focus of this review is on the inositol pyrophosphates, which are a novel group of InsP signaling molecules containing diphosphate or triphosphate chains (i.e., PPx) attached to the inositol ring. These PPx-InsPs are emerging as critical players in the integration of cellular metabolism and stress signaling in non-plant eukaryotes. Most eukaryotes synthesize the precursor molecule, myo-inositol (1,2,3,4,5,6)-hexakisphosphate (InsP₆), which can serve as a signaling molecule or as storage compound of inositol, phosphorus, and minerals (referred to as phytic acid). Even though plants produce huge amounts of precursor InsP₆ in seeds, almost no attention has been paid to whether PPx-InsPs exist in plants, and if so, what roles these molecules play. Recent work has delineated that *Arabidopsis* has two genes capable of PP-InsP₅ synthesis, and PPx-InsPs have been detected across the plant kingdom. This review will detail the known roles of PPx-InsPs in yeast and animal systems, and provide a description of recent data on the synthesis and accumulation of these novel molecules in plants, and potential roles in signaling.

Keywords: plant inositol signaling, inositol hexakisphosphate, VIP, inositol pyrophosphate, energy metabolism

Myo-inositol (inositol) signaling is much like a language in that each molecular species used in the pathway, whether lipid or soluble in nature, can convey specific information to the cell, like a word. In this analogy, each combination of different numbers and positions of phosphates on the inositol ring and the presence of diacylglycerol linked via the C1 of inositol, also convey unique information (see Figure 1). Comprehensive analyses of both inositol and inositol phospholipids in signaling have been previously reviewed (Van Leeuwen et al., 2004; Gillaspy, 2011; Heilmann and Heilmann, 2014), so this review focuses on new inositol signaling molecules, the di-phospho (PP) and tri-phospho (PPP) inositol phosphates (PPx-InsPs), also known as inositol pyrophosphates. These high-energy molecules have been studied in non-plant eukaryotes, however, their existence and role in plants is newly emerging. The main questions regarding PPx-InsPs are: can these molecules be detected in plants, how are they synthesized and what type of information do they convey? Recent work addressing these questions will be discussed in the broader context of understanding how PPx-InsPs function in eukaryotes.

HISTORY AND STRUCTURE OF PPx-INSPS

PPx-InsPs were first identified in *Dictyostelium* in 1993 (Glennon and Shears, 1993; Hawkins et al., 1993; Menniti et al., 1993; Stephens et al., 1993). They are similar to ATP and polyphosphates in that they contain a linear chain of two (PP) or three (PPP) phosphates separated by pyrophosphate bonds, linked to an InsP molecule (see Figure 2).

The PPx moieties at one or more positions on the inositol ring in PPx-InsPs are synthesized from InsP₅ or InsP₆ (Menniti et al., 1993; Shears et al., 2011), resulting in InsPs containing seven or eight phosphates (i.e., InsP₇ and InsP₈). The high energy pyrophosphate bonds present in PPx-InsPs may serve as a way to store energy in the cell, with the standard free energy of hydrolysis of InsP₇ and InsP₈ higher than that of ADP and ATP, respectively (Stephens et al., 1993). Indeed, the initial role proposed for PPx-InsPs was simply as a high energy molecules, as they can be broken down to generate ATP (Voglmaier et al., 1996; Huang et al., 1998). However, PPx-InsPs are present at very low amounts and they have high turnover rates, suggesting that they serve as more than energy storage molecules (Glennon and Shears, 1993; Menniti et al., 1993). Recently new physiological roles have been discovered for PPx-InsPs, supporting their role as dynamic and important signaling molecules.

Only a few of the theoretically possible PPx-InsP structures have been confirmed. The naming convention is to describe the position and number of the pyrophosphates first, followed by the name of the InsP. For example, *Dictyostelium* contains 6PP-InsP₅ and 5PP-InsP₅, and these contain a pyrophosphate on the 6th and 5th carbons of InsP₅, respectively. *Dictyostelium* also contains 5,4/6(PP)₂-InsP₄ or 1/3,5(PP)₂-InsP₄, and in these cases the slash indicates one of the pyrophosphates present can occur at either of two carbons (i.e., at the C4 or C6 position, or at C1 or C3, respectively). The ratios of these different PPx-InsPs differ in various *Dictyostelium* species examined (Laussmann et al., 1997,

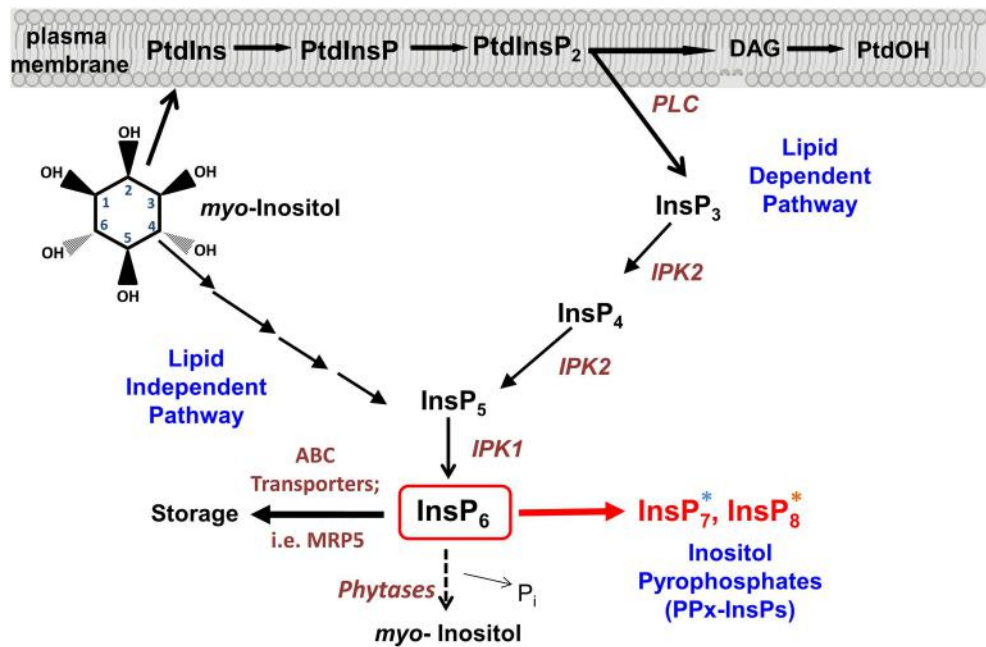


FIGURE 1 | Synthesis of inositol pyrophosphate. Overview of the Inositol phosphate pathway, including both lipid dependent and lipid independent routes for synthesis of InsP₆. Inositol Pyrophosphate (PPx-InsP) synthesis is indicated in red. Major lipid and inositol

species are indicated in black and key enzymes are indicated in brown. A more detailed outline of PPx-InsP synthesis is depicted in **Figure 2**. The blue and orange asterisks correspond to the colored boxes in **Figure 2**.

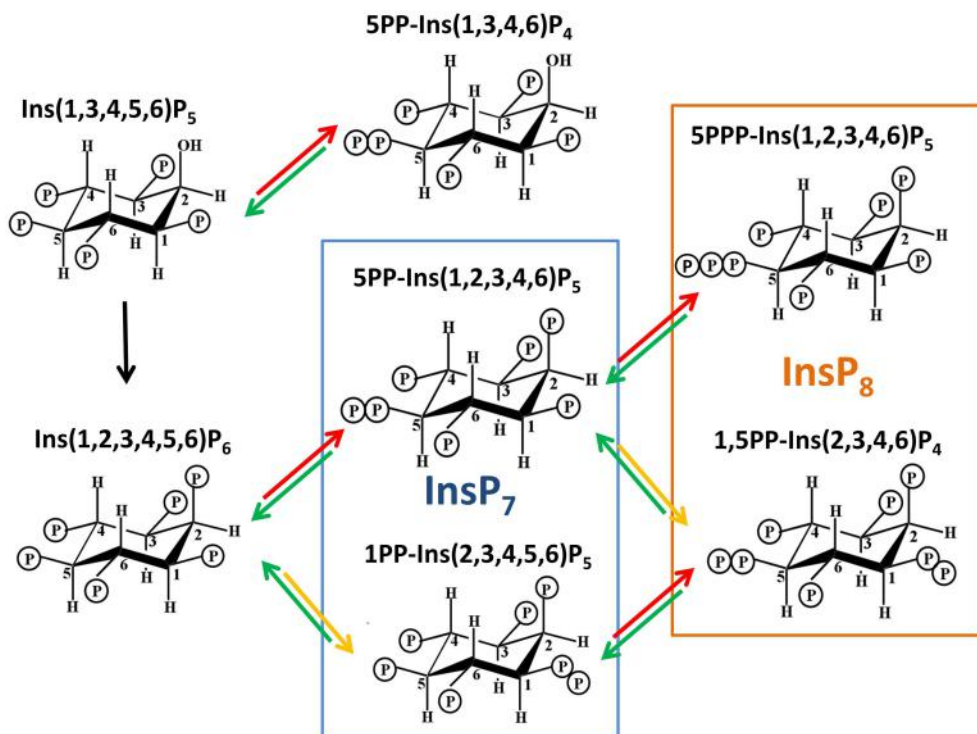


FIGURE 2 | Structures of PPx-InsPs and pathway of proposed synthesis.

The unboxed area is the last step in InsP₆ synthesis, catalyzed by the IPK1 enzyme in plants. The boxed areas in blue and orange indicate InsP₇ and

InsP₈ synthesis. The colored arrows indicate known enzymes in yeast. Red arrows indicate KCS1 activity, while yellow arrows indicate VIP activity. The green arrows indicate phosphatase activity by DDP1.

1998). Another member of the Amoebozoa kingdom, *Entamoeba histolytica*, has further diversity in that a PPx-InsP was identified containing *neo*-inositol, rather than *myo*-inositol (Martin et al., 2000). This difference could produce even more diversity in the language of InsPs, but it is not yet known if this occurs in other organisms.

In Dictyostelium and the animal kingdom, PPx-InsPs synthesized from InsP₅ exist (Laussmann et al., 1997, 1998; Draskovic et al., 2008), however at present there is no data indicating they are found in plants. This review will focus on the PPx-InsP species synthesized from InsP₆. The most abundant InsP₇ isomer has been confirmed through NMR as 5PP-InsP₅ (Mulugu et al., 2007; Draskovic et al., 2008). A second InsP₇ was first speculated to be pyrophosphorylated at C4 or C6 (i.e., 4/6), but was later conclusively identified as 1/3PP-InsP₅ (Lin et al., 2009). Recent work in animals has shown that the 1- rather than 3- position is phosphorylated, thus 1PP-InsP₅ is likely to be the second type of InsP₇ present in animals (Wang et al., 2012). Given this, we use 1PP-InsP₅ as the updated nomenclature for this second molecular species of InsP₇. Studies in yeast and humans identified that both of these InsP₇ molecules are present. The InsP₈ species confirmed are 1,5(PP)₂-InsP₄ (*in vivo*) and 5PPP-InsP₅ (*in vitro*) (Draskovic et al., 2008; Lin et al., 2009).

METHODS USED TO DETECT PPx-INSPS

Several methods have been used to detect PPx-InsPs, each having distinct strengths and limitations. The most common method is to introduce a radiolabeled precursor, often ³H-*myo*-inositol or ³H-InsP₆, followed by HPLC separation of InsP species produced after a given time (Azevedo and Saiardi, 2006). This method is very sensitive, but labor-intensive, and while it can resolve isomers of the lower InsPs, currently it is not possible to separate different PPx-InsP isomers. As well, one is limited to analysis of cells/tissues that can take up the radiolabelled precursor. However, this method has an advantage in that one can be fairly certain of the identity of the resulting labeled peaks on the HPLC chromatograms. A nonradioactive high-performance anion-exchange chromatographic method based on metal dye detection (MDD)-HPLC can also be used to detect PPx-InsPs. The advantage of this method is that it can separate different isomers of InsP₇, however this method requires a 3 pump HPLC unit which increases the complexity of the system and limits its use (Mayr, 1988). Another method of separation of InsPs is thin layer chromatography, which utilizes either radiolabeling or dye for detection of InsP species (Otto et al., 2007). This method, in general, does not have great sensitivity, and is most often used with purified PPx-InsPs.

Since acidic conditions can cause the degradation of PPx-InsPs, HPLC analyses may underestimate the amount of PPx-InsPs present (Losito et al., 2009). A new method developed to limit exposure of extracted PPx-InsPs to acid buffers is polyacrylamide gel separation by electrophoresis (PAGE), and subsequent staining with either DAPI or toluidine blue to detect InsPs (Losito et al., 2009). The PAGE technique is sensitive enough to visualize PPx-InsPs from cell/tissue extracts, and it can separate different InsP₇ and InsP₈ isomers. However, its distinct advantage is that it may allow for a better estimation of PPx-InsP abundance because

of the speed of analysis. The disadvantage of using PAGE is that conclusive identification of stained “bands” as PPx-InsPs is best verified with a separate technology, as other molecules could be present and give rise to bands. It is important to note that co-migration with InsP and PPx-InsP standards is required for all of these methods, and follow-up NMR is needed to conclusively identify the specific structure of PPx-InsP species.

PLANTS CONTAIN PPx-INSPS

Plants have large amounts of one of the precursors to PPx-InsPs, InsP₆, which is well studied as a phosphorous storage molecule (Raboy, 2003). Given this, it seems likely that plants also synthesize the PPx-InsPs. Previous studies had noted InsP molecules more polar than InsP₆ in barley, duckweed, and potato (Breakley and Hanke, 1996; Flores and Smart, 2000; Lemtiri-Chlieh et al., 2000; Dorsch et al., 2003). Acting on this information, we recently utilized both HPLC separation of radiolabelled plant tissues and PAGE to delineate the presence of InsP₇ and InsP₈ in higher plants including Arabidopsis, *Camelina sativa*, cotton, and maize (Desai et al., 2014). These two methods provided a complementary analysis of higher phosphorylated InsPs, including the PPx-InsPs. Since PPx-InsPs are low abundance molecules, it is not surprising that Arabidopsis seeds were found to contain less than 2% of the total inositol pool as inositol pyrophosphates (1.33% InsP₇, 0.24% InsP₈). Vegetative tissue from Arabidopsis was also analyzed and PPx-InsPs were found in both seedlings (0.64% InsP₇, 0.14% InsP₈) and mature leaves (1.00% InsP₇). InsP₇ was detected in other plant species as well, including another member of the Brassica family, *Camelina sativa* (1.40% in seedlings), and an unrelated dicot, cotton (*Gossypium hirsutum*) in the leaves and in shoots and roots of seedlings. PAGE analysis was used to detect PPx-InsPs in both Arabidopsis and maize seed in this same work (Desai et al., 2014). These findings indicate that PPx-InsPs may play a role during the plant life cycle throughout the plant kingdom, both in monocots and dicots.

Critical to our detection of the PPx-InsPs in plants was the use of a mutant containing elevated InsP₇ and InsP₈. The Multidrug Resistance associated Protein 5 (MRP5) is a high affinity ABC-binding cassette transporter that specifically binds to InsP₆ (Nagy et al., 2009) (Figure 1). Studies on MRP5 have indicated the likely role of this transporter is in moving InsP₆ into the storage vacuole (Nagy et al., 2009). The subcellular localization of MRP5 has been reported as both the plasma membrane (Suh et al., 2007) and the vacuolar membrane (Nagy et al., 2009), however it has been suggested that the plasma membrane localization is an artifact resulting from ectopic expression (Nagy et al., 2009). MRP5 was first identified as an important player in stomatal responses, since guard cells of the loss-of-function *mrp5* mutant are insensitive to ABA and Ca²⁺ (Klein et al., 2003). This alteration in guard cell function results in reduction of water loss and use, allowing *mrp5* mutants some resistance to drought (Klein et al., 2003). The maize parologue of MRP5 (called MRP4), results in decreased levels of InsP₆ in seeds when mutated (Shi et al., 2007; Nagy et al., 2009). Our recent study showed that in addition to decreased levels of InsP₆, *mrp5* mutants have elevated levels of InsP₇ and InsP₈ in seeds (Desai et al., 2014). These changes are less striking in vegetative tissue, perhaps as a result of overall lower levels of InsP₆

(Desai et al., 2014), or reduced MRP5 expression (Nagy et al., 2009) in vegetative tissues. The guard cell phenotype of *mrp5* mutants has been attributed to an increase in cytosolic InsP₆, which could mobilize Ca²⁺, leading to inhibition of inward rectifying K⁺ channels, and changes in turgor pressure resulting in a decreased stomatal aperture (Lemtiri-Chlieh et al., 2000, 2003; Nagy et al., 2009). With the identification of elevated PPx-InsPs in *mrp5* mutants, an alternative hypothesis for alterations in *mrp5* guard cell signaling is that changes in InsP₇ and InsP₈ may be involved.

It should be noted that the recent study identifying PPx-InsPs in plants was not able to discern the enantiomers present (Desai et al., 2014). Thus, it is not known whether plants contain 5PP-InsP₇ or 1PP-InsP₇ similar to yeast and animals, or (4/6)PP-InsP₇, similar to *Dictyostelium*. Efforts were made to purify the plant PPx-InsPs, however no informative NMR data was obtained (Desai et al., 2014). The identity of the plant isomers is key, and in itself may yield insights into the pathway, as different types of enzymes in other organisms give rise to specific PPx-InsP isomers. The following section describes this relationship between PPx-InsP synthesis and isomers in detail.

SYNTHESIS OF PPx-InsPs BY KCS1/IP6K ENZYMES

There are two classes of genes shown to encode enzymes required for synthesis of PPx-InsPs. **Figure 3** shows the presence and names of these genes in species relevant to this review. These two classes of genes encode distinct enzymes that catalyze the

addition of pyrophosphates at specific positions on the inositol ring (**Figure 2**). The first class is named the IP6Ks, and the kinase activity of these enzymes phosphorylates the 5-position of InsP₅, InsP₆, and InsP₇, yielding 5PP-InsP₄ or 5PP-InsP₅ and two possible forms of InsP₈: 1/3,5PP-InsP₅ and 5PPP-InsP₅ (Draskovic et al., 2008). In yeast, this class of enzymes is named KCS1, and was first identified in a suppressor screen of the yeast Protein Kinase C (*pkc1*) mutant (Huang and Symington, 1995). *Kcs1* encodes a protein closely related to the bZIP family of transcription factors, although analysis of its two potential leucine zipper motifs indicates the secondary alpha-helical structure for DNA binding is not formed (Huang and Symington, 1995). Instead, the altered structure of this alpha helix in addition to a two-turn 3₁₀ helix, forms a pocket for InsP₆ binding (Wang et al., 2014).

Under low energy conditions, KCS1 can generate ATP from InsP₆ (Wunderberg et al., 2014). This dual function of KCS1 to both degrade InsP₆ and generate InsP₇ presents the possibility of KCS1 acting as an ATP/ADP ratio sensor (Wunderberg et al., 2014). Given the considerable amount of InsP₆ in plants, if present, a KCS1-like enzyme could generate a significant source of ATP under low energy conditions. However, sequence homology searches using the yeast KCS1 and human IP6K proteins indicate that there are no KCS1/IP6K homologs in plants (Bennett et al., 2006; Desai et al., 2014).

In the absence of a plant KCS1/IP6K, one might expect that 5PP-InsP₅ could not be synthesized. However, there is the

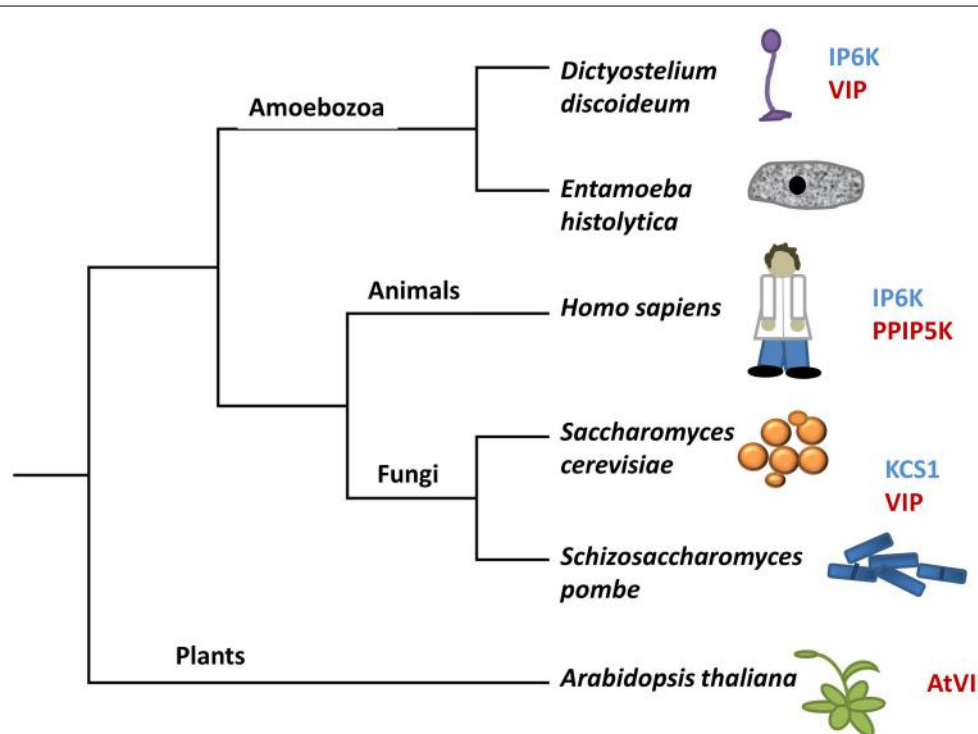


FIGURE 3 | A modified tree of life indicating the composition of genes in different species that encode kinases capable of phosphorylating InsP₆. Genes in blue have sequence identity with

KCS1, whereas genes in red have sequence identity with VIP. The tree depicts evolutionary relationships between groups discussed in the review.

possibility of another InsP kinase in plants acting as a KCS1/IP6K in the synthesis of 5PP-InsP₅. The larger InsP kinase family (Pfam PF03770) has a PxxxDxKxG (“PDKG”) catalytic motif and includes the InsP₃ kinases (IP3Ks), IP6K, and inositol polyphosphate multikinases (IPMKs). Recent phylogenetic studies on these enzymes have suggested that the InsP kinase family common ancestor is an IP6K precursor (Bennett et al., 2006). The rationale is that the substrate-binding pocket for InsP₆ is larger, and from this common ancestor, the binding pocket would shrink to become more specific for other InsPs (Wang et al., 2014). Not all extant species have developed kinases solely acting on InsP₃: *Entamoeba histolytica* still has an IP3K which retains IP6K activity (Wang et al., 2014), presenting the possibility that if plants have a KCS1/IP6K, it may be distinct from that of yeast and mammals.

SYNTHESIS OF PP_x-InsPs BY VIP/PPIP5K ENZYMES

The second class of enzymes capable of synthesizing PP_x-InsPs are the VIPs, which are also known as diphosphoinositol pentakisphosphate kinases (PPIP5Ks) in animals (Shears et al., 2013) (Figures 2, 3). In quick succession, two groups identified VIPs in yeast and mammalian cells (Choi et al., 2007; Fridy et al., 2007; Mulugu et al., 2007). The name PPIP5K originated as scientists were looking for an enzyme capable of phosphorylating PP-InsP₅ to produce the InsP₈, which had been observed in

mammalian cell extracts (Stephens et al., 1993). The PPIP5K that was identified has a higher affinity for InsP₇ than InsP₆ (Choi et al., 2007). These enzymes produce a structurally distinct InsP₇ with recent NMR work delineating 1PP-InsP₇ as the product (Wang et al., 2012). These enzymes can also phosphorylate 5PP-InsP₅ to produce 1,5(PP)₂-InsP₄ (Figure 2) or speculatively, even 1PPP-InsP₅.

The *Vip* genes are conserved across eukaryotes, including plants (Mulugu et al., 2007; Desai et al., 2014). They have a dual domain structure consisting of an N-terminal ATP grasp domain with kinase activity and a C-terminal histidine acid phosphatase domain or “phytase” domain (Mulugu et al., 2007) (see Figure 4). The human PPIP5K1 phosphatase domain is not active with InsP₅, InsP₆, PP-InsP₄, or PP-InsP₅ as the substrate or even *p*-nitrophenyl phosphate, a generic substrate for acid phosphatases (Gokhale et al., 2011). This is probably due to the fact that PPIP5Ks lack a conserved histidine essential for phosphatase activity. In addition, the phosphatase catalytic region is interrupted by a Pleckstrin Homology (PH) domain (Gokhale et al., 2011). The PH domain is found in signaling proteins and is responsible for binding phospholipids or molecules derived from their head group (Scheffzek and Welti, 2012). The hybrid PH domain in PPIP5K1 preferentially binds PtdIns(3,4,5)P₃ and can also bind InsP₆ allowing PPIP5K1 to translocate from the

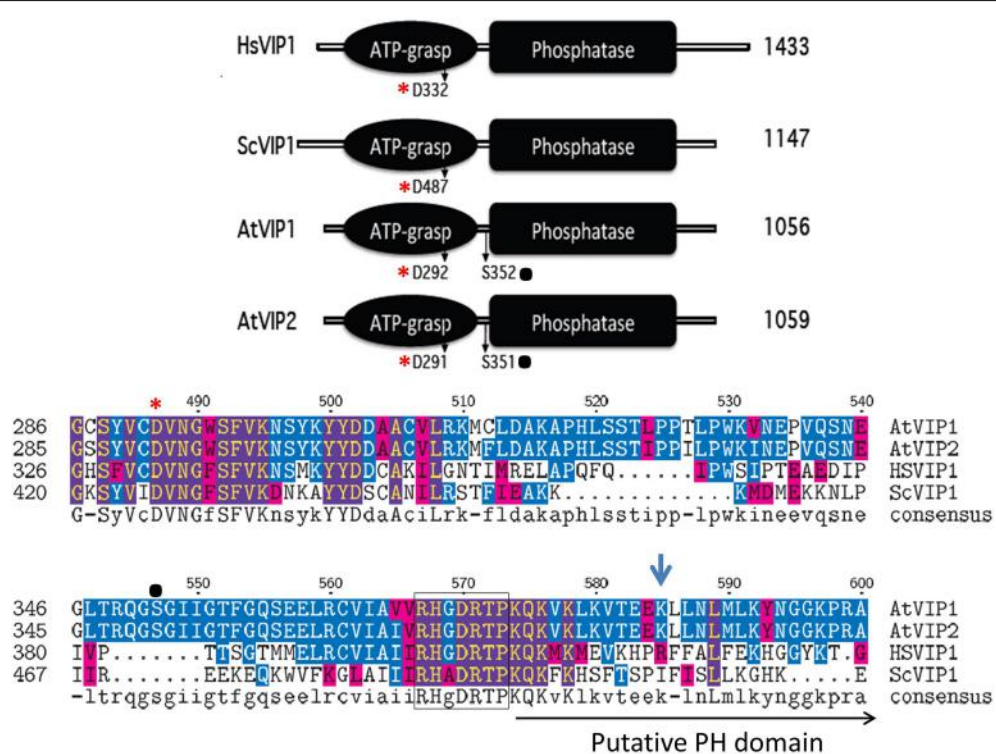


FIGURE 4 | Schematic alignment of the kinase and phosphatase domains of VIPs. The ATP grasp/RimK/ kinase (ATP-grasp) and the histidine acid Phosphatase (Phosphatase) domains within the VIP proteins from *Homo sapiens* (Hs, Genbank AAH57395), *Saccharomyces cerevisiae* (Sc, NP_013514) and *Arabidopsis thaliana* (*AtVip1* Gene ID, 821297; *AtVip2* Gene ID, 831359). The red asterisks denotes in both panels the conserved aspartic acid residue (D) required for kinase activity, and the black dot, the known phosphorylated serine residues within the *Arabidopsis* VIPs. The lower panel contains the amino acid alignment of the boundary region between the ATP-Grasp and Phosphatase domains. The beginning of the Histidine Acid phosphatase domain is boxed, followed by the PH domain and Arg417 is marked by the blue arrow.

acid residue (D) required for kinase activity, and the black dot, the known phosphorylated serine residues within the *Arabidopsis* VIPs. The lower panel contains the amino acid alignment of the boundary region between the ATP-Grasp and Phosphatase domains. The beginning of the Histidine Acid phosphatase domain is boxed, followed by the PH domain and Arg417 is marked by the blue arrow.

cytoplasm to the plasma membrane when the PtdIns(3,4,5)P₃ signaling pathway is activated (Gokhale et al., 2011). Critical to ligand binding is arginine 417 in the PH domain of PPIP5K1 (Gokhale et al., 2011).

All plant species searched through BLAST contained multiple expressed Vip homologs (Desai et al., 2014). Arabidopsis contains two conserved *Vip* genes, *AtVip1* (*At3g01310*) and *AtVip2* (*At5g15070*) and the encoded proteins have 94% similarity to each other, but only 50% and 59% similarity to yeast ScVIP1 and human HsVIP1 respectively (Desai et al., 2014). As with yeast and human VIPs, Arabidopsis VIP1 and VIP2 contain a RimK/ATP-Grasp domain (kinase domain) and a histidine acid-phosphatase domain (Figure 4). A BLAST analysis identifies potential *Vip* genes in several other plant species indicating that PPx-InsP synthesis is conserved across the plant kingdom. The kinase domain of the Arabidopsis VIPs contains a conserved aspartic acid (D), which as in yeast and humans, is necessary for activity (Choi et al., 2007; Mulugu et al., 2007; Desai et al., 2014). This residue is also conserved in mouse and *Drosophila* VIPs, however its role in activity has yet to be confirmed (Fridy et al., 2007). The AtVIP1 and AtVIP2 phosphatase domains are also interrupted with a putative PH domain (Gokhale et al., 2011) (Figure 4), however binding to PtdInsPs has not been tested to date. The arginine residue required for PtdInsP-binding of the human PPIP5K is not conserved in the AtVIPs, however, the substituted lysine at this position provides a similar charge as arginine and there are other arginine residues located nearby (Figure 4). Phosphoproteomics has shown that AtVIPs have a serine adjacent to the phosphatase domain that is phosphorylated. This is not conserved in ScVIP and HsVIP (<http://phosphat.mpimp-golm.mpg.de>) and may represent a unique mechanism for regulation of VIP activity specific to plants (Desai et al., 2014).

Importantly, both AtVIPs encode catalytically active proteins that allow specific yeast mutants to synthesize InsP₇ (Desai et al., 2014). There appears to be an intriguing difference in the AtVIPs as compared to the human and yeast VIPs. In the human PPIP5K and yeast VIPs the kinase domain alone is more active than the full-length protein (Fridy et al., 2007; Mulugu et al., 2007), while both full-length AtVIPs are more active than their kinase domains alone (Desai et al., 2014). One explanation for this difference is that the phosphatase domain in the yeast VIP and human PPIP5K may auto-inhibit the kinase activity, and this control may be missing in the AtVIPs. Data from yeast supports this idea of auto-inhibition (Fridy et al., 2007). A second explanation is that the unique presence of a phosphorylated serine in the AtVIPs might provide regulatory control.

Although NMR data on the plant PPx-InsPs is not yet available, it seems reasonable to speculate that only the 1PP-PPx-InsPs should be synthesized in plants, since VIP enzymes are known to phosphorylate at this position. Indeed, the architecture of the VIP catalytic site is what determines the position of phosphorylation (Shears et al., 2013), and as discussed above, 5PP-InsPs may not be synthesized. Intriguing however, both InsP₇ and InsP₈ have been found in plants (Desai et al., 2014). This argues for the presence of a plant enzyme capable of 5PP-InsP synthetic ability, since the only structurally verified isomers of InsP₈ in any organism, 1,5(PP)₂-InsP₄ and 5PPP-InsP₅, both require

phosphorylation at a C5 position (Laussmann et al., 1997, 1998; Draskovic et al., 2008; Lin et al., 2009). Further, in yeast, KCS1 and VIP are known to act sequentially to phosphorylate each other's InsP₇ product, resulting in 1,5(PP)₂-InsP₄ synthesis (Figure 2). Alternatively, the plant InsP₈ molecule may be unique in nature and may not require phosphorylation at the 5-position. Thus, either the plant VIPs are different enough that they can phosphorylate a different position, or there are other enzymes in the plant that can phosphorylate InsP₆ or InsP₇. It is important to note one final structural implication of PPx-InsPs: InsP₇ produced by either IP6K or VIP may not be equivalent since the charge from phosphate is distributed differently in each, and the shapes are not superimposable. As a result, different InsP₇ enantiomers may interact with different proteins and act in different signaling conditions or pathways.

The similarity of AtVIP1 and AtVIP2 proteins (94% similarity), and the ability of each gene product to restore InsP₇ synthesis in yeast, suggests that these two genes function similarly at the biochemical level. Thus, the expression patterns of each gene may provide information on where and when InsP₇ is synthesized. Recent studies showed that *AtVip1* expression is high in vegetative tissues, including shoot of seedlings as well as mature leaf and stem. In contrast, *AtVip2* is most abundantly expressed in roots and reproductive tissues (Desai et al., 2014) suggesting differential spatial regulation. Additionally, since both *AtVip1* and *AtVip2* are expressed together in some vegetative tissues, they may be differentially regulated at a subcellular level. Using subcellular prediction tools, we found compelling predictions for AtVIP1 nuclear localization and an AtVIP2 cytosolic location within the plant cell. Discerning whether the two AtVIPs really do function in these compartments will require experimental validation.

MEANING OF PPx-InsPs: HOW ARE THEY LIKELY TO FUNCTION IN PLANTS?

If we continue the analogy of InsP as words, our next challenge will be to understand what these words mean and what information they convey. We will describe how InsP₇ is known to modify or interact with proteins in other model systems, and how these actions lead to changes in known signaling functions in yeast and animals. Although little is known about PPx-InsPs function in plants and mechanisms regulating inositol signaling differ between plants and animals, it is likely that InsP₇ conveys plant signaling information by virtue of modifying or interacting with proteins. Drawing parallels from the known and hypothesized roles of InsP₇ in other organisms, we speculate that PPx-InsPs function in several plant signaling pathways, including, but not limited to energy homeostasis, phosphate (P_i) sensing, and immune responses. In the following sections, we will elaborate on published data from other model systems that indicates a role for PPx-InsPs in these pathways.

ENERGY HOMEOSTASIS

PPx-InsPs are involved in energy homeostasis both at the cellular and organismal level. Maintaining energy homeostasis, or the balance of intake/production, storage and use of energy often in the form of ATP or sugar, is essential for all living organism. In animals, the AMP Kinase (AMPK) is often named as an

energy sensor. Under low energy conditions, AMP is bound, activating the AMP kinase and reprogramming the cell to maximize energy acquisition and minimize energy use (Hardie, 2011). In opposition is mammalian Target Of Rapamycin (mTOR), which under high energy conditions promotes growth and cell division (Dunlop and Tee, 2009). In plants, these two enzymes also form the base for maintaining energy homeostasis.

At the cellular level, PPx-InsPs regulate ATP levels through what has been referred to as the “glycolic/mitochondrial metabolic ratio” in yeast (Szijgyarto et al., 2011). Yeast mutants lacking KCS1 have up to five fold higher level of ATP than their wild type controls while overexpression of KCS1 results in a decrease of ATP (Szijgyarto et al., 2011). A similar result is seen with *kcs1* mutant mouse embryonic fibroblast (MEF) cells, where levels of ADP and AMP are low. Further studies showed that the yeast *kcs1* and *kcs1/vip1* mutants as well as MEF *ip6k* mutants have reduction or loss of functional mitochondria. This loss of mitochondrial function with high ATP levels can be explained by an increase in glycolysis and a reduction of ATP used in metabolic pathways. Thus, the lack of InsP₇ synthesis in these mutants leads to changes in ATP synthesis and utilization. InsP₇ in this system most likely affects ATP levels by altering transcription of genes that control glycolysis. Specifically, in yeast promoters of glycolytic regulatory genes have a CT-box that binds to the General Control Response 1 (GCR1) transcription factor. InsP₇ may function to regulate GCR1 directly by a non-catalytic transfer of the β-phosphate from InsP₇ to an already phosphorylated serine residue in GCR1, resulting in a pyrophosphorylated serine. This modification likely causes a conformational change in GCR1, allowing it to bind the CT-box, thereby regulating the expression of glycolytic regulatory genes (Szijgyarto et al., 2011).

This addition of a new pyrophosphate bond on an already phosphorylated serine residue in a target substrate protein is a proposed mechanism unique to InsP₇. First demonstrated in yeast, InsP₇ was shown to modify proteins important for ribosomal biogenesis and endosomal trafficking (Saiardi et al., 2004). The pyrophosphorylated serine in target proteins is surrounded by acidic residues, possibly enhancing the recruitment of Mg²⁺ as a cofactor. This modification would be more permanent than phosphorylation by ATP (Bhandari et al., 2007), as no known enzymes exist to remove the pyrophosphate. One limitation to acceptance of this mechanism is that it has been difficult to verify whether such pyrophosphorylated serines occur *in vivo*.

At the whole organism level, InsP₇ functions in sugar homeostasis through regulating insulin release and glucose uptake in animals. In mammals, InsP₇ acts as an inhibitor of the Protein Kinase B (also known as Akt) pathway, reducing glucose uptake, insulin sensitivity and protein translation. In response to growth factors, Akt is normally phosphorylated by a protein kinase named PDK1 (3-phosphoinositide-dependent protein kinase 1), which activates the GSK3β (Glycogen synthase kinase 3) and mTOR signaling pathways. Activation of Akt requires binding of its PH domain to PtdIns(3,4,5)P₃, associated with the plasma membrane. When bound to PtdIns(3,4,5)P₃, Akt undergoes a conformational change which exposes its activation domain, allowing Akt to be phosphorylated and activated by PDK1 (Calleja et al., 2007). InsP₇, produced by IP6K1, acts

as an inhibitor of Akt by competing for binding to the PH domain within Akt. This effectively prevents the phosphorylation of T308 of Akt (Chakraborty et al., 2010), and dampens Akt signaling. *ip6k1* loss-of-function mutant mice are smaller than their wild type littermates and have lower circulating levels of insulin, but are not diabetic and they have normal blood glucose levels (Bhandari et al., 2008). These genetic data underscore the role of InsP₇ in global metabolic control.

While insulin is not made by plants, gene homologs functioning in the Akt, GSK3β, and mTOR pathways exist in plants, and have been implicated in growth control pathways. Plants contain homologs of both Akt (i.e., Adi3: AvrPto-dependent Pto-interacting protein 3) and the kinase that activates Akt, PDK1. Most studies indicate that plants do not synthesize PtdIns(3,4,5)P₃, however plant PDK1 is known to bind phosphatidic acid via its PH domain, allowing membrane localization (Anthony et al., 2004) and the subsequent activation of Adi3 (Devarenne and Martin, 2007). Adi3 can suppress the activity of a major regulator of plant metabolism and AMPK homolog, SnRK1 (Sucrose non-fermenting Related Kinase 1), through phosphorylation of a SnRK1 multiple subunit complex (Avila et al., 2012). GSK-3 kinases are negative regulators of signal transduction pathways controlling metabolism and developmental events across the animal kingdom. In plants, GSK3 homologs are involved in brassinosteroid (BR) signaling pathways. Specifically, the brassinosteroid insensitive 2 (BIN2) protein is a GSK-3 that functions as a negative regulator of BR signal transduction (Yan et al., 2009; Clouse, 2011). As with the animal GSK-3 signaling, BR signal transduction is required for proper metabolic and developmental control throughout the life of a plant. In the case of mTOR, the Arabidopsis gene homologs are known to be important regulators of metabolic changes in response to glucose. Arabidopsis TOR signaling has been linked to transcriptional reprogramming of central and secondary metabolism and other processes within plants (Xiong and Sheen, 2014).

We do not yet know whether InsP₇ in plants regulates transcription via pyrophosphorylation or whether InsP₇ can compete with binding to PH domains of plant proteins, however, both are potential mechanisms by which InsP₇ could act. Determining whether plants use InsP₇ to regulate metabolism or growth, and the mechanistic details of such regulation will benefit from the development of genetic resources to examine *Atvip* loss-of-function mutants. In addition, we need to know whether PPx-InsPs levels are altered by changes in energy or metabolic status. Answering these questions is now possible as the basis for detecting and measuring PPx-InsPs in plants has been established, and the *AtVip* genes have been cloned and shown to encode active proteins.

P_i SENSING

PPx-InsPs are also involved in perceiving and maintaining P_i levels and numerous studies link PPx-InsPs to low P_i responses in other organisms. Plant P_i homeostasis is a highly regulated process (Zhang et al., 2014) and it is important to consider whether PPx-InsPs play a role in this process in plants. P_i sensing involves the perception of P_i present in the environment, followed by acquisition, remobilization and recycling of P_i to maintain P_i

homeostasis. In yeast, the response to P_i starvation is regulated by the P_i -responsive (PHO) signaling pathway, including the Pho80-Pho85 cyclin-CDK (cyclin dependent kinase) complex (Lenburg and O'shea, 1996; Carroll and O'shea, 2002). When P_i levels are low, the Pho80-Pho85 protein complex is inactive. As a result, the Pho4 transcription factor is not phosphorylated and remains in the nucleus where it acts to activate PHO genes (Kaffman et al., 1994; O'neill et al., 1996).

Though there is some lack of consensus for the exact mechanism by which PPx-InsPs control P_i sensing, it is clear that they play a role in P_i homeostasis. One group found that low P_i elevates InsP₇, and genetic evidence suggested that it was 1PP-InsP₅, although this was not experimentally confirmed (Lee et al., 2007). This group showed that InsP₇ physically interacts with Pho81, inactivating the Pho80-Pho85 complex, and ultimately leading to changes in gene expression required to maintain metabolic homeostasis under low P_i conditions. In addition, this pathway was dependent on the activity of the yeast VIP genes (Lee et al., 2007). The finding that InsP₇ is elevated in yeast in response to low P_i has been contested by other investigators. Exposure of wild type yeast to P_i -free medium for 20 min resulted in a decrease of intracellular PPx-InsPs levels by 80%, without affecting InsP₆ levels (Lonetti et al., 2011).

The change in InsP₇ levels is not the only phenotype that suggests KCS1 is involved in the yeast low P_i response. An intriguing connection between KCS1 and P_i sensing comes from recent studies that found that Pho4 binds to intragenic regions of the *Kcs1* gene, promoting the transcription of intragenic and antisense RNA. The authors suggested that the truncated KCS1 protein produced could down-regulate KCS1 function (Nishizawa et al., 2008). An alternative hypothesis is that this truncated KCS1 protein has an altered enzymatic property yet to be determined (Saiardi, 2012). Further work is needed to examine these possibilities and determine the function of intragenic and antisense *Kcs1* RNA. In addition, recent work examining the lipidome of numerous yeast mutants found similarities in changes in sphingolipids of *pho85* and *kcs1*, but not *vip1* mutants, suggesting that similar metabolic changes take place in *pho85* and *kcs1* mutants (Da Silveira Dos Santos et al., 2014). Together these data suggest that either *Vip* or *Kcs1* genes, or possibly both, are linked to P_i sensing and sphingolipid homeostasis in yeast.

In animal cells, IP6K has been identified as a stimulator of P_i uptake in response to low nutrients. A study found that the mRNAs expressed in rabbit duodenum from a rabbit fed a low P_i diet can stimulate Na⁺-dependent P_i uptake when injected into *Xenopus* oocytes (Yagci et al., 1992). From this pool of mRNAs, the P_i uptake stimulator (PiUS) gene was isolated and confirmed to increase P_i uptake when expressed in *Xenopus* oocytes (Norbis et al., 1997). The *PiUS* gene was later found to encode an IP6K, and the gene is now known as *Ip6k2* (Saiardi et al., 1999).

In plants, InsPs are essential for P_i response and homeostasis. Arabidopsis mutants in *ipk1*, which catalyzes the addition of a phosphate at the 2-position to select substrates, have a 83% reduction in InsP₆ levels compared to wild type, and are hypersensitive to P_i (Stevenson-Paulik et al., 2005). These mutants have increased uptake of P_i and root to shoot translocation of P_i (Kuo et al., 2014). Many plant responses to P_i starvation (PSR) are

regulated at a transcriptional and post-transcriptional level. A recent study has shown that a sub set of PSR genes involved in P_i uptake, translocation and remobilization are up regulated in the *ipk1* mutant under P_i sufficient conditions (Kuo et al., 2014). Additionally, increased expression of a subset of PSR genes was shown to correlate with a reduction of histone H2A.Z occupancy (Smith et al., 2010) and interestingly, H2A.Z occupancy at chromatin sites associated with several PSR genes was found to be significantly reduced in *ipk1* (under both sufficient and low P_i) compared to wild type (Kuo et al., 2014). However, Arabidopsis mutants with lower InsP₆ levels including *mips1* (myo-inositol 1-phosphate synthase), do not show an accumulation of P_i , indicating that InsP₆ *per se* is probably not the molecule utilized for sensing P_i (Kuo et al., 2014). This implicates other InsPs or the PPx-InsPs as controllers of P_i sensing. In particular, since PPx-InsPs are synthesized from InsP₆ substrates, these molecules might serve as critical players in sensing P_i . We note that the conversion between InsP₆ and the PPx-InsPs might be important as InsP₆ serves an important function in phosphorous storage (Raboy, 2003).

Studies on yeast and animal mutant responses to low P_i were among the first to highlight a specific property of InsPs that may be especially important for understanding PPx-InsP function. Response to environmental stress, including P_i starvation, requires the fine tuning of TOR and the TORC1 complex activity. This results in the down regulation of ribosomal and protein synthesis regulatory genes, as well as the up regulation of stress response genes (Loewith et al., 2002). Working in parallel with the inactivation of TORC1, the histone deacetylase (HDAC) enzyme is recruited to turn off expression of ribosomal and protein synthesis regulatory genes (Alejandro-Osorio et al., 2009). This HDAC activity is dependent on InsP₄, which is known to act as a "molecular glue" allowing the HDAC Rpd3L complex to interact with its co-repressor, SMRT (silencing mediator of retinoic acid and thyroid hormone receptor) (Watson et al., 2012). InsP₇ has been hypothesized to interact with this same complex (Worley et al., 2013), suggesting that PPx-InsPs may play a role in chromatin remodeling thereby regulating gene expression.

There are other known cases of InsPs serving a role as a type of molecular glue, and these bear mentioning. InsP₆ and InsP₅ have been found in the auxin (TIR1; Transport Inhibitor Response 1) (Tan et al., 2007) and jasmonic acid receptor, COI1 (Coronatine Insensitive 1) (Sheard et al., 2010; Mosblech et al., 2011), respectively. In both of these examples, InsPs are lodged between the F-Box and the repressor protein target in the E3 ubiquitin ligase complex. When the hormone is present, the repressors for auxin and jasmonic acid, Aux/IAA (Auxin inducible) and JAZ (Jasmonate Zim-domain protein) respectively, are degraded, allowing for transcription of hormone responsive genes. TIR1 is a member of a family of F-box proteins whose five members differ slightly in expression, biochemical activity or function (Parry et al., 2009) and Aux/IAA belongs to an even larger family of 29 proteins (Remington et al., 2004). Like TIR1, COI1 is a member of the F-Box family while JAZ is a 12 member subgroup of TIFY (named for the shared TIF[F/Y]XG motif) (Chini et al., 2007; Vanholme et al., 2007). With all the potential combinations of hormone receptors and repressor proteins, it is interesting to

speculate whether other InsPs, including PPx-InsPs, may function as cofactors in hormone signaling to regulate transcription.

IMMUNE RESPONSE

The innate immune system is the first line of defense in both plants and animals. The first step in the innate immune response pathway involves the recognition of pathogen-associated molecular patterns (PAMPs) by the host pattern recognition receptors (PRRs) on the cell surface or cytoplasm. In plants, pathogen detection, signaling, and immune response takes place in most cells, while animal immune systems have evolved specialized mobile immune cells. Detection of PAMPs by PRRs initiate signaling cascades which can result in Ca^{2+} release, activation of kinases, and transcription factors, production of reactive oxygen species and alterations in other signaling pathways within the organism (Jones and Dangl, 2006). In animals, RIG-1 (retinoic acid-inducible gene 1) is a PRR in the cytoplasm, which detects double stranded viral DNA and activates a signaling cascade in which the transcription factor IRF3 (Interferon regulatory factor 3) is phosphorylated. IRF3 then moves into the nucleus and promotes the expression of type-1 interferon genes. The interferon proteins then stimulate anti-viral or anti-bacterial activity in leukocytes (Trinchieri, 2010). Recently, this innate response pathway was linked to PPx-InsPs. An *in vitro* study found both InsP₇ and InsP₈ are capable of inducing an interferon response through the RIG-1 signaling pathway. The authors of this study speculated that 1PP-InsP₅ is the physiologically relevant molecule and acts a co-factor for protein interactions or by β -phosphorylation of a serine residue on IRF3, a type of PPx-InsP-driven protein pyrophosphorylation event that we have previously discussed (Pulloor et al., 2014).

The innate immune system in plants and animals share many similarities in the use of PAMPs and PRR as a method of detecting pathogens. Plants have a large diversity of PRR and Resistance (R) genes, however homologs of the RIG-1/IRF3 pathway have not been found in plants. Therefore, while it is interesting to speculate that PPx-InsPs may regulate specific defense transcription factors in plants, the lack of RIG-1 and IRF-3 homologs suggests that this pathway may be unique to animal innate immunity signaling.

A second role of PPx-InsPs in the animal innate immune response involves the afore-mentioned PDK1/Akt signaling pathway. This complex pathway regulates multiple central biological processes including cell survival, proliferation, growth, and metabolism (Hemmings and Restuccia, 2012). In the immune system, neutrophil activation is tightly controlled, with 5PP-InsP₅ acting as a negative regulator. As described previously, 5PP-InsP₅ competes for binding with Akt through the PH domain. Upon infection, 5PP-InsP₅ levels drop allowing Akt to translocate to the membrane and allow for the induction of PtdIns(3,4,5)P₃ signaling, leading to neutrophil activation and superoxide production. *ip6k* mutant neutrophils have increased bactericidal activity and ROS production (Prasad et al., 2011). Akt triggers reactive oxygen species and nitric oxide production, and is not limited to neutrophils, it can also regulate programmed cell death in other cell types (Lam, 2004). The inhibition of Akt signaling by InsP₇ is a general phenomenon, however, the mechanism of regulation

and the biological outcome may differ depending on tissue and signaling context (Prasad et al., 2011).

A common characteristic of the innate immune response is the programed cell death of infected cells to reduce the spread of disease. In plants, localized programed cell death stimulated by the hypersensitive response occurs rapidly in response to pathogen infection (Morel and Dangl, 1997). As mentioned previously, plants have a homologous pathway to the PDK1/Akt pathway in mammals. In plants, the homolog to Akt is Adi3, which acts in the immune response as a negative regulator of cell death through the MAPK kinase cascade. Akt and Adi3 kinases may be a target for pathogen manipulation of the host. In the case of *Pseudomonas* infection of tomato, the bacterial effector protein AvrPto interacts with the Adi3 presumably to manipulate cell death (Devarenne et al., 2006). It is intriguing to speculate whether PPx-InsPs may serve as innate immunity signaling molecules in plants, perhaps by acting to antagonize Adi3 signaling. However it should be noted that although functionally similar, Akt and Adi3 share only 21.4% amino acid identity, suggesting differences in regulation and possibly function (Devarenne et al., 2006).

A final connection between PPx-InsPs and plant innate immune signaling involves plant mutants defective in the synthesis or metabolism of InsPs. Transgenic plants constitutively expressing the human type 1 inositol polyphosphate 5-phosphatase (InsP 5-ptase, the enzyme which dephosphorylates InsP₃), showed a compromised defense response, including decreased expression of defense genes and a reduction in the systemic acquired immunity in response to a bacterial pathogen (Hung et al., 2014). Furthermore, plants defective in synthesis of *myo*-inositol and InsP₆ were also more susceptible to disease, including viral, bacterial and fungal pathogen infection (Murphy et al., 2008). It was concluded that InsP₆ and not its precursors is the critical InsP for this phenotype, however, the authors of this study could not rule out a role for PPx-InsPs in this process due to the difficulty in detection (Murphy et al., 2008). Crops with altered InsP profiles, specifically low InsP₆, have been developed to combat issues of nutrition and P_i pollution (Raboy, 2007). If InsP₆ or PPx-InsPs play a role in pathogen resistance and immune response, it could negatively impact the performance of these so-called low phytate crops.

CONCLUDING REMARKS

PPx-InsPs have recently been identified in higher plants, adding new molecular players in the plant inositol signaling pathway. Both InsP₇ and InsP₈ have been detected in a handful of plant species. With two *Vip/PIP5K* gene homologs as the only identified kinase to synthesize PPx-InsPs, the predicted species are 1PP-InsP₅ and either 1,3(PP)₂-InsP₄ or 1PPP-InsP₅. Further work is needed to identify the stereochemistry of plant PPx-InsPs and to clarify the regulatory components involved in their synthesis and metabolism. Drawing parallels to known roles of PPx-InsPs in other eukaryotes, plant PPx-InsPs may have a role in energy, P_i sensing, and innate immunity signaling pathways. Thus, identification of PPx-InsPs in plants presents a new avenue and tool that may be useful for improving crop yield, reduced fertilizer demand, and improved growth under stress.

ACKNOWLEDGMENTS

This work was supported by a NSF collaborative grant (MCB1051646 to GG and MCB 1052034 to IYP) and a NIFA award (2013-02277 to GG and IYP).

REFERENCES

- Alejandro-Osorio, A. L., Huebert, D. J., Porcaro, D. T., Sonntag, M. E., Nillasithanukroh, S., Will, J. L., et al. (2009). The histone deacetylase Rpd3p is required for transient changes in genomic expression in response to stress. *Genome Biol.* 10:R57. doi: 10.1186/gb-2009-10-5-r57
- Anthony, R. G., Henriques, R., Helfer, A., Meszaros, T., Rios, G., Testerink, C., et al. (2004). A protein kinase target of a PDK1 signalling pathway is involved in root hair growth in Arabidopsis. *EMBO J.* 23, 572–581. doi: 10.1038/sj.emboj.7600068
- Avila, J., Gregory, O. G., Su, D., Deeter, T. A., Chen, S., Silva-Sanchez, C., et al. (2012). The beta-subunit of the SnRK1 complex is phosphorylated by the plant cell death suppressor Adi3. *Plant Physiol.* 159, 1277–1290. doi: 10.1104/pp.112.198432
- Azevedo, C., and Saiardi, A. (2006). Extraction and analysis of soluble inositol polyphosphates from yeast. *Nat. Protoc.* 1, 2416–2422. doi: 10.1038/nprot.2006.337
- Bennett, M., Onnebo, S. M., Azevedo, C., and Saiardi, A. (2006). Inositol pyrophosphates: metabolism and signaling. *Cell. Mol. Life Sci.* 63, 552–564. doi: 10.1007/s00018-005-5446-z
- Bhandari, R., Juluri, K. R., Resnick, A. C., and Snyder, S. H. (2008). Gene deletion of inositol hexakisphosphate kinase 1 reveals inositol pyrophosphate regulation of insulin secretion, growth, and spermiogenesis. *Proc. Natl. Acad. Sci. U.S.A.* 105, 2349–2353. doi: 10.1073/pnas.0712227105
- Bhandari, R., Saiardi, A., Ahmadibeni, Y., Snowman, A. M., Resnick, A. C., Kristiansen, T. Z., et al. (2007). Protein pyrophosphorylation by inositol pyrophosphates is a posttranslational event. *Proc. Natl. Acad. Sci. U.S.A.* 104, 15305–15310. doi: 10.1073/pnas.0707338104
- Brearley, C. A., and Hanke, D. E. (1996). Inositol phosphates in barley (*Hordeum vulgare* L.) aleurone tissue are stereochemically similar to the products of breakdown of InsP6 in vitro by wheat-bran phytase. *Biochem. J.* 318(Pt 1), 279–286.
- Calleja, V., Alcor, D., Laguerre, M., Park, J., Vojnovic, B., Hemmings, B. A., et al. (2007). Intramolecular and intermolecular interactions of protein kinase B define its activation in vivo. *PLoS Biol.* 5:e95. doi: 10.1371/journal.pbio.0050095
- Carroll, A. S., and O'shea, E. K. (2002). Pho85 and signaling environmental conditions. *Trends Biochem. Sci.* 27, 87–93. doi: 10.1016/S0968-0004(01)02040-0
- Chakraborty, A., Koldobskiy, M. A., Bello, N. T., Maxwell, M., Potter, J. J., Juluri, K. R., et al. (2010). Inositol pyrophosphates inhibit Akt signaling, thereby regulating insulin sensitivity and weight gain. *Cell* 143, 897–910. doi: 10.1016/j.cell.2010.11.032
- Chini, A., Fonseca, S., Fernandez, G., Adie, B., Chico, J. M., Lorenzo, O., et al. (2007). The JAZ family of repressors is the missing link in jasmonate signalling. *Nature* 448, 666–671. doi: 10.1038/nature06006
- Choi, J. H., Williams, J., Cho, J., Falck, J. R., and Shears, S. B. (2007). Purification, sequencing, and molecular identification of a mammalian PP-InsP5 kinase that is activated when cells are exposed to hyperosmotic stress. *J. Biol. Chem.* 282, 30763–30775. doi: 10.1074/jbc.M704655200
- Clouze, S. D. (2011). Brassinosteroid signal transduction: from receptor kinase activation to transcriptional networks regulating plant development. *Plant Cell* 23, 1219–1230. doi: 10.1105/tpc.111.084475
- Da Silveira Dos Santos, A. X., Riezman, I., Aguilera-Romero, M. A., David, F., Piccolis, M., Loewenthal, R., et al. (2014). Systematic lipidomic analysis of yeast protein kinase and phosphatase mutants reveals novel insights into regulation of lipid homeostasis. *Mol. Biol. Cell* 25, 3234–3246. doi: 10.1091/mbc.E14-03-0851
- Desai, M., Rangarajan, P., Donahue, J. L., Williams, S. P., Land, E. S., Mandal, M. K., et al. (2014). Two inositol hexakisphosphate kinases drive inositol pyrophosphate synthesis in plants. *Plant J.* 80, 642–653. doi: 10.1111/tpj.12669
- Devarenne, T. P., Ekengren, S. K., Pedley, K. F., and Martin, G. B. (2006). Adi3 is a Pdk1-interacting AGC kinase that negatively regulates plant cell death. *EMBO J.* 25, 255–265. doi: 10.1038/sj.emboj.7600910
- Devarenne, T. P., and Martin, G. B. (2007). Manipulation of plant programmed cell death pathways during plant-pathogen interactions. *Plant Signal. Behav.* 2, 188–189. doi: 10.4161/psb.2.3.4150
- Dorsch, J. A., Cook, A., Young, K. A., Anderson, J. M., Bauman, A. T., Volkmann, C. J., et al. (2003). Seed phosphorus and inositol phosphate phenotype of barley low phytic acid genotypes. *Phytochemistry* 62, 691–706. doi: 10.1016/S0031-9422(02)00610-6
- Draskovic, P., Saiardi, A., Bhandari, R., Burton, A., Ilc, G., Kovacevic, M., et al. (2008). Inositol hexakisphosphate kinase products contain diphosphate and triphosphate groups. *Chem. Biol.* 15, 274–286. doi: 10.1016/j.chembiol.2008.01.011
- Dunlop, E. A., and Tee, A. R. (2009). Mammalian target of rapamycin complex 1: signalling inputs, substrates and feedback mechanisms. *Cell. Signal.* 21, 827–835. doi: 10.1016/j.cellsig.2009.01.012
- Flores, S., and Smart, C. C. (2000). Abscisic acid-induced changes in inositol metabolism in *Spirodela polyrrhiza*. *Planta* 211, 823–832. doi: 10.1007/s004250000348
- Fridy, P. C., Otto, J. C., Dollins, D. E., and York, J. D. (2007). Cloning and characterization of two human VIP1-like inositol hexakisphosphate and diphosphoinositol pentakisphosphate kinases. *J. Biol. Chem.* 282, 30754–30762. doi: 10.1074/jbc.M704656200
- Gillaspy, G. E. (2011). The cellular language of myo-inositol signaling. *New Phytol.* 192, 823–839. doi: 10.1111/j.1469-8137.2011.03939.x
- Glennon, M. C., and Shears, S. B. (1993). Turnover of inositol pentakisphosphates, inositol hexakisphosphate and diphosphoinositol polyphosphates in primary cultured hepatocytes. *Biochem. J.* 293(Pt 2), 583–590.
- Gokhale, N. A., Zaremba, A., and Shears, S. B. (2011). Receptor-dependent compartmentalization of PPIP5K1, a kinase with a cryptic polyphosphoinositide binding domain. *Biochem. J.* 434, 415–426. doi: 10.1042/BJ20101437
- Hardie, D. G. (2011). AMPK and autophagy get connected. *EMBO J.* 30, 634–635. doi: 10.1038/embj.2011.12
- Hawkins, P. T., Stephens, L. R., and Piggott, J. R. (1993). Analysis of inositol metabolites produced by *Saccharomyces cerevisiae* in response to glucose stimulation. *J. Biol. Chem.* 268, 3374–3383.
- Heilmann, M., and Heilmann, I. (2014). Plant phosphoinositides-complex networks controlling growth and adaptation. *Biochim. Biophys. Acta* doi: 10.1016/j.bbaply.2014.09.018. [Epub ahead of print].
- Hemmings, B. A., and Restuccia, D. F. (2012). PI3K-PKB/Akt pathway. *Cold Spring Harb. Perspect. Biol.* 4:a011189. doi: 10.1101/cshperspect.a011189
- Huang, C. F., Voglmaier, S. M., Bembenek, M. E., Saiardi, A., and Snyder, S. H. (1998). Identification and purification of diphosphoinositol pentakisphosphate kinase, which synthesizes the inositol pyrophosphate bis(diphospho)inositol tetrakisphosphate. *Biochemistry* 37, 14998–15004. doi: 10.1021/bi981920l
- Huang, K. N., and Symington, L. S. (1995). Suppressors of a *Saccharomyces cerevisiae* pck1 mutation identify alleles of the phosphatase gene PTC1 and of a novel gene encoding a putative basic leucine zipper protein. *Genetics* 141, 1275–1285.
- Hung, C. Y., Aspasia, P. Jr., Hunter, M. R., Lomax, A. W., and Perera, I. Y. (2014). Phosphoinositide-signaling is one component of a robust plant defense response. *Front. Plant Sci.* 5:267. doi: 10.3389/fpls.2014.00267
- Jones, J. D., and Dangl, J. L. (2006). The plant immune system. *Nature* 444, 323–329. doi: 10.1038/nature05286
- Kaffman, A., Herskowitz, I., Tjian, R., and O'shea, E. K. (1994). Phosphorylation of the transcription factor PHO4 by a cyclin-CDK complex, PHO80-PHO85. *Science* 263, 1153–1156. doi: 10.1126/science.8108735
- Klein, M., Perfus-Barbeoch, L., Frelet, A., Gaedeke, N., Reinhardt, D., Mueller-Roeber, B., et al. (2003). The plant multidrug resistance ABC transporter AtMRP5 is involved in guard cell hormonal signalling and water use. *Plant J.* 33, 119–129. doi: 10.1046/j.1365-313X.2003.016012.x
- Kuo, H. F., Chang, T. Y., Chiang, S. F., Wang, W. D., Charng, Y. Y., and Chiou, T. J. (2014). Arabidopsis inositol pentakisphosphate 2-kinase, AtIPK1, is required for growth and modulates phosphate homeostasis at the transcriptional level. *Plant J.* 80, 503–515. doi: 10.1111/tpj.12650
- Lam, E. (2004). Controlled cell death, plant survival and development. *Nat. Rev. Mol. Cell Biol.* 5, 305–315. doi: 10.1038/nrm1358
- Laussmann, T., Hansen, A., Reddy, K. M., Reddy, K. K., Falck, J. R., and Vogel, G. (1998). Diphospho-myo-inositol phosphates in *Dictyostelium* and *Polysphondylium*: identification of a new bisdiphospho-myo-inositol tetrakisphosphate. *FEBS Lett.* 426, 145–150. doi: 10.1016/S0014-5793(98)00329-9
- Laussmann, T., Reddy, K. M., Reddy, K. K., Falck, J. R., and Vogel, G. (1997). Diphospho-myo-inositol phosphates from *Dictyostelium* identified

- as D-6-diphospho-myoinositol pentakisphosphate and D-5,6-bisdiphospho-myoinositol tetrakisphosphate. *Biochem. J.* 322(Pt 1), 31–33.
- Lee, Y. S., Mulugu, S., York, J. D., and O'shea, E. K. (2007). Regulation of a cyclin-CDK-CDK inhibitor complex by inositol pyrophosphates. *Science* 316, 109–112. doi: 10.1126/science.1139080
- Lemtiri-Chlieh, F., Mac Robbie, E. A., and Brearley, C. A. (2000). Inositol hexakisphosphate is a physiological signal regulating the K⁺-inward rectifying conductance in guard cells. *Proc. Natl. Acad. Sci. U.S.A.* 97, 8687–8692. doi: 10.1073/pnas.140217497
- Lemtiri-Chlieh, F., Mac Robbie, E. A., Webb, A. A., Manison, N. F., Brownlee, C., Skepper, J. N., et al. (2003). Inositol hexakisphosphate mobilizes an endomembrane store of calcium in guard cells. *Proc. Natl. Acad. Sci. U.S.A.* 100, 10091–10095. doi: 10.1073/pnas.1133289100
- Lenburg, M. E., and O'shea, E. K. (1996). Signaling phosphate starvation. *Trends Biochem. Sci.* 21, 383–387. doi: 10.1016/0968-0004(96)10048-7
- Lin, H., Fridy, P. C., Ribeiro, A. A., Choi, J. H., Barma, D. K., Vogel, G., et al. (2009). Structural analysis and detection of biological inositol pyrophosphates reveal that the family of VIP/diphosphoinositol pentakisphosphate kinases are 1/3-kinases. *J. Biol. Chem.* 284, 1863–1872. doi: 10.1074/jbc.M805686200
- Loewith, R., Jacinto, E., Wullschleger, S., Lorberg, A., Crespo, J. L., Bonenfant, D., et al. (2002). Two TOR complexes, only one of which is rapamycin sensitive, have distinct roles in cell growth control. *Mol. Cell* 10, 457–468. doi: 10.1016/S1097-2765(02)00636-6
- Lonetti, A., Szijgyarto, Z., Bosch, D., Loss, O., Azevedo, C., and Saiardi, A. (2011). Identification of an evolutionarily conserved family of inorganic polyphosphate endopolyphosphatases. *J. Biol. Chem.* 286, 31966–31974. doi: 10.1074/jbc.M111.266320
- Losito, O., Szijgyarto, Z., Resnick, A. C., and Saiardi, A. (2009). Inositol pyrophosphates and their unique metabolic complexity: analysis by gel electrophoresis. *PLoS ONE* 4:e5580. doi: 10.1371/journal.pone.00005580
- Martin, J. B., Laussmann, T., Bakker-Grunwald, T., Vogel, G., and Klein, G. (2000). Neo-inositol polyphosphates in the amoeba *Entamoeba histolytica*. *J. Biol. Chem.* 275, 10134–10140. doi: 10.1074/jbc.275.14.10134
- Mayr, G. W. (1988). A novel metal-dye detection system permits picomolar-range h.p.l.c. analysis of inositol polyphosphates from non-radioactively labelled cell or tissue specimens. *Biochem. J.* 254, 585–591.
- Menniti, F. S., Miller, R. N., Putney, J. W. Jr., and Shears, S. B. (1993). Turnover of inositol polyphosphate pyrophosphates in pancreaticoma cells. *J. Biol. Chem.* 268, 3850–3856.
- Morel, J. B., and Dangl, J. L. (1997). The hypersensitive response and the induction of cell death in plants. *Cell Death Differ.* 4, 671–683. doi: 10.1038/sj.cdd.4400309
- Mosblech, A., Thurow, C., Gatz, C., Feussner, I., and Heilmann, I. (2011). Jasmonic acid perception by COI1 involves inositol polyphosphates in *Arabidopsis thaliana*. *Plant J.* 65, 949–957. doi: 10.1111/j.1365-313X.2011.04480.x
- Mulugu, S., Bai, W., Fridy, P. C., Bastidas, R. J., Otto, J. C., Dollins, D. E., et al. (2007). A conserved family of enzymes that phosphorylate inositol hexakisphosphate. *Science* 316, 106–109. doi: 10.1126/science.1139099
- Murphy, A. M., Otto, B., Brearley, C. A., Carr, J. P., and Hanke, D. E. (2008). A role for inositol hexakisphosphate in the maintenance of basal resistance to plant pathogens. *Plant J.* 56, 638–652. doi: 10.1111/j.1365-313X.2008.03629.x
- Nagy, R., Grob, H., Weder, B., Green, P., Klein, M., Frelet-Barrand, A., et al. (2009). The Arabidopsis ATP-binding cassette protein AtMRP5/AtABC5 is a high affinity inositol hexakisphosphate transporter involved in guard cell signaling and phytate storage. *J. Biol. Chem.* 284, 33614–33622. doi: 10.1074/jbc.M109.030247
- Nishizawa, M., Kormai, T., Morohashi, N., Shimizu, M., and Toh-e, A. (2008). Transcriptional repression by the Pho4 transcription factor controls the timing of SNZ1 expression. *Eukaryot. Cell* 7, 949–957. doi: 10.1128/EC.00366-07
- Norbis, F., Boll, M., Stange, G., Markovich, D., Verrey, F., Biber, J., et al. (1997). Identification of a cDNA/protein leading to an increased Pi-uptake in *Xenopus laevis* oocytes. *J. Membr. Biol.* 156, 19–24. doi: 10.1007/s002329900183
- O'neill, E. M., Kaffman, A., Jolly, E. R., and O'shea, E. K. (1996). Regulation of PHO4 nuclear localization by the PHO80-PHO85 cyclin-CDK complex. *Science* 271, 209–212. doi: 10.1126/science.271.5246.209
- Otto, J. C., Mulugu, S., Fridy, P. C., Chiou, S. T., Armbruster, B. N., Ribeiro, A. A., et al. (2007). Biochemical analysis of inositol phosphate kinases. *Meth. Enzymol.* 434, 171–185. doi: 10.1016/S0076-6879(07)34010-X
- Parry, G., Calderon-Villalobos, L. I., Prigge, M., Peret, B., Dharmasiri, S., Itoh, H., et al. (2009). Complex regulation of the TIR1/AFB family of auxin receptors. *Proc. Natl. Acad. Sci. U.S.A.* 106, 22540–22545. doi: 10.1073/pnas.0911967106
- Prasad, A., Jia, Y., Chakraborty, A., Li, Y., Jain, S. K., Zhong, J., et al. (2011). Inositol hexakisphosphate kinase 1 regulates neutrophil function in innate immunity by inhibiting phosphatidylinositol-(3,4,5)-trisphosphate signaling. *Nat. Immunol.* 12, 752–760. doi: 10.1038/ni.2052
- Pulloor, N. K., Nair, S., Kostic, A. D., Bist, P., Weaver, J. D., Riley, A. M., et al. (2014). Human genome-wide RNAi screen identifies an essential role for inositol pyrophosphates in Type-I interferon response. *PLoS Pathog.* 10:e1003981. doi: 10.1371/journal.ppat.1003981
- Raboy, V. (2003). myo-Inositol-1,2,3,4,5,6-hexakisphosphate. *Phytochemistry* 64, 1033–1043. doi: 10.1016/S0031-9422(03)00446-1
- Raboy, V. (2007). The ABCs of low-phytate crops. *Nat. Biotechnol.* 25, 874–875. doi: 10.1038/nbt0807-874
- Remington, D. L., Vision, T. J., Guilfoyle, T. J., and Reed, J. W. (2004). Contrasting modes of diversification in the Aux/IAA and ARF gene families. *Plant Physiol.* 135, 1738–1752. doi: 10.1104/pp.104.039669
- Saiardi, A. (2012). How inositol pyrophosphates control cellular phosphate homeostasis? *Adv. Biol. Regul.* 52, 351–359. doi: 10.1016/j.jbior.2012.03.002
- Saiardi, A., Bhandari, R., Resnick, A. C., Snowman, A. M., and Snyder, S. H. (2004). Phosphorylation of proteins by inositol pyrophosphates. *Science* 306, 2101–2105. doi: 10.1126/science.1103344
- Saiardi, A., Erdjument-Bromage, H., Snowman, A. M., Tempst, P., and Snyder, S. H. (1999). Synthesis of diphosphoinositol pentakisphosphate by a newly identified family of higher inositol polyphosphate kinases. *Curr. Biol.* 9, 1323–1326. doi: 10.1016/S0960-9822(00)80055-X
- Scheffzek, K., and Welti, S. (2012). Pleckstrin homology (PH) like domains – versatile modules in protein-protein interaction platforms. *FEBS Lett.* 586, 2662–2673. doi: 10.1016/j.febslet.2012.06.006
- Sheard, L. B., Tan, X., Mao, H., Withers, J., Ben-Nissan, G., Hinds, T. R., et al. (2010). Jasmonate perception by inositol-phosphate-potentiated COII-JAZ co-receptor. *Nature* 468, 400–405. doi: 10.1038/nature09430
- Shears, S. B., Gokhale, N. A., Wang, H., and Zaremba, A. (2011). Diphosphoinositol polyphosphates: what are the mechanisms? *Adv. Enzyme Regul.* 51, 13–25. doi: 10.1016/j.advenzreg.2010.09.008
- Shears, S. B., Weaver, J. D., and Wang, H. (2013). Structural insight into inositol pyrophosphate turnover. *Adv. Biol. Regul.* 53, 19–27. doi: 10.1016/j.jbior.2012.10.002
- Shi, J., Wang, H., Schellin, K., Li, B., Faller, M., Stoop, J. M., et al. (2007). Embryo-specific silencing of a transporter reduces phytic acid content of maize and soybean seeds. *Nat. Biotechnol.* 25, 930–937. doi: 10.1038/nbt1322
- Smith, A. P., Jain, A., Deal, R. B., Nagarajan, V. K., Poling, M. D., Raghothama, K. G., et al. (2010). Histone H2A.Z regulates the expression of several classes of phosphate starvation response genes but not as a transcriptional activator. *Plant Physiol.* 152, 217–225. doi: 10.1104/pp.109.145532
- Stephens, L., Radenberg, T., Thiel, U., Vogel, G., Khoo, K. H., Dell, A., et al. (1993). The detection, purification, structural characterization, and metabolism of diphosphoinositol pentakisphosphate(s) and bisdiphosphoinositol tetrakisphosphate(s). *J. Biol. Chem.* 268, 4009–4015.
- Stevenson-Paulik, J., Bastidas, R. J., Chiou, S. T., Frye, R. A., and York, J. D. (2005). Generation of phytate-free seeds in *Arabidopsis* through disruption of inositol polyphosphate kinases. *Proc. Natl. Acad. Sci. U.S.A.* 102, 12612–12617. doi: 10.1073/pnas.0504172102
- Suh, S. J., Wang, Y. F., Frelet, A., Leonhardt, N., Klein, M., Forestier, C., et al. (2007). The ATP binding cassette transporter AtMRP5 modulates anion and calcium channel activities in *Arabidopsis* guard cells. *J. Biol. Chem.* 282, 1916–1924. doi: 10.1074/jbc.M607926200
- Szijgyarto, Z., Garedew, A., Azevedo, C., and Saiardi, A. (2011). Influence of inositol pyrophosphates on cellular energy dynamics. *Science* 334, 802–805. doi: 10.1126/science.1211908
- Tan, X., Calderon-Villalobos, L. I., Sharon, M., Zheng, C., Robinson, C. V., Estelle, M., et al. (2007). Mechanism of auxin perception by the TIR1 ubiquitin ligase. *Nature* 446, 640–645. doi: 10.1038/nature05731
- Trinchieri, G. (2010). Type I interferon: friend or foe? *J. Exp. Med.* 207, 2053–2063. doi: 10.1084/jem.20101664
- Vanholme, B., Grunewald, W., Bateman, A., Kohchi, T., and Gheysen, G. (2007). The tify family previously known as ZIM. *Trends Plant Sci.* 12, 239–244. doi: 10.1016/j.tplants.2007.04.004

- Van Leeuwen, W., Okresz, L., Bogre, L., and Munnik, T. (2004). Learning the lipid language of plant signalling. *Trends Plant Sci.* 9, 378–384. doi: 10.1016/j.tplants.2004.06.008
- Voglmaier, S. M., Bembeneck, M. E., Kaplin, A. I., Dorman, G., Olszewski, J. D., Prestwich, G. D., et al. (1996). Purified inositol hexakisphosphate kinase is an ATP synthase: diphosphoinositol pentakisphosphate as a high-energy phosphate donor. *Proc. Natl. Acad. Sci. U.S.A.* 93, 4305–4310. doi: 10.1073/pnas.93.9.4305
- Wang, H., Derose, E. F., London, R. E., and Shears, S. B. (2014). IP6K structure and the molecular determinants of catalytic specificity in an inositol phosphate kinase family. *Nat. Commun.* 5:4178. doi: 10.1038/ncomms5178
- Wang, H., Falck, J. R., Hall, T. M., and Shears, S. B. (2012). Structural basis for an inositol pyrophosphate kinase surmounting phosphate crowding. *Nat. Chem. Biol.* 8, 111–116. doi: 10.1038/nchembio.733
- Watson, P. J., Fairall, L., Santos, G. M., and Schwabe, J. W. (2012). Structure of HDAC3 bound to co-repressor and inositol tetraphosphate. *Nature* 481, 335–340. doi: 10.1038/nature10728
- Worley, J., Luo, X., and Capaldi, A. P. (2013). Inositol pyrophosphates regulate cell growth and the environmental stress response by activating the HDAC Rpd3L. *Cell Rep.* 3, 1476–1482. doi: 10.1016/j.celrep.2013.03.043
- Wunderberg, T., Grabinski, N., Lin, H., and Mayr, G. W. (2014). Discovery of InsP6-kinases as InsP6-dephosphorylating enzymes provides a new mechanism of cytosolic InsP6 degradation driven by the cellular ATP/ADP ratio. *Biochem. J.* 462, 173–184. doi: 10.1042/BJ20130992
- Xiong, Y., and Sheen, J. (2014). The role of target of rapamycin signaling networks in plant growth and metabolism. *Plant Physiol.* 164, 499–512. doi: 10.1104/pp.113.229948
- Yagci, A., Werner, A., Murer, H., and Biber, J. (1992). Effect of rabbit duodenal mRNA on phosphate transport in *Xenopus laevis* oocytes: dependence on 1,25-dihydroxy-vitamin-D3. *Pflugers Arch.* 422, 211–216. doi: 10.1007/BF00376204
- Yan, Z., Zhao, J., Peng, P., Chihara, R. K., and Li, J. (2009). BIN2 functions redundantly with other Arabidopsis GSK3-like kinases to regulate brassinosteroid signaling. *Plant Physiol.* 150, 710–721. doi: 10.1104/pp.109.138099
- Zhang, Z., Liao, H., and Lucas, W. J. (2014). Molecular mechanisms underlying phosphate sensing, signaling, and adaptation in plants. *J. Integr. Plant Biol.* 56, 192–220. doi: 10.1111/jipb.12163

Conflict of Interest Statement: The authors declare that the research was conducted in the absence of any commercial or financial relationships that could be construed as a potential conflict of interest.

Received: 24 November 2014; accepted: 26 January 2015; published online: 12 February 2015.

Citation: Williams SP, Gillaspy GE and Perera IY (2015) Biosynthesis and possible functions of inositol pyrophosphates in plants. Front. Plant Sci. 6:67. doi: 10.3389/fpls.2015.00067

This article was submitted to Plant Physiology, a section of the journal Frontiers in Plant Science.

Copyright © 2015 Williams, Gillaspy and Perera. This is an open-access article distributed under the terms of the Creative Commons Attribution License (CC BY). The use, distribution or reproduction in other forums is permitted, provided the original author(s) or licensor are credited and that the original publication in this journal is cited, in accordance with accepted academic practice. No use, distribution or reproduction is permitted which does not comply with these terms.



Overexpression of patatin-related phospholipase $\text{AIII}\beta$ altered the content and composition of sphingolipids in *Arabidopsis*

Maoyin Li^{1,2*}, Jonathan E. Markham³ and Xuemin Wang^{1,2}

¹ Department of Biology, University of Missouri, St. Louis, MO, USA

² Donald Danforth Plant Science Center, St. Louis, MO, USA

³ Department of Biochemistry, University of Nebraska-Lincoln, Lincoln, NE, USA

Edited by:

Olga Valentova, Institute of Chemical Technology Prague, Czech Republic

Reviewed by:

Daniel Hofius, Swedish University of Agricultural Sciences, Sweden
Günther F. E. Scherer, Leibniz Universität Hannover, Germany

***Correspondence:**

Maoyin Li, Department of Biology, University of Missouri and Donald Danforth Plant Science Center, St. Louis, MO 63121, USA
e-mail: mali@danforthcenter.org

In plants, fatty acids are primarily synthesized in plastids and then transported to the endoplasmic reticulum (ER) for synthesis of most of the complex membrane lipids, including glycerolipids and sphingolipids. The first step of sphingolipid synthesis, which uses a fatty acid and a serine as substrates, is critical for sphingolipid homeostasis; its disruption leads to an altered plant growth. Phospholipase As have been implicated in the trafficking of fatty acids from plastids to the ER. Previously, we found that overexpression of a patatin-related phospholipase, *pPLAIII* β , resulted in a smaller plant size and altered anisotropic cell expansion. Here, we determined the content and composition of sphingolipids in *pPLAIII* β -knockout and overexpression plants (*pPLAIII* β -KO and -OE). 3-keto-sphinganine, the product of the first step of sphingolipid synthesis, had a 26% decrease in leaves of *pPLAIII* β -KO while a 52% increase in *pPLAIII* β -OE compared to wild type (WT). The levels of free long-chain base species, dihydroxy-C18:0 and trihydroxy-18:0 (d18:0 and t18:0), were 38 and 97% higher, respectively, in *pPLAIII* β -OE than in WT. The level of complex sphingolipids ceramide d18:0-16:0 and t18:1-16:0 had a twofold increase in *pPLAIII* β -OE. The level of hydroxy ceramide d18:0-h16:0 was 72% higher in *pPLAIII* β -OE compared to WT. The levels of several species of glucosylceramide and glycosylinositolphosphoceramide tended to be higher in *pPLAIII* β -OE than in WT. The total content of the complex sphingolipids showed a slightly higher in *pPLAIII* β -OE than in WT. These results revealed an involvement of phospholipase-mediated lipid homeostasis in plant growth.

Keywords: *Arabidopsis thaliana*, patatin-related phospholipase, sphingolipid, plant growth, fatty acyl flux

INTRODUCTION

Lipids are structural components of membrane bilayers and play important metabolic and regulatory roles in plant growth, development, and stress responses. Phospholipases are major enzyme families that catalyze many of the reactions in lipid metabolism and signaling. Recently, multiple biological functions have been revealed for patatin-related phospholipase As (pPLAs; Li and Wang, 2014). Patatin-related PLAs in *Arabidopsis* comprise pPLAI, pPLAI (α,β,γ,δ,ε), and pPLAII (α,β,γ,δ; Scherer et al., 2010). *pPLAI* has a positive role in plant resistance to the fungus pathogen *Botrytis cinerea*, possibly by mediating the production of jasmonates (Yang et al., 2007). Deficiency of *pPLAII*α decreases resistance to bacterial pathogens and impedes oxylipin production under drought stress (La Camera et al., 2005; Yang et al., 2012). *pPLAII*γ, *pPLAII*δ, and *pPLAII*ε are involved in the response to phosphorus deficiency and auxin treatment in terms of root elongation (Rietz et al., 2004, 2010).

pPLAIIIs possess a distinctive non-canonical esterase motif GxGxG, instead of GxSxG, which is present in pPLAI and pPLAIIIs (Scherer et al., 2010). Overexpression of *pPLAII*δ leads to a stunted plant stature (Huang et al., 2001). Overexpression

of *pPLAIII* β results in smaller plant size and reduced cellulose content in stems (Li et al., 2011). Disruption of rice *DEP3*, a homolog of *pPLAII*δ, results in taller rice plants (Qiao et al., 2011). Heterogeneous overexpression of an *Oncidium OSAG78*, another homolog of *pPLAII*δ, results in a smaller plant size and a delayed flowering time in *Arabidopsis* (Lin et al., 2011). These lines of evidence indicate *pPLAIIIs* are important for plant growth and development.

In plants, sphingolipids are major components of cellular membranes and determine the membrane physical properties. They have functions on environmental stress tolerance (Chao et al., 2011; Chen et al., 2012), programmed cell death (Alden et al., 2011), and polar auxin transport (Markham et al., 2011; Yang et al., 2013). Sphingolipids include free long chain bases, such as long chain bases (LCBs) and long chain base phosphate (LCBPs), and complex sphingolipids, such as ceramide (Cer), hydroxyceramide (hCer), glucosylceramide (GlcCer), and glycosylinositolphosphoceramide (GIPC; Markham et al., 2013). Sphingolipid synthesis begins by the condensation of palmitoyl-CoA and serine catalyzed by serine palmitoyltransferase (SPT; Hanada, 2003). SPT are heterodimer proteins with two subunits, LCB1 and LCB2. In *Arabidopsis*, LCB1 is encoded by a single gene

(Chen et al., 2006), while LCB2 is encoded by two functionally redundant genes, *LCB2a* and *LCB2b* (Dietrich et al., 2008).

Maintenance of sphingolipid homeostasis is critical for plant growth and development (Chen et al., 2006; Dietrich et al., 2008; Teng et al., 2008; Kimberlin et al., 2013). T-DNA disruption of *LCB1* gene in *Arabidopsis* results in an arrested development of the embryo at the globular stage (Chen et al., 2006). Partial RNA interference suppression of *LCB1* results in reduced cell expansion, a smaller plant, and elevated levels of saturated sphingolipid LCBs (Chen et al., 2006). There is no apparent growth phenotype for mutants deficient in either *LCB2a* or *LCB2b*, however, the deficiency of both is lethal for gametophyte (Dietrich et al., 2008). Inducible suppression of *LCB2b* results in cell necrosis and reduced levels of LCBs in adult *Arabidopsis* plants (Dietrich et al., 2008).

The function of SPT can be regulated by small polypeptides designated as small subunits of SPT (ssSPT). ssSPT α and ssSPT β interact with SPT and stimulate its activity in *Arabidopsis* (Kimberlin et al., 2013). T-DNA disruption of ssSPT α results in reduced plant growth and pollen lethality in *Arabidopsis* (Kimberlin et al., 2013). Overexpression of ssSPT α leads to increased levels of free LCBs and LCBPs compared with that of WT, while RNA interference suppression of ssSPT α has opposite effects (Kimberlin et al., 2013). Overexpression of ssSPT α results in a greater reduction in plant growth than suppression does, when plants are treated by fumonisin B1, an inhibitor of sphingolipid synthesis (Kimberlin et al., 2013).

Previously, we reported that overexpression of *pPLAIIIβ* results in a reduced plant growth in *Arabidopsis* (Li et al., 2011). Here we report the effects of overexpression of *pPLAIIIβ* on the content and composition of sphingolipids, including free sphingolipids and complex ones. Our results show that overexpression of *pPLAIIIβ* results in an elevated level of 3-keto-sphinganine (3-KS), the product of the first step of sphingolipid synthesis, as well as altered levels of many of the species of complex sphingolipids.

RESULTS

OVEREXPRESSION OF *pPLAIIIβ* INCREASED LEVELS OF 3-KETO-SPHINGANINE AND FREE LONG-CHAIN BASES

Overexpression of *pPLAIIIβ* by constitutive 35S cauliflower mosaic virus promoter in *Arabidopsis* resulted in stunted plant growth (Figure 1A). The sphingolipids were profiled in leaves of WT, *pPLAIIIβ*-knockout (β -KO), and *pPLAIIIβ*-overexpressors (β -OE). The first step of sphingolipid synthesis is the production of 3-KS catalyzed by the serine palmitoyltransferase using substrates of 16:0-CoA and serine (Figure 1B). The reduction of 3-KS forms a dihydroxy C18 long chain base (sphinganine), designated as LCB d18:0 (Figures 1B,C). The reduction of LCB d18:0 forms the trihydroxy LCB (phytosphingosine), designated as LCB t18:0. Desaturation of LCB d18:0 and t18:0 produces LCB d18:1 and t18:1. The LCB d18:0, d18:1, t18:0, and t18:1 can be phosphorylated to form LCBP d18:0, d18:1, t18:0, and t18:1 (Figures 1B,C). LCBs and LCBPs belong to free sphingolipids.

The level of 3-KS was 26% lower in β -KO and 52% higher in β -OE compared with that of WT (Figure 2A). The levels of LCB t18:0 and t18:1 were approximately 15 times higher than LCB d18:0

and d18:1 in leaves of WT (Figure 2B). Among the LCB species, the levels of d18:0 and t18:0 were 38 and 97% higher, respectively, in leaves of β -OE compared to those of WT (Figure 2B). The level of LCB t18:0 tended to be lower in β -KO than in WT (Figure 2B). Of the LCBP species, the level of t18:0 tended to be 85% higher while it was 43% lower in β -KO than in WT (Figure 2C).

OVEREXPRESSION OF *pPLAIIIβ* ALTERED THE LEVELS OF CERAMIDE AND HYDROXYCERAMIDE

Ceramide was synthesized by CS using substrates of LCBs and acyl-CoAs (Figure 1B). A Cer molecule contains two components, a LCB and a fatty acid chain, linked by an amide bond. For example, Cer d18:0–16:0 comprises a LCB d18:0 and a fatty acyl chain 16:0 (Figure 1C). The levels of Cer molecules containing one of four types of LCBs and one of the 14 types of fatty acyl chains were quantified by mass spectrometry (Figure 3). The four types of LCBs are d18:0, d18:0, t18:0, and t18:1, and the most abundant fatty acyl chains are 16:0, 22:0, 24:0, and 26:0 (Figure 3). The levels of 16:0-containing Cers, including d18:0–16:0, d18:1–16:0, t18:0–16:0, and t18:1–16:0, tended to be lower in β -KO while higher in β -OE than in WT (Figure 3). The levels of Cer d18:0–16:0 and t18:0–16:0 were about twofold higher in β -OE than in WT (Figure 3). The levels of 24:0-, 24:1-, and 26:0-containing Cers, including t18:0–24:0, t18:1–24:1, and t18:1–26:0, tended to be lower in β -OE than in WT (Figure 3). Generally the levels of Cers containing fatty acyl chain of 16–22 carbons tended to be higher while those containing fatty acyl chain of 24–26 carbons tended to be lower in leaves of β -OE than in WT, and the β -KO behaved oppositely (Figure 3).

The fatty acyl chains of Cer can be hydroxylated to produce hydroxyl ceramide (hCer; Figure 1B). For example, the hydroxylation of 16:0 in Cer d18:0–16:0 led to the formation of hCer d18:0–h16:0 (Figure 1C). The levels of hCer species containing one of the four types of LCBs and one of the 14 types of hydroxylated fatty acyl chains were profiled (Figure 4). The most profound alteration was the level of hCer d18:0–h16:0; it was 24% lower in β -KO and 72% higher in β -OE than in WT (Figure 4). The levels of the other hCer species did not display any significant alteration between WT and β -OE (Figure 4).

OVEREXPRESSION OF *pPLAIIIβ* CHANGED THE LEVELS OF GLUCOSYLCERAMIDE AND GLYCOSYLINOSITOLPHOSPHOCERAMIDE

A sugar-containing polar head group can be linked to the hydroxyl ceramide to form GlcCer and GIPC (Figure 1B). For example, GluCer d18:0–h16:0 has a glycosyl head group and GIPC d18:0–h16:0 has a phosphoryl-inositol-hexose-hexuronic acid head group (Figure 1C). Some GlcCer species displayed higher levels in leaves of β -OE than in WT, including GlcCer d18:0–h20:0, d18:1–h24:0, t18:1–h24:0, and t18:1–h24:1 (Figure 5). The level of GlcCer t18:0–h24:0 was 80% lower in β -KO (Figure 5). The profound alteration of GIPC species was d18:0–h26:0; its levels increased 64% in β -OE compared to WT (Figure 6). The levels of GIPC d18:0–h16:0, d18:1–h16:0, and t18:0–h16:0 tended to be lower in β -KO while higher in β -OE than in WT (Figure 6). Generally most of the GIPC species tended to be lower in β -KO and higher in β -OE than in WT (Figure 6).

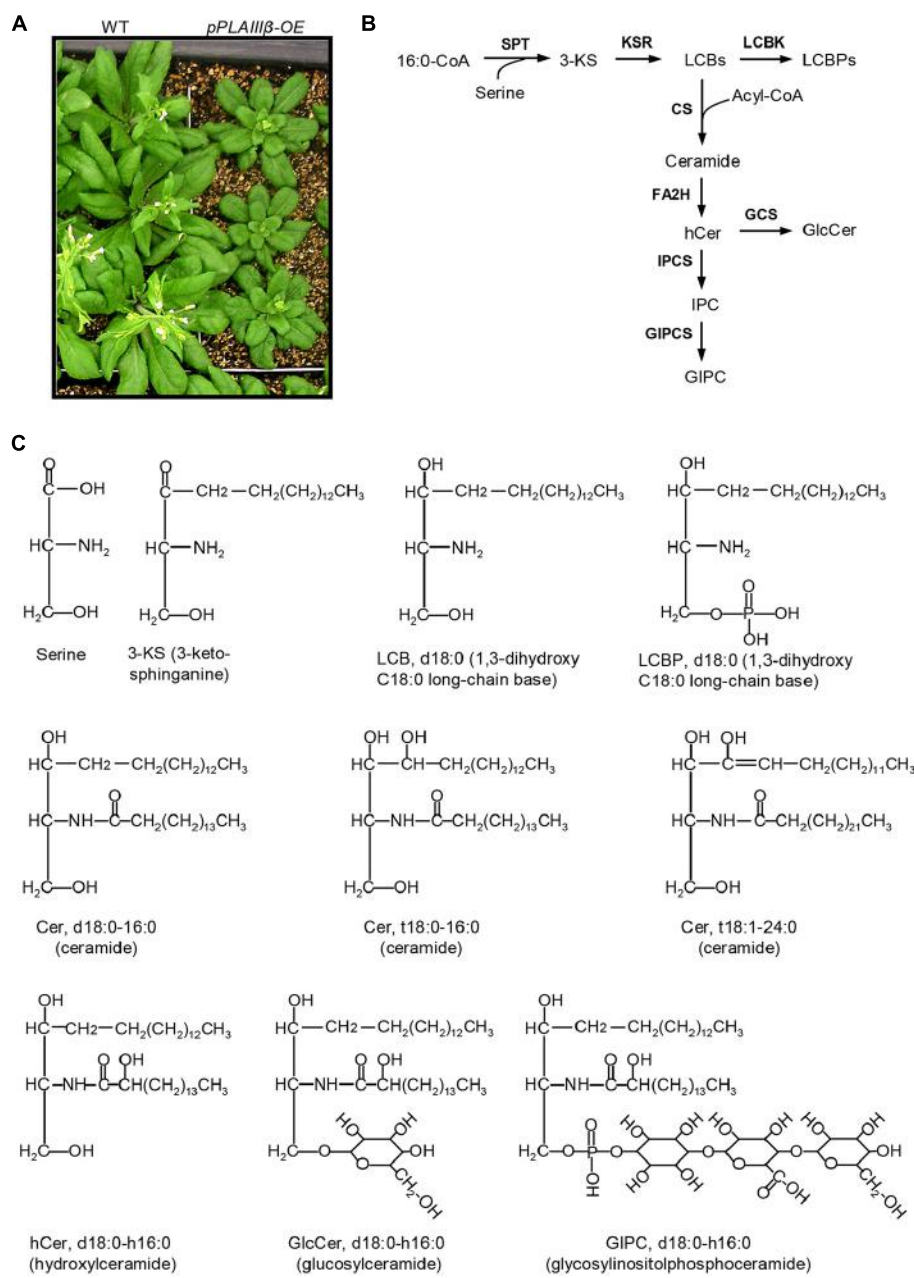


FIGURE 1 | Schematic representation of sphingolipid biosynthesis in *Arabidopsis*. **(A)** *pPLAIIIb*-overexpressing mutants (β -OE) were smaller than wild type (WT). **(B)** Representative diagram of the sphingolipid biosynthesis pathways (Markham et al., 2013). **(C)** Representative sphingolipid molecules. 3-KS, 3-keto-sphinganine; Cer, ceramide; CS, ceramide synthase; FA2H, fatty acid 2-hydroxylase; GCS, glucosylceramide

synthase; GIPC, glycosylinositolphosphoceramide; GIPCS, glycosylinositolphosphoceramide synthase; GlcCer, glucosylceramide; hCer, hydroxyceramide; IPC, inositolphosphoceramide; IPCS, inositolphosphoceramide synthase; KSR, 3-ketosphinganine reductase; LCBK, long-chain base kinase; LCBP, LCB phosphate; LCBs, long-chain bases; SPT, serine-palmitoyltransferase.

Of the measured free sphingolipids, the level of total LCBs was 32% higher in β -OE than in WT (**Figure 7A**). The level of total LCBPs tended to be lower in β -KO than in WT (**Figure 7B**). Of the measured complex sphingolipids, the most abundant classes were GIPC (50%), followed by GlcCer (37%), Cer (8%), and hCer (5%; **Figure 7C**). The level of total Cer tended to be lower while the levels of total GlcCer and total GIPC tended to be higher in

β -OE than in WT (**Figure 7C**). The total content of complex sphingolipids tended to be slightly higher in β -OE than in WT (**Figure 7D**).

DISCUSSION

These data show that overexpression of *pPLAIIIB* results in a 52% increase and knockout mutant has a 26% decrease of 3-KS, the

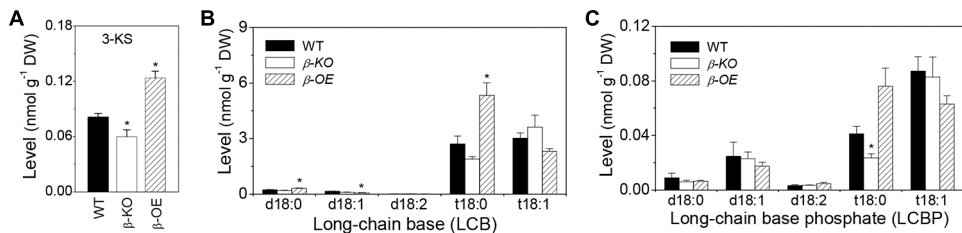


FIGURE 2 | Levels of 3-KS, LCBs, and LCBP in *pPLAIII β* -knockout and overexpression plant leaves. (A) The level of 3-keto-sphinganine (3-KS). **(B)** The level of long-chain bases (LCBs). **(C)** The level of long chain base-phosphates (LCBPs). β -KO, T-DNA knockout of *pPLAIII β*

(Salk_057212). β -OE, overexpression mutant of *pPLAIII β* driven by cauliflower mosaic 35S promoter. Values are means \pm SE ($n = 5$). *Significant difference at $P < 0.05$ compared with the WT, based on Student's *t*-test.

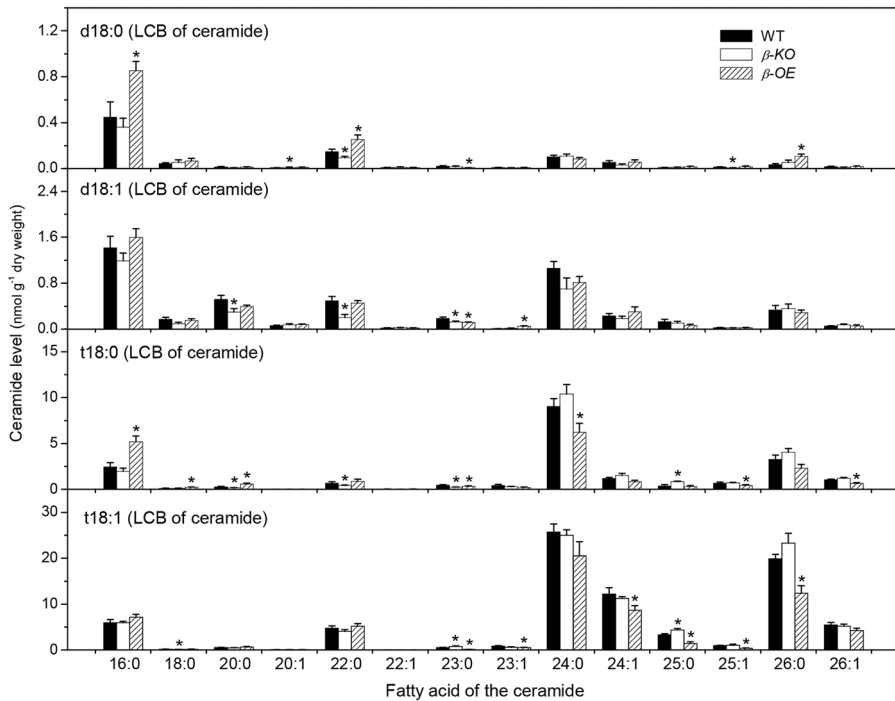


FIGURE 3 | Levels of Cer species in *pPLAIII β* -knockout and overexpression plant leaves. β -KO, T-DNA knockout of *pPLAIII β* (Salk_057212). β -OE, overexpression mutant of *pPLAIII β* driven by cauliflower mosaic 35S promoter. Values are means \pm SE ($n = 5$). *Significant difference at $P < 0.05$ compared with the WT, based on Student's *t*-test.

product of the first step of sphingolipid synthesis. Overexpression of *pPLAIII β* leads to increase of several complex sphingolipid species with saturated long chain base and saturated fatty acid chains, such as Cer d18:0–16:0 (90%), Cer t18:0–16:0 (112%), hCer d18:0–h16:0 (72%), GlcCer d18:0–h20:0 (379%), and GIPC t18:0–h16:0 (24%). The total amount of each complex sphingolipid class has no significant difference between WT and *pPLAIII β* -overexpression plants. It is not clear how the overexpression of *pPLAIII β* leads to the alteration of sphingolipid homeostasis.

pPLAIII β and *pPLAIII δ* can hydrolyze PC and generate LPC and FA (Li et al., 2011, 2013a). It is implicated that *pPLAIII δ* are involved in the fatty acyl trafficking from plastids to ER (Li et al., 2013a). Overexpression of *pPLAIII β* may promote the fatty

acyl flux from plastids to ER and enlarge certain fatty acyl pools that provide fatty acyl substrates for sphingolipid synthesis. We observed that the level of 3-KS, the precursor of sphingolipid synthesis, was significantly increased in *pPLAIII β* -overexpression plants. The alteration of this critical first step of sphingolipid synthesis could lead to the observed changes in sphingolipid homeostasis (Figure 8).

Sphingolipids are the major components of the plasma membrane (Sperling et al., 2004). Changes in sphingolipid homeostasis may alter structure integrity of raft-like domains in the plasma membrane and therefore influence cell surface activities, such as lipid trafficking and cell wall metabolism (Mongrand et al., 2004; Borner et al., 2005; Melser et al., 2011). Overexpression of *pPLAIII β* results in a decreased level of cellulose content,

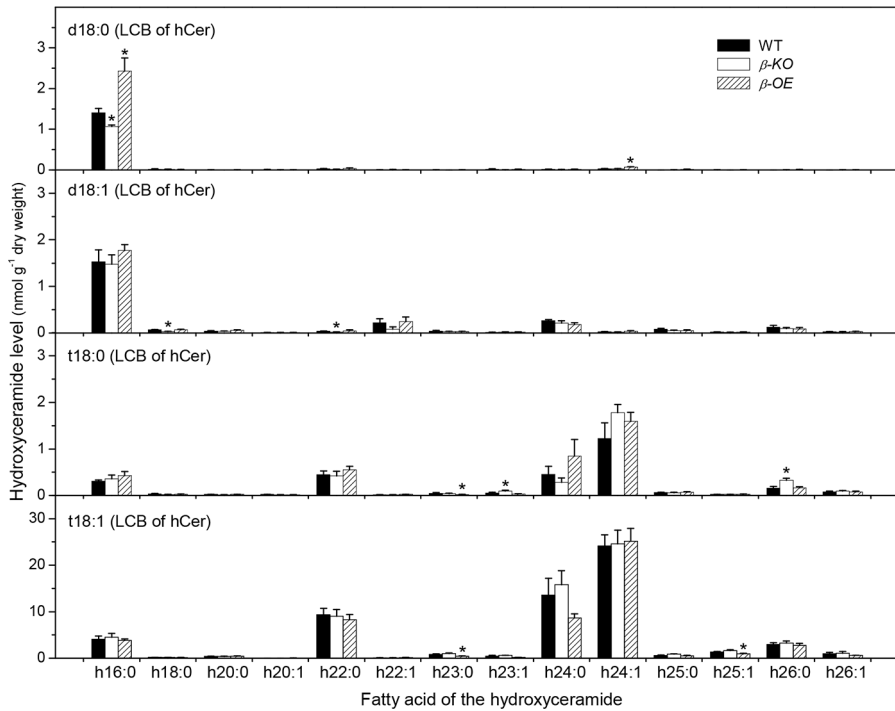


FIGURE 4 | Levels of hCer species in *pPLAIII β* -knockout and overexpression plant leaves. β -KO, T-DNA knockout of *pPLAIII β* (Salk_057212). β -OE, overexpression mutant of *pPLAIII β* driven by cauliflower mosaic 35S promoter. Values are means \pm SE ($n = 5$). *Significant difference at $P < 0.05$ compared with the WT, based on Student's *t*-test.

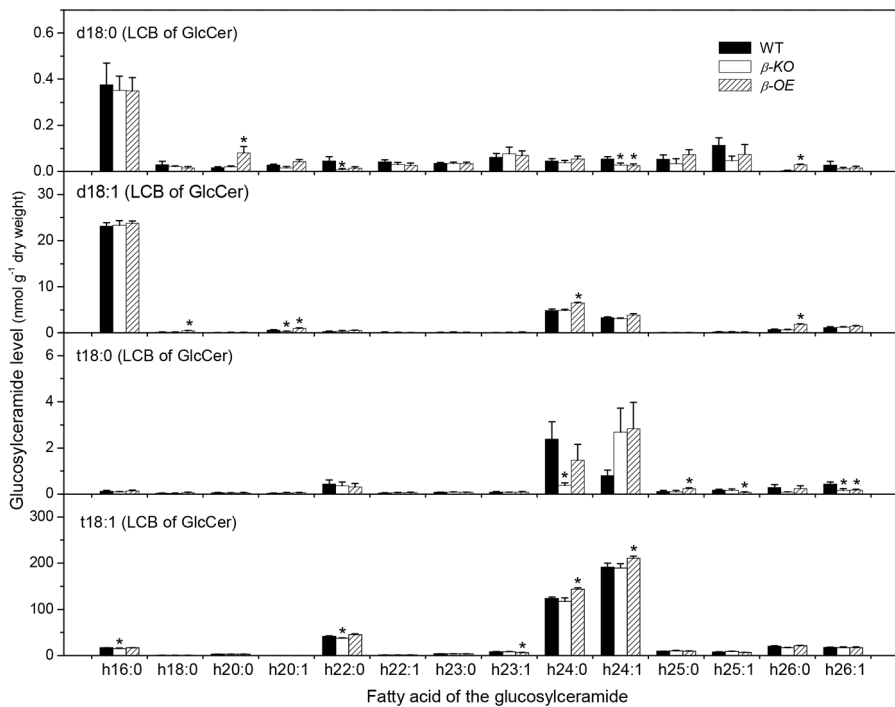


FIGURE 5 | Levels of GlcCer species in *pPLAIII β* -knockout and overexpression plant leaves. β -KO, T-DNA knockout of *pPLAIII β* (Salk_057212). β -OE, overexpression mutant of *pPLAIII β* driven by cauliflower mosaic 35S promoter. Values are means \pm SE ($n = 5$). *Significant difference at $P < 0.05$ compared with the WT, based on Student's *t*-test.

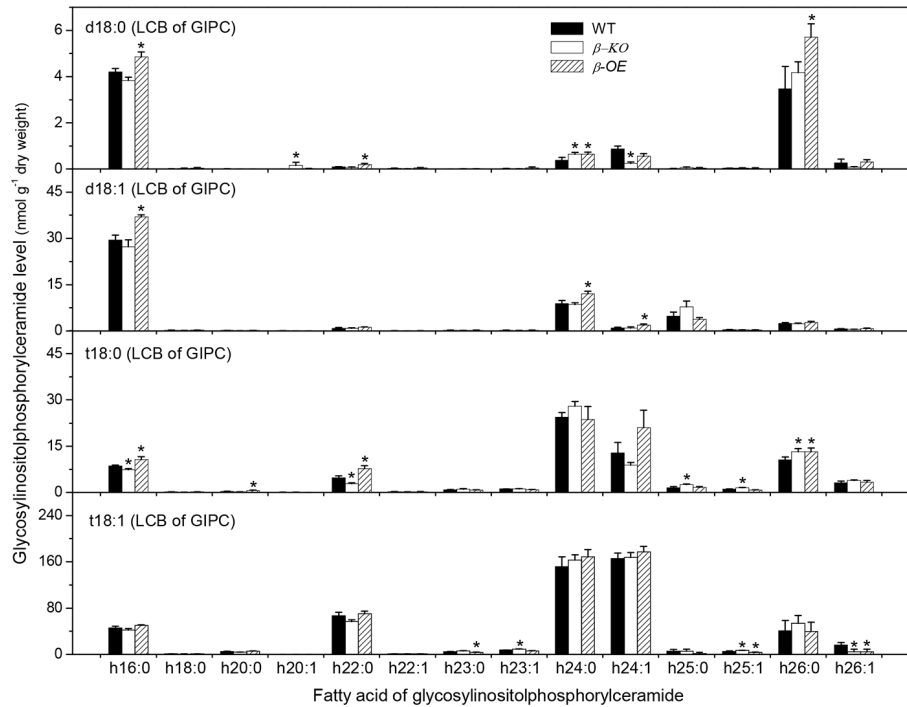


FIGURE 6 | Levels of GIPC species in *pPLAIII β* -knockout and overexpression plant leaves. β -KO, T-DNA knockout of *pPLAIII β* (Salk_057212). β -OE, overexpression mutant of *pPLAIII β* driven by cauliflower mosaic 35S promoter. Values are means \pm SE ($n = 5$). *Significant difference at $P < 0.05$ compared with the WT, based on Student's *t*-test.

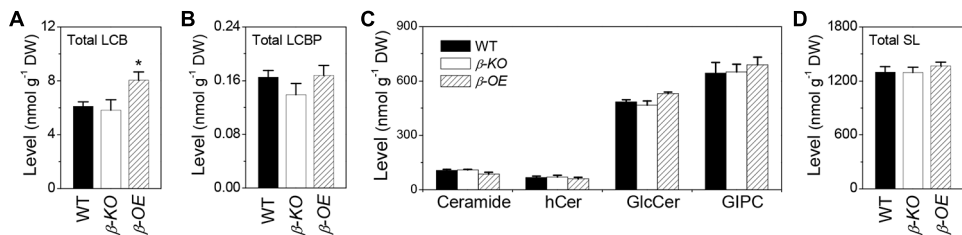


FIGURE 7 | Levels of total LCBs, total LCBPs, and total complex sphingolipids in *pPLAIII β* -knockout and overexpression plant leaves. (A) The level of total LCBs, summarized from individual species in Figure 2B. (B) The level of total LCBPs, summarized from individual species in Figure 2C. (C) The levels of total complex sphingolipids, including Cer, hCer, GlcCer, and GIPC, summarized from individual species in Figures 3–6. (D) The

total content of sphingolipids (SL), including free sphingolipids, such as LCBs and LCBPs, and complex sphingolipids, such as Cer, hCer, GlcCer, and GIPC. β -KO, T-DNA knockout of *pPLAIII β* (Salk_057212). β -OE, overexpression mutant of *pPLAIII β* driven by cauliflower mosaic 35S promoter. Values are means \pm SE ($n = 5$). *Significant difference at $P < 0.05$ compared with the WT, based on Student's *t*-test.

a loss of anisotropic cell expansion, and a thinner cell wall (Li et al., 2011). Plasma membrane dynamics contribute significantly to the buildup of the cell wall (Li et al., 2013b). It could be possible that the altered sphingolipid homeostasis in *pPLAIII β* mutants impairs cell membrane activities which consequently results in a reduced cellulose production and plant growth.

Multiple lines of evidence suggest that *pPLAIII β* plays a role in auxin transport. In the early seedling stage, some auxin-related phenotypes were shown for *pPLAIII β* mutants, such as slightly longer roots and hypocotyls in *pPLAIII β -KO* mutants and much shorter roots and hypocotyls, as well

as smaller leaves in *pPLAIII β -OE* (Li et al., 2011). Reduced lobe formation in the interdigitating pattern of leaf epidermis cells in *pPLAIII β -OE* resembles those observed in auxin receptor mutant *abp1* (auxin-binding protein1; Xu et al., 2011). In addition, the induction of early auxin response genes was delayed in *pPLAIII β -KO* mutants (Labusch et al., 2013).

The altered sphingolipid composition in *pPLAIII β* mutants may disturb the auxin transport. Alteration of *pPLAIII β* expression changed the levels of sphingolipid metabolites, particularly species with saturated long chain base and saturated fatty acyl chain, such as Cer d18:0–16:0 and hCer d18:0–h16:0,

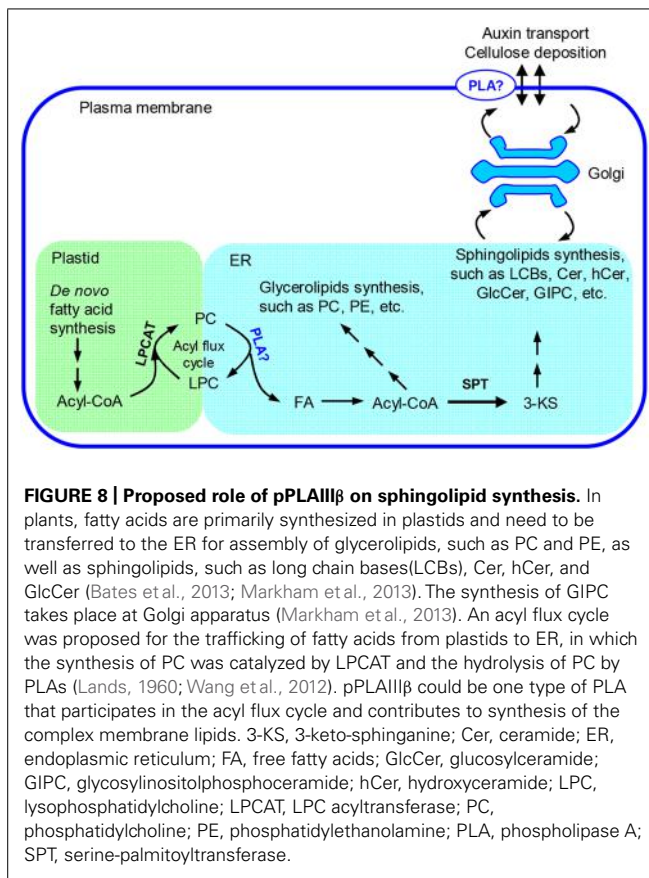


FIGURE 8 | Proposed role of pPLAIII β on sphingolipid synthesis. In plants, fatty acids are primarily synthesized in plastids and need to be transferred to the ER for assembly of glycerolipids, such as PC and PE, as well as sphingolipids, such as long chain bases(LCBs), Cer, hCer, and GlcCer (Bates et al., 2013; Markham et al., 2013). The synthesis of GIPC takes place at Golgi apparatus (Markham et al., 2013). An acyl flux cycle was proposed for the trafficking of fatty acids from plastids to ER, in which the synthesis of PC was catalyzed by LPCAT and the hydrolysis of PC by PLAs (Lands, 1960; Wang et al., 2012). pPLAIII β could be one type of PLA that participates in the acyl flux cycle and contributes to synthesis of the complex membrane lipids. 3-KS, 3-keto-sphinganine; Cer, ceramide; ER, endoplasmic reticulum; FA, free fatty acids; GlcCer, glucosylceramide; GIPC, glycosylinositolphosphoceramide; hCer, hydroxyceramide; LPC, lysophosphatidylcholine; LPCAT, LPC acyltransferase; PC, phosphatidylcholine; PE, phosphatidylethanolamine; PLA, phospholipase A; SPT, serine-palmitoyltransferase.

and GIPC d18:0–h16:0, and t18:0–h16:0 (Figures 3–6). Disruption of CS genes diminished the production of sphingolipids with very long chain fatty acids (>18C), impaired the auxin transport, and led to auxin defective phenotypes (Markham et al., 2011). Important functions of sphingolipids on the trafficking of auxin carriers PIN1 (PIN-Formed 1) and AUX1 (Auxin Resistant 1) were evidenced by detailed analyses of an auxin transporter, ATP-binding cassette B19 (ABCB19) auxin transporter (Yang et al., 2013). Sphingolipids are essential components of membrane microdomains or lipid rafts where they attract a unique subset of proteins and together are transported to the plasma membrane (Klemm et al., 2009). The presence of very long chain fatty acids and saturated long carbon chains in sphingolipids can increase their hydrophobicity and the transition from a fluid to a gel phase, which are required for microdomain or lipid raft formation. The altered levels of sphingolipids with saturated acyl chains in *pPLAIII β* mutants may impact the membrane physical properties, the membrane functions on auxin transport, the induction of auxin response gene expression, and subsequently the auxin-related growth.

In summary, our data show that overexpression of *pPLAIII β* alters sphingolipid homeostasis. Our study implies that *pPLAIII β* may influence the substrate availability of the first step of sphingolipid synthesis, which may alter the sphingolipid homeostasis, change the membrane integrity, and eventually impede plant growth.

MATERIALS AND METHODS

PLANT GROWTH CONDITION AND GENERATION OF OVEREXPRESSION MUTANTS

Plants were grown in growth chambers with a 12 h light/12 h-dark cycle, at 23/21°C, in 50% humidity, under 200 $\mu\text{mol m}^{-2} \text{ sec}^{-1}$ of light intensity, and watered with fertilizer once a week. The WT and the mutant *Arabidopsis* are in Columbia-0 background (Col-0). To overexpress *pPLAIII β* , the genomic sequence of *pPLAIII β* was obtained by PCR using Col-0 *Arabidopsis* genomic DNA as a template. The genomic DNA was cloned into the pMDC83 vector before the GFP-His coding sequence. The expression was under the control of the 35S cauliflower mosaic virus promoter. The detailed procedure to generate overexpression lines of *pPLAIII β* was described previously (Li et al., 2011).

SPHINGOLIPID PROFILING

Leaves from 4 week old plants were harvested and immediately immersed into liquid nitrogen. The frozen samples were lyophilized and stored at -80°C before sphingolipid extraction. Approximately 30 mg of freeze-dried *Arabidopsis* leaves was processed for the sphingolipid profiling using mass spectrometry. The detailed protocols of sphingolipid extraction, detection, and quantification were described previously (Markham and Jaworski, 2007; Markham, 2013).

ACKNOWLEDGMENTS

The authors were grateful to Brian Fanella for critical reading and Kevin Reilly at the Donald Danforth Plant Science Center's Plant Growth Facility for assistance on *Arabidopsis* growth. Work by Xuemin Wang was supported by the U.S. Department of Energy (DOE), Office of Science, Office of Basic Energy Sciences (BES), Materials Sciences and Engineering Division under Award # DE-SC0001295. Work by Maoyin Li and Xuemin Wang was supported by the National Science Foundation (MCB-0922879).

REFERENCES

- Alden, K. P., Dhondt-Cordelier, S., McDonald, K. L., Reape, T. J., Ng, C. K., McCabe, P. F., et al. (2011). Sphingolipid long chain base phosphates can regulate apoptotic-like programmed cell death in plants. *Biochem. Biophys. Res. Commun.* 410, 574–580. doi: 10.1016/j.bbrc.2011.06.028
- Bates, P. D., Stymne, S., and Ohlrogge, J. (2013). Biochemical pathways in seed oil synthesis. *Curr. Opin. Plant Biol.* 16, 358–364. doi: 10.1016/j.pbi.2013.02.015
- Borner, G. H., Sherrier, D. J., Weimar, T., Michaelson, L. V., Hawkins, N. D., Macaskill, A., et al. (2005). Analysis of detergent-resistant membranes in *Arabidopsis*. Evidence for plasma membrane lipid rafts. *Plant Physiol.* 137, 104–116. doi: 10.1104/pp.104.053041
- Chao, D. Y., Gable, K., Chen, M., Baxter, I., Dietrich, C. R., Cahoon, E. B., et al. (2011). Sphingolipids in the root play an important role in regulating the leaf ionome in *Arabidopsis thaliana*. *Plant Cell* 23, 1061–1081. doi: 10.1105/tpc.110.079095
- Chen, M., Han, G., Dietrich, C. R., Dunn, T. M., and Cahoon, E. B. (2006). The essential nature of sphingolipids in plants as revealed by the functional identification and characterization of the *Arabidopsis* LCB1 subunit of serine palmitoyltransferase. *Plant Cell* 18, 3576–3593. doi: 10.1105/tpc.105.040774
- Chen, M., Markham, J. E., and Cahoon, E. B. (2012). Sphingolipid $\Delta 8$ unsaturation is important for glucosylceramide biosynthesis and low-temperature performance in *Arabidopsis*. *Plant J.* 69, 769–781. doi: 10.1111/j.1365-313X.2011.04829.x

- Dietrich, C. R., Han, G., Chen, M., Berg, R. H., Dunn, T. M., and Cahoon, E. B. (2008). Loss-of-function mutations and inducible RNAi suppression of *Arabidopsis* LCB2 genes reveal the critical role of sphingolipids in gametophytic and sporophytic cell viability. *Plant J.* 54, 284–298. doi: 10.1111/j.1365-313X.2008.03420.x
- Hanada, K. (2003). Serine palmitoyltransferase, a key enzyme of sphingolipid metabolism. *Biochim. Biophys. Acta* 1632, 16–30. doi: 10.1016/S1388-1981(03)00059-3
- Huang, S., Cerny, R. E., Bhat, D. S., and Brown, S. M. (2001). Cloning of an *Arabidopsis* patatin-like gene, STURDY, by activation T-DNA tagging. *Plant Physiol.* 125, 573–584. doi: 10.1104/pp.125.2.573
- Kimberlin, A. N., Majumder, S., Han, G., Chen, M., Cahoon, R. E., Stone, J. M., et al. (2013). *Arabidopsis* 56-amino acid serine palmitoyltransferase-interacting proteins stimulate sphingolipid synthesis, are essential, and affect mycotoxin sensitivity. *Plant Cell* 25, 4627–4239. doi: 10.1105/tpc.113.116145
- Klemm, R. W., Ejsing, C. S., Surma, M. A., Kaiser, H. J., Gerl, M. J., Sampaio, J. L., et al. (2009). Segregation of sphingolipids and sterols during formation of secretory vesicles at the trans-Golgi network. *J. Cell Biol.* 185, 601–612. doi: 10.1083/jcb.200901145
- La Camera, S., Geoffroy, P., Samaha, H., Ndiaye, A., Rahim, G., Legrand, M., et al. (2005). A pathogen-inducible patatin-like lipid acyl hydrolase facilitates fungal and bacterial host colonization in *Arabidopsis*. *Plant J.* 44, 810–825. doi: 10.1111/j.1365-313X.2005.02578.x
- Labusch, C., Shishova, M., Effendi, Y., Li, M., Wang, X., and Scherer, G. F. (2013). Patterns and timing in expression of early auxin-induced genes imply involvement of phospholipases A (pPLAs) in the regulation of auxin responses. *Mol. Plant* 6, 1473–1486. doi: 10.1093/mp/sst053
- Lands, W. E. M. (1960). Metabolism of glycerolipids. 2. The enzymatic acylation of lysolecithin. *J. Biol. Chem.* 235, 2233–2237.
- Li, M., Bahn, S. C., Fan, C., Li, J., Phan, T., Ortiz, M., et al. (2013a). Patatin-related phospholipase pPLAII β increases seed oil content with long-chain fatty acids in *Arabidopsis*. *Plant Physiol.* 162, 39–51. doi: 10.1104/pp.113.216994
- Li, X., Luu, D. T., Maurel, C., and Lin, J. (2013b). Probing plasma membrane dynamics at the single-molecule level. *Trends Plant Sci.* 18, 617–624. doi: 10.1016/j.tplants.2013.07.004
- Li, M., Bahn, S. C., Guo, L., Musgrave, W., Berg, H., Welti, R., et al. (2011). Patatin-related phospholipase pPLAII β -induced changes in lipid metabolism alter cellulose content and cell elongation in *Arabidopsis*. *Plant Cell* 23, 1107–1123. doi: 10.1105/tpc.110.081240
- Li, M., and Wang, X. (2014). “pPLA: patatin-related phospholipase as with multiple biological functions,” in *Phospholipases in Plant Signaling*, ed. X. Wang (Berlin: Springer-Verlag), 93–108.
- Lin, C. C., Chu, C. F., Liu, P. H., Lin, H. H., Liang, S. C., Hsu, W. E., et al. (2011). Expression of an *Oncidium* gene encoding a patatin-like protein delays flowering in *Arabidopsis* by reducing gibberellin synthesis. *Plant Cell Physiol.* 52, 421–435. doi: 10.1093/pcp/pcq206
- Markham, J. E. (2013). Detection and quantification of plant sphingolipids by LC-MS. *Methods Mol. Biol.* 1009, 93–101. doi: 10.1007/978-1-62703-401-2_10
- Markham, J. E., and Jaworski, J. G. (2007). Rapid measurement of sphingolipids from *Arabidopsis thaliana* by reversed-phase high-performance liquid chromatography coupled to electrospray ionization tandem mass spectrometry. *Rapid Commun. Mass Spectrom.* 21, 1304–1314. doi: 10.1002/rct.2962
- Markham, J. E., Lynch, D. V., Napier, J. A., Dunn, T. M., and Cahoon, E. B. (2013). Plant sphingolipids: function follows form. *Curr. Opin. Plant Biol.* 16, 350–357. doi: 10.1016/j.pbi.2013.02.009
- Markham, J. E., Molino, D., Gissot, L., Belloc, Y., Hématy, K., Marion, J., et al. (2011). Sphingolipids containing very-long-chain fatty acids define a secretory pathway for specific polar plasma membrane protein targeting in *Arabidopsis*. *Plant Cell* 23, 2362–2378. doi: 10.1105/tpc.110.080473
- Melser, S., Molino, D., Batailler, B., Peypelut, M., Laloi, M., WatteletBoyer, V., et al. (2011). Links between lipid homeostasis, organelle morphodynamics and protein trafficking in eukaryotic and plant secretory pathways. *Plant Cell Rep.* 30, 177–193. doi: 10.1007/s00299-010-0954-1
- Mongrand, S., Morel, J., Laroche, J., Claverol, S., Carde, J. P., Hartmann, M. A., et al. (2004). Lipid rafts in higher plant cells: purification and characterization of Triton X-100-insoluble microdomains from tobacco plasma membrane. *J. Biol. Chem.* 279, 36277–36286. doi: 10.1074/jbc.M403440200
- Qiao, Y., Piao, R., Shi, J., Lee, S. I., Jiang, W., Kim, B. K., et al. (2011). Fine mapping and candidate gene analysis of dense and erect panicle 3, DEP3, which confers high grain yield in rice (*Oryza sativa* L.). *Theor. Appl. Genet.* 122, 1439–1449. doi: 10.1007/s00122-011-1543-6
- Rietz, S., Dermendjiev, G., Oppermann, E., Tafesse, F. G., Effendi, Y., Holk, A., et al. (2010). Roles of *Arabidopsis* patatin-related phospholipases A in root development are related to auxin responses and phosphate deficiency. *Mol. Plant* 3, 524–538. doi: 10.1093/mp/ssp109
- Rietz, S., Holk, A., and Scherer, G. F. (2004). Expression of the patatin-related phospholipase A gene AtPLA IIa in *Arabidopsis thaliana* is up-regulated by salicylic acid, wounding, ethylene, and iron and phosphate deficiency. *Planta* 219, 743–753. doi: 10.1007/s00425-004-1275-9
- Scherer, G. F., Ryu, S. B., Wang, X., Matos, A. R., and Heitz, T. (2010). Patatin-related phospholipase A: nomenclature, subfamilies and functions in plants. *Trends Plant Sci.* 15, 693–700. doi: 10.1016/j.tplants.2010.09.005
- Sperling, P., Warnecke, D., and Heinz, E. (2004). “Plant sphingolipids,” in *Topics in Current Genetics*, Vol. 6, *Lipid Metabolism and Membrane Biogenesis*, ed. G. Daum (Berlin: Springer-Verlag).
- Teng, C., Dong, H., Shi, L., Deng, Y., Mu, J., Zhang, J., et al. (2008). Serine palmitoyltransferase, a key enzyme for de novo synthesis of sphingolipids, is essential for male gametophyte development in *Arabidopsis*. *Plant Physiol.* 146, 1322–1332. doi: 10.1104/pp.107.113506
- Wang, L., Shen, W., Kazachkov, M., Chen, G., Chen, Q., Carlsson, A. S., et al. (2012). Metabolic interactions between the lands cycle and the Kennedy pathway of glycerolipid synthesis in *Arabidopsis* developing seeds. *Plant Cell* 24, 4652–4669. doi: 10.1105/tpc.112.104604
- Xu, T., Nagawa, S., and Yang, Z. (2011). Uniform auxin triggers the Rho GTPase-dependent formation of interdigititation patterns in pavement cells. *Small GTPases* 2, 227–232. doi: 10.4161/sgrp.2.4.16702
- Yang, H., Richter, G. L., Wang, X., Mlodzinska, E., Carraro, N., Ma, G., et al. (2013). Sterols and sphingolipids differentially function in trafficking of the *Arabidopsis* ABCB19 auxin transporter. *Plant J.* 74, 37–47. doi: 10.1111/tpj.12103
- Yang, W., Devaiah, S. P., Pan, X., Isaac, G., Welti, R., and Wang, X. (2007). AtPLAI is an acyl hydrolase involved in basal jasmonic acid production and *Arabidopsis* resistance to *Botrytis cinerea*. *J. Biol. Chem.* 282, 18116–18128. doi: 10.1074/jbc.M700405200
- Yang, W., Zheng, Y., Bahn, S. C., Pan, X., Li, M., Vu, H., et al. (2012). The patatin-containing phospholipase A pPLAII α modulates oxylipin formation and water loss in *Arabidopsis thaliana*. *Mol. Plant* 5, 452–460. doi: 10.1093/mp/ssr118

Conflict of Interest Statement: The Review Editor Dr. Daniel Hofius declares that, despite having collaborated with author Jonathan E. Markham, the review process was handled objectively. The Review Editor Dr. Günther F. E. Scherer declares that, despite having collaborated with authors Maoyin Li and Xuemin Wang, the review process was handled objectively. The authors declare that the research was conducted in the absence of any commercial or financial relationships that could be construed as a potential conflict of interest.

Received: 13 June 2014; accepted: 27 September 2014; published online: 21 October 2014.

Citation: Li M, Markham JE and Wang X (2014) Overexpression of patatin-related phospholipase AII β altered the content and composition of sphingolipids in *Arabidopsis*. *Front. Plant Sci.* 5:553. doi: 10.3389/fpls.2014.00553

This article was submitted to Plant Physiology, a section of the journal *Frontiers in Plant Science*.

Copyright © 2014 Li, Markham and Wang. This is an open-access article distributed under the terms of the Creative Commons Attribution License (CC BY). The use, distribution or reproduction in other forums is permitted, provided the original author(s) or licensor are credited and that the original publication in this journal is cited, in accordance with accepted academic practice. No use, distribution or reproduction is permitted which does not comply with these terms.



Zn²⁺-dependent surface behavior of diacylglycerol pyrophosphate and its mixtures with phosphatidic acid at different pHs

Ana L. Villasuso^{1*†}, Natalia Wilke^{2†}, Bruno Maggio² and Estela Machado¹

¹ Departamento de Biología Molecular, FCEFQN, Universidad Nacional de Río Cuarto, Río Cuarto, Argentina

² Facultad de Ciencias Químicas, Departamento de Química Biológica-Centro de Investigaciones en Química Biológica de Córdoba, Universidad Nacional de Córdoba, Ciudad Universitaria, Córdoba, Argentina

Edited by:

Eric Ruelland, Centre National de la Recherche Scientifique, France

Reviewed by:

Alain Zachowski, Université Pierre et Marie Curie, France

Rhoderick E. Brown, University of Minnesota, USA

***Correspondence:**

Ana L. Villasuso, Departamento de Biología Molecular, FCEFQN, Universidad Nacional de Río Cuarto, Ruta Nacional 36, Km 601, X5804BYA Río Cuarto, Córdoba, Argentina
e-mail: lvillasuso@exa.unrc.edu.ar

[†]Ana L. Villasuso and Natalia Wilke have contributed equally to this work.

Diacylglycerol pyrophosphate (DGPP) is a minor lipid that attenuates the phosphatidic acid (PA) signal, and also DGPP itself would be a signaling lipid. Diacylglycerol pyrophosphate is an anionic phospholipid with a pyrophosphate group attached to diacylglycerol that was shown to respond to changes of pH, thus affecting the surface organization of DGPP and their interaction with PA. In this work, we have investigated how the presence of Zn²⁺ modulates the surface organization of DGPP and its interaction with PA at acidic and basic pHs. Both lipids formed expanded monolayers at pHs 5 and 8. At pH 5, monolayers formed by DGPP became stiffer when Zn²⁺ was added to the subphase, while the surface potential decreased. At this pH, Zn²⁺ induced a phase transition from an expanded to a condensed-phase state in monolayers formed by PA. Conversely, at pH 8 the effects induced by the presence of Zn²⁺ on the surface behaviors of the pure lipids were smaller. Thus, the interaction of the bivalent cation with both lipids was modulated by pH and by the ionization state of the polar head groups. Mixed monolayers of PA and DGPP showed a non-ideal behavior and were not affected by the presence of Zn²⁺ at pH 8. This could be explained considering that when mixed, the lipids formed a closely packed monolayer that could not be further modified by the cation. Our results indicate that DGPP and PA exhibit expanded- and condensed-phase states depending on pH, on the proportion of each lipid in the film and on the presence of Zn²⁺. This may have implications for a possible role of DGPP as a signaling lipid molecule.

Keywords: diacylglycerol pyrophosphate, phosphatidic acid, plant lipid signaling, membrane packing, glycerophospholipid monolayers, Zn²⁺

INTRODUCTION

Phospholipids are mostly conceived as playing a structural role in lipid bilayers but important aspects on the implications of several phospholipids in lipid-mediated signal transduction have emerged over the past decade (Wang et al., 2006).

Diacylglycerol pyrophosphate (DGPP) is a minor phospholipid found in biological membranes, with a relatively simple chemical structure within the glycerophospholipid family (Wissing and Behrbohm, 1993a). Diacylglycerol pyrophosphate is synthesized from phosphatidic acid (PA) and ATP via the reaction catalyzed by phosphatidate kinase (PAK) and dephosphorylated to PA by the enzyme DGPP phosphatase (Wissing and Behrbohm, 1993b). The average concentration of DGPP in cell membranes is usually very low but evidence suggests that DGPP may act as a novel second messenger with important roles in diverse cellular processes in plants that are related to drought and osmotic stress or salinity (van Schooten et al., 2006). Diacylglycerol pyrophosphate formation is transient and it is always associated with variations of the amount of PA, therefore its synthesis may also be involved in attenuating PA levels (Munnik et al., 1996; van Schooten et al., 2006; Racagni et al., 2008; Paradis et al., 2011). The concentration

of PA is maintained at low levels in the cell as a result of its continuous conversion into other lipid species (Arisz et al., 2009; Villasuso et al., 2013).

Phosphatidic acid, the lipid precursor of DGPP, is the glycerophospholipid with the simplest chemical structure in biological membranes; its behavior is crucial for cell survival since it is a phospholipid involved in the synthesis of phospholipids and triacylglycerols thus playing a focal role in cell signaling (Athenstaedt and Daum, 1999). Phosphatidic acid signaling acts by binding effector proteins and recruiting them to a membrane, which regulates the proteins' activity in cellular pathways (Testerink and Munnik, 2011). Binding is mainly dependent on the concentration of the lipid in the bilayer and it depends on non-specific electrostatic interactions between clusters of positively charged amino acids in the protein and the negatively charged phosphomonoester head group of PA (Shin and Loewen, 2011).

Diacylglycerol pyrophosphate is an anionic phospholipid with a pyrophosphate group attached to diacylglycerol. It was shown that, depending on the pH, the pyrophosphate moiety of DGPP could display 2 or 3 negative charges making it a highly polar molecule (Villasuso et al., 2010; Strawn et al., 2012). Consequently,

the ionization of the pyrophosphate group may be important for allowing electrostatic interactions between DGPP and proteins as well as with bivalent cations such as Zn^{2+} and Ca^{2+} (Han et al., 2001; Zalejski et al., 2006; Strawn et al., 2012). This can participate in regulating Zn^{2+} -mediated enzyme activities (Han et al., 2001; Kim et al., 2013). Therefore, it is possible that PA and DGPP could be involved in Zn^{2+} binding thus affecting the lipid signal although the interaction between zinc and DGPP has not been directly demonstrated.

Zinc (Zn) is an essential element in all organisms that plays a fundamental role in numerous cellular functions (Broadley et al., 2007; Cherif et al., 2011). Zn is involved in the catalytic function of many enzymes and structural stability of various cell proteins (Vallee and Falchuk, 1993). Moreover, it has an important role in stabilization and protection of the biological membranes against oxidative stress and the loss of plasma membrane integrity (Aravind and Prasad, 2003). Therefore, Zn deficiency can cause an increase in membrane permeability and a decrease in detoxification mechanisms (Cakmak, 2000). Respect to, it has been shown that the plant roots treated with Cd, an heavy metal that frequently accompanies Zn in the environment, generated oxidative stress, while in combined treatments it was less prominent, indicating that Zn could alleviate oxidative damage (Tkalec et al., 2014). On the other hand, high levels of Zn inhibit many metabolic processes in plants, which can result in limited growth and root development and induce plant senescence (Uruc Parlak and Demirezen Yilmaz, 2012). The extent of Zn phytotoxicity varies in a wide range but mostly depends on plant species, age, environmental conditions, and combinations with other heavy metals (Tsonev and Lidon, 2012). Consequently, the study of the interaction of simple systems with Zn^{2+} may be relevant and a starting point for future studies with other bivalent ions in relation to abiotic stress and the DGPP and PA signaling.

Although, several aspects of DGPP are unknown, it has been shown that the effective lipid molecular shape and the ionization properties of the phosphomonoester head group of DGPP are similar to PA (Kooijman et al., 2007; Kooijman and Burger, 2009). Thus, the ionization properties of the phosphomonoester of DGPP mimic those of PA following the electrostatic-hydrogen bond switch model (Strawn et al., 2012). However, DGPP is not a cone-shaped lipid, i.e., it is not capable of imparting negative curvature stress to the membrane that could facilitate the insertion of hydrophobic protein domains in the membrane (Strawn et al., 2012).

Little is known on the interaction of PA with DGPP and how these are affected by pH and divalent cations, whether these lipids can molecularly mix, or undergo interactions that may modify their individual properties. Within the context briefly reviewed above, it becomes important to understand details of the effects of Zn^{2+} and pH on the surface packing and electrostatic behavior of DGPP, and on its interaction with PA. In a previous study with Langmuir monolayers, we demonstrated that the packing and electrostatic properties of films of pure DGPP and PA were affected by the subphase pH as a consequence of changes in the ionization state of the molecules and that the lipids molecularly mix to form closely packed monolayers at basic pHs (Villasuso et al., 2010). In the present work, we provide further evidences

on the molecular packing, in-plane elasticity, and surface electrostatic of films of pure DGPP and 1-palmitoyl-2-oleoyl-*sn*-glycerol 3 phosphate (POPA) and their mixtures on subphases with $ZnCl_2$ at different pHs. In addition, we show how the cation affects the monolayer organization by using fluorescence and Brewster angle microscopy (BAM).

MATERIALS AND METHODS

Langmuir monolayers of the individual lipids and their binary mixtures were spread from premixed solutions in chloroform/methanol (2:1, v/v) onto different subphases at a molecular area larger than the lift off area. Before isometric compression of the film, the solvent was allowed to evaporate for 5 min. All experiments were performed at $24 \pm 1^\circ\text{C}$. Temperature was maintained within $\pm 1^\circ\text{C}$ with a refrigerated Haake F3C thermocirculator and air-conditioning the room temperature. DGPP, POPA, and the lipophilic, fluorescent probe 1- α -phosphatidylethanolamine-*N*-(lissaminerhodamine B sulfonyl)-ammonium salt were purchased from Avanti polar lipids Inc. (Alabaster, AL, USA). The lipids were dissolved in chloroform/methanol (2:1, v/v) to a final concentration of $1 \text{ nmol } \mu\text{L}^{-1}$. In all the experiments, the subphase was 150 mM NaCl , 5 mM EDTA , pH 8 or 5, with or without 8 mM ZnCl_2 . The pH was stable during the time of the experiment. The subphase was prepared with ultra-pure water obtained from a Millipore purification system ($18.2 \text{ M}\Omega$). Solvents were of the highest available purity from Merck (Darmstadt Germany).

Surface pressure and surface potential versus molecular area isotherms were obtained at $24 \pm 1^\circ\text{C}$ in a Teflon trough of a Langmuir film balance (Monofilmeter, Mayer Feintechnik, Germany).

Surface pressure was measured with a platinized-PtWilhelmy plate. The surface potential measurements were carried out with a high-impedance millivoltmeter connected to a surface ionizing ^{241}Am electrode positioned 5 mm above the monolayer surface and to a reference $\text{Ag}/\text{AgCl}/\text{Cl}^-$ (3 M) electrode connected to the aqueous subphase.

Absence of surface-active impurities in the subphase and in the spreading solvents was routinely controlled as described elsewhere (Maggio, 2004). At least triplicate monolayer isotherms were obtained and averaged at a compression rate of $0.45\text{--}0.60 \text{ nm}^2 \text{ molecule}^{-1} \text{ min}^{-1}$; for each mixture, it was ascertained that reducing the compression speed produced no change in the isotherms and that recompression after 5 min equilibration of the expanded isotherm at surface pressures below 2 mN m^{-1} led to no significant changes of the limiting mean molecular areas which rules out film loss or kinetically limited artifacts.

Reproducibility was within a maximum SEM of $\pm 1 \text{ mN m}^{-1}$ for surface pressure, $\pm 30 \text{ mV}$ for surface potential, and $\pm 0.04 \text{ nm}^2$ for molecular areas. The monolayers of the pure components and of all mixed films were stable and reproducible by recompression.

The monolayer compressibility modulus (κ), also known as in-plane elasticity, was calculated for the pure monolayers and for each mixture in the different conditions as $\kappa = -A_m(\partial\pi/\partial A_m)_T$. The effect of $ZnCl_2$ in the subphase as well as the interactions and molecular miscibility were ascertained from the behavior of the mean molecular area, of the compressibility modulus, and of

the average dipole potential per unit of molecular surface density ($\Delta V \cdot A$, being ΔV the surface (dipole) potential and A the mean molecular area at a defined surface pressure); this magnitude is directly proportional to the overall resultant dipole moment in the direction perpendicular to the interface (Gaines, 1966).

The surfaces of the films were observed by fluorescence microscopy (FM), while simultaneously registering the surface pressure vs. molecular area isotherms. The setup consisted of an automated Langmuir balance (KIBRON microtrough) with a Wilhelmy plate for surface pressure determination, mounted on the stage of a Zeiss Axiovert 200 (Carl Zeiss, Oberkochen, Germany) fluorescence microscope with a CCD video camera Zeiss commanded through the Axiovision software of the Zeiss microscope. Long-distance 20 \times and 40 \times objectives were employed. Monolayers with different mole fractions of lipids were spread from chloroform/methanol (2:1, v/v) solutions onto different subphases at a molecular area larger than the lift off area. The fluorescent probe was incorporated in the lipid solution before spreading (1 mol %). Before isometric compression of the film, the solvent was allowed to evaporate for 5 min. All experiments were performed at 24 \pm 1°C. This method allows analyzing the presence of micron-sized domains of lipids in different phase state and thus, studying bidimensional phase transitions and phase diagrams of mixtures in different conditions (Rosetti et al., 2010; Vega Mercado et al., 2011; Mangiarotti et al., 2014).

For the BAM experiments, an EP3 Imaging ellipsometer (Accurion, Goettingen, Germany) with a 20 \times objective was used. These observations were performed in order to ensure that the textures on the micron scale observed in FM experiments were not a consequence of the presence of the fluorescent probe; the latter was reported for some systems (Rosetti et al., 2010), while in others the same texture was observed with both techniques (Mangiarotti et al., 2014). All the experiments were performed at 24 \pm 1°C.

RESULTS

In a previous article, the surface behavior of monolayers prepared with DGPP and POPA was described at different pHs. The mixture of both lipids was also analyzed on subphases at basic pHs. As mentioned above, the polar head group of DGPP is a pyrophosphate moiety, and the net charge on the molecule change with the subphase pH (Villasuso et al., 2010). Thus, the polar head group of DGPP may bear from 1 to 3 negative charges, depending on pH (Strawn et al., 2012). Taking the pyrophosphoric acid pKa's in consideration, we performed compression isotherms on subphases with or without ZnCl₂ at pH 5 (pyrophosphate moiety with 1 or 2 negative charges), and at pH 8 (pyrophosphate moiety with 2 or 3 negative charges) with the aim of analyzing the effect of Zn²⁺ on the molecular packing behavior of DGPP and POPA monolayers in different ionization states.

Figure 1 shows the compression isotherms of DGPP (A) and POPA (C) on subphases at pH 5 with and without 8 mM ZnCl₂. The compression isotherms in the absence of ZnCl₂ have been previously reported (Villasuso et al., 2010). Briefly, both lipids formed expanded monolayers with compressibility moduli increasing

continuously up to about 100 mN m⁻¹ at collapse (**Figures 1B,D**, black lines), which occurred at about 40 mN m⁻¹ for both lipids on acid subphases.

The presence of Zn²⁺ in the subphase caused a shift of the whole isotherm of DGPP to smaller average molecular area (**Figure 1A**, solid gray line) with a concomitant increase of the compressibility modulus at high molecular densities (**Figure 1B**, gray line), without an appreciable change of the collapse pressure (collapse point: 42 mN m⁻¹ at 0.58 nm²). The lift off area with zinc in the subphase was 1.05 nm². The compressibility modulus ranged from 25–30 mN m⁻¹ to 130 mN m⁻¹, indicating that in the presence of Zn²⁺, DGPP also formed monolayers with a liquid-expanded behavior (Davies and Rideal, 1963) but with a more condensed character under compression compared to the behavior on subphases without Zn²⁺.

In order to explore the electrostatics of these monolayers, the surface potential was determined in the absence and in the presence of Zn²⁺. The cation induced a three to fivefold diminution in $\Delta V \cdot A$ depending on the film packing (**Figure 1A**, dotted lines).

For POPA, the presence of zinc in the subphase induced a phase transition from a liquid-expanded to a liquid-condensed state at about 11.5 mN m⁻¹ (**Figure 1C**, solid gray line). The phase transition was clearly observed as a minimum in the compressibility modulus (**Figure 1D**, gray line). The condensed state showed compressibility moduli up to 150 mN m⁻¹ at collapse (**Figure 1D**, gray line), corresponding to a liquid-condensed character (Davies and Rideal, 1963). The phase transition induced by Zn²⁺ probably reflects a decrease of lateral repulsion in the charged polar head groups caused by the divalent cation as previously observed for POPA monolayers in the presence of Mg²⁺ (Brockman et al., 2003).

The Zn²⁺ induced phase transition corresponded to a first-order, phase transition since micron-sized domains formed by lipids in the condensed state were observed in the two-phase coexistence region using BAM and FM. In **Figure 1D**, representative images for POPA on solutions with Zn²⁺ at the indicated surface pressure obtained with FM are shown; similar images were obtained using BAM while in the absence of Zn²⁺ domains were not observed at any surface pressure (data not shown).

The effect of ZnCl₂ on $\Delta V \cdot A$ at pH 5 was similar to that observed for DGPP, i.e., Zn²⁺ inducing a 2–4 times decrease depending on the molecular packing density. The phase transition was detected as a change of slope of the $\Delta V \cdot A$ vs. A isotherm at about 0.65 nm² (see arrow in **Figure 1C** inset). In **Figure 2**, the effect of Zn²⁺ ions is shown at basic pH. At pH 8, the films of DGPP were loosely packed (Villasuso et al., 2010) and the effect of Zn²⁺ was less marked than at acid pH (**Figure 2A**). However, a small condensation of the film could still be observed when the cation was added to the subphase and the compressibility modulus increased from 60 to 80 mN m⁻¹ at collapse (**Figure 2B**). A similar effect was induced by Zn²⁺ in POPA monolayers (see **Figures 2C,D**). Regarding the interfacial electrostatics, the presence of Zn²⁺ at this pH induced an increase of $\Delta V \cdot A$, contrary to the effect observed on subphases at acid pH. The increase of $\Delta V \cdot A$ was of about 20%.

It was shown that the effective molecular shape of PA is highly influenced by pH, temperature, and the presence of

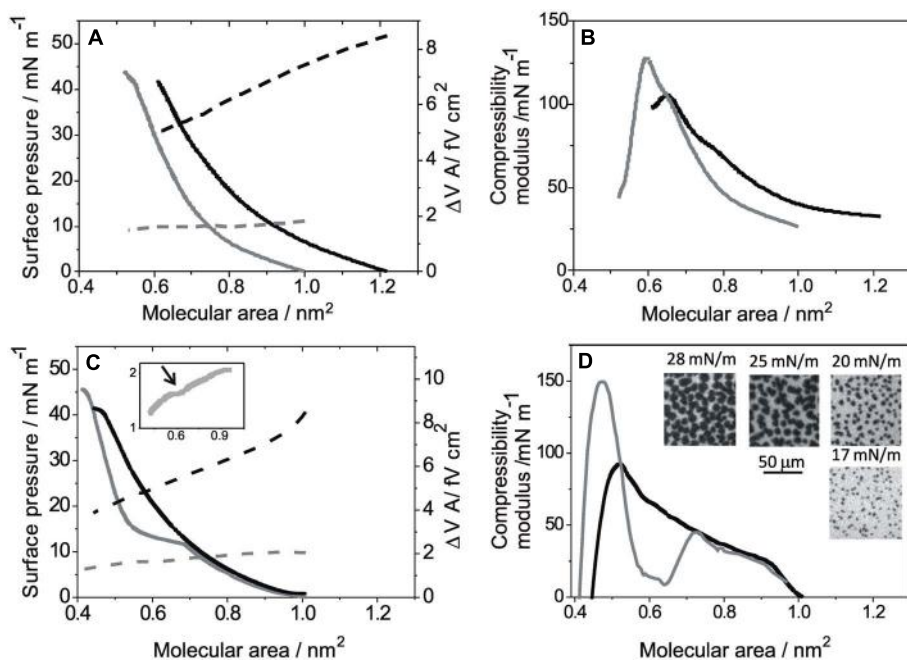


FIGURE 1 | Compression isotherms for monolayers of diacylglycerol pyrophosphate (DGPP) and palmitoyl-2-oleoyl-sn-glycerol 3 phosphate (POPA) on subphases at pH 5: (A) Lateral pressure (solid lines, left scale) and $\Delta V \cdot A$ (dashed line, right scale) as a function of the mean molecular area for DGPP monolayers. (B) Compressibility modulus for the isotherms shown in A. (C) Lateral pressure (solid lines, left scale) and $\Delta V \cdot A$ (dashed line, right scale) as a function of the mean molecular area for POPA monolayers. Inset:

zoom for $\Delta V \cdot A$ of POPA on solutions with Zn^{2+} (same as in the main plot). (D) Compressibility modulus for the isotherms shown in C. Insets: representative images for POPA films on solutions with Zn^{2+} obtained with FM at the indicated lateral pressures. Real size: $100 \mu\text{m} \times 100 \mu\text{m}$. Subphase composition: $0.15 \text{ M NaCl} + 5 \text{ mM EDTA}$, pH 5 (black lines) and 0.15 M NaCl , $5 \text{ mM EDTA} + 8 \text{ mM ZnCl}_2$, pH 5 (gray line). All curves show a single representative experiment from a set of triplicates.

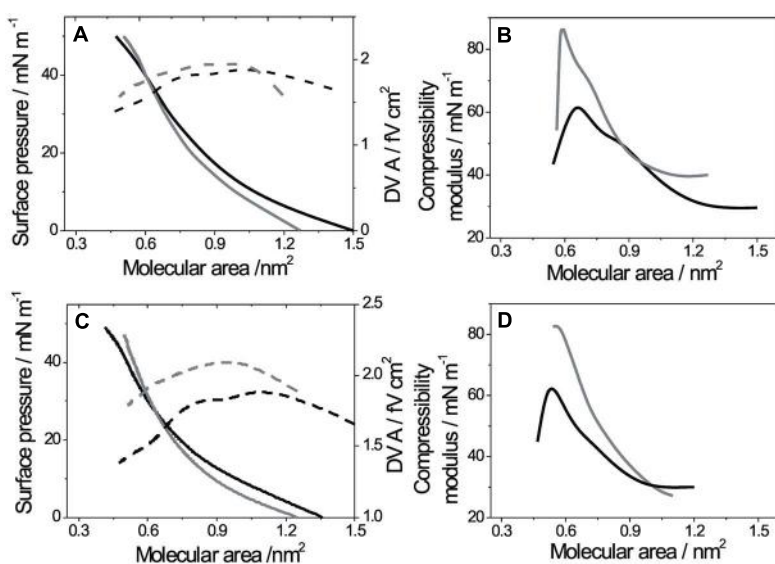


FIGURE 2 | Compression isotherms for monolayers of DGPP and POPA on subphases at pH 8: (A) Lateral pressure (solid lines, left scale) and $\Delta V \cdot A$ (dashed line, right scale) as a function of the mean molecular area for DGPP monolayers. (B) Compressibility modulus for the isotherms shown in A. (C) Lateral pressure (solid lines, left scale) and $\Delta V \cdot A$ (dashed line, right scale)

as a function of the mean molecular area for POPA monolayers. (D) Compressibility modulus for the isotherms shown in C. Subphase composition: $0.15 \text{ M NaCl} + 5 \text{ mM EDTA}$, pH 8 (black lines) and 0.15 M NaCl , $5 \text{ mM EDTA} + 8 \text{ mM ZnCl}_2$, pH 8 (gray line). All curves show a single representative experiment from a set of triplicates.

divalent cations (Minones et al., 2002; Kooijman et al., 2003, 2005; Villasuso et al., 2010). At pH 7 in the presence of magnesium ion, PA acquires a cylindrical shape and thus stabilizes the bilayer. However, once subjected to an acid environment, the head group of PA decreases its effective size, and the lipid undergoes a shape change to a cone-like shape, thus affecting the membrane by promoting an increase of negative membrane curvature (Kooijman et al., 2003). Diacylglycerol pyrophosphate formation after stimulus takes place after a transient increase of the PA levels (Munnik et al., 1995). As a consequence, a temporary and local accumulation of DGPP and its precursor at the membrane interface should be expected. Since the monolayer packing properties are affected by the interactions of POPA and DGPP at pH 8 (Villasuso et al., 2010), the phospholipid packing may be affected during the signaling processes. Therefore, we studied the packing properties of mixed films of DGPP and POPA in the presence of Zn^{2+} on subphases at acidic and basic pHs.

Figure 3 shows the behavior of mixed monolayers of DGPP and POPA when $ZnCl_2$ is added to the subphase at pHs 5 and 8. **Figure 3A** shows the compression isotherm for a 1:1 mixture at pH 5 with Zn^{2+} compared with the isotherm in the absence of Zn^{2+} . Similar to the pure lipids, the cation decreased

the potential from 8–6 to 3–2 fV cm^2 and a phase transition from a liquid-expanded to a liquid-condensed film was induced. However, the transition occurred at 30 mN m^{-1} and was less marked. As shown in **Figure 2B**, the phase transition of POPA induced by Zn^{2+} was observed at increasing pressures and in a less marked fashion as the proportion of DGPP in the mixtures increased. The fact that the lateral pressure for the phase transition was higher as the proportion of DGPP increased in the film indicates that DGPP mixed preferentially with POPA in the liquid-expanded state, thus stabilizing the latter with respect to the condensed phase. **Figure 3C** shows representative FM images of mixed monolayers at the surface pressures in which the phase coexistence is observed in each case, similar images were obtained using BAM (data not shown). At 75% of DGPP, no domains were observed up to 36 mN m^{-1} . Nevertheless, as the monolayer approached the collapse point, the fluorescent probe was segregated in bright spots indicating that the monolayer acquired a more condensed character, expelling the bulky probe (see image in **Figure 3C**).

At pH 8, the surface pressure- and $\Delta V \cdot A$ -mean molecular area compression isotherms for mixed monolayers of DGPP with POPA were only slightly affected by the presence of the divalent cation (see **Figure 3D**).

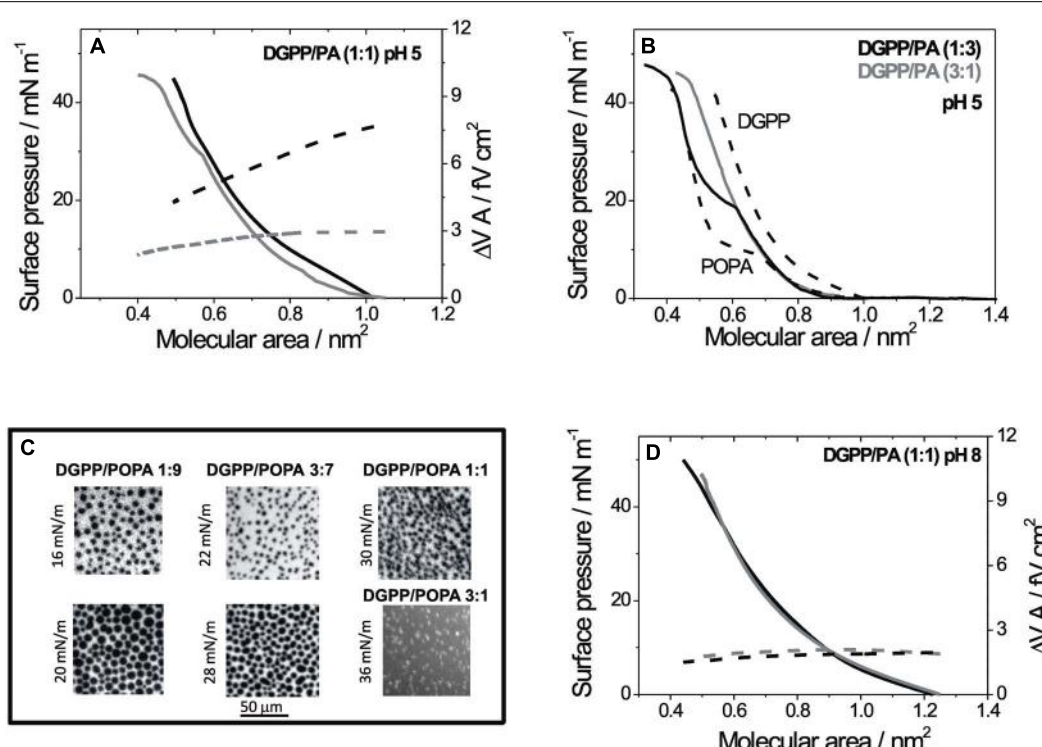


FIGURE 3 | Compression isotherms for mixed monolayers of DGPP and POPA on subphases at different pHs: (A) Lateral pressure (solid lines, left scale) and $\Delta V \cdot A$ (dashed line, right scale) as a function of the mean molecular area for monolayers composed of DGPP/POPA (1:1) on subphases at pH 5. (B) Lateral pressure as a function of the mean molecular area for monolayers composed pure DGPP and POPA (dashed lines) or mixtures of DGPP/POPA in a proportion (1:3) (black line) and (3:1) (gray line). (C) Representative images

of mixed films at the indicated proportions and pressures obtained with FM on subphases at pH 5 with Zn^{2+} . Real size: 100 $\mu m \times 100 \mu m$. (D) Lateral pressure (solid lines, left scale) and $\Delta V \cdot A$ (dashed line, right scale) as a function of the mean molecular area for monolayers composed of DGPP/POPA (1:1) on subphases at pH 8. Subphase composition: 0.15 M NaCl + 5 mM EDTA, pH 8 (black lines) and 0.15 M NaCl, 5 mM EDTA + 8 mM $ZnCl_2$, pH 8 (gray line).

DISCUSSION

The behavior upon compression of films composed of DGPP, POPA, and their mixtures in the presence of ZnCl_2 was investigated on acid and basic subphases. **Figure 4** summarizes the effect of the presence of ZnCl_2 at 10 and 40 mN m^{-1} at pH 5 (left panels) compared to pH 8 (right panels). The mean molecular area, the compressibility of the film, and $\Delta V/A$ are shown as a function of the mole fraction of DGPP in mixed films with POPA. The same scale was used for both pHs in panels A–D in order to facilitate comparison. For panels E and F, different scales were used for better understanding of the data.

At pH 5, the molecular density of pure DGPP and of films enriched in this lipid was markedly increased by the divalent cation while the effect was reduced in films with a high proportion of POPA (**Figure 4A**). This effect was more marked at low than at high surface pressure, where the mean molecular area decreased 0.1–0.2 nm^2 . This is probably a consequence that the mean molecular

area at 30 mN m^{-1} or higher pressures was close to the minimal area occupied by two hydrocarbon chains (0.38–0.40 nm^2), and thus the cation was not able to further reduce the area occupied by the lipid. However, slope of the isotherms in the whole range of surface pressures was higher in the presence of Zn^{2+} with a concomitant increase in the surface compressibility modulus. At pH 5, monolayers in the presence of Zn^{2+} were less compressible than in its absence (see **Figure 4C**). Exceptions were observed for the proportions in which the induced phase transition coincides with the lateral pressure analyzed (25% at 10 mN m^{-1} and 75% at 40 mN m^{-1}). The compression isotherms of monolayers for a particular lipid species depends on the length and unsaturation of the hydrocarbon chain and on the bulkiness and charge of the polar head group. Long and saturated hydrocarbon chains generally promote more condensed monolayer. In contrast, ionization of the lipid head groups should result in repulsive interaction, leading to loosely packed monolayers (Brown and Brockman, 2007). Thus,

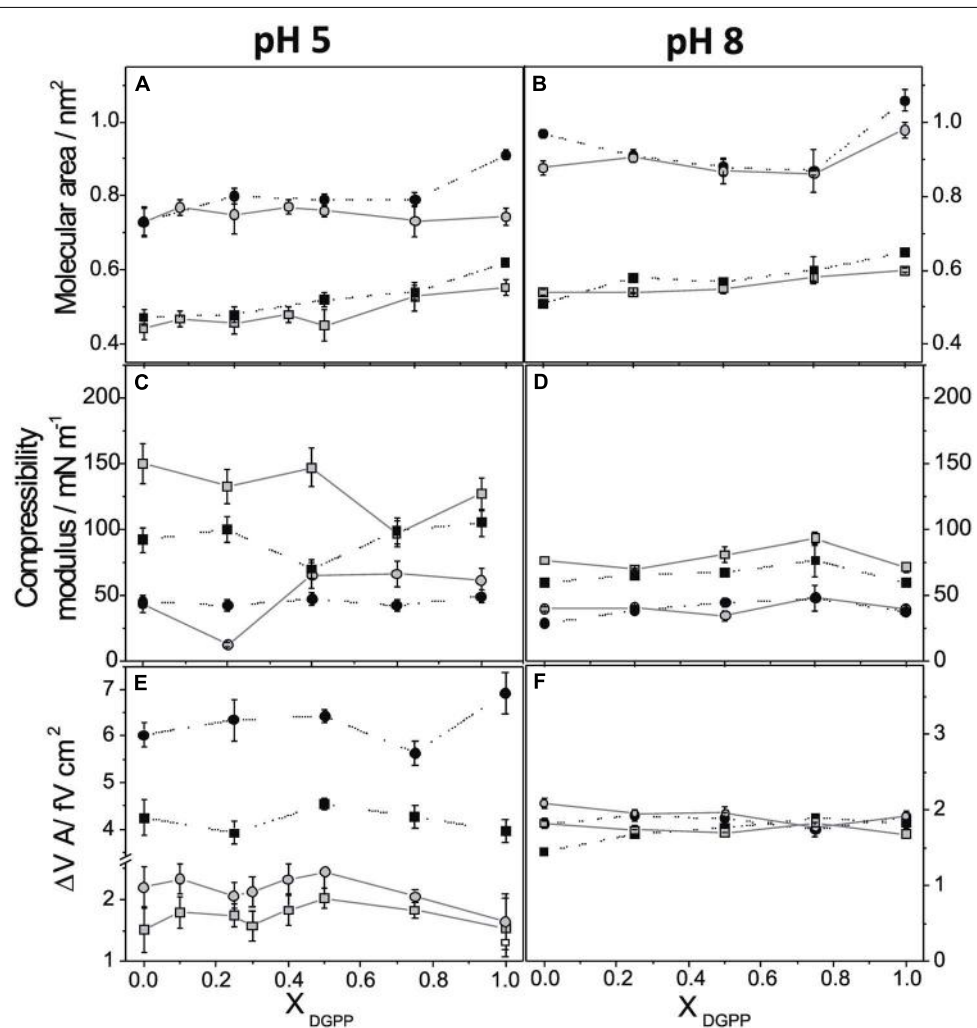


FIGURE 4 | Mean molecular area (A,B), compressibility modulus (C,D), and surface potential density (E,F) as a function of the mole fraction of DGPP in the mixture at pH 5 (left panel) and pH 8 (right panel). The lateral

pressures are: 10 mN m^{-1} (circles) and 40 mN m^{-1} (squares). Subphase composition: 0.15 M NaCl + 5 mM EDTA, (black circle) and 0.15 M NaCl, 5 mM EDTA + 8 mM ZnCl_2 , (gray circle).

the observed compression isotherms of DGPP and POPA at pH 5 in the presence of the cation are in agreement with a decreased electrostatic repulsion where a lower net charge is expected. In similar experiments, it was observed that DPPA monolayers are also influenced by pH as a consequence of the change in the ionization of the lipid (Minones et al., 2002). At pH 3, DPPA molecules are uncharged showing a more rigid monolayer structure compared to monolayer spread on subphases at higher pHs. It is possible that hydrogen bonding between protonated PA groups of adjacent molecules could lead to a more stable and coherent monolayer. In contrast, DPPA monolayer at pH 6 exhibits a larger molecular area due to the ionization of the first phosphate of PA, decreasing the possibility for intermolecular hydrogen bonding. The effect of divalent cations on the interfacial behavior of anionic lipid was also evaluated with other phospholipids in model system. Apparently some divalent cations at high concentration may induce the formation of clusters of phospholipids. In the case of the precursor of second messenger PIP₂, only Ca²⁺, but not Mg²⁺, Zn²⁺, or polyamines induces a surface pressure drop that coincides with the formation of PIP₂ clusters (Wang et al., 2012). Our results with Zn²⁺ at high concentration (ca. 3 mM free ion) indicated that the ion promotes the generation of domains of POPA in a condensed phase state. Which is the lower amount of this ion capable of induce a phase transition in monolayers of this lipid is however, not investigated, since it is beyond the scope of this research.

At pH 8, only the monolayers composed of pure DGPP or POPA were condensed by Zn²⁺, while the film density of the mixed monolayers was unaffected by this cation (**Figure 4B**). This is probably a consequence of the fact that the mixture at basic pHs forms closely packed films and the process of mixing is thermodynamically favored (Villasuso et al., 2010), therefore, the Zn²⁺ ions are probably not able to penetrate and further modify the compact film formed by the mixture. The compressibility modulus as a function of the proportion of DGPP in the mixture at pH 8 is shown in **Figure 4D**, and the comparison with **Figure 4C** indicates that at this pH only a slight increase of the compressibility was observed at 10 mN m⁻¹ while the effect was negligible at 40 mN m⁻¹.

Regarding the surface electrostatics, **Figures 4E,F** show that the $\Delta V \cdot A$ of the pure lipids and their mixtures changed from 4–6 to 2 fV cm² when the pH increased. The negative charge on the lipids signifies an anionic surface with a corresponding distribution of mobile ions in the immediate aqueous milieu (the double-layer potential) which is also included in the surface potential measured. It was previously observed in stearic acid monolayers that an increase of the negative charge in the monolayer may decrease the double-layer potential by values as high as 200 mV (Vega Mercado et al., 2011). The surface potential of charged films depends in a rather complex manner on the double-layer potential because of the simultaneous contribution of hydrocarbon chain dipoles, of water dipoles from the polar head group hydration shell, and intrinsic polar head group dipoles, as well as from the electrostatic field brought about from the relative position of mobile ions close to the monolayer. Therefore, a decrease of the double-layer potential when the lipid becomes ionized may result in a lower surface potential even if the overall

lipid dipole is being increased in the negatively charged molecule (Vega Mercado et al., 2011). Thus, the decrease of $\Delta V \cdot A$ observed at pH 8 compared to pH 5 could most probably be a consequence of the decrease of the double-layer potential as the monolayer charge increased. Studies of the interaction between PA and Ba²⁺ suggested that PA is extremely effective in binding divalent ions through its oxygen atoms, with a broad distribution of binding constants and exhibiting the phenomenon of charge inversion (a total number of bound counterion charges that exceeds the negative PA charge; Faraudo and Travesset, 2007). The authors predict that a PA-rich domain undergoes a drastic reorganization when divalent cations as Ca²⁺ and Ba²⁺ reach micromolar concentrations (i.e., typical physiological conditions), as PA lipids become doubly charged by releasing their protons. Although restricted to PA, those results could be qualitatively similar for other phospholipids, as DGPP, which play somewhat similar roles as PA.

When Zn²⁺ was present in the subphase, the measured $\Delta V \cdot A$ was about 2 fV cm² at both pHs. This leads to the conclusion that this parameter is very sensitive to the Zn²⁺ cation at pH 5 and at all pressures, while at pH 8 only the pure POPA monolayers were affected by the cation and, in a less marked manner than at pH 5. Besides, at pH 8 the interface was slightly depolarized while at pH 5 it became highly hyperpolarized.

The relatively low response of the surface electrostatics at pH 8 may be explained by considering that in this condition, the charge density of the interface was quite negative, and a compact, double layer was already formed in the absence of Zn²⁺. The addition of this cation may not induce further changes in the system, in spite of any specific binding with the film molecules. Also, it is possible that at basic pHs, Zn²⁺ did not interact specifically with the film and thus, only changed slightly the ionic strength of the subphase with correspondingly small changes in the film properties (**Figures 4B,D,F**).

At pH 5, on the other hand, the divalent cation appeared to interact with the film and to induce changes in the film properties studied (**Figures 4A,C,E**). The important changes induced by Zn²⁺ clearly indicate an interaction with the phosphate groups, decreasing the in-plane repulsion and hyperpolarizing the interface. How this interaction may translate to changes in $\Delta V \cdot A$ is not easy to explain because this parameter depends on the location of Zn²⁺ ions relative to the polar head groups and to the interface.

CONCLUSION

Our results indicate that the film properties of DGPP and its precursor PA were sensitive to Zn²⁺ in a pH-dependent manner, and thus depend on the ionization state of the molecules forming the film. This effect was further modulated by the relative proportions of DGPP and POPA in the film. The changes promoted by Zn²⁺ were more marked on subphases at pH 5, while at pH 8 the influence of the cation in the film surface properties was attenuated.

Regarding the ionization behavior of PA, it was recently proposed that upon initial ionization, the remaining hydrogen may form hydrogen bonds with this phosphomonoester head group, resulting in an easier deprotonation compared to the situation

lacking the hydrogen bond. This peculiar ionization behavior was summarized in the electrostatic-hydrogen bond switch model. Similarly, the phosphomonoester head group of DGPP was proposed to follow this behavior. In addition, it was observed that at constant pH, DGPP carries more negative charge than the phosphomonoester head group (Strawn et al., 2012). Strawn et al. (2012) suggested that the higher charges would favor the interaction of positive domains of proteins and might result in a displacement of a PA-bound protein to DGPP. If in the complex mixture, POPA and DGPP also form a stable film when locally mixed, then in the presence of DGPP, POPA would not be as free as in its absence. Furthermore, the interaction of both molecules with Zn^{2+} ions would be precluded in the mixed film.

If the surface behavior described could happen in biomembranes, it may be speculated that such effects could occur locally when DGPP is generated by PAK or hydrolyzed by DGPP phosphatase. In this work, we demonstrate that a local increase in the proportion of this lipid can affect the local film properties, in a pH-dependent manner which is also sensitive to the ionic composition of the aqueous milieu. Taking together, all these effects may constitute structural-electrostatic signal transduction mechanism involving DGPP in the turning off/on of PA signaling.

AUTHOR CONTRIBUTIONS

Ana L. Villasuso and Natalia Wilke conceived and designed the experiments. Ana L. Villasuso performed the experiments. Ana L. Villasuso and Natalia Wilke analyzed the data. Estela Machado and Bruno Maggio contributed reagents/materials/analysis tools. Ana L. Villasuso, Natalia Wilke, Estela Machado, and Bruno Maggio involved in the Result discussion. Ana L. Villasuso, Natalia Wilke, Estela Machado, and Bruno Maggio wrote the paper. Ana L. Villasuso, Natalia Wilke, Estela Machado, and Bruno Maggio edited the manuscript, wrote figure legends, and helped with the outline of the paper.

ACKNOWLEDGMENTS

This work was supported in part by SECyT-UNRC, SECyT-UNC, FONCYT (PICT, 2006-1513; 2007-02212; 2010-0415), CONICET and Agencia Cordoba-Ciencia. Bruno Maggio, Natalia Wilke, and Ana L. Villasuso are Career Investigators of CONICET.

REFERENCES

- Aravind, P., and Prasad, M. N. V. (2003). Zinc alleviates cadmium induced toxicity in *Ceratophyllum demersum*, a fresh water macrophyte. *Plant Physiol. Biochem.* 41, 391–397. doi: 10.1016/S0981-9428(03)00035-4
- Arisz, S. A., Testerink, C., and Munnik, T. (2009). Plant PA signaling via diacylglycerol kinase. *Biochim. Biophys. Acta* 1791, 869–875. doi: 10.1016/j.bbapplied.2009.04.006
- Athenstaedt, K., and Daum, G. (1999). Phosphatidic acid, a key intermediate in lipid metabolism. *Eur. J. Biochem.* 266, 1–16. doi: 10.1046/j.1432-1327.1999.00822.x
- Broadley, M. R., White, P. J., Hammond, J. P., Zelko, I., and Lux, A. (2007). Zinc in plants. *New Phytol.* 173, 677–702. doi: 10.1111/j.1469-8137.2007.01996.x
- Brockman, H. L., Applegate, K. R., Momsen, M. M., King, W. C., and Glomset, J. A. (2003). Packing and electrostatic behavior of sn-2-docosahexaenoyl and -arachidonoyl phosphoglycerides. *Biophys. J.* 85, 2384–2396. doi: 10.1016/S0006-3495(03)74662-1
- Brown, R. E., and Brockman, H. L. (2007). Using monomolecular films to characterize lipid lateral interactions. *Methods Mol. Biol.* 398, 41–58. doi: 10.1007/978-1-59745-513-8_5
- Cakmak, I. (2000). Role of zinc in protecting plant cells from reactive oxygen species. *New Phytol.* 146, 185–205. doi: 10.1046/j.1469-8137.2000.00630.x
- Cherif, J., Mediouni, C., Ben Ammar, W., and Jemal, F. (2011). Interactions of zinc and cadmium toxicity in their effects on growth and in antioxidative systems in tomato plants (*Solanum lycopersicum*). *J. Environ. Sci. (China)* 23, 837–844. doi: 10.1016/S1001-0742(10)60415-9
- Davies, J. T., and Rideal, E. K. (1963). *Interfacial Phenomena*, 2nd Edn. New York: Academic Press.
- Faraudo, J., and Travesset, A. (2007). Phosphatidic acid domains in membranes: effect of divalent counterions. *Biophys. J.* 92, 2806–2818. doi: 10.1529/biophys.106.092015
- Gaines, G. L. (1966). “Insoluble monolayers at liquid-gas interfaces,” in *Interscience Monographs on Physical Chemistry*, ed. I. Prigogine (New York: John Wiley and Sons), 136–207.
- Han, G. S., Johnston, C. N., Chen, X., Athenstaedt, K., Daum, G., and Carman, G. M. (2001). Regulation of the *Saccharomyces cerevisiae* DPP1-encoded diacylglycerol pyrophosphate phosphatase by zinc. *J. Biol. Chem.* 276, 10126–10133. doi: 10.1074/jbc.M011421200
- Kim, S.-C., Guo, L., and Wang, X. (2013). Phosphatidic acid binds to cytosolic glyceraldehyde-3-phosphate dehydrogenase and promotes its cleavage in *Arabidopsis*. *J. Biol. Chem.* 288, 11834–11844. doi: 10.1074/jbc.M112.427229
- Kooijman, E. E., and Burger, K. N. (2009). Biophysics and function of phosphatidic acid: a molecular perspective. *Biochim. Biophys. Acta* 1791, 881–888. doi: 10.1016/j.bbapplied.2009.04.001
- Kooijman, E. E., Carter, K. M., Van Laar, E. G., Chupin, V., Burger, K. N., and De Kruijff, B. (2005). What makes the bioactive lipids phosphatidic acid and lysophosphatidic acid so special? *Biochemistry* 44, 17007–17015. doi: 10.1021/bi0518794
- Kooijman, E. E., Chupin, V., De Kruijff, B., and Burger, K. N. (2003). Modulation of membrane curvature by phosphatidic acid and lysophosphatidic acid. *Traffic* 4, 162–174. doi: 10.1034/j.1600-0854.2003.00086.x
- Kooijman, E. E., Tielemans, D. P., Testerink, C., Munnik, T., Rijkers, D. T., Burger, K. N., et al. (2007). An electrostatic/hydrogen bond switch as the basis for the specific interaction of phosphatidic acid with proteins. *J. Biol. Chem.* 282, 11356–11364. doi: 10.1074/jbc.M609737200
- Maggio, B. (2004). Favorable and unfavorable lateral interactions of ceramide, neutral glycosphingolipids and gangliosides in mixed monolayers. *Chem. Phys. Lipids* 132, 209–224. doi: 10.1016/j.chemphyslip.2004.07.002
- Mangiariotti, A., Caruso, B., and Wilke, N. (2014). Phase coexistence in films composed of DLPC and DPPC: a comparison between different model membrane systems. *Biochim. Biophys. Acta* 1838, 1823–1831. doi: 10.1016/j.bbamem.2014.02.012
- Minones, J. Jr., Rodriguez Patino, J. M., Minones, J., Dynarowicz-Latka, P., and Carrera, C. (2002). Structural and topographical characteristics of dipalmitoyl phosphatidic acid in Langmuir monolayers. *J. Colloid Interf. Sci.* 249, 388–397. doi: 10.1006/jcis.2002.8285
- Munnik, T., Arisz, S. A., De Vrije, T., and Musgrave, A. (1995). G protein activation stimulates phospholipase D signaling in plants. *Plant Cell* 7, 2197–2210. doi: 10.1105/tpc.7.12.2197
- Munnik, T., De Vrije, T., Irvine, R. F., and Musgrave, A. (1996). Identification of diacylglycerol pyrophosphate as a novel metabolic product of phosphatidic acid during G-protein activation in plants. *J. Biol. Chem.* 271, 15708–15715. doi: 10.1074/jbc.271.26.15708
- Paradis, S., Villasuso, A. L., Aguayo, S. S., Maldiney, R., Habricot, Y., Zalejski, C., et al. (2011). *Arabidopsis thaliana* lipid phosphate phosphatase 2 is involved in abscisic acid signalling in leaves. *Plant Physiol. Biochem.* 49, 357–362. doi: 10.1016/j.plaphy.2011.01.010
- Racagni, G., Villasuso, A. L., Pasquare, S. J., Giusto, N. M., and Machado, E. (2008). Diacylglycerol pyrophosphate inhibits the alpha-amylase secretion stimulated by gibberellin acid in barley aleurone. *Physiol. Plant.* 134, 381–393. doi: 10.1111/j.1399-3054.2008.01148.x
- Rosetti, C. M., Maggio, B., and Wilke, N. (2010). Micron-scale phase segregation in lipid monolayers induced by myelin basic protein in the presence of a cholesterol analog. *Biochim. Biophys. Acta* 1798, 498–505. doi: 10.1016/j.bbapplied.2009.11.006
- Shin, J. J., and Loewen, C. J. (2011). Putting the pH into phosphatidic acid signaling. *BMC Biol.* 9:85. doi: 10.1186/1741-7007-9-85

- Strawn, L., Babb, A., Testerink, C., and Kooijman, E. E. (2012). The physical chemistry of the enigmatic phospholipid diacylglycerol pyrophosphate. *Front. Plant Sci.* 3:40. doi: 10.3389/fpls.2012.00040
- Testerink, C., and Munnik, T. (2011). Molecular, cellular, and physiological responses to phosphatidic acid formation in plants. *J. Exp. Bot.* 62, 2349–2361. doi: 10.1093/jxb/err079
- Tkalec, M., Štefanić, P. P., Cyjetko, P., Šikić, S., Pavlica, M., and Balen, B. (2014). The effects of cadmium–zinc interactions on biochemical responses in tobacco seedlings and adult plants. *PLoS ONE* 9:e87582. doi: 10.1371/journal.pone.0087582
- Tsonev, T., and Lidon, F. J. C. (2012). Zinc in plants – an overview. *Emir. J. Food Agric.* 24, 322–333.
- Uruc Parlak, K., and Demirezen Yilmaz, D. (2012). Response of antioxidant defences to Zn stress in three duckweed species. *Ecotoxicol. Environ. Saf.* 85, 52–58. doi: 10.1016/j.ecoenv.2012.08.023
- Vallee, B. L., and Falchuk, K. H. (1993). The biochemical basis of zinc physiology. *Physiol. Rev.* 73, 79–118.
- van Schooten, B., Testerink, C., and Munnik, T. (2006). Signalling diacylglycerol pyrophosphate, a new phosphatidic acid metabolite. *Biochim. Biophys. Acta* 1761, 151–159. doi: 10.1016/j.bbalip.2005.12.010
- Vega Mercado, F., Maggio, B., and Wilke, N. (2011). Phase diagram of mixed monolayers of stearic acid and dimyristoylphosphatidylcholine. Effect of the acid ionization. *Chem. Phys. Lipids* 164, 386–392. doi: 10.1016/j.chemphyslip.2011.05.004
- Villasuso, A. L., Di Palma, M. A., Aveldano, M., Pasquare, S. J., Racagni, G., Giusto, N. M., et al. (2013). Differences in phosphatidic acid signalling and metabolism between ABA and GA treatments of barley aleurone cells. *Plant Physiol. Biochem.* 65, 1–8. doi: 10.1016/j.plaphy.2013.01.005
- Villasuso, A. L., Wilke, N., Maggio, B., and Machado, E. (2010). The surface organization of diacylglycerol pyrophosphate and its interaction with phosphatidic acid at the air-water interface. *Chem. Phys. Lipids* 163, 771–777. doi: 10.1016/j.chemphyslip.2010.09.002
- Wang, X., Devaiah, S. P., Zhang, W., and Welti, R. (2006). Signaling functions of phosphatidic acid. *Prog. Lipid Res.* 45, 250–278. doi: 10.1016/j.plipres.2006.01.005
- Wang, Y. H., Collins, A., Guo, L., Smith-Dupont, K. B., Gai, F., Svitkina, T., et al. (2012). Divalent cation-induced cluster formation by polyphosphoinositides in model membranes. *J. Am. Chem. Soc.* 134, 3387–3395. doi: 10.1021/ja208640t
- Wissing, J. B., and Behrbohm, H. (1993a). Diacylglycerol pyrophosphate, a novel phospholipid compound. *FEBS Lett.* 315, 95–99. doi: 10.1016/0014-5793(93)81141-L
- Wissing, J. B., and Behrbohm, H. (1993b). Phosphatidate kinase, a novel enzyme in phospholipid metabolism (Purification, Subcellular Localization, and Occurrence in the Plant Kingdom). *Plant Physiol.* 102, 1243–1249. doi: 10.1104/pp.102.4.1243
- Zalejski, C., Paradis, S., Maldiney, R., Habricot, Y., Miginiac, E., Rona, J. P., et al. (2006). Induction of abscisic acid-regulated gene expression by diacylglycerol pyrophosphate involves Ca^{2+} and anion currents in *Arabidopsis* suspension cells. *Plant Physiol.* 141, 1555–1562. doi: 10.1104/pp.106.080218

Conflict of Interest Statement: The authors declare that the research was conducted in the absence of any commercial or financial relationships that could be construed as a potential conflict of interest.

Received: 09 June 2014; accepted: 11 July 2014; published online: 29 July 2014.

Citation: Villasuso AL, Wilke N, Maggio B and Machado E (2014) Zn^{2+} - dependent surface behavior of diacylglycerol pyrophosphate and its mixtures with phosphatidic acid at different pHs. *Front. Plant Sci.* 5:371. doi: 10.3389/fpls.2014.00371

This article was submitted to Plant Physiology, a section of the journal Frontiers in Plant Science.

Copyright © 2014 Villasuso, Wilke, Maggio and Machado. This is an open-access article distributed under the terms of the Creative Commons Attribution License (CC BY). The use, distribution or reproduction in other forums is permitted, provided the original author(s) or licensor are credited and that the original publication in this journal is cited, in accordance with accepted academic practice. No use, distribution or reproduction is permitted which does not comply with these terms.



Structural divergence and loss of phosphoinositide-specific phospholipase C signaling components during the evolution of the green plant lineage: implications from structural characteristics of algal components

Koji Mikami*

Division of Marine Life Science, Genetics and Genomics, Faculty of Fisheries Sciences, Hokkaido University, Hakodate, Japan

*Correspondence: komikami@fish.hokudai.ac.jp

Edited by:

Eric Ruelland, Centre National de la Recherche Scientifique, France

Reviewed by:

Imara Yasmin Perera, North Carolina State University, USA

Eric Ruelland, Centre National de la Recherche Scientifique, France

Keywords: alga, phosphoinositide-specific phospholipase C, phosphatidylinositol phosphate-kinase, protein domain, genome

Phosphatidylinositol (PtdIns) is involved not only in the structural composition of eukaryotic cellular membranes but also in the regulation of a wide variety of physiological processes influencing growth and development (Xue et al., 2009; Janda et al., 2013). Because molecules that participate in PtdIns signaling are generated via PtdIns metabolism, extensive attention has been paid to genes encoding enzymes involved in this metabolism in order to elucidate developmental and stress-response mechanisms. PtdIns is synthesized from CDP-diacylglycerol and cytoplasmic inositol by PtdIns synthase (PIS) and is phosphorylated sequentially on its inositol ring to produce PtdIns4P and PtdIns(4,5)P₂ by PtdIns 4-kinase (PI4K) and PtdIns phosphate-kinase (PIP), respectively (Xue et al., 2009; Janda et al., 2013). Subsequently, PtdIns(4,5)P₂ is cleaved by phosphoinositide-specific phospholipase C (PI-PLC) into the second messengers diacylglycerol and inositol-1,4,5-trisphosphate [Ins(1,4,5)P₃, IP₃] (Xue et al., 2009; Janda et al., 2013), which then activate protein kinase C (PKC) and the IP₃ receptor involved in release of Ca²⁺ from the ER into the cytoplasm, respectively, in animal cells (Rebecchi and Pentyala, 2000; Suh et al., 2008). In fact, genes encoding orthologs of PKC and the IP₃ receptor are not found in terrestrial plant genomes, suggesting differences in second messenger systems between animals and plants.

Significant genomic information has been accumulated for unicellular algae including the green alga *Chlamydomonas reinhardtii* (Merchant et al., 2007), the red alga *Cyanidioschyzon merolae* (Matsuzaki et al., 2004), for the diatoms *Thalassiosira pseudonana* and *Phaeodactylum tricornutum* (Armbrust et al., 2004; Bowler et al., 2008), and also for multicellular seaweeds such as the red seaweeds *Pyropia yezoensis* (Nakamura et al., 2013) and *Chondrus crispus* (Collén et al., 2013), and brown seaweed *Ectocarpus siliculosus* (Cock et al., 2010). In addition, large-scale EST information has been accumulated for the red seaweeds *Porphyra umbilicalis* and *Porphyra purpurea* (Chan et al., 2012; Stiller et al., 2012). Because understanding the evolutionary aspects of PtdIns signaling can help us to understand the process of establishment of the plant PtdIns signaling system, algal PI-PLC and PIPK protein structures have been compared with those of terrestrial plants.

PI-PLC

The first record of the PI-PLC gene in plants was presented by Hirayama et al. (1995). Since then, information on PI-PLC genes from terrestrial plants and green algae has accumulated from results of molecular cloning and *in silico* analysis based on genome sequence data. In mammals, PI-PLC isozymes have been divided into six groups according to their domain structural characteristics (Rebecchi and Pentyala, 2000; Suh et al., 2008). For

example, PLC δ consists the Pleckstrin homology (PH) domain, the EF hand, and X, Y, and C2 domains (Figure 1), although PLC γ and PLC ϵ contain the SH2 and SH3 domains and the Ras-GEF and RA domains, respectively, in addition to domains found in PLC δ . The PH domain participates in membrane binding, whereas the X and Y domains are responsible for catalytic activity. Plant PI-PLCs reported so far, however, lack the PH domain, similar in that to the mammalian PI-PLC ζ isoform (Pokotylo et al., 2014). They consist of an N-terminal EF-hand, a central X/Y catalytic domain, and a C-terminal C2 domain (Figure 1). The EF hand plays an important role in Ca²⁺-dependent activation of PI-PLC ζ , suggesting a similar function in plant PI-PLCs. Indeed, it has been demonstrated that the activities of PI-PLCs from plants were stimulated by Ca²⁺ in a concentration dependent manner (for instance, Hirayama et al., 1995; Otterhag et al., 2001; Hunt et al., 2004; Mikami et al., 2004). Although the EF hand in mammalian PI-PLC has four repeats of helix-loop-helix structure, plant enzymes carry only two of these repeats due to truncation (Figure 1). The C2 domain in plant PI-PLCs was suggested to have evolved separately from animal PI-PLCs and is possibly involved in membrane localization (Rupwate and Rajasekharan, 2012).

Genome analysis has identified nine copies of the PI-PLC genes (AtPLC1-AtPLC9) in *A. thaliana*, although AtPLC8

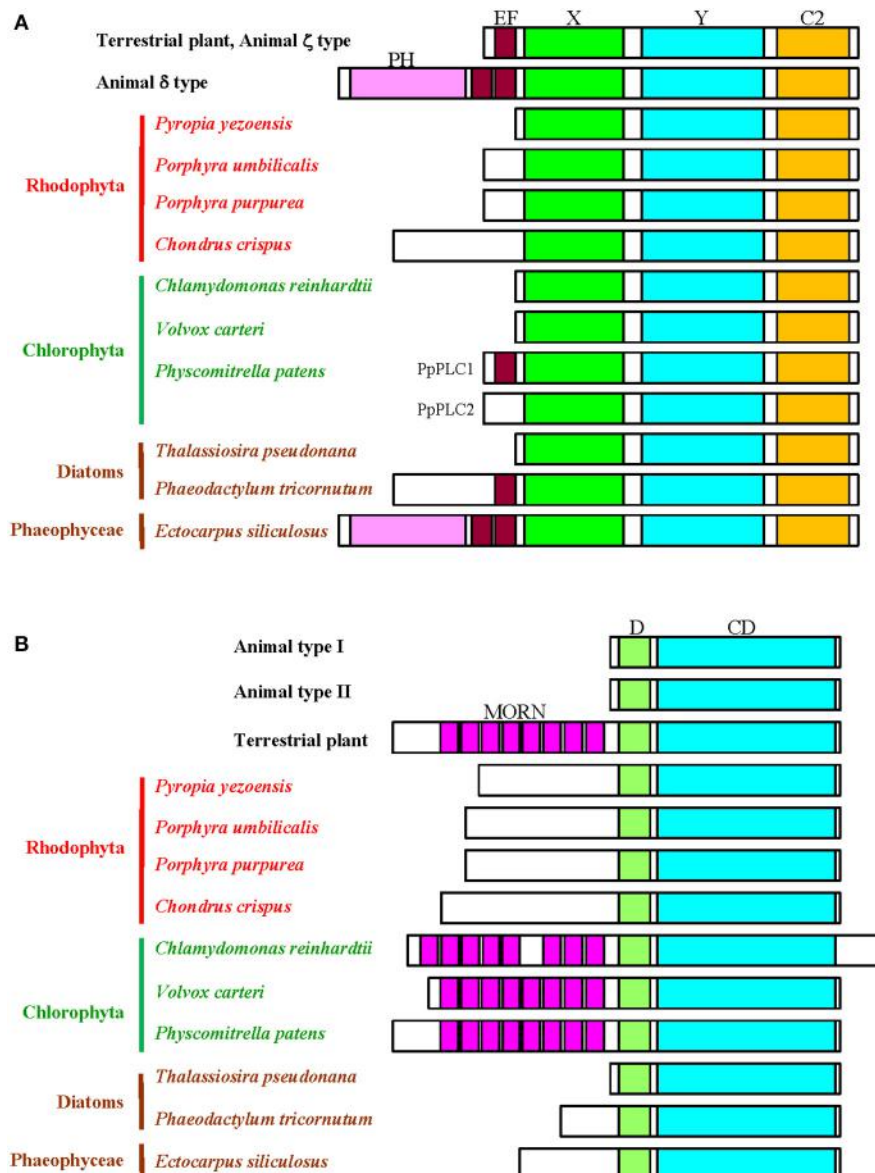


FIGURE 1 | Schematic comparison of the domain structures of the PI-PLC signaling components. (A), PI-PLC; (B), PIPK. D, dimerization domain; CD, catalytic domain.

and AtPLC9 with amino acid substitutions in the Y domain do not group into the clade containing other PLCs during phylogenetic analysis (Mueller-Roeber and Pical, 2002; Hunt et al., 2004). However, only one and two copies of PI-PLC genes have been found in *C. reinhardtii* and *Physcomitrella patens*, respectively (Mikami et al., 2004; Awasthi et al., 2012). Moreover, because red and brown seaweeds as well as green microalgae have only a single copy of the PI-PLC gene, amplification and

functional diversification of these genes likely occurred during evolution of streptophytes (land plants and charophytic algae) with establishment of multicellularity and vascular systems after the colonization of land.

It is worth noting that *P. patens* has a novel PI-PLC without PtdIns(4,5)P₂-hydrolyzing activity, with an insertion at its N-terminal EF hand (Mikami et al., 2004). **Figure 1** shows the absence of the EF hand in unicellular and multicellular algae from aqueous environments, except

for the diatom *P. tricornutum* and the brown seaweed *E. siliculosus* (**Figure 1**). The EF hand might have appeared after the colonization of land by green algal lineages and, subsequently, PI-PLCs lacking the EF hand disappeared during the evolution of terrestrial green plants. Thus, the EF-hand-mediated regulatory mode of PI-PLC activation seems to have evolved in the green plant lineages after the colonization of land.

The evolutionary establishment of the domain structure of PI-PLC in brown

seaweeds is highly complex. As shown in **Figure 1**, *P. tricornutum* and *E. siliculosus* have the EF hand motif. Thus, the EF hand was acquired during the evolution of diatoms and brown seaweeds. Surprisingly, PI-PLC in *E. siliculosus* contains the non-truncated EF hand and the PH domain, just as does the mammalian PI-PLC δ isoform (**Figure 1**). The reason that only the brown seaweed has an isoform of the PI-PLC δ type remains to be resolved.

PIPK

The first molecular characterization of the plant PIPK gene was performed by Mikami et al. (1998), following molecular cloning and *in silico* identification based on the genome sequences of land plant PIPKs. Due to their substrate specificity in animals, PIKs can be divided into three subfamilies, known as types I, II, and III. Types I and II enzymes convert PtdIns(4)P and PtdIns(5)P, respectively, to produce PtdIns(4,5)P₂ (Anderson et al., 1999), whereas type III enzymes use PI(3)P to produce PI(3,5)P₂ similar to yeast Fab1 (Mueller-Roeber and Pical, 2002). Despite such differences in substrate specificity, the structures of type I and II PIPKs are highly similar in animals; however, based on substrate specificity and structure, the plant enzymes are classified as type I/II PIPKs (Mueller-Roeber and Pical, 2002; Thole and Nielsen, 2008; Saavedra et al., 2012).

The genome of *A. thaliana* contains 11 PIPKs, subdivided into A and B subfamilies according to their structural differences. The domain structure of subfamily A (AtPIP10 and AtPIP11) shows similarity to animal PIPKs, whereas the domain structure of subfamily B members (AtPIP5K1-AtPIP5K9) includes a long N-terminal extension containing a repeat of the membrane occupation and recognition nexus (MORN) motif (Mueller-Roeber and Pical, 2002; Saavedra et al., 2012). Although the domain containing MORN motifs has been hypothesized to be a module involved in plasma membrane-localization and phosphatidic acid (PA)-dependent enzymatic activation (Im et al., 2007), it was recently demonstrated that the activation loop conserved in the lipid kinase domain is responsible for both plasma membrane localization and PA-dependent activation of *A. thaliana* and

P. patens PIPKs (Mikami et al., 2010a,b; Saavedra et al., 2012). Plant genomes other than that of *A. thaliana* contain only the B subfamily and a small number of genes for PIPK orthologs exist in *C. reinhardtii* (single copy; Awasthi et al., 2012) and *P. patens* (two copies; Saavedra et al., 2009, 2011, 2012). Because red and brown seaweeds as well as green microalgae have only a single copy of the PIPK gene, amplification and functional diversification of PIPK genes also likely occurred during evolution, as in PI-PLC.

As shown in **Figure 1**, the MORN motifs are not found in PIPKs from red algae, diatoms, and brown *E. siliculosus*, indicating the presence of the MORN repeats is restricted into the green lineage, although PIPKs without the MORN motifs are conserved in *A. thaliana*, as mentioned above. Because the common origin of the red and green algae can be ascribed to a single symbiosis (Keeling, 2010), there are two possibilities for the presence of the MORN motifs in the green lineage. One is that although an ancestral plant cell has a MORN motif-containing PIPK, this motif disappeared from red algae after the divergence of red and green algae. The other is that an ancestral plant cell has a PIPK consisting of the dimerization and catalytic domains and the MORN motifs appeared only in green algae after the divergence of red and green algae. The absence of the MORN motifs in the brown seaweed can be explained by either possibility. According to these findings, the activation mode of PIPK differs between green plants and red and brown algae. Elucidation of the functions of the MORN motif is necessary to fully explain such a difference.

CONCLUSIONS

Comparative genomics provide an evolutionary insight into the taxonomic origin of enzymes and their isoforms, which is generally drawn based on the presence and number of gene family members. Here, it is demonstrated that analysis of domain structure can allow novel evolutionary conclusions. Because domain structure is involved in the regulation of the active state of each protein, comparison of plant genomes with a focus on the structure of and changes in protein domains could open new scenarios regarding the origin

and evolution of signaling networks that regulate development and stress responses in plants.

ACKNOWLEDGMENT

This work was supported in part by a KAKENHI Grant (Number 2566016003) from the Japan Society for the Promotion of Science.

REFERENCES

- Anderson, R. A., Boronenkov, I. V., Doughman, S. D., Kunz, J., and Loijens, J. C. (1999). Phosphatidylinositol phosphate kinases, a multi-faceted family of signaling enzymes. *J. Biol. Chem.* 274, 9907–9910. doi: 10.1074/jbc.274.15.9907
- Armbrust, E. V., Berge, J. A., Bowler, C., Green, B. R., Martinez, D., Putnam, N. H., et al. (2004). The genome of the diatom *Thalassiosira pseudonana*: ecology, evolution, and metabolism. *Science* 306, 781–786. doi: 10.1126/science.1101156
- Awasthi, M., Batra, J., and Kateriya, S. (2012). Disulphide bridges of phospholipase C of *Chlamydomonas reinhardtii* modulates lipid interaction and dimer stability. *PLoS ONE* 7:e39258. doi: 10.1371/journal.pone.0039258
- Bowler, C., Allen, A. E., Badger, J. H., Grimwood, J., Jabbari, K., Kuo, A., et al. (2008). The *Phaeodactylum* genome reveals the evolutionary history of diatom genomes. *Nature* 456, 239–244. doi: 10.1038/nature07410
- Chan, C. X., Zäuner, S., Wheeler, G., Grossman, A. R., Prochnik, S. E., Blouin, N. A., et al. (2012). Analysis of *Porphyra* membrane transporters demonstrates gene transfer among photosynthetic eukaryotes and numerous sodium-coupled transport systems. *Plant Physiol.* 158, 2001–2012. doi: 10.1104/pp.112.193896
- Cock, J. M., Sterck, L., Rouzé, P., Scornet, D., Allen, A. E., Amoutzias, G., et al. (2010). The *Ectocarpus* genome and the independent evolution of multicellularity in brown algae. *Nature* 465, 617–621. doi: 10.1038/nature09016
- Collén, J., Porcel, B., Carré, W., Ball, S. G., Chaparro, C., Tonon, T., et al. (2013). Genome structure and metabolic features in the red seaweed *Chondrus crispus* shed light on evolution of the Archaeplastida. *Proc. Natl. Acad. Sci. U.S.A.* 110, 5247–5252. doi: 10.1073/pnas.1221259110
- Hiroyama, T., Ohto, C., Mizoguchi, T., and Shinozaki, K. (1995). A gene encoding a phosphatidylinositol-specific phospholipase C is induced by dehydration and salt stress in *Arabidopsis thaliana*. *Proc. Natl. Acad. Sci. U.S.A.* 92, 3903–3907. doi: 10.1073/pnas.92.9.3903
- Hunt, L., Otterhag, L., Lee, J. C., Lasheen, T., Hunt, J., Seki, M., et al. (2004). Gene-specific expression and calcium activation of *Arabidopsis thaliana* phospholipase C isoforms. *New Phytol.* 162, 643–654. doi: 10.1111/j.1469-8137.2004.01069.x
- Im, Y. J., Davis, A. J., Perera, I. Y., Johannes, E., Allen, N. S., and Boss, W. F. (2007). The N-terminal membrane occupation and recognition nexus domain of *Arabidopsis* phosphatidylinositol phosphate kinase 1 regulates enzyme activity. *J. Biol. Chem.* 282, 5443–5452. doi: 10.1074/jbc.M611342200

Conclusion and Perspectives

The establishment and maintenance of apical polarity relies on a dynamic, mobile network of signaling mechanisms. Currently, our conceptual models focus mostly on apical and sub-apical localization (of ions, proteins, lipids), particularly at the plasma membrane (or associated with). Here we provided examples of four classes of proteins related to ion and lipid signaling which indicates that a careful analysis of localization, activity and mobility is required in order to fully assign their role in apical growth. This rationale can probably be extended to other equally relevant signaling components identified in these cells (e.g., Rop GTPases, Ca^{2+} -dependent protein kinases, actin and actin-binding proteins, etc; **Figure 1**; for a review see Onelli and Moscatelli, 2013). The results obtained with FAB kinases further suggest the importance of plasma membrane—endomembrane signaling raising new perspectives in the study of apical growth mechanisms. Signaling to other organelles and compartments is also likely to play key roles in the establishment of polarity.

We have discussed the hypothesis that, in nature, and upon a myriad of environmental (extracellular) cues, cellular responses

involve flexible positioning of proteins, lipids and ion fluxes. Such dynamics may go partly unnoticed in the set-ups we devise for our experimental planning which are conditioned by the species under study, the technical approach, the pre-existing knowledge and, most importantly, by the requirements to test individual stimuli. Thus, transient gradients or peaks of activity/localization may or not be recorded (even dismissed) depending on the experimental set-up, cellular conditions and our biased previous background. Large single cell analysis and settings mimicking (or bearing in mind) the natural environment where cells develop, are required but may be difficult to implement. To compare and interpret results obtained with different experimental as well as plant systems will be a challenge, but one that must be tackled.

Acknowledgments

This work was supported by Fundação Ciência e Tecnologia (FCT/MCTES/PIDDAC, Portugal) with post-doc fellowship to LS (SFRH/BPD/63619/2009), FD (SFRH/BPD/81635/2011), and research funds to RM (PEst-OE/BIA/UI4046/2014; UID/MULTI/04046/2013).

References

- Bak, G., Lee, E.-J., Lee, Y., Kato, M., Segami, S., Sze, H., et al. (2013). Rapid structural changes and acidification of guard cell vacuoles during stomatal closure require phosphatidylinositol 3,5-bisphosphate. *Plant Cell* 25, 2202–2216. doi: 10.1105/tpc.113.110411
- Bove, J., Vaillancourt, B., Krueger, J., Hepler, P. K., Wiseman, P. W., and Geitmann, A. (2008). Magnitude and direction of vesicle dynamics in growing pollen tubes using spatiotemporal image correlation spectroscopy and fluorescence recovery after photobleaching. *Plant Physiol.* 147, 1646–1658. doi: 10.1104/pp.108.120212
- Camacho, L., and Malhó, R. (2003). Endo-exocytosis in the pollen tube apex is differentially regulated by Ca^{2+} and GTPases. *J. Exp. Bot.* 54, 83–92. doi: 10.1093/jxb/erg043
- Castanho Coelho, P., and Malhó, R. (2006). Correlative analysis of apical secretion and $[\text{Ca}^{2+}]_c$ in pollen tube growth and reorientation. *Plant Signal. Behav.* 1, 152–157. doi: 10.4161/psb.1.3.2999
- Cheung, A., and Wu, H. M. (2008). Structural and signaling networks for the polar cell growth machinery in pollen tubes. *Annu. Rev. Plant Biol.* 59, 547–572. doi: 10.1146/annurev.arplant.59.032607.092921
- Dove, S. K., Dong, K., Kobayashi, T., Williams, F. K., and Michell, R. H. (2009). Phosphatidylinositol 3,5-bisphosphate and Fab1p/PIKfyve under PPIn endolysosome function. *Biochem. J.* 419, 1–13. doi: 10.1042/BJ20081950
- Dowd, P. E., Courso, S., Skirpan, A. L., Kao, T.-H., and Gilroy, S. (2006). Petunia phospholipase C1 is involved in pollen tube growth. *Plant Cell* 18, 1438–1453. doi: 10.1105/tpc.106.041582
- Frietsch, S., Wang, Y.-F., Sladek, C., Poulsen, L. R., Romanowsky, S. M., Schroeder, J. I., et al. (2007). A cyclic nucleotide-gated channel is essential for polarized tip growth of pollen. *Proc. Natl. Acad. Sci. U.S.A.* 104, 14531–14536. doi: 10.1073/pnas.0701781104
- Gary, J. D., Wurmser, A. E., Bonangelino, C. J., Weisman, L. S., and Emr, S. D. (1998). Fab1p is essential for PtdIns(3)P 5-kinase activity and the maintenance of vacuolar size and membrane homeostasis. *J. Cell Biol.* 143, 65–79. doi: 10.1083/jcb.143.1.65
- Gui, C. P., Dong, X., Liu, H. K., Huang, W. J., Zhang, D., Wang, S. J., et al. (2014). Overexpression of the tomato pollen receptor kinase LePRK1 rewires pollen tube growth to a blebbing mode. *Plant Cell* 26, 3538–3555. doi: 10.1105/tpc.114.127381
- Guo, F., and McCubbin, A. (2012). The pollen-specific R-SNARE/longin PiVAMP726 mediates fusion of endo- and exocytic compartments in pollen tube tip growth. *J. Exp. Bot.* 63, 3083–3095. doi: 10.1093/jxb/ers023
- Heilmann, M., and Heilmann, I. (2015). Plant phosphoinositides-complex networks controlling growth and adaptation. *Biochim. Biophys. Acta* 1851, 759–769. doi: 10.1016/j.bbalip.2014.09.018
- Helling, D., Possart, A., Cottier, S., Klahre, U., and Kost, B. (2006). Pollen tube tip growth depends on plasma membrane polarization mediated by tobacco PLC3 activity and endocytic membrane recycling. *Plant Cell* 18, 3519–3534. doi: 10.1105/tpc.106.047373
- Hepler, P. K., Kunkel, J. G., Rounds, C. M., and Winship, L. J. (2012). Calcium entry into pollen tubes. *Trends Plant Sci.* 17, 32–38. doi: 10.1016/j.tplants.2011.10.007
- Hirano, T., Matsuzawa, T., Takegawa, K., and Sato, M. H. (2011). Loss-of-function and gain-of-function mutations in FAB1A/B impair endomembrane homeostasis, conferring pleiotropic developmental abnormalities in *Arabidopsis*. *Plant Physiol.* 155, 797–807. doi: 10.1104/pp.110.167981
- Hope, M. J., Redelmeier, T. E., Wong, K. F., Rodriguez, W., and Cullis, P. R. (1989). Phospholipid asymmetry in large unilamellar vesicles induced by transmembrane pH gradients. *Biochemistry* 28, 4181–4187. doi: 10.1021/bi00436a009
- Hurtado-Lorenzo, A., Skinner, M., El Annan, J., Futai, M., Sun-Wada, G. H., Bourgois, S., et al. (2006). V-ATPase interacts with ARNO and Arf6 in early endosomes and regulates the protein degradative pathway. *Nat. Cell Biol.* 8, 124–136. doi: 10.1038/ncb1348
- Ischebeck, T., Stenzel, I., and Heilmann, I. (2008). Type B phosphatidylinositol-4-phosphate 5-kinases mediate *Arabidopsis* and *Nicotiana tabacum* pollen tube growth by regulating apical pectin secretion. *Plant Cell* 20, 3312–3330. doi: 10.1105/tpc.108.059568
- Ischebeck, T., Stenzel, I., Hempel, F., Jin, X., Mosblech, A., and Heilmann, I. (2010). Phosphatidylinositol-4,5-bisphosphate influences Nt-Rac5-mediated cell expansion in pollen tubes of *Nicotiana tabacum*. *Plant J.* 65, 453–468. doi: 10.1111/j.1365-313X.2010.04435.x
- Jose, M., Tollis, S., Nair, D., Mitteau, R., Velours, C., Massoni-Laporte, A., et al. (2015). A quantitative imaging-based screen reveals the exocyst as a network hub connecting endocytosis and exocytosis. *Mol. Biol. Cell* 26, 2519–2534. doi: 10.1091/mbc.E14-11-1527
- Kost, B., Lemichez, E., Spielhofer, P., Hong, Y., Tolias, K., Carpenter, C., et al. (1999). Rac homologues and compartmentalized phosphatidylinositol 4, 5-bisphosphate act in a common pathway to regulate polar pollen tube growth. *J. Cell Biol.* 145, 317–330. doi: 10.1083/jcb.145.2.317
- Kusano, H., Testerink, C., Vermeer, J. E., Tsuge, T., Shimada, H., Oka, A., et al. (2008). The *Arabidopsis* phosphatidylinositol phosphate 5-kinase PIP5K3 is a key regulator of root hair tip growth. *Plant Cell* 20, 367–380. doi: 10.1105/tpc.107.056119

Advantages of publishing in Frontiers



OPEN ACCESS

Articles are free to read,
for greatest visibility



COLLABORATIVE PEER-REVIEW

Designed to be rigorous
– yet also collaborative,
fair and constructive



FAST PUBLICATION

Average 85 days from
submission to publication
(across all journals)



COPYRIGHT TO AUTHORS

No limit to article
distribution and re-use



TRANSPARENT

Editors and reviewers
acknowledged by name
on published articles



SUPPORT

By our Swiss-based
editorial team



IMPACT METRICS

Advanced metrics
track your article's impact



GLOBAL SPREAD

5'100'000+ monthly
article views
and downloads



LOOP RESEARCH NETWORK

Our network
increases readership
for your article

Frontiers

EPFL Innovation Park, Building I • 1015 Lausanne • Switzerland
Tel +41 21 510 17 00 • Fax +41 21 510 17 01 • info@frontiersin.org
www.frontiersin.org

Find us on

